U.S. Department of the Interior
U.S. Geological Survey

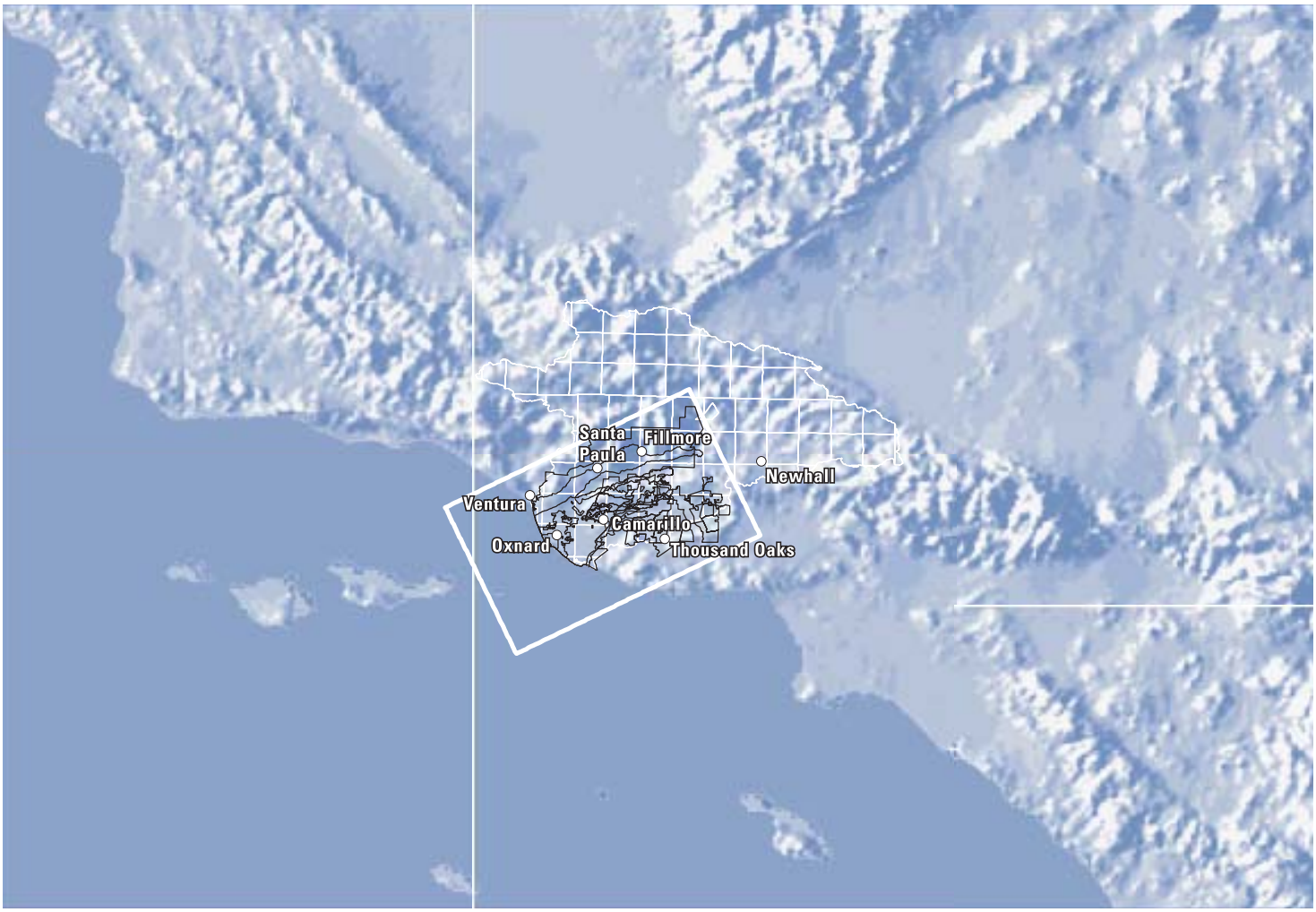

SIMULATION OF GROUND-WATER/ SURFACE-WATER FLOW IN THE SANTA CLARA-CALLEGUAS BASIN, VENTURA COUNTY, CALIFORNIA

A contribution of the
Southern California Regional Aquifer-System Analysis Program

USGS
science for a changing world

Water-Resources Investigations Report 02-4136

Simulation of Ground-Water/Surface-Water Flow in the Santa Clara–Calleguas Ground-Water Basin, Ventura County, California

By R.T. HANSON, PETER MARTIN, *and* K.M. KOCZOT

U.S. GEOLOGICAL SURVEY

Water-Resources Investigations Report 02-4136

A contribution of the
Southern California Regional Aquifer-System Analysis Program

5030-38

Sacramento, California
2003

U.S. DEPARTMENT OF THE INTERIOR

GALE A. NORTON, *Secretary*

U.S. GEOLOGICAL SURVEY

Charles G. Groat, *Director*

For additional information write to:

District Chief
U.S. Geological Survey
Placer Hall, Suite 2012
6000 J Street
Sacramento, CA 95819-6129
http://water.wr.usgs.gov/

Copies of this report can be purchased from:

U.S. Geological Survey
Information Services
Building 810
Box 25286, Federal Center
Denver, CO 80225-0286

CONTENTS

FIGURES

TABLES

CONVERSION FACTORS, VERTICAL DATUM, ABBREVIATIONS AND WELL-NUMBERING SYSTEM

CONVERSION FACTORS

Multiply	By	To obtain
Length		
inch (in.)	2.54	centimeter
foot (ft)	0.3048	meter
mile (mi)	1.609	kilometer
Area		
acre	0.4047	hectare
square mile (mi^2)	259.0	hectare
Volume		
acre-foot (acre-ft)	1,233	cubic meter
Flow rate		
acre-foot per day (acre-ft/d)	0.01427	meter per day
acre-foot per year (acre-ft/yr)	1,233	cubic meter per year
foot per year (ft/yr)	0.3048	meter per year
cubic foot per second (ft^3/s)	0.3048	cubic meter per second
foot per day per foot [(ft/d)/ft]	1.0000	meter per day per meter
gallon per minute (gal/min)	0.06309	liter per minute
inch per year (in/yr)	25.4	millimeter per year
Hydraulic conductivity		
foot per day (ft/d)	0.3048	meter per day
Transmissivity		
foot squared per day (ft^2/d)	0.09290	meter squared per day

Temperature in degrees Celsius (°C) may be converted to degrees Fahrenheit (°F) as follows:

$$°F = (1.8 \times °C) + 32$$

Temperature in degrees Fahrenheit (°F) may be converted to degrees Celsius (°C) as follows:

$$°C = (°F - 32) / 1.8$$

VERTICAL DATUM

Sea level: In this report, "mean sea level" refers to the National Geodetic Vertical Datum of 1929 (NGVD of 1929)—a geodetic datum derived from a general adjustment of the first-order level nets of both the United States and Canada, formerly called Sea Level Datum of 1929.

Abbreviations

AR	autoregressive
ASR	artificial storage and recovery system
BM	bench mark
CMWD	Calleguas Municipal Water District
DWR	[California] Department of Water Resources
EM	electromagnetic induction
ET	evapotranspiration
FGMA	Fox Canyon Groundwater Management District
GIS	Geographic Information System
InSAR	Interferometric Synthetic Aperture Radar
LSA	land surface altitude
ME	mean error
MODFLOW	U.S. Geological Survey's modular flow model
PTP	pumping-trough pipeline
PVCWD	Pleasant Valley County Water District
RASA	Southern California Regional Aquifer-System Analysis
RMSE	root mean square error
SSA	singular-spectrum analysis
STR1	streamflow routing package 1
USGS	U.S. Geological Survey
UWCD	United Water Conservation District
VCFCD	Ventura County Flood Control District
VCPWD	Ventura County Public Works Department

Well-Numbering System

Wells are identified and numbered according to their location in the rectangular system for the subdivision of public lands. Identification consists of the township number, north or south; the range number, east or west; and the section number. Each section is divided into sixteen 40-acre tracts lettered consecutively (except I and O), beginning with "A" in the northeast corner of the section and progressing in a sinusoidal manner to "R" in the southeast corner. Within the 40-acre tract, wells are sequentially numbered in the order they are inventoried. The final letter refers to the base line and meridian. In California, there are three base lines and meridians; Humboldt (H), Mount Diablo (M), and San Bernardino (S). Well numbers consist of 15 characters and follow the format 002N002W12F001S. In this report, well numbers may be abbreviated and written 2N/2W-12F1. The following diagram shows how the number for well 2N/2W-12F1 is derived.

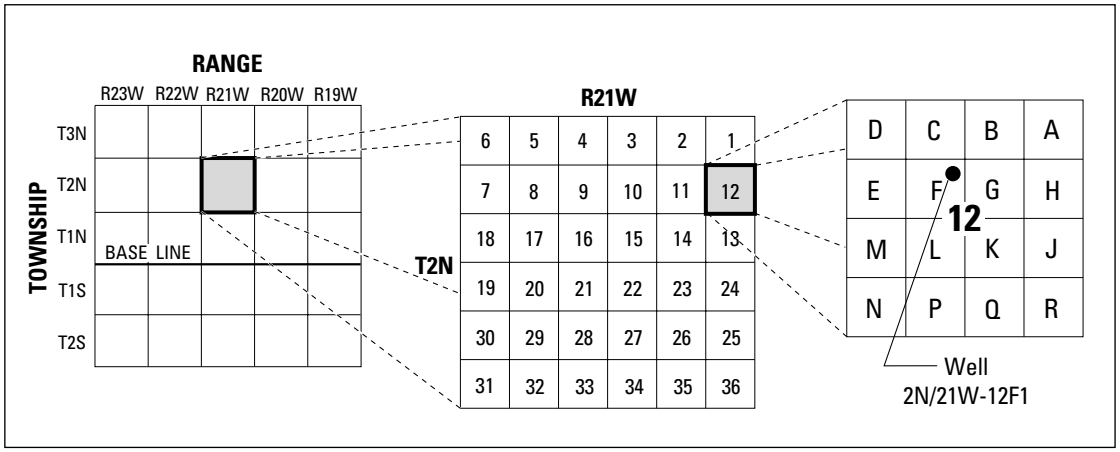

Well-numbering diagram

Simulation of Ground-Water/Surface-Water Flow in the Santa Clara–Calleguas Ground-Water Basin, Ventura County, California

By R.T. Hanson, Peter Martin, *and* K.M. Koczot

ABSTRACT

Ground water is the main source of water in the Santa Clara–Calleguas ground-water basin that covers about 310 square miles in Ventura County, California. A steady increase in the demand for surface- and ground-water resources since the late 1800s has resulted in streamflow depletion and ground-water overdraft. This steady increase in water use has resulted in seawater intrusion, inter-aquifer flow, land subsidence, and ground-water contamination.

The Santa Clara–Calleguas Basin consists of multiple aquifers that are grouped into upper- and lower-aquifer systems. The upper-aquifer system includes the Shallow, Oxnard, and Mugu aquifers. The lower-aquifer system includes the upper and lower Hueneme, Fox Canyon, and Grimes Canyon aquifers. The layered aquifer systems are each bounded below by regional unconformities that are overlain by extensive basal coarse-grained layers that are the major pathways for ground-water production from wells and related seawater intrusion. The aquifer systems are bounded below and along mountain fronts by consolidated bedrock that forms a relatively impermeable boundary to ground-water flow. Numerous faults act as additional exterior and interior boundaries to ground-water flow. The aquifer systems extend offshore where they crop out along the edge of the submarine shelf and within the coastal submarine canyons. Submarine canyons have dissected these regional aquifers, providing a hydraulic connection to the ocean through the submarine outcrops of the aquifer systems. Coastal landward flow (seawater intrusion) occurs within both the upper- and lower-aquifer systems.

A numerical ground-water flow model of the Santa Clara–Calleguas Basin was developed by the U.S. Geological Survey to better define the geohydrologic framework of the regional ground-water flow system and to help analyze the major problems affecting water-resources management of a typical coastal aquifer system. Construction of the Santa Clara–Calleguas Basin model required the compilation of geographic, geologic, and hydrologic data and estimation of hydraulic properties and flows. The model was calibrated to historical surface-water and ground-water flow for the period 1891–1993.

Sources of water to the regional ground-water flow system are natural and artificial recharge, coastal landward flow from the ocean (seawater intrusion), storage in the coarse-grained beds, and water from compaction of fine-grained beds (aquitards). Inflows used in the regional flow model simulation include streamflows routed through the major rivers and tributaries; infiltration of mountain-front runoff and infiltration of precipitation on bedrock outcrops and on valley floors; and artificial ground-water recharge of diverted streamflow, irrigation return flow, and treated sewage effluent.

Most natural recharge occurs through infiltration (losses) of streamflow within the major rivers and tributaries and the numerous arroyos that drain the mountain fronts of the basin. Total simulated natural recharge was about 114,100 acre-feet per year (acre-ft/yr) for 1984–93: 27,800 acre-ft/yr of mountain-front and bedrock recharge, 24,100 acre-ft/yr of valley-floor recharge, and 62,200 acre-ft/yr of net streamflow recharge.

Artificial recharge (spreading of diverted streamflow, irrigation return, and sewage effluent) is a major source of ground-water replenishment. During the 1984–93 simulation period, the average rate of artificial recharge at the spreading grounds was about 54,400 acre-ft/yr, 13 percent less than the simulated natural recharge rate for streamflow infiltration within the major rivers and tributaries. Estimated recharge from infiltration of irrigation return flow on the valley floors averaged about 51,000 acre-ft/yr, and treated sewage effluent averaged about 9,000 acre-ft/yr. Artificial recharge as streamflow diversion to the spreading grounds has occurred since 1929, and treated-sewage effluent has been discharged to stream channels since 1930.

Under predevelopment conditions, the largest discharge from the ground-water system was outflow as coastal seaward flow and evapotranspiration. Pumpage of ground water from thousands of water-supply wells has diminished these outflows and is now the largest outflow from the ground-water flow system. The distribution of pumpage for 1984–93 indicates that most of the pumpage occurs in the Oxnard Plain subareas (37 percent) and in the upper Santa Clara River Valley subareas (37 percent). The total average simulated pumpage was about 247,000 acre-ft/yr (59 percent); of which about 146,000 acre-ft/yr was from the Fox Canyon Groundwater Management Agency (FGMA) subareas and 101,000 acre-ft/yr (41 percent) from the non-FGMA subareas. Of the total 1984–93 pumpage, 46 percent was contributed by natural recharge, 22 percent was contributed by artificial recharge from diverted streamflow, 20 percent was contributed by irrigation return flow, 4 percent was contributed from sewage-effluent infiltration, 6 percent was contributed from storage depletion, and 2 percent was contributed from coastal landward flow (seawater intrusion).

Seawater intrusion was first suspected in 1931 when water levels were below sea level in a large part of the Oxnard Plain. The simulation of regional ground-water flow indicated that coastal landward flow (seawater intrusion) began in 1927 and continued to the end of the period of simulation (1993). During wet periods or periods of reduced demand for ground water, the direction of coastal flow in the upper-aquifer system reverses from landward to seaward. During the 1984–93 period, the simulated total net seaward flow was 9,500 acre-feet in the upper-aquifer system, which is considerably less than that simulated for predevelopment conditions. During the same period, total simulated landward flow in the lower-aquifer system was 64,200 acre-feet.

Water-level declines in the basin have induced land subsidence that was first measured in 1939 and have resulted in as much as 2.7 feet land subsidence in the southern part of the Oxnard Plain. The model simulated a total of 3 feet of land subsidence in the southern part of the Oxnard Plain and as much as 5 feet in the Las Posas Valley subbasins. Model simulations indicate that most of the land subsidence occurred after the drought of the late 1920s and during the agricultural expansion of the 1950s and 1960s. The results also indicate that subsidence occurred primarily in the upper-aquifer system prior to 1959, but in the lower-aquifer system between 1959–93 owing to an increase in pumpage from the lower-aquifer system.

The calibrated ground-water flow model was used to assess future ground-water conditions based on proposed water-supply projects in the existing management plan for the Santa Clara–Calleguas ground-water basin. All the projections of the proposed water-supply projects in the existing management plan have reduced pumpage in the FGMA areas which resulted in a reduction but not an elimination of storage depletion and related coastal landward flow (seawater intrusion) and subsidence, a reduction in streamflow recharge, and an increase in coastal seaward flow and underflow to adjacent subareas from the Oxnard Plain. A comparison of management simulations based on historical inflows and a spectral estimate of inflows shows increased coastal landward flow (seawater intrusion), storage depletion, and increased land subsidence due to a drought projected earlier in the spectral estimate of inflows than in the historical inflows. The spectral estimate probably provides a smoother and more realistic transition between historical and future climatic conditions.

The model also was used to simulate potential alternative water-supply projects in the Santa Clara–Calleguas ground-water basin. These seven alternative water-supply projects were proposed to help manage the effects of increasing demand and variable supply on seawater intrusion, subsidence, increased withdrawal from storage, and vertical and lateral flow between subareas and aquifers systems. Stopping pumpage primarily in the lower-aquifer system in the South Oxnard Plain subarea had the largest effect on reducing coastal landward flow (seawater intrusion) of all the potential cases evaluated. Shifting pumpage from the lower- to the upper-aquifer system in the South Oxnard Plain subarea yielded the largest combined effect on coastal flow with a reduction of coastal landward flow in the lower-aquifer system and coastal seaward flow from the upper-aquifer system. A seawater-barrier injection project stopped coastal landward flow (seawater intrusion) in the upper-aquifer system but also resulted in large quantities of coastal seaward flow. The recharge of water in Happy Camp Canyon resulted in water-level rises that were above land surface (not feasible) in the East Las Posas Valley subarea but in no significant changes in hydrologic conditions in other parts of the basin.

INTRODUCTION

Ground water from the regional alluvial-aquifer systems is the main source of water in the Santa Clara and Calleguas watersheds in southern California. In Ventura County, for the purposes of this study, the alluvial ground-water basins of these watersheds are referred to as the Santa Clara–Calleguas ground-water basin. Development of the water resources of the Santa Clara–Calleguas ground-water basin has steadily increased since the late 1800s, resulting in streamflow depletion, ground-water overdraft, seawater intrusion, inter-aquifer flow, land subsidence, and ground-water contamination. The extent of ground-water overdraft, which is the withdrawal of potable water from an aquifer system in excess of replenishment from natural and artificial recharge, varies throughout the basin. Overdraft is also dependent on climatic variability and associated increases in water use. Overdraft has been larger within selected subareas of the ground-water basin and in the deeper aquifers. However, there has been an increased amount of conjunctive use to compensate for the effects of the variability of surface-water supplies and to mitigate the effects of ground-water overdraft.

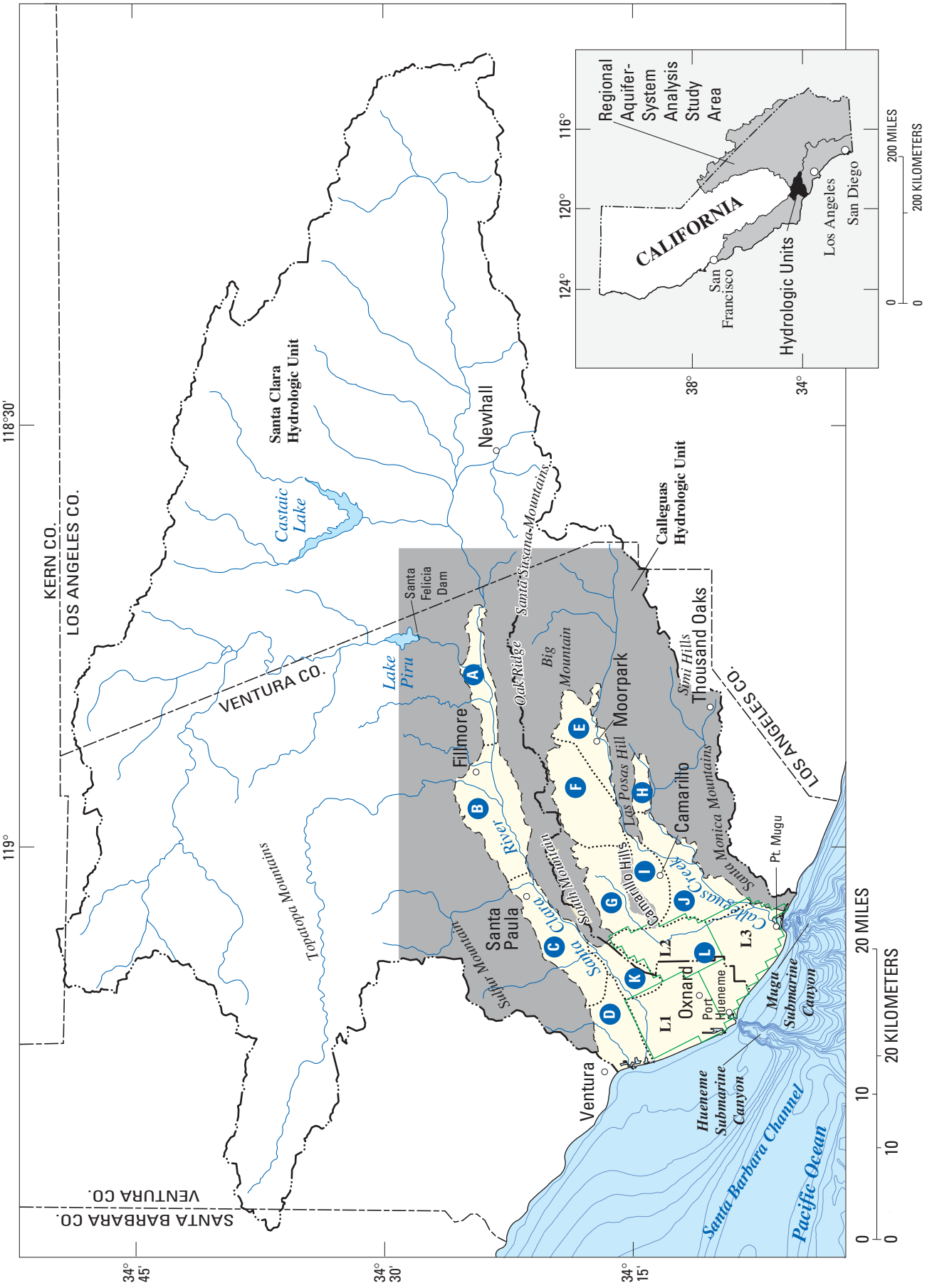

Figure 1. Santa Clara–Calleguas Hydrologic Unit and ground-water basin. (Modified from California State Water Resources Board, 1956)

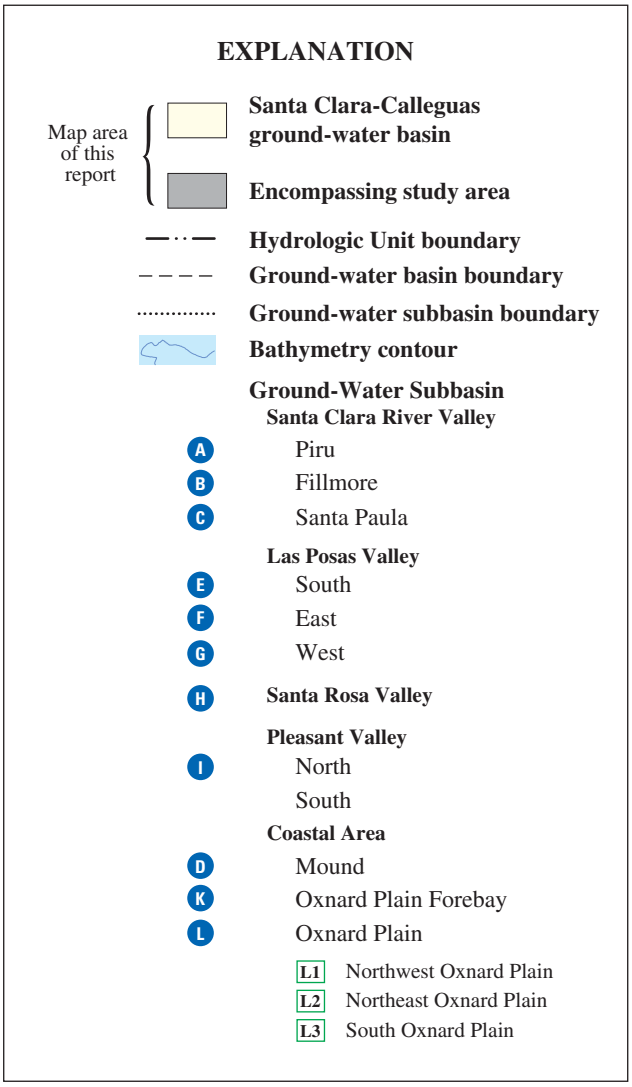

A U.S. Geological Survey (USGS) study of the hydrogeology of the Santa Clara–Calleguas Basin was completed as part of the Southern California Regional Aquifer-System Analysis (RASA) Program (Martin, 1986). The purpose of the Southern California RASA Program was to analyze the major problems and issues affecting ground-water use in southern California, including ground-water overdraft, streamflow depletion, subsidence, seawater intrusion, and ground-water contamination. Because of the large size of the study area and the large number of basins involved, only two, the Santa Clara–Calleguas Basin (coastal) and the Mojave River ground-water basin (desert), of the 89 hydrologic subunits identified by the California Department of Water Resources (1964) were studied for the Southern California RASA Program (Martin, 1993). The basic assumption of the program was that certain characteristics of the geohydrologic processes and human activities that control or influence water resources are common to many of the basins or groups of basins. The development of the Santa Clara–Calleguas Basin study is an extension of previous investigations in the nearby coastal aquifer systems in Santa Barbara, California (Martin and Berenbrock, 1986; Freckleton and others, 1998).

Purpose and Scope

The purpose of this study is to acquire a better understanding of the hydrogeologic system in the Santa Clara–Calleguas Basin (fig. 1) and to develop a tool to help analyze the major problems affecting water-resources management of a typical coastal aquifer system. The study included a reevaluation of the basin structure and stratigraphy of the water-bearing rocks and an evaluation of the hydrologic system under predevelopment, historical development, and future development conditions. The purposes of this report are to describe the regional ground-water flow model that was constructed for the RASA Program, to summarize the results of simulations of historical and future periods using the RASA model, and to describe the model limitations and the data needed for future model refinements. Also described in this report are ground-water recharge, movement, and discharge.

Approach

A regional model of ground-water flow that simulates the hydrologic system under pre- and post-development conditions was developed to evaluate the natural and human-induced controls on the regional water resources. Because water-resources development began relatively early in the coastal basins of California, there is very little quantitative information on predevelopment ground-water and surface-water conditions. This lack of data required coupling the calibration of the steady- and transient-state simulations to arrive at a combined fit for pre- and post-development conditions.

Previous studies of the aquifer systems (Mann and Associates, 1959; Turner, 1975) and numerical models of the hydrologic system (California Department of Water Resources, 1974a,b; Reichard, 1995) were used as the starting point for the reevaluation of the stratigraphy and structure of the water-bearing units and to provide estimates of hydraulic properties of each unit. Reevaluation was based on additional geophysical data, geochemical data, and hydraulic data from selected existing production wells and from 23 new monitoring wells drilled throughout the basin by the USGS (Izbicki and others, 1995; Densmore, 1996). Estimates for many of the hydraulic properties and for the quantities and locations of recharge and discharge needed to simulate ground-water flow in the major water-bearing units generally were unavailable; therefore, indirect estimates, which were modified during the calibration of the numerical model, were required.

Description of Study Area

The Santa Clara (hydrologic unit 18070102) and Calleguas (hydrologic unit 18070103) Basins are coastal watersheds that principally drain parts of Ventura and Los Angeles Counties; they have a total drainage area of 2,010 mi^2 (fig. 1). Almost 90 percent of the basin surface is characterized by rugged topography; the remainder consists of valley floor and coastal plain composed of a northeast-trending set of anticlinal mountains and synclinal valleys in the Transverse Ranges physiographic province. The onshore part of the Santa Clara–Calleguas alluvial basin is about 32 mi long and includes about 310 mi^2. The ground-water basin extends as much as 10 miles offshore and includes an additional 193 mi^2. The sloping offshore plain and underlying aquifers are truncated by steeply dipping submarine cliffs that are dissected by several submarine canyons.

The Santa Clara–Calleguas Basin is a regional ground-water basin that can be divided into 12 onshore subbasins (fig. 1). The coastal subbasins extend offshore beneath the gently sloping submarine shelf. The ground-water subbasins are subareas within the surface-water drainage subbasins, and many of their boundaries are aligned with known faults and other geologic features. The Piru, Fillmore, Santa Paula, and Mound subbasins and the northern part of the Oxnard Plain known as the Oxnard Plain Forebay subbasin compose the Santa Clara River Valley. The Santa Rosa Valley, East and South Las Posas Valley, and North and South Pleasant Valley subbasins and the southern part of the Oxnard Plain subbasin compose the Arroyo Simi–Arroyo Las Posas–Conejo Creek–Calleguas Creek drainage basin. In the West Las Posas Valley subbasin, Arroyo Hondo and Beardsley Wash flow into Revolon Slough, which flows along with Calleguas Creek into Mugu Lagoon (see figure 4 in the "Surface Water" section). These three drainages cross parts of the coastal subbasin known as the Oxnard Plain.

The Santa Clara River and the Calleguas Creek discharge directly to the Pacific Ocean. The onshore ground-water basin is bounded by the Sulfur Mountain and the Topatopa Mountains on the north, the Santa Susana Mountains and the Simi Hills on the east, and the Santa Monica Mountains on the south (fig. 1). Mountain peaks, which exceed 6,700 ft in altitude, rise above numerous narrow valleys and streams that are tributary to the Santa Clara River and Calleguas Creek drainage basins. The west-trending Oak Ridge, South Mountain, and Santa Susana Mountains separate the Santa Clara River Valley from the Las Posas Valley. The west-trending Las Posas and Camarillo Hills separate Las Posas Valley from Pleasant Valley. These intermontane alluvial valleys grade into the coastal flood plains in the Oxnard Plain and the Mound subbasins. The coastal flood plain continues offshore as a gently sloping submarine shelf of the Santa Barbara Channel. The submarine shelf is bounded on the west by steeply sloping submarine cliffs where the water-bearing formations crop out. The shelf is dissected by the Hueneme and the Mugu submarine canyons and several unnamed smaller submarine canyons (fig. 1). The larger submarine canyons dissect the submarine shelf to the present-day shoreline.

Climate

The climate of the basin is of the mediterranean type with 85 percent of the rainfall occurring between November and April, typical of the southern California coastal area. Average annual precipitation is about 14 in. at Port Hueneme along the coast, about 17 in. near Santa Paula in the intermediate altitudes of the Santa Clara River Valley, and more than 25 in. in the surrounding mountains (Ventura County Public Works Agency, 1990, 1993). Daily mean temperatures range from as high as 89°F along the coast in late summer and early fall to below freezing in the bordering mountains during winter. Mean pan-evaporation rates range from 59 in/yr at Casitas Dam at Ventura County Flood Control District (VCFCD) Station Number 4 to 73 in/yr at Lake Bard at VCFCD Station Number 227 (Ventura County Public Works Agency, 1990, 1993).

The climate is seasonally variable and has been variable through time (fig. 2). The cumulative departure of tree-ring indices and precipitation can be used to divide periods of the climatic record into wet and dry climatic periods. Wet climatic periods are determined using the rising limb of the cumulative departure curve, and dry climatic periods are determined using the falling limb of the cumulative departure curve. The cumulative departure of tree-ring indices for southern California for 1458–1966 (National Atmospheric and Oceanic Administration, 1994) indicates an apparent shift in the frequency and amplitude of wet and dry periods after the early 1700s. Prior to the early 1700s, wet and dry periods were relatively long (20 to more than 60 years); whereas after the early 1700s, wet and dry periods were shorter (5 to 20 years) (fig. *2A*). The wet and dry periods determined from tree-ring indices for 1770–1965 generally are in agreement with available precipitation records for Port Hueneme and Santa Paula and are related to periods of major droughts and floods (fig. 2B).

Population

The Santa Clara–Calleguas Basin was settled and populated by Native American Indians of the Shumash Tribes. Spanish missionaries established Mission San Buena Ventura in 1787. In the early 1800s, Jesuit Fathers from the San Buena Ventura Mission established an asistencia (Ventura Mission outpost) where the city of Santa Paula is now located (Freeman, 1968). These colonies and related Spanish land grants developed the initial agrarian and ranching industry in the river valleys. The town of San Buena Ventura (hereinafter referred to as "Ventura") became the county seat. By 1930, Ventura County had a total population of 54,976; Ventura and Santa Paula were the most populous cities. Ventura, which was largely supported by the oil industry, had a population of 11,603. Santa Paula and Fillmore, which were the principal towns in the citrus area, had populations of 7,452 and 2,890, respectively. Oxnard, the center of the beet-sugar industry in Ventura County, had a population of 6,285 (California Department of Public Works, 1934). By 1970, the population in Ventura County increased to 378,497 as various small unincorporated settlements grew into towns. The population increased to 535,700 by 1980, and to 686,900 by 1992—a 28 percent increase. Since the 1960s, a large part of the population increase was related to the urbanization of Ventura County.

Land and Water Use

Prior to the 1900s, most land in the Santa Clara–Calleguas Basin was used for grazing cattle and dry-land farming. In the early 1900s, agricultural and petroleum production became the chief economic activities. As in all the coastal basins, urbanization since the late 1940s resulted in the transfer of agricultural lands to residential and commercial uses, especially in the Oxnard Plain. In the late 1940s, the turbine pump was introduced for pumping ground water, and in the early 1950s, the introduction of the refrigerated railroad car provided long-range markets for fresh produce. As a result, agriculture was transformed from predominantly seasonal dry-land farming of walnuts and field crops to predominantly year-round irrigated farming of citrus, avocados, and truck crops, and water use increased to a historical high during the 1950s. Currently, about 80 percent of the ground-water and surface-water supply is used for agriculture. Agricultural land use increased less than 5 percent and urban land use increased from 39 to 51 percent between 1969 and 1980. Since 1980, urban growth has continued and urban land use has remained the dominant land use in the basin. Because of the proximity to the Los Angeles metropolitan area, growth may continue with further transformation from an agriculture-based economy to an urban and industrial economy. An excellent summary of the development of water in Ventura County is given by Freeman (1968).

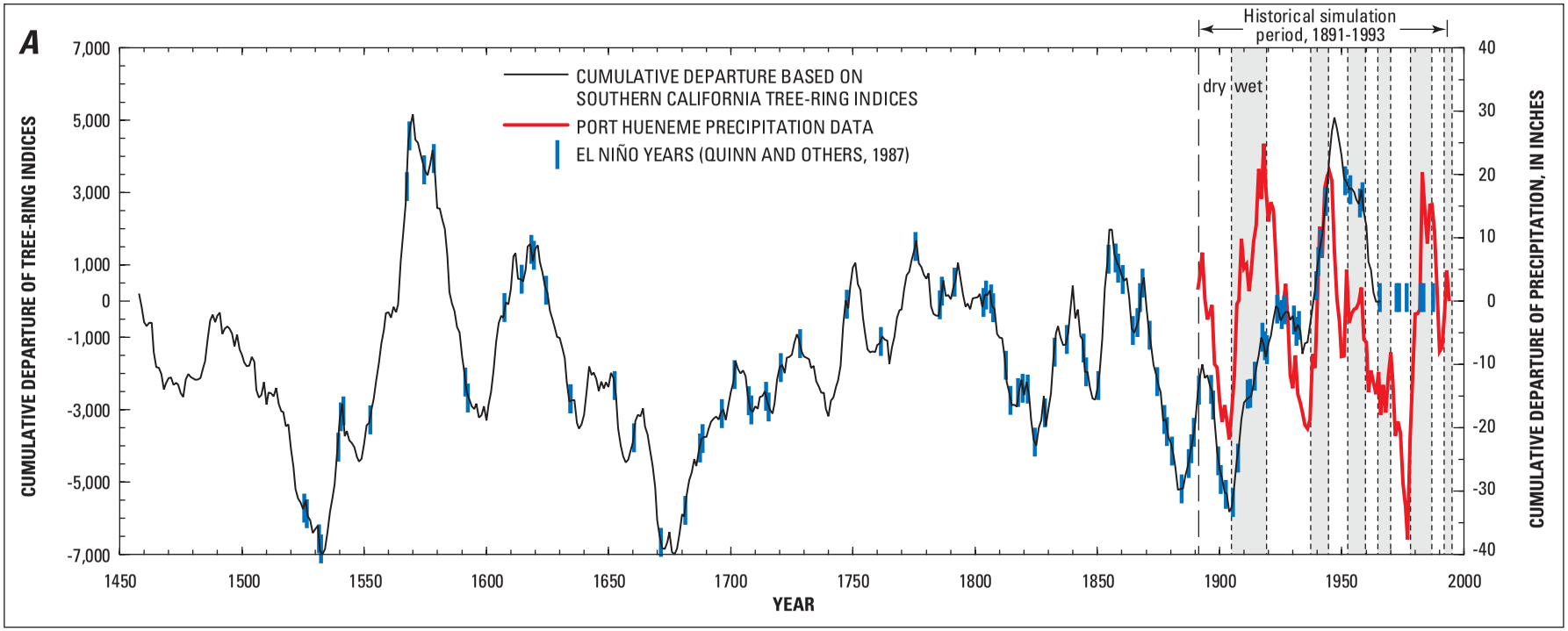

Figure 2. ***A***, Cumulative departure of tree-ring indices for southern California (1458–1966), cumulative departure of precipitation at Port Hueneme (1891–1993), and wet and dry climatic periods for the historical simulation period (1891–1993), and ***B***, Cumulative departure of tree-ring indices for southern California, cumulative departure of precipitation at Port Hueneme and Santa Paula, wet and dry climatic periods, and major climatic events (1770–1965), Ventura County, California.

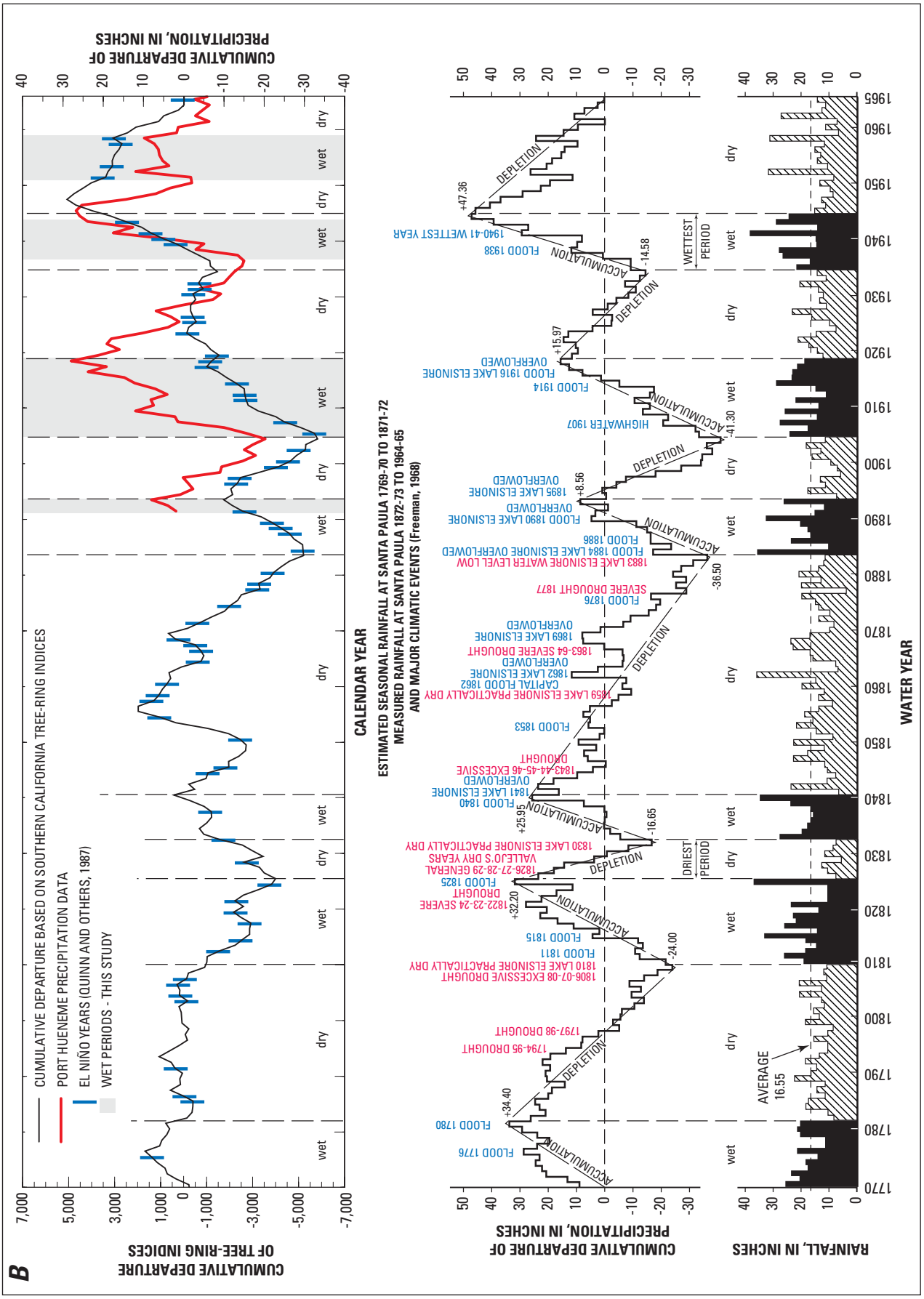

Figure 2. Continued.

Acknowledgments

This study could not have been accomplished without the assistance of personnel from the United Water Conservation District (UWCD), the hydrology section of the Ventura County Public Works Department (VCPWD), the Fox Canyon Groundwater Management Agency (FGMA), the Calleguas Municipal Water District (CMWD), the U.S. Department of the Navy, the Pleasant Valley County Water District (PVCWD), local municipalities and water mutuals, and numerous other well owners that provided data and allowed access to their wells for sampling and well testing. The authors are also indebted to Wesley Danskin, USGS, for assistance with the modifications to the diversion component of the streamflow-routing package (Appendix 2), and to Michael Dettinger, USGS, for assistance with the analysis of historical precipitation and estimation of future precipitation (Appendix 3). The authors would also like to thank Larry Schneider for his extraordinary effort in creating the scientific illustrations for this report. An additional special thanks also goes out to Myrna L. DeBortoli and Mary Gibson for editing this large and complicated report.

SURFACE WATER

Runoff from precipitation in the upland areas that surround the Santa Clara–Calleguas Basin is the predominant source of natural streamflow and ground-water recharge. As agriculture developed, some streamflow was diverted for irrigation. Since the 1950s, imported water from northern California has been combined with local surface water and collectively used for artificial recharge. Discharge of reclaimed sewage effluent, which began in the late 1930s, provides an additional source of water to the surface-water and ground-water systems in parts of the basin.

Precipitation Estimates

Precipitation, and related surface-water flow, has been variable through time, and is the major source of ground-water recharge. For this study, precipitation and streamflow data and statistical relations determined from these data were segregated into wet and dry seasonal periods to reconstruct historical runoff and streamflow. The cumulative departure curve of precipitation for Port Hueneme was used to divide periods of record into wet and dry climatic periods (fig. 2). The wet and dry climatic periods were determined using the rising and falling limbs of the cumulative departure curve, respectively.

As noted earlier, for the past few centuries, cumulative departure of the tree-ring indices for southern California indicates an apparent shift in the frequency and amplitude of the wet and dry periods after the early 1700s; prior to the early 1700s wet and dry periods were relatively long (20 to more than 60 years) whereas after the early 1700s these periods were relatively short (5 to 20 years) (fig. *2A*). Frequency analyses (spectral) of tree rings, precipitation, and ground-water levels indicate climatic cycles of 22, 5.3, and 2.2–2.9 years for the period of record (Appendix 3; Hanson and Dettinger, 1996). Collectively, these cycles account for 60 percent of the variation in precipitation. Winter and spring rainfall is derived largely from arctic-northern frontal storms that may be related to the long term (22 year) climatic cycles of the Pacific decadal oscillation. Intermediate (5.3 year) cycles contribute to fall and winter rainfall and may be related to a combination of storms related to a northerly flow of moisture from El Niño and monsoonal flow from the central Pacific Ocean. Additional moisture may be associated with meridianal flow of the jetstream and related extracyclonic storms that occur during the short-term (2.2–2.9 year) cycles of El Niño years in both wet and dry periods (fig. *2A*). Examples of exceptional storm-type related events that may be attributed to subtropical extracyclonic storms include a short-lived, intense rain storm, such as occurred in September of 1910 during a dry period; a relatively wet year, such as 1962, during a dry period; and historic flooding, such as in 1853. Freeman (1968) originally segregated wet and dry periods on the basis of precipitation records from Santa Paula and precipitation estimates reconstructed from crop indices for 1769 through 1965. Freeman demonstrated a strong correlation between the longer term wet and dry periods and observed hydrologic events in southern California, such as changes in stage of lakes and reservoirs, and droughts and floods (fig. *2B*).

For this study, six alternating climate cycles that resulted in six wet and six dry periods between 1891 and 1993 were identified on the basis of the cumulative departure curve for precipitation measured at Port Hueneme (fig. 2A). The climate cycles were separated into wet-year and dry-year periods as follows:

CYCLE	DRY-YEAR PERIOD	WET-YEAR PERIOD
1	1891–1904	1905–1918
2	1919–1936	1937–1944
3	1945–1951	1952–1958
4	1959–1964	1965–1969
5	1970–1977	1978–1986
6	1987–1991	1992–1993

This segregation shows good agreement with the tree-ring indices and the climate periods delineated by Freeman (1968) (fig. 2A,B). Selected coastal precipitation stations at Ventura, Oxnard, Port Hueneme, and Camarillo were used to assess the segregation of data within the wet- and dry-year seasons (fig. 3, table 1). Although there are some wet years in dry periods and dry years in wet periods, the seasonal mean coastal precipitation for these multiple-year wet- and dry-year period groupings is not significantly different from the seasonal mean precipitation grouped for individual wet and dry years (independent of wet- and dry-year periods) but is significantly different from the period-of-record mean for all seasons except summer (table 1). This general segregation of recent historical climatic variability into wet- and dry-year periods were used to reconstruct the historical estimates of precipitation and streamflow. Ground-water recharge and changes in ground-water demand measured or estimated from pumpage data were categorized on the basis of these wet and dry periods.

Kriged estimates of average total seasonal precipitation for wet and dry winters, springs, summers, and falls were made from available data from the Ventura County Flood Control District precipitation stations for 1891 to 1991 (fig. 3A–H). Data were not available for individual stations for the entire period of estimation. The spatial distributions of seasonal precipitation for wet and dry periods were similar for winter and fall. Spring and summer precipitation patterns, however, showed a small shift from relatively more precipitation in the northern mountains during wet springs and summers to relatively more precipitation in the southeastern mountains during dry springs and summers (fig. 3C–F). The largest increase in seasonal precipitation was between wet and dry winters (fig. 3A,B). The ratio of wet- to dry-season precipitation was 1.8 for winter, 1.6 for spring, 1.1 for summer, and 1.2 for fall.

Streamflow

The Santa Clara River Basin drains the area to the north and east of the Santa Clara–Calleguas ground-water basin; its major tributaries are Piru, Hopper, Pole, Sespe, Santa Paula, and Ellsworth Creeks (fig. 4). Calleguas Creek and its major tributaries, Conejo Creek and Arroyo Simi–Las Posas, drain the areas to the south and east of the alluvial basin. Revolon Slough and its major tributaries, Arroyo Hondo and Beardsley Wash (fig. 4), drain the western part of the Las Posas Valley and the southwestern part of the Oxnard Plain. Streamflow represents the major natural source ground-water recharge to the basin. The steadily increasing use of the surface-water and ground-water resources of the Santa Clara–Calleguas Basin since the late 1800s has resulted in streamflow depletion.

Streamflow measurements were made as early as the late 1800s (Grunsky, 1925), but continuous measurement at permanent gaging stations was not undertaken until 1912 on Piru Creek and not until 1927 on the Santa Clara River (fig. 4). Gaging stations also were established on other Santa Clara River tributaries (fig. 4) starting in 1927. Streamflow gaging stations were first established on the Arroyo Simi in 1934 and on Conejo Creek in the 1970s. Continuous gaging of streamflow at downstream sites began at Montalvo on the Santa Clara River (11114000) in 1955, on the Calleguas Creek above U.S. Highway 101 (11106550) in 1971, and at Camarillo (11106000) in 1968 (fig. 4).

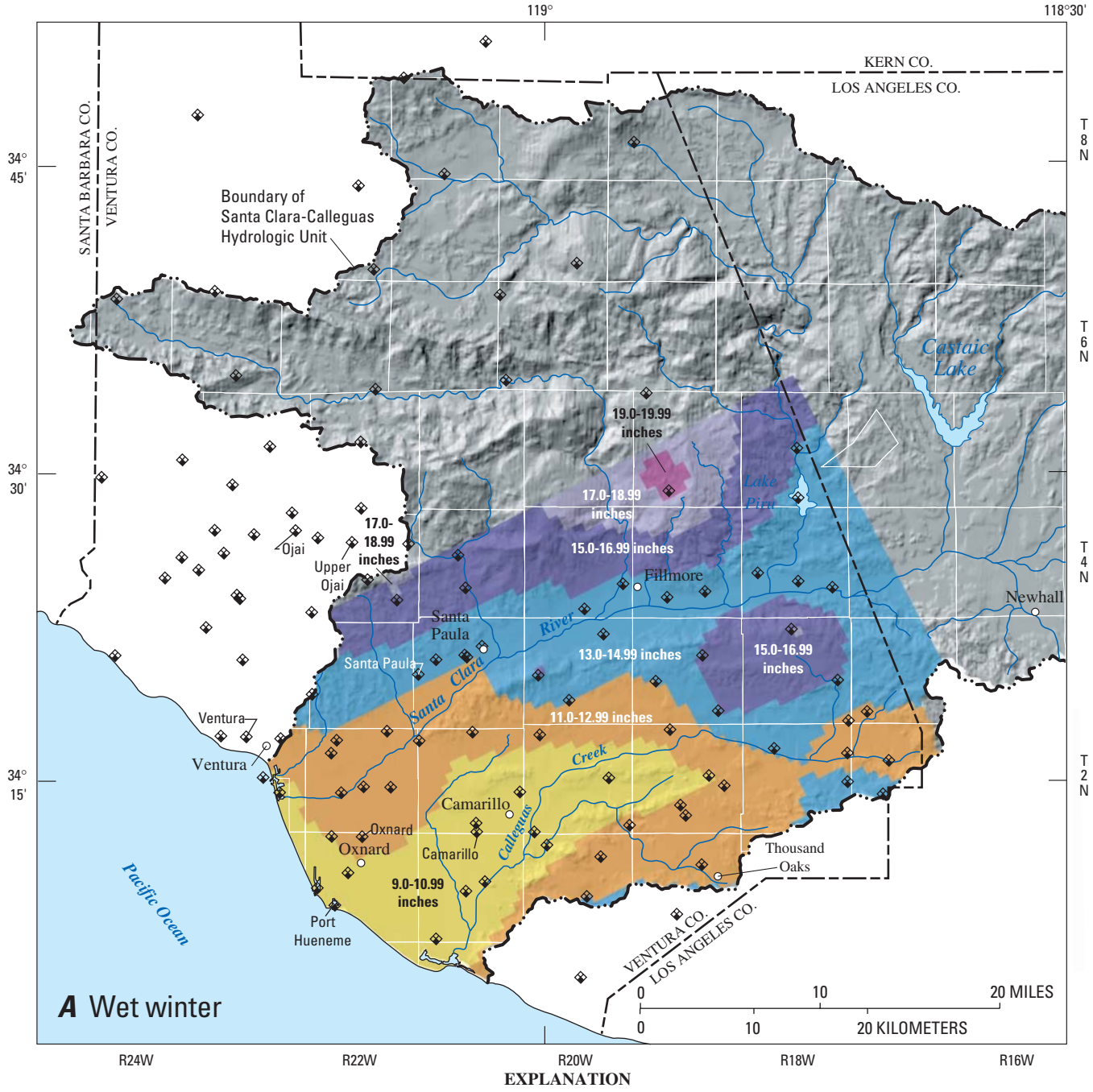

Figure 3. Kriged average total seasonal precipitation 1891–1991 for wet and dry climatic periods by season. ***A***, Wet winter. ***B***, Dry winter. ***C***, Wet spring. ***D***, Dry spring. ***E***, Wet summer. ***F***, Dry summer. ***G***, Wet fall. ***H***, Dry fall. Number of seasons available varies between stations.

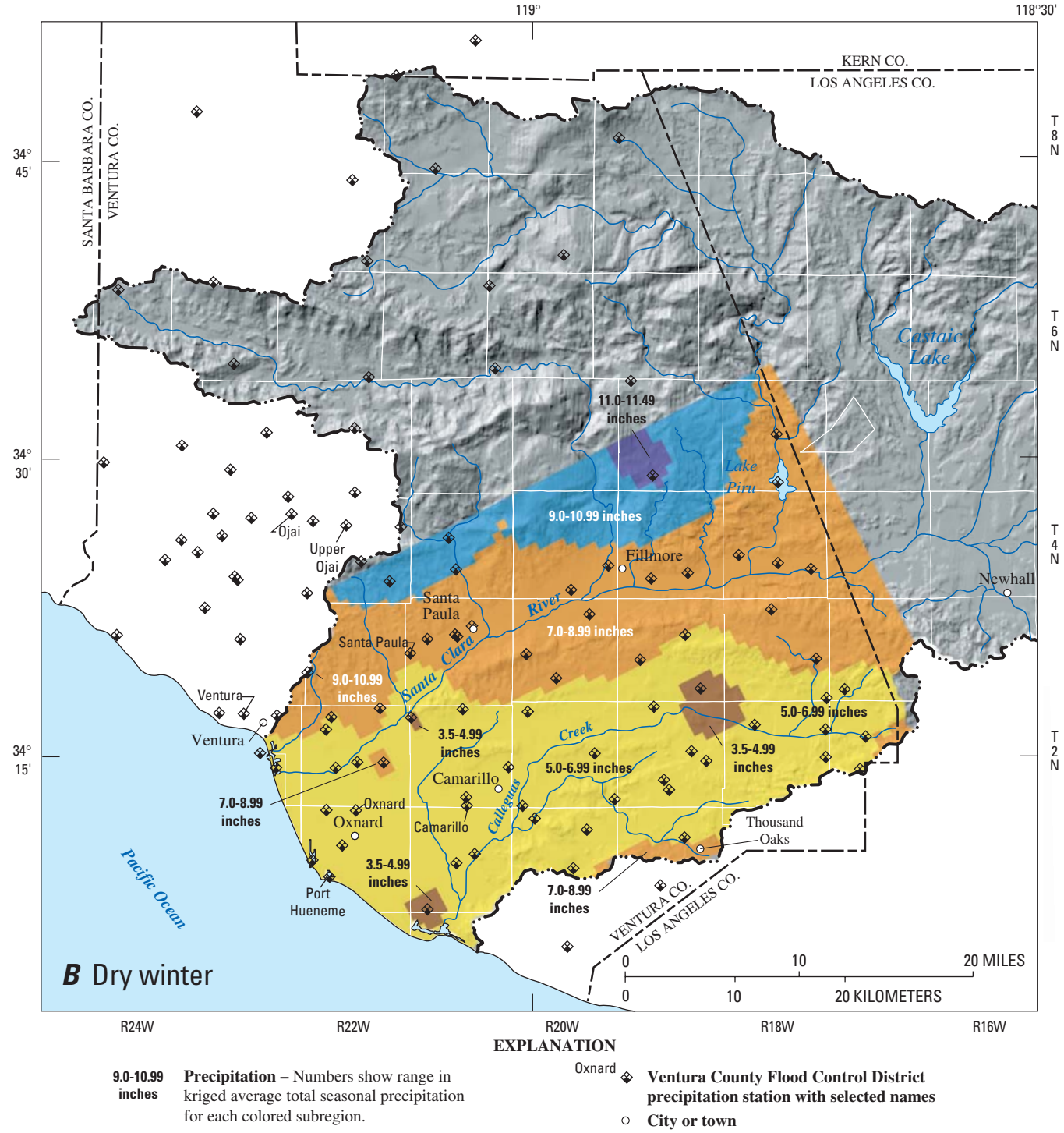

Figure 3—Continued. Kriged average total seasonal precipitation 1891–1991 for wet and dry climatic periods by season. ***B***, Dry winter.

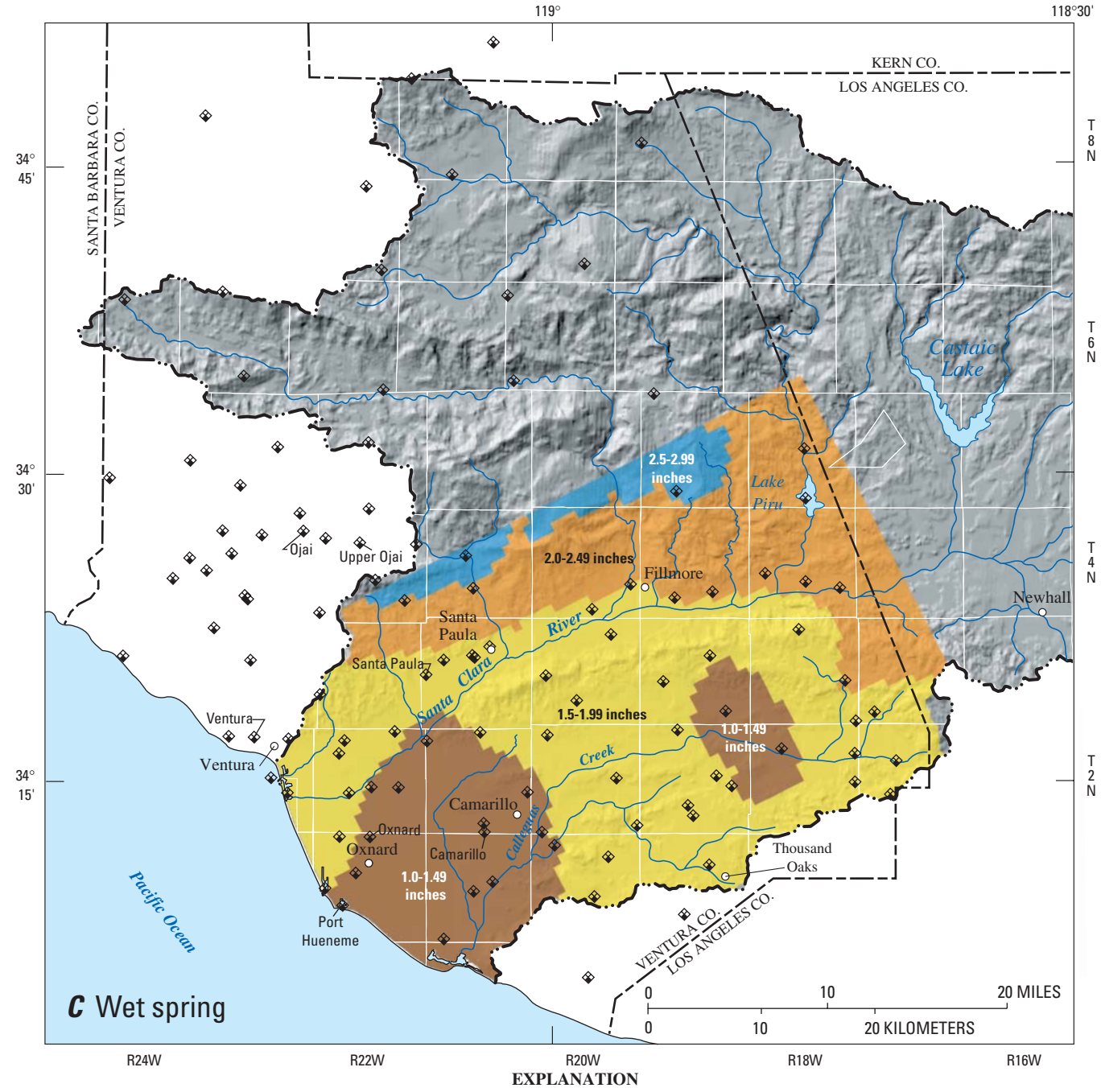

Figure 3—Continued. Kriged average total seasonal precipitation 1891–1991 for wet and dry climatic periods by season. ***C***, Wet spring.

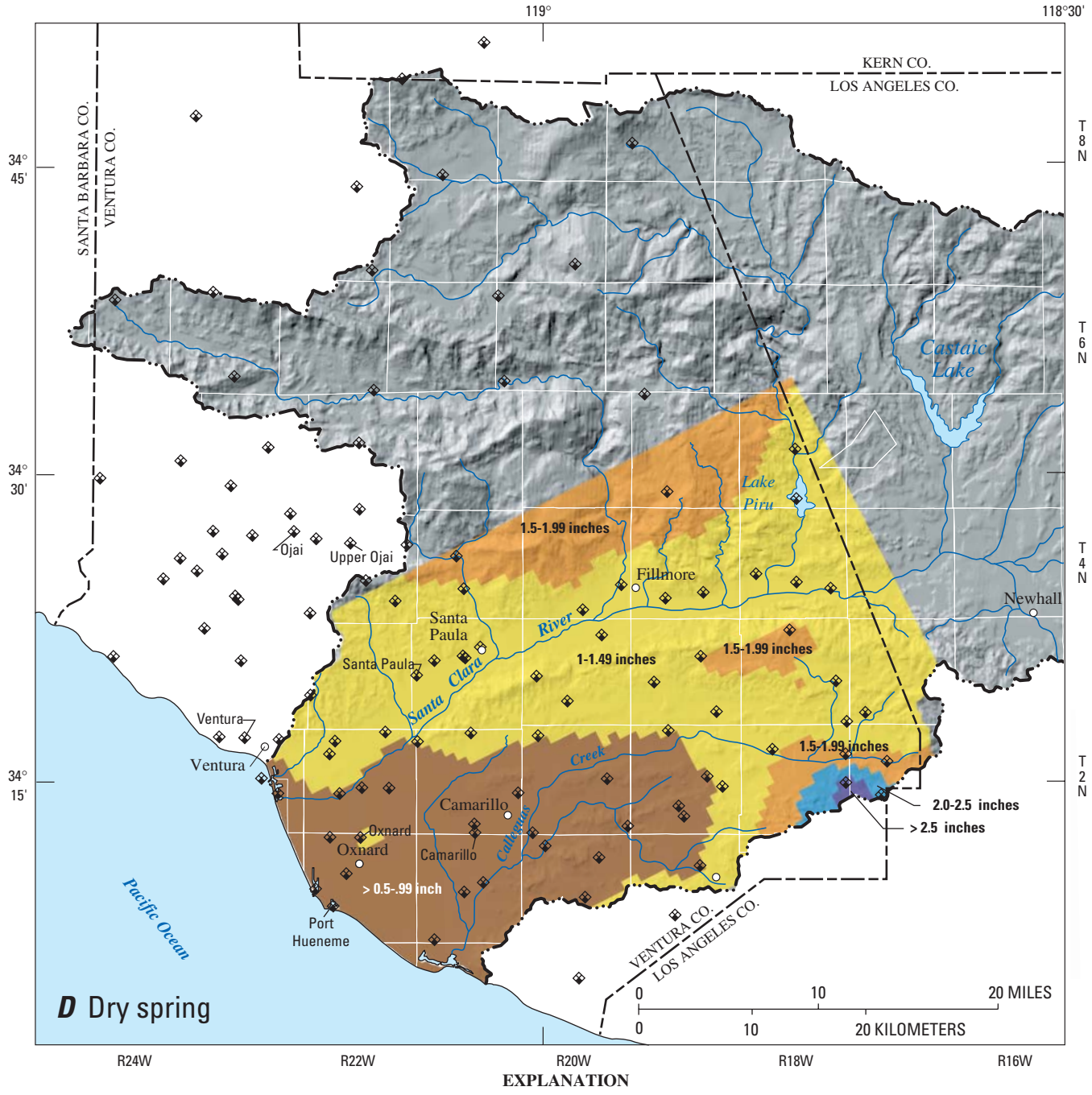

Figure 3—Continued. Kriged average total seasonal precipitation 1891–1991 for wet and dry climatic periods by season. ***D***, Dry spring.

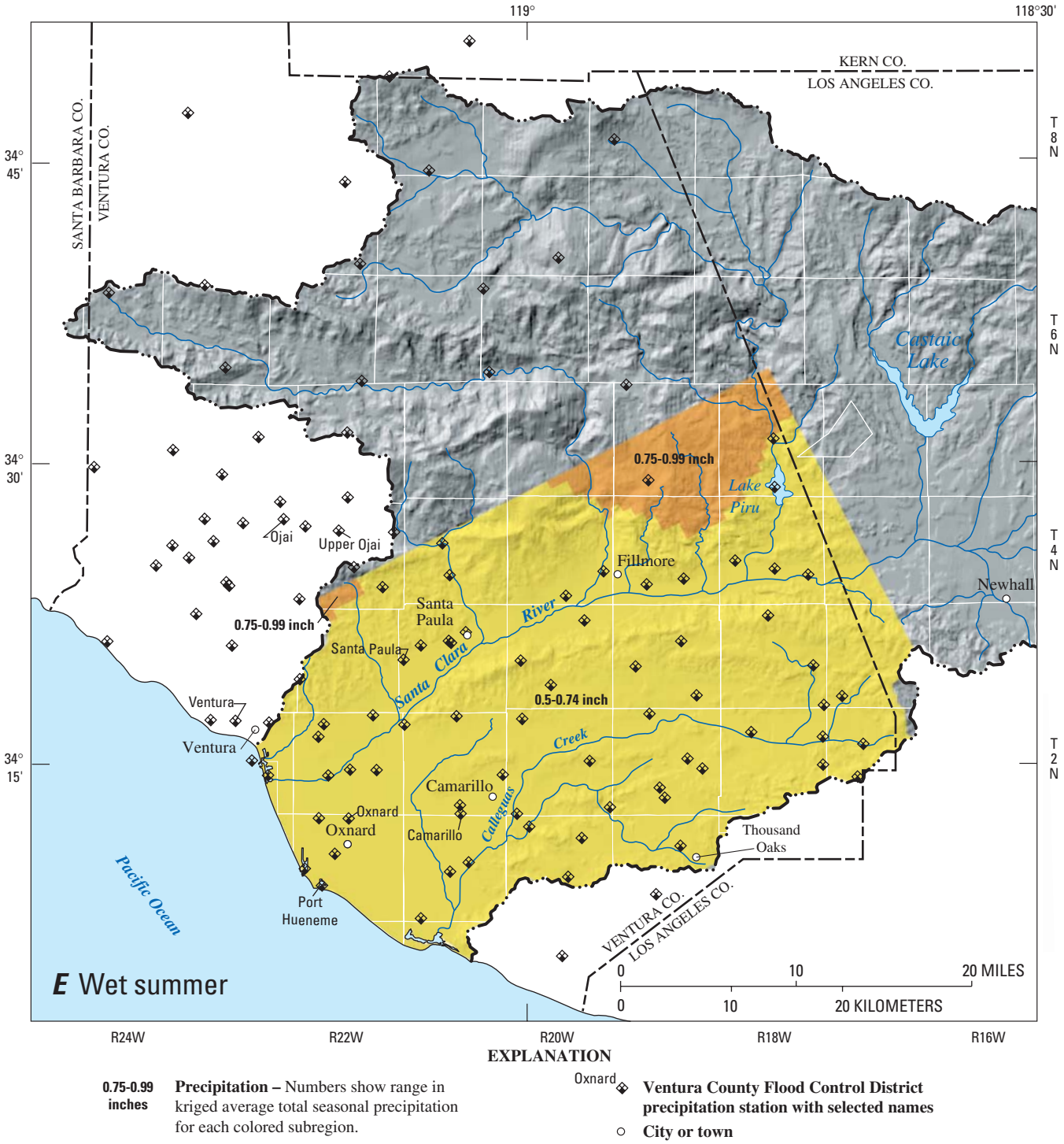

Figure 3—Continued.Kriged average total seasonal precipitation 1891–1991 for wet and dry climatic periods by season. ***E***, Wet summer.

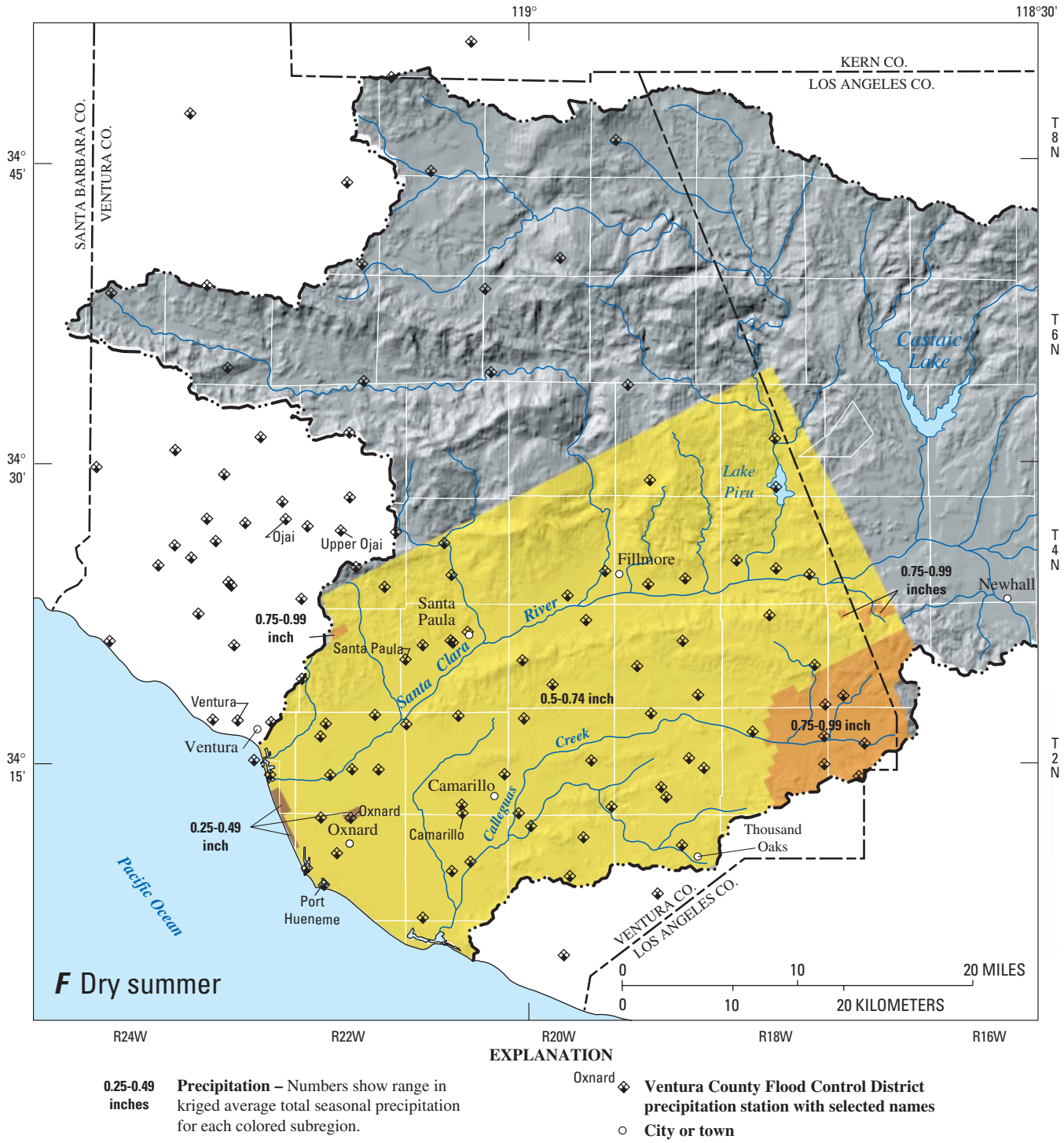

Figure 3—Continued. Kriged average total seasonal precipitation 1891–1991 for wet and dry climatic periods by season. ***F***, Dry summer.

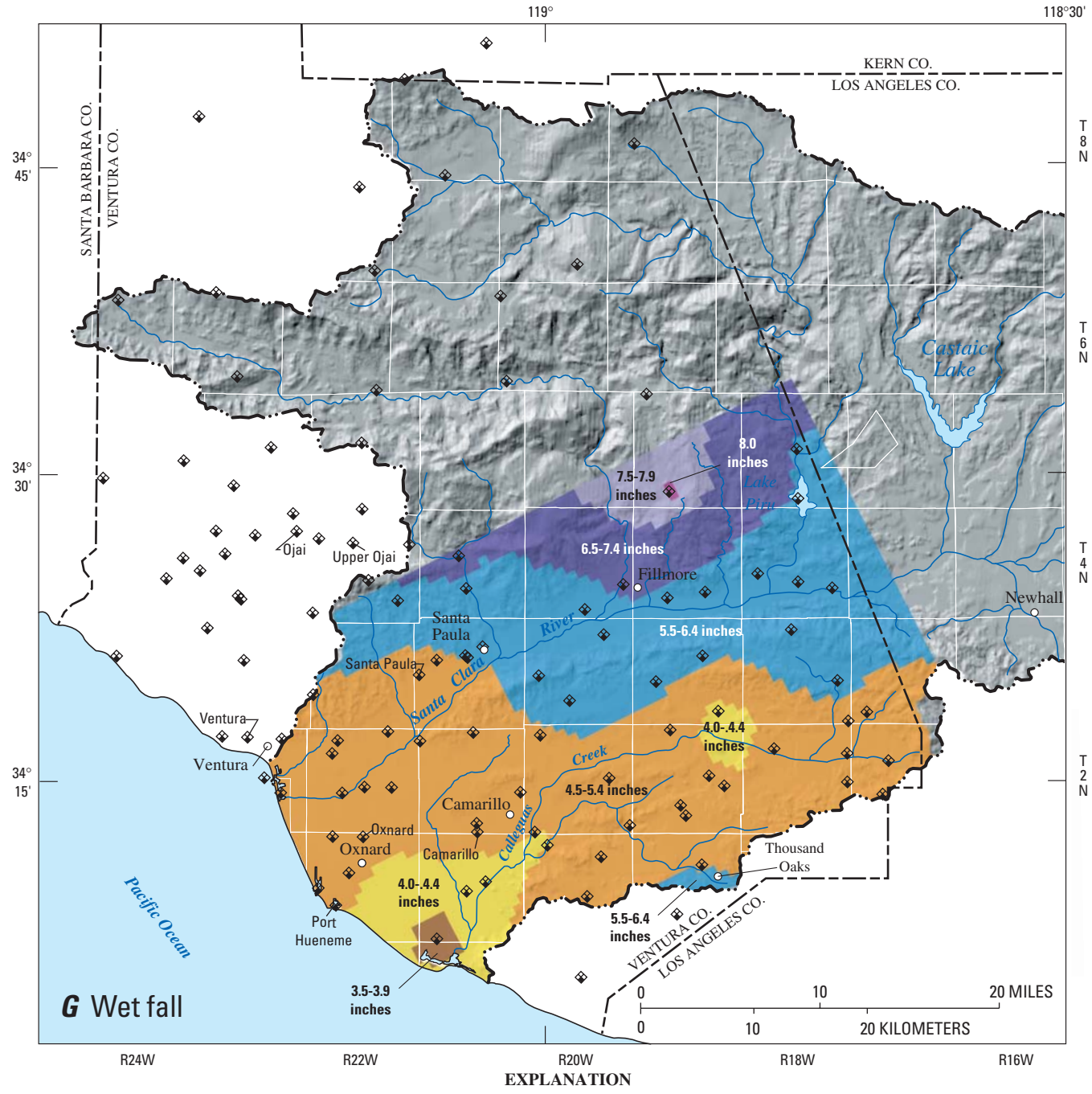

Figure 3—Continued. Kriged average total seasonal precipitation 1891–1991 for wet and dry climatic periods by season. ***G***, Wet fall.

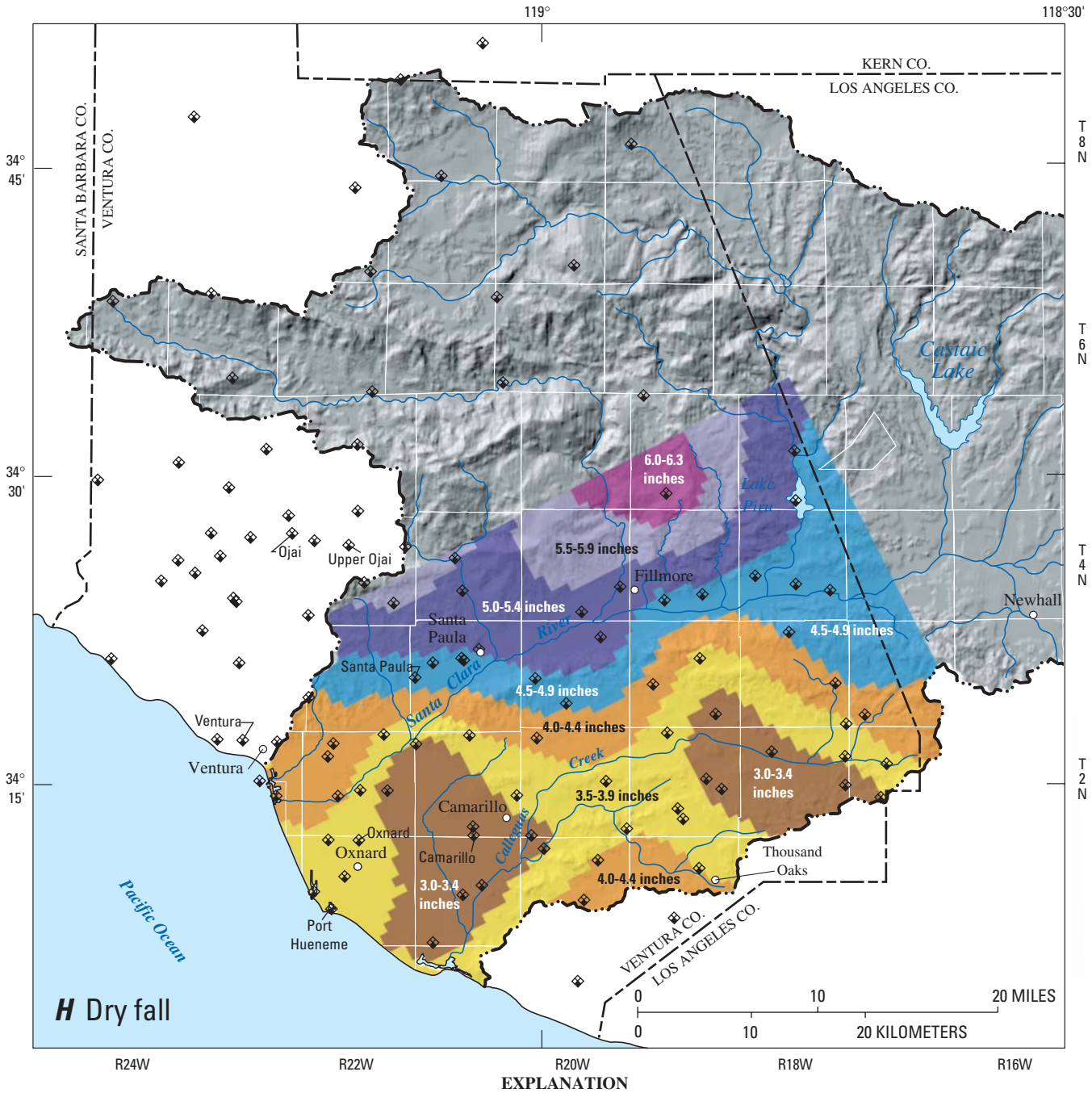

Figure 3—Continued. Kriged average total seasonal precipitation 1891–1991 for wet and dry climatic periods by season. ***H***, Dry fall.

Table 1. Summary of coastal precipitation statistics for the Santa Clara–Calleguas Basin, Ventura County, California

[Data from Ventura County, Department of Public Works (Dolores Taylor, written commun., 1992). Grouping: Dry years represent all years in which precipitation was less than the mean for the period of record; wet years represent all years in which precipitation was more than the mean for the period of record. Dry-year periods are periods of decreasing cumulative departure for precipitation for the period of record and wet-year periods are periods of increasing cumulative departure. W is a value of Shapiro–Wilk Statistic normality test where values close to 1 indicate a significant probability of a normally distributed group of mean total seasonal precipitation.%, percent; —, reference group]

Precipitation period (group number)	Grouping	Mean/standard deviation, in inches (number of samples)	W: Normality test	Significant difference in means at 95-percent level between groups?
Coastal winter (1)	All years	8.37/5.19(101)	0.93	—
Coastal winter (2)	Dry years	5.47/2.48(70)	.97	(1)–(2):Yes (2)–(3): No
Coastal winter (3)	Dry-year periods	6.24/3.28(58)	.93	(1)–(3):Yes
Coastal winter (4)	Wet years	14.93/3.20(31)	.94	(1)–(4):Yes (4)–(5): Yes
Coastal winter (5)	Wet-year periods	11.19/5.85(43)	.96	(1)–(5):Yes
Coastal spring (1)	All years	1.15/1.13(100)	.83	—
Coastal spring (2)	Dry years	.31/.73(70)	.48	(1)–(2):Yes (2)–(3): Yes
Coastal spring (3)	Dry-year periods	1.05/.96(57)	.87	(1)–(3):No
Coastal spring (4)	Wet years	1.03/1.10(30)	.83	(1)–(4):No (4)–(5): No
Coastal spring (5)	Wet-year periods	1.30/1.33(43)	.84	(1)–(5):No
Coastal summer (1)	All years	.30/.66(100)	.53	—
Coastal summer (2)	Dry years	.30/.73(70)	.48	(1)–(2):No (2)–(3): No
Coastal summer (3)	Dry-year periods	.26/.68(57)	.43	(1)–(3):No
Coastal summer (4)	Wet years	.28/.48(30)	.66	(1)–(4):No (4)–(5): No
Coastal summer (5)	Wet-year periods	.36/.65(43)	.64	(1)–(5):No
Coastal fall (1)	All years	4.11/2.74(99)	.94	—
Coastal fall (2)	Dry years	4.01/2.68(69)	.95	(1)–(2):No (2)–(3): No
Coastal fall (3)	Dry-year periods	3.86/2.63(56)	.94	(1)–(3):No
Coastal fall (4)	Wet years	4.33/2.90(30)	.94	(1)–(4):No (4)–(5): No
Coastal fall (5)	Wet-year periods	4.44/2.87(43)	.95	(1)–(5):No

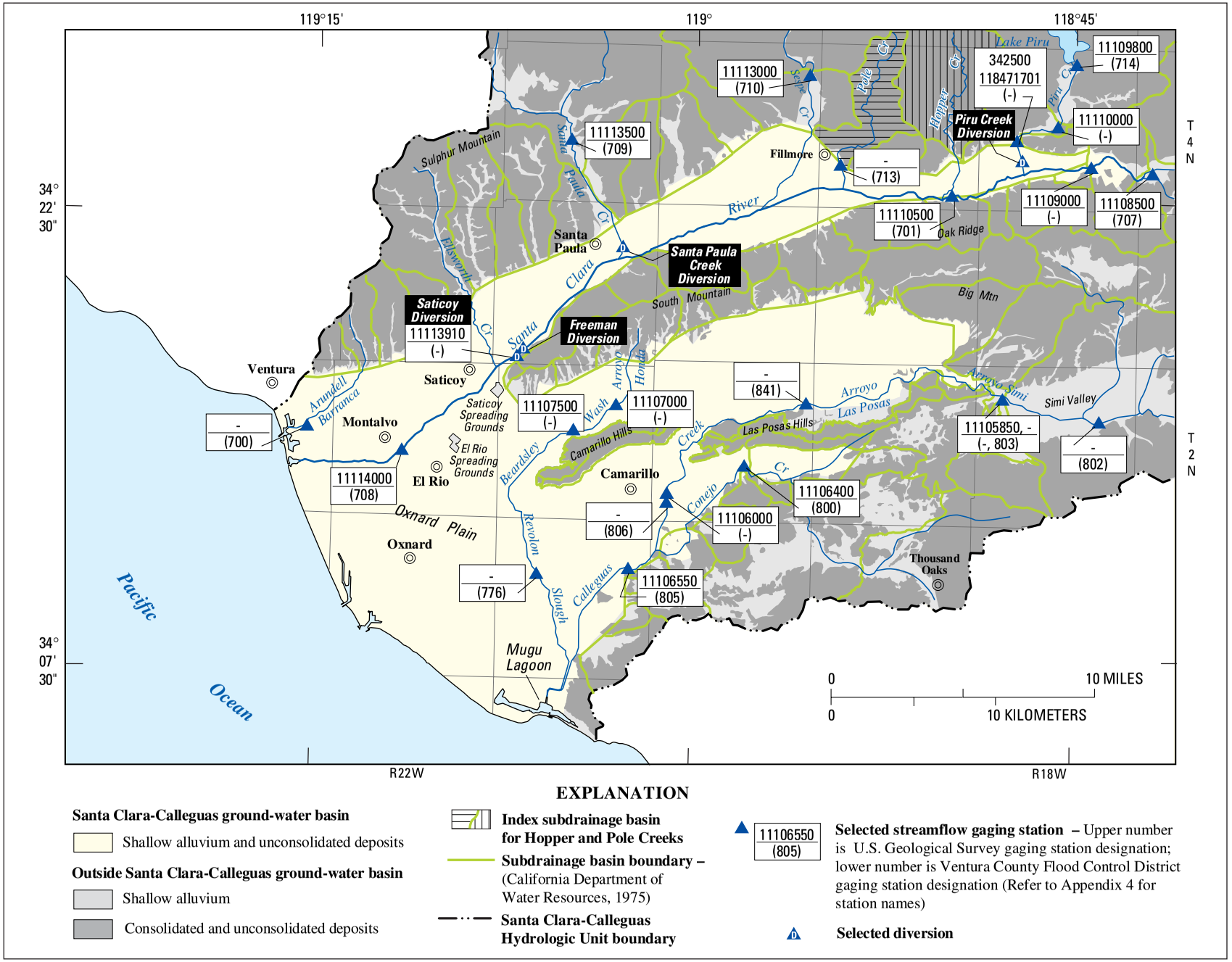

Figure 4. Surface-water drainage features, selected gaging stations, and selected diversions in the Santa Clara–Calleguas ground-water basin, Ventura County, California.

Hydrographs of daily mean streamflow for eight gaging stations in the Santa Clara–Calleguas Basin are presented in figure 5. Natural streamflow in all the major streams and tributaries in the basin is intermittent to ephemeral (fig. 5). Runoff from precipitation primarily during December through April results in natural streamflow in the winter and spring. Most of the streamflow occurs as floodflow. Some of the flows recharge the ground-water system and the remainder discharges into the Pacific Ocean. Sespe Creek is the largest contributor of streamflow to the Santa Clara River system and Piru Creek is the second largest (table 2). Major streams generally have fewer intermittent reaches or become perennial during wet-year periods and have more floodflows and larger baseflows (fig. 5). The Santa Clara River, Piru Creek, Arroyo Simi, and Conejo Creek all have components of regulated flow. The average and median streamflow, and the number of days of flow for the total period of record and for the wet and dry periods defined for this study (fig. 2) are summarized in table 2. These components of regulated flow increased the mean flow and decreased the number of days with no flow (table 2).

Major floods generally occur during wet periods but can occur during dry-year periods (figs. 2 and 5). In 1969, the peak discharge for the largest flood for the period of record was more than 110,000 ft^3/s at the Montalvo gage (11114000) on the Santa Clara River (not shown in figure 5). In the Santa Clara River and most of its major tributaries, multiple-year recession periods generally follow wet periods for unregulated streamflow (fig. 5). During these subsequent years, the gaged outflow at Montalvo can be greater than the gaged inflow of the Santa Clara River and its major tributaries.

Streamflow-duration curves of gaged streams show major differences between wet and dry periods (fig. 6). Streamflow on Piru, Pole, Sespe, and Santa Paula Creeks is perennial during wet years (fig. 6 *C*,*D*,*F*,*G*). The magnitude of daily streamflow increases by a factor of three to five from dry to wet years for streamflows of the same frequency at the seven gaging stations in the Santa Clara–Calleguas ground-water basin (fig. 6 *A*–*G*).

Since the construction of the Santa Felicia Dam in 1955, controlled releases of water from Lake Piru have resulted in fewer days of no flow in the Santa Clara River; however, average annual streamflow in the river was reduced by 35 percent during the 21-year period (1956–75) after construction of the dam (Taylor and others, 1977). Since 1969, discharge owing to the release of treated wastewater from Los Angeles County and imported water from Castaic Lake has increased the minimum flow in the Santa Clara River across the Los Angeles–Ventura County line from less than 10 ft^3/s to about 20 ft^3/s (fig. 5*A*). In the Calleguas Creek drainage, regulated flow has resulted in additional baseflow owing to discharge of treated municipal sewage along Arroyo Simi and Conejo Creek since about 1970 (fig. 5*B*) and discharge of shallow ground water from dewatering wells. Since 1962, the release of sewage effluent in Conejo Creek has resulted in an increase in baseflow from 0.5 to 15 ft^3/s (fig. 5). The pumping of shallow ground water for dewatering upstream in Simi Valley has resulted in additional baseflow on the Arroyo Simi at the Madera Road Bridge (fig. 5*G*)—an increase from less than 0.1 ft^3/s to about 4 ft^3/s since 1969. Streamflow has become more intermittent on the Santa Clara River at Montalvo since 1929 owing to diversions at Saticoy and Freeman. Based on historical basinwide estimates of streamflow and runoff, ungaged tributary runoff provides the second (California Department of Water Resources, 1975; tables 23 and 24) or third (California Department of Public Works, 1934; table 59) largest contribution to streamflow. Diversion from Sespe Creek, as well as numerous smaller intermittent diversions from the Santa Clara River for irrigation, is still occurring. Diversions from Piru Creek below Santa Felicia Dam and from the Santa Clara River at the Freeman Diversion provide water for artificial recharge. Controlled releases from Lake Piru Reservoir are conveyed down the natural stream channel to these artificial-recharge spreading grounds, supplementing the intermittent natural streamflow during the generally dry summer and fall months.

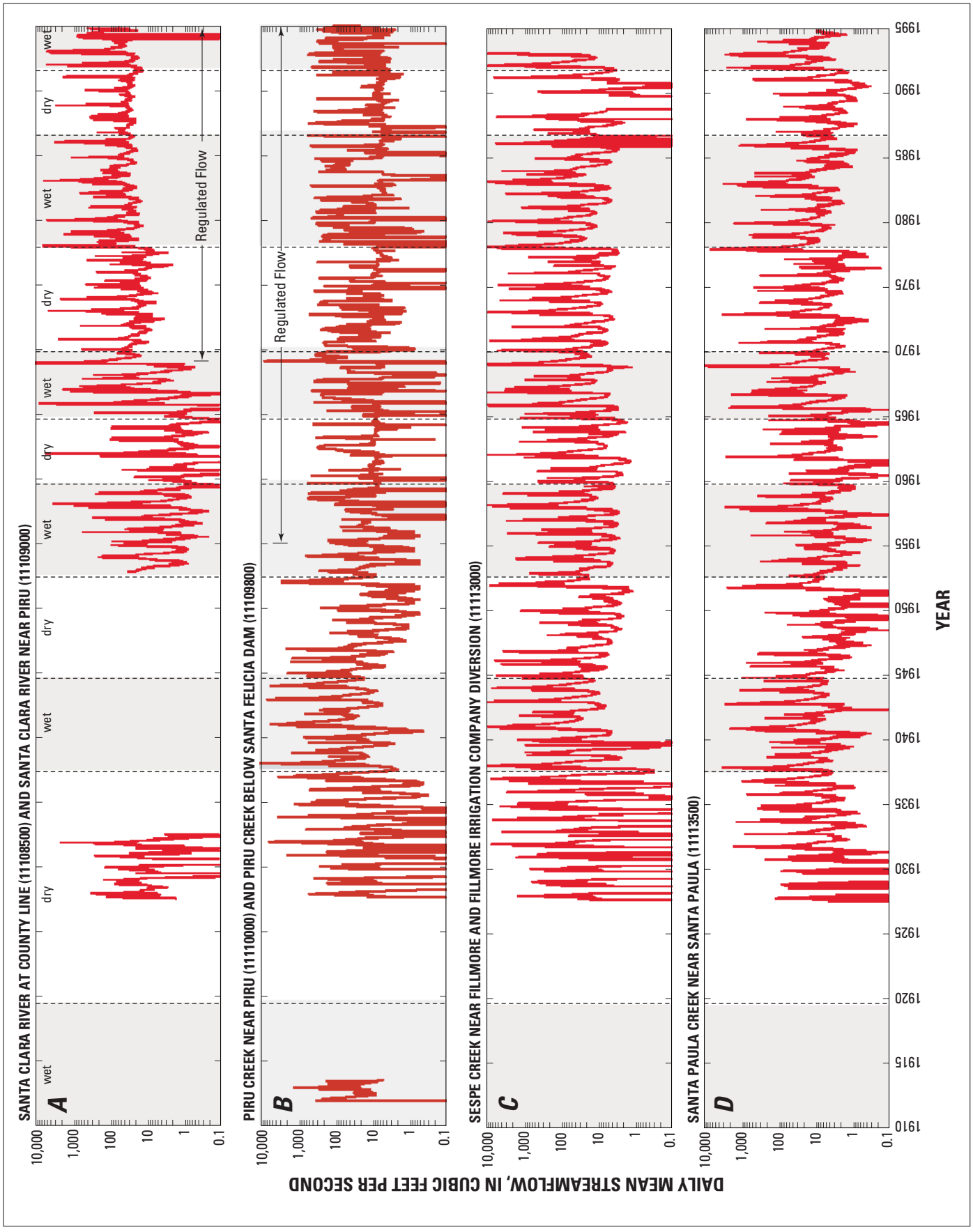

Figure 5. Daily mean streamflow for wet and dry periods at the major rivers and tributaries in the Santa Clara–Calleguas ground-water basin, Ventura County, California.

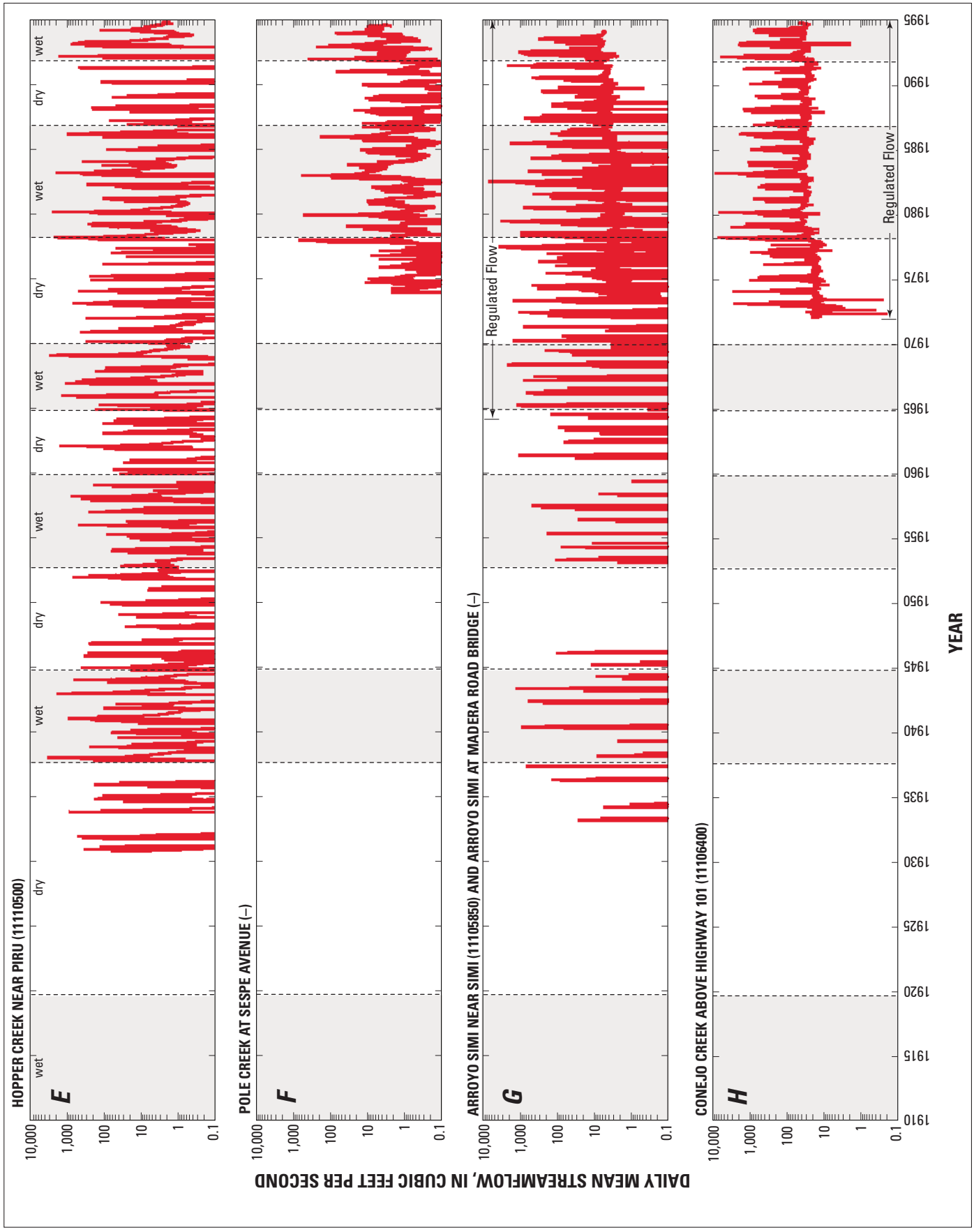

Figure 5—Continued.

Table 2. Summary of gaged streamflow data for selected streams in the Santa Clara–Calleguas Basin, Ventura County, California

[Streamflow gaging station (station number): preceding the slash is the U.S. Geological Survey gaging station number and following the slash is the Ventura County Flood Control District gaging station number. --, no station number provided; —, no estimate provided]

Streamflow gaging station (station No.) [period of record]	Arithmetic average streamflow (cubic feet per second)			Median/geometric mean streamflow (cubic feet per second)			Number of no-flow days			Time averaged streamflow used in predevelopment model (cubic feet per second)
	Total period	Wet periods	Dry periods	Total period	Wet periods	Dry periods	Total period	Wet periods	Dry periods	
Santa Clara River at county line[1] (11108500 / 707) Unregulated flow [1928–32, 1953–71]	32.1	52.5	14.5	2.6/4.3	3.2/4.6	1.9/4.0	801	100	701	2.0
Santa Clara River at county line (11108500 / 707) Regulated and unregulated flow [1953–91][2]	48.3	69.3	26.2	17.0/11.4	20.0/ 13.1	14.0/ 9.7	464	100	364	—
Piru Creek near Piru (11110000 / —) [1912–13, 1927–54]	57.3	100	23.7	12.0/12.8	22.0/23.4	5.1/7.2	1,038	4	1,034	13.0
Piru Creek below Santa Felicia Dam (11109800 / 714) [1956–92]	42.1	54.6	28.7	12.0/12.2	8.7/14.5	7.2/10.3	544	450	94	—
Hopper Creek near Piru (11110500 / 701) [1931–90]	6.2	9.7	2.4	.3/1.1	.7/ 1.6	.01/.6	7,765	2,660	4,032	0.3
Pole Creek at Sespe Avenue, Fillmore (–/ 713) [1974–91]	2.3	3.5	.7	.6/.6	1.0/1.0	.3/.3	25	2	23	0.6
Sespe Creek near Fillmore (11113000 / 710)[3] [1940–91]	125.4	179.8	64.2	17.0/20.7	26.0/30.7	10.0/13.2	0	0	0	18.0
Santa Paula Creek near Santa Paula (11113500 / 709) [1928–91].....	22.5	36.5	10.8	4.5/5.4	7.2/8.7	2.9/3.5	854	0	854	4.5
Santa Clara River at Montalvo (11114000 / 708)[4] [1955–71][5]	222.2	319.8	113.0	25.0/47.9	33.9/71.5	18.2/30.7	1,244	669	575	—
Santa Clara River at Montalvo (11114000 / 708)[4] [1955–92][6]	257.4	385.4	114.2	46.1/59.7	96.0/106.8	24.5/32.2	1,392	671	721	—
Arroyo Simi near Simi (11105850/—)[7] and Arroyo Simi at Royal Avenue (–1/802) [1934–64].....	1.3	2.1	.5	0/.6	0/.8	0/.3	10,282	4,801	5,481	0
Arroyo Simi near Simi (11105850/--)[7] and Arroyo Simi at Royal Avenue (–/802) [1934–69]	2.3	3.7	.5	0/.9	0/1.5	0/.3	11,942	6,461	5,481	0

[1]Streamflow data combined with streamflow data from Santa Clara River near Piru (11109000) for period 1927–32. Numbers represent the period without wastewater flowing into the basin along the Santa Clara River from Los Angeles County for climate periods.

[2]Values are for the periods with and without wastewater flowing into the basin along the Santa Clara River from Los Angeles County.

[3]Streamflow data was combined with streamflow data from Fillmore Irrigation Canal diversion (11113001/—) for period 1940–91.

[4]Streamflow data was combined with streamflow data from Santa Clara River Diversion at Saticoy (11113910/—) for period 1928–92. Values also represent the period with releases from Lake Piru.

[5]Values represent the period without wastewater flowing into the basin along the Santa Clara River from Los Angeles County.

[6]Values represent the period with and without wastewater flowing into the basin along the Santa Clara River from Los Angeles County, respectively. Values also represent the period with releases from Lake Piru.

[7]Values represent the period without dewatering pumpage flowing into the basin along Arroyo Simi.

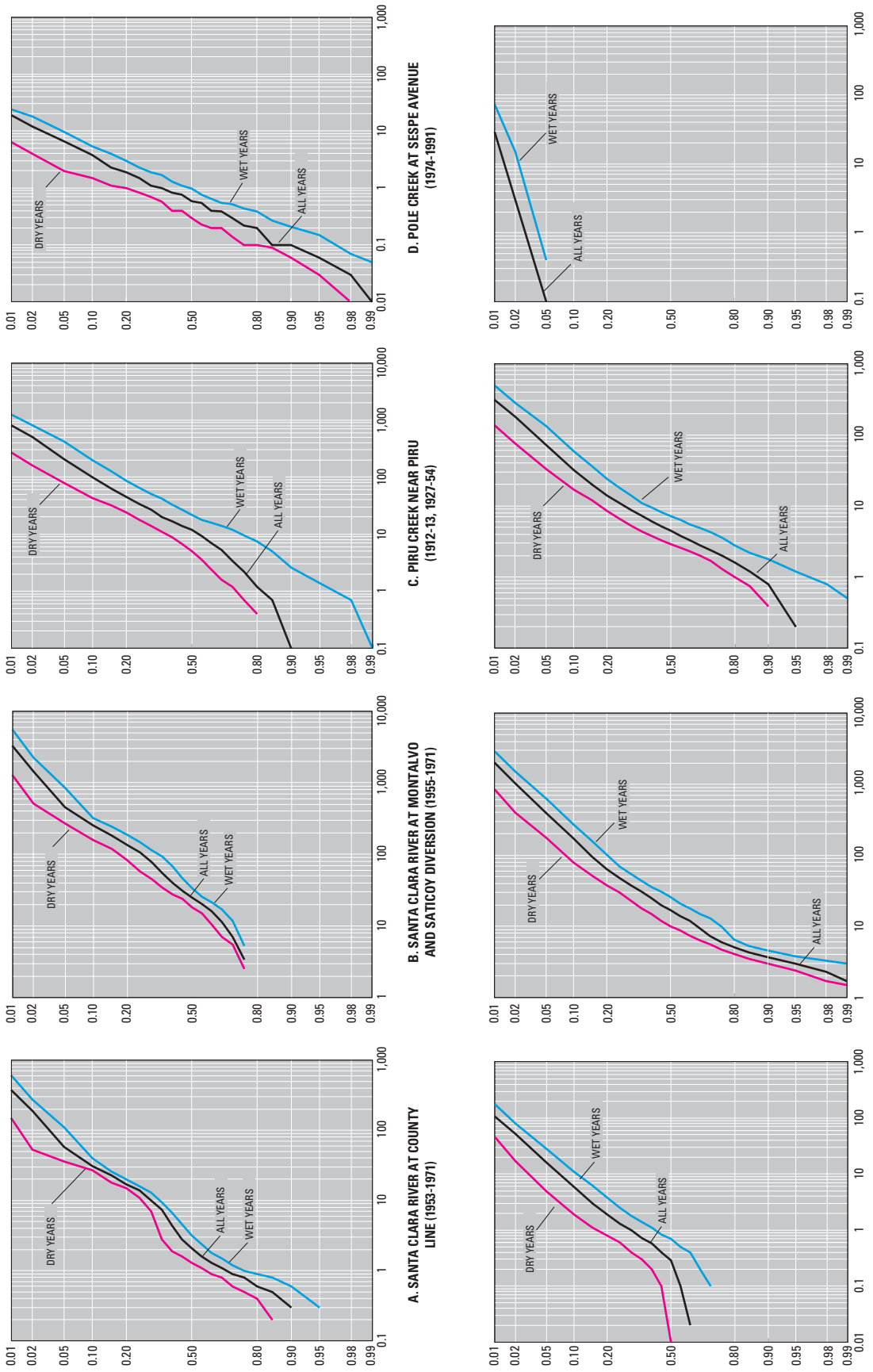

Figure 6. Streamflow duration during wet and dry periods at the major rivers and tributaries in the Santa Clara–Calleguas ground-water basin, Ventura County, California. (See table 2 for gaging station numbers and figure for gaging station locations.)

Irrigation Diversions

Diversion of natural streamflow (fig. 4) was the first water-resources development for agricultural use in the Santa Clara–Calleguas ground-water basin. Major diversions from the Santa Clara River and its tributaries were constructed in the middle to late 1800s. The continued growth of agriculture resulted in irrigation and return-flow diversions in the early 1900s that captured most of nonflood flows from the Santa Clara River. The diversions on the tributaries generally were small, permanent structures on bedrock designed to capture the low perennial baseflows (less than 1 to 10 ft^3/s) during summer and fall. Mainstem diversions, however, commonly were temporary structures that were rebuilt within the shifting channel after the recession of floodflows. Other historically larger diversion canals (not shown on figure 4), such as Farmers Ditch, Santa Clara Water and Irrigation Company Canal, Camulos Ranch Ditch on the Santa Clara River, and Fillmore Land and Water Company Canal on Sespe Creek, conveyed diversions of 10 to 40 ft^3/s [shown in Adams (1913, pl. XVI), and Predmore and others (1997)]. Most of these diversions operated within the subbasins and supplied irrigation water to crops on the adjacent flood plain. The larger mainstem diversions typically were located where there was sustained flow, which generally occurs below the confluence with major tributaries where natural sediment deposited by inflow causes riffles and ponding of streamflow. Some of the mainstem diversions along the Santa Clara River were built near the upstream side of the constrictions at the subbasin boundaries where there is a mixture of streamflow and ground-water discharge. The diversions of surface water supplied a significant amount of the water used for irrigation prior to the early 1930s when irrigation demand exceeded the surface-water supplies largely owing to the 1923–36 drought.

Imported water

Since 1971, surface water has been imported from northern California and routed through a series of reservoirs constructed by the UWCD for controlled release during the growing season. Water from northern California is imported by the UWCD to Pyramid Lake and Lake Piru where it periodically is released into Piru Creek and the Santa Clara River channels. Water has been imported to Castaic Lake since the 1970s where it is released into the Santa Clara River channel. This imported water, along with treated sewage effluent from Los Angeles County, increases the perennial baseflow at the streamflow-gaging station on the Santa Clara River at the Los Angeles–Ventura County Line (fig. 5*A*). Most of the water brought into the basin since 1964 was imported by the CMWD using Metropolitan Water District (MWD) pipelines—about 1,863,000 acre-ft of water from 1964 through 1993. The water was used primarily for municipal supplies (91 percent), and a small part (9 percent) was used for irrigation. Some of this water may have entered the ground-water flow system as sewage-effluent discharge or as percolation of excess applied irrigation water (hereinafter referred to as irrigation return flow) in the Las Posas Valley and Pleasant Valley subbasins. Even though most of the water imported by the CMWD that is used for municipal supply becomes treated sewage effluent that is discharged to the Pacific Ocean, this imported water has helped reduce growth in ground-water pumping in the Oxnard Plain, Pleasant Valley, and Las Posas Valley subbasins.

Sewage Effluent

Sewage effluent is discharged directly to the Pacific Ocean, the Santa Clara River, Calleguas Creek, and Conejo Creek and to percolation ponds for direct infiltration or it was reused for irrigation. Most of the sewage effluent is either directly discharged to the Pacific Ocean or is discharged to stream channels in the Oxnard Plain, where low-permeability channels do not allow significant infiltration to the regional ground-water flow system. Treated sewage effluent is included in the streamflow that enters the basin at the county line along the Santa Clara River, Calleguas River, and Conejo Creek. These contributions to streamflow are part of the gaged streamflow on these rivers.

GROUND WATER

The Santa Clara–Calleguas drainage basin is part of the tectonically active Transverse Ranges physiographic province. The mountains are composed of a variety of consolidated marine and terrestrial sedimentary and volcanic rocks of Late Cretaceous through Quaternary age. The subbasins of the Santa Clara–Calleguas Basin are filled with a mixture of consolidated and unconsolidated marine and terrestrial coastal deposits of Tertiary and Quaternary age. These basin-fill sediments and consolidated rocks form a complex set of aquifer systems that have been the primary source of water supplies since the early 1900s. Agriculture has been the main user of ground water, and in recent years public supply and industry have become significant users of ground water. The geohydrology of the basin is discussed in detail in reports by California Department of Public Works (1934), California Department of Water Resources (1954, 1958, 1974a,b, and 1975), California State Water Resources Board (1956), Mann and Associates (1959), and Turner (1975). The reader is referred to these reports for a more complete description of the geohydrology of the Santa Clara–Calleguas Basin.

Geologic Framework

For this report, the lithologic units mapped by Webber and others (1976), Dibblee (1988, 1990a,b, 1991, 1992a,b,c,d), and Dibblee and Ehrenspeck (1990) in the Santa Clara–Calleguas Basin and surrounding area were grouped into two general categories: (1) upper Cretaceous and Tertiary bedrock, and (2) Quaternary unconsolidated deposits. The outcrop pattern of these combined units is shown in figure 7*A* and their stratigraphic relations are shown in figure 7*B*.

Consolidated Rocks

The upper Cretaceous and Tertiary consolidated rocks include sedimentary, volcanic, igneous, and metamorphic rocks. These rocks are virtually non-water bearing and form the base of the Santa Clara–Calleguas Basin. Although these rocks are not an important source of ground water, the erosion and subsequent deposition of these rocks are the source of the unconsolidated deposits that form the Santa Clara–Calleguas ground-water basin. The sedimentary rocks of Cretaceous age are exposed in the Topatopa Mountains north of the ground-water basin and in the Simi Hills and Santa Susana Mountains south of the basin (California State Water Resources Board, 1956, pl. 10). These rocks are generally non-water bearing except within the poorly cemented and fractured sandstones in the hills near Simi Valley (Turner, 1975, p. 3).

The consolidated Tertiary sedimentary rocks underlie most of the ground-water basin and compose the surrounding mountains and hills. These rocks are predominantly marine in origin and are nearly impermeable except for the slightly permeable sandstones and within fracture zones. Some of these Miocene formations contain oil and tar sand beds, natural gas, and related methane and brines. The Pico Sandstone of Pliocene and Pleistocene epochs underlies the unconsolidated deposits throughout most of the ground-water basin and crops out in the mountains on the north side of the Santa Clara River Valley (California State Water Resources Board, 1956, pl. 10). These rocks are also considered to be of low permeability and non-water bearing.

Volcanic rocks and related intrusive rocks of Miocene age underlie parts of the southern Oxnard Plain, South Pleasant Valley, and Santa Rosa Valley subbasins (figs. 7 and 8*D*,*E*). Although these rocks are considered non-water bearing, they have been developed for water supply where alluvial deposits are absent, such as in the Santa Rosa Valley subbasin. These volcanic and intrusive rocks also crop out in the Santa Monica Mountains along the southern and southeastern boundaries of the ground-water basin (California State Water Resources Board, 1956, pl. 10) and in the offshore submarine canyons along the southwestern boundary of the basin (Kennedy and others, 1987, pl. 2A).

Unconsolidated Deposits

The Quaternary unconsolidated deposits consist of the Santa Barbara Formation (Weber and others, 1976), the Las Posas Sand (Dibblee, 1988, 1990a,b, 1991, 1992a,b,c,d; Dibblee and Ehrenspeck, 1990), the San Pedro Formation (Weber and others, 1976), and the Saugus Formation (Weber and others, 1976; Dibblee, 1988, 1990a,b, 1991, 1992 a,b,c,d), all of the Pleistocene epoch, and unconsolidated alluvial and fluvial deposits of the Pleistocene to Holocene epoch. In the Santa Clara–Calleguas Basin, the unconsolidated deposits are grouped together into the upper-aquifer system and the lower-aquifer system (fig. 7*B*).

The Santa Barbara Formation, mapped by Weber and others (1976), overlies consolidated Tertiary rocks in most of the ground-water basin and consists of marine sandstone, siltstone, mudstone, and shale. The thickness and lithology of the formation varies considerably throughout the basin, but the formation is thickest, more than 5,000 ft, in the Ventura area (Yerkes and others, 1987). The formation is of low permeability and generally contains water of poor quality throughout most of the basin (Turner, 1975) and, therefore, is not considered an important source of ground water. In the East Las Posas Valley subbasin, the Santa Barbara Formation contains layers of sands and gravels that are an important source of water to wells in areas where younger unconsolidated deposits are absent or are unsaturated. The coarse-grained section of the Santa Barbara Formation in the East Las Posas Valley subbasin is commonly referred to as the "Grimes Canyon" member (California Department of Water Resources, 1956).

The Santa Barbara Formation and the lower part of the San Pedro Formation mapped by Weber and others (1976) consist of shallow marine sand and gravel beds that were indicated as a separate formation, the Las Posas Sand, by Dibblee (1988, 1990a,b, 1991, 1992a,b,c,d) and Dibblee and Ehrenspeck (1990). These deposits reach a maximum thickness of more than 2,000 ft in the Santa Clara River Valley near Ventura (Dibblee, 1992a,b,c,d) and consist of a series of relatively uniform fine-grained sand layers 100 to 300 ft thick separated by silt and clay layers 10 to 20 ft thick. The upper part of San Pedro Formation consists of lenticular layers of sand, gravel, silt, and clay of marine and continental origin. The continental fluvial silt, sand, and gravel deposits within the upper part of the San Pedro Formation are referred to as the Saugus Formation by Dibblee (1988, 1990a,b, 1991, 1992a,b,c,d) and Dibblee and Ehrenspeck (1990). These deposits reach a maximum thickness of more than 5,000 ft in the Piru subbasin in the Santa Clara River Valley (Dibblee, 1991). The sand and gravel layers range from 10 to 100 ft thick and are separated by silt and clay layers that generally are 10 to 20 ft thick. The Santa Barbara and San Pedro Formations are absent in the Santa Rosa Valley subbasin east of the San Pedro Fault and in the South Pleasant Valley subbasin southeast of the Bailey Fault. In the eastern part of the Santa Rosa Valley subbasin and in the eastern part of the South Pleasant Valley subbasin, recent alluvial and terrace deposits were deposited unconformably on the marine shale and sandstone beds of the Santa Margarita Formation (Late Miocene) or rest unconformably on the Conejo Volcanics (Middle Miocene). For this study, the Santa Margarita Formation in the Santa Rosa Valley subbasin is grouped with the unconsolidated sediments of the lower system. During the Pleistocene epoch, major changes in sea level resulted in cycles of erosion and deposition (Dahlen, 1992). The sequence of deposits above the erosional unconformities typically starts with a basal conglomerate that is laterally extensive, relatively more permeable than the underlying deposits, and a potential major source of water to wells perforated in these deposits. These coarse-grained layers of fluvial and beach deposits are interbedded with extensive fine-grained layers.

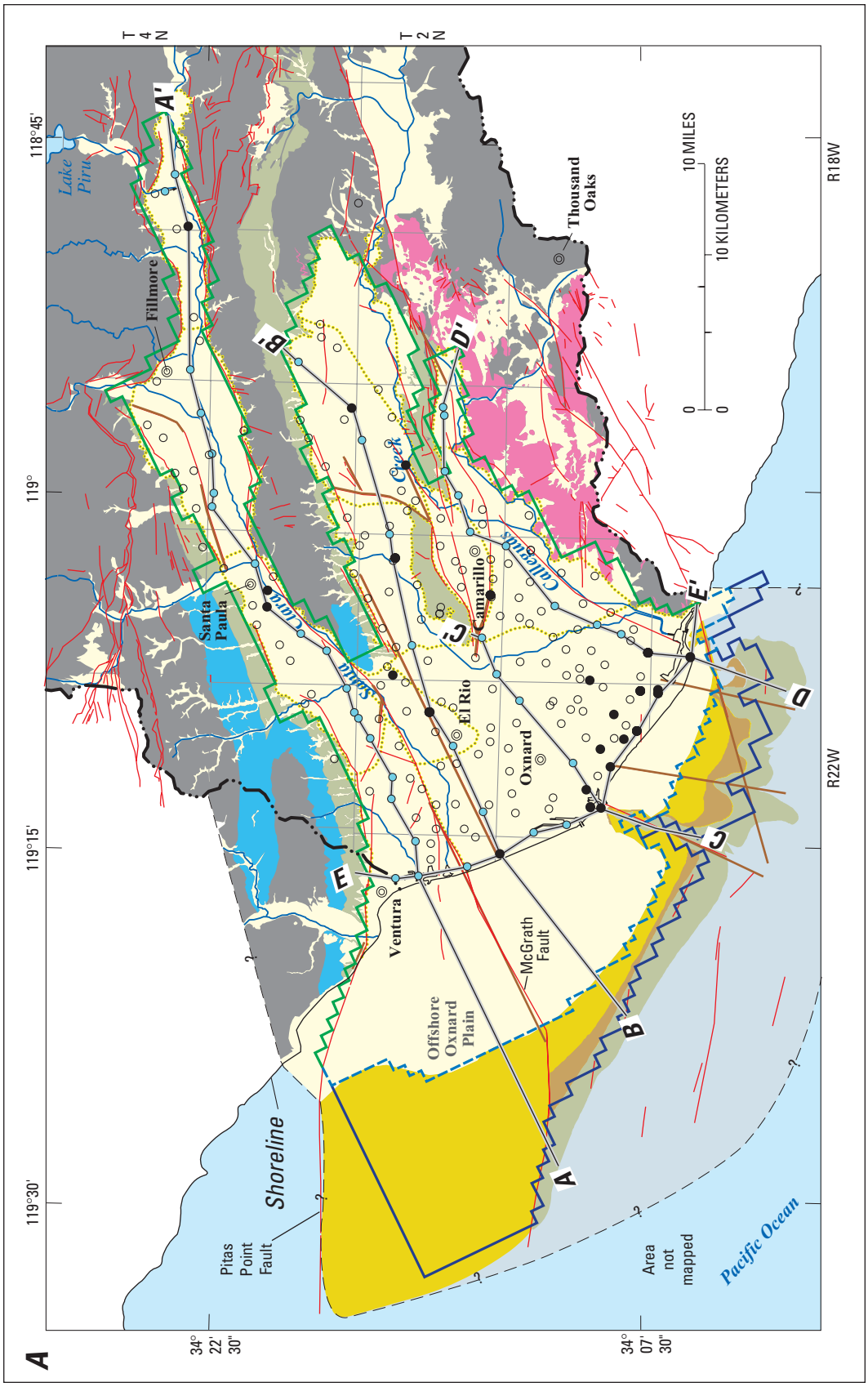

Figure 7. ***A,*** Generalized surficial geology of the Santa Clara–Calleguas ground-water basin and extents of layers in the numerical ground-water flow model, and ***B***, stratigraphic column and related aquifer designations of geologic units by source and aquifer-system model layers, Ventura County, California. (Modified from Weber and others, 1976).

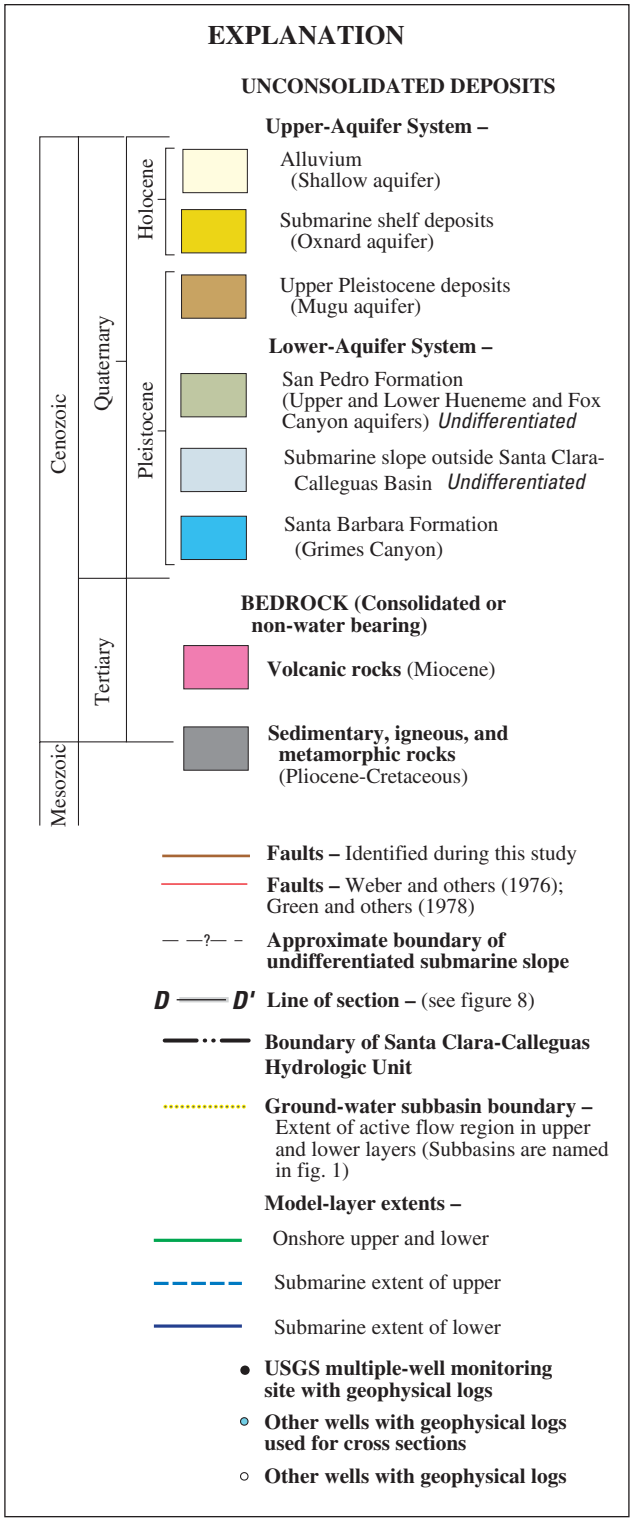

Figure 7—Continued.

The Late Pleistocene and Holocene deposits are unnamed, consist of relatively flat-lying marine and continental unconsolidated deposits, and are regionally grouped into the upper system of water-bearing deposits (fig. 7*B*). These deposits, which were derived from local sources and from the Santa Clara River and Calleguas Creek, were deposited unconformably on the older unconsolidated deposits and contain basal conglomerates that are laterally extensive and produce substantial ground-water supplies. In the Mound and Oxnard Plain subbasins, the basal zones are overlain with fine-grained deposits of low permeability. Alluvial and fluvial sand and gravel deposits with interbedded fine-grained deposits of the Holocene epoch unconformably overlie the Late Pleistocene deposits. The basal deposits of the Holocene epoch consist of gravel and sand, which are overlain by fine-grained deposits throughout most of the Santa Clara River Valley and Oxnard Plain subbasins. These basal deposits are relatively more permeable than underlying deposits, and are potential major sources of water to wells completed in the saturated parts of these deposits. Interbedded sand layers occur within the fine-grained deposits throughout most of the Oxnard Plain. With the exception of recent coarse-grained channel deposits along the Santa Clara River and Calleguas Creek, the thin layer of Holocene deposits that are not coincident with minor tributaries are relatively fine grained and relatively low in permeability.

Figure 7B. Stratigraphic column and related aquifer designations of geologic units by source and aquifer system model layers in the ground-water and surface-water flow model of the Santa Clara–Calleguas Basin, Ventura County, California—Continued

Geologic era	Geologic system	Geologic series (epoch)	Weber and others (1976)	Dibblee[1]	Turner (1975) Green and others (1978)[2]	RASA[3]	Aquifer system model layers
			Lithologic units and Formations		Aquifers		
Cenozoic	Quaternary	Holocene	**Recent Alluvium** (Lagoonal, beach, river and flood plain deposits, artificial fill, and alluvial fan deposits)		Recent alluvial and semiperched	Shallow	Upper-aquifer system[4], layer 1
			Recent Alluvium (Lagoonal, beach, river and flood plain deposits and alluvial fan deposits)		Oxnard[5]		
		Late (Upper) Pleistocene[6]	***Older Alluvium*** (Lagoonal, beach, river and flood plain, alluvial fan, terrace, and marine terrace deposits)		Mugu[2]		
			Saugus Formation[7] (Terrestrial fluvial sediments)	Saugus Formation	Hueneme	Upper Hueneme	Lower-aquifer system, layer 2
			San Pedro Formation[8] (Marine clays and sands and terrestrial fluvial sediments)			Lower Hueneme	
				Las Posas Sand (Marine shallow regressive sands)	Fox Canyon	Fox Canyon	
		Early (Lower) Pleistocene[6]	***Santa Barbara Formation***[8] (Marine shallow regressive sands)		Grimes Canyon[9,10]	Grimes Canyon	
			Pico Formation[11] (Marine siltstones, sandstones, and conglomerates)		Formation not included in regional flow model		Formation not included in regional flow model
	Tertiary	Pliocene[6]	***Repetto formation*** (Terrestrial conglomerates, sandstones, and shales)				
		Miocene	***Santa Margarita Formation, Monterey Shale, Rincon Mudstone, Towsley Formation*** (Terrestrial fluvial sandstones and fine-grained lake deposits)		Not Included	Santa Margarita sandstones included in northeastern Santa Rosa Valley	Lower-aquifer system, layer 2
			Conejo Volcanics (Terrestrial and marine extrusive and intrusive, felsic-andesites to basalts)		Formation not included in regional flow model		Formation not included in regional flow model
			Lower Topanga Formation, Topanga-Vaqueros Sandstones, Modelo Formation, Sisquoc Formation (Marine transgressive sands and siltstones)				
		Oligocene	***Sespe Formation*** (Terrestrial fluvial claystones and sandstones)				
		Eocene	***Llajas Formation, Coldwater Sandstone, Cozy Dell Shale, Matilija Sandstone, Juncal Formation, Santa Susana Formation*** (Marine sandstones, mudstones, and claystones)				
		Paleocene	***Martinez Formation*** (Terrestrial conglomerate, sandstones, and marine shales)				
Mesozoic	Upper Cretaceous		Chico Formation (Sandstones with shales)				

Figure 7B. Stratigraphic column and related aquifer designations of geologic units by source and aquifer system model layers in the ground-water and surface-water flow model of the Santa Clara–Calleguas Basin, Ventura County, California—Continued

[1]Formations from Dibblee (1988; 1990a,b; 1991; 1992a,b,c,d) and Dibblee and Ehrenspeck (1990).
[2]Perched aquifer designated in parts of the Oxnard Plain only.
[3]From the current study as part of the Southern California Regional Aquifer-System Analysis Program of the U.S. Geological Survey.
[4]Shallow aquifer included in the Oxnard Plain Forebay and inland subbasins. Semiperched part of Shallow aquifer not included in remainder of Oxnard Plain.
[5]Restricted to the Oxnard Plain and Forebay by Turner (1975).
[6]Modified on the basis of ash-deposit age dates (Yerkes and others, 1987, fig.11.2).
[7]Mapped in eastern Ventura County subbasins of Santa Paula, Fillmore, Piru, and Las Posas Valley and may be time equivalent to parts of the San Pedro and Santa Barbara Formations (Weber and others, 1976, fig. 3).
[8]Mapped in western Ventura County subbasins.
[9]San Pedro Formation everywhere except in Pleasant Valley where the Santa Barbara Formation was assigned to the Grimes Aquifer.
[10]Las Posas and Pleasant Valley subbasins only.
[11]Includes Mud Pit and Claystone Members.

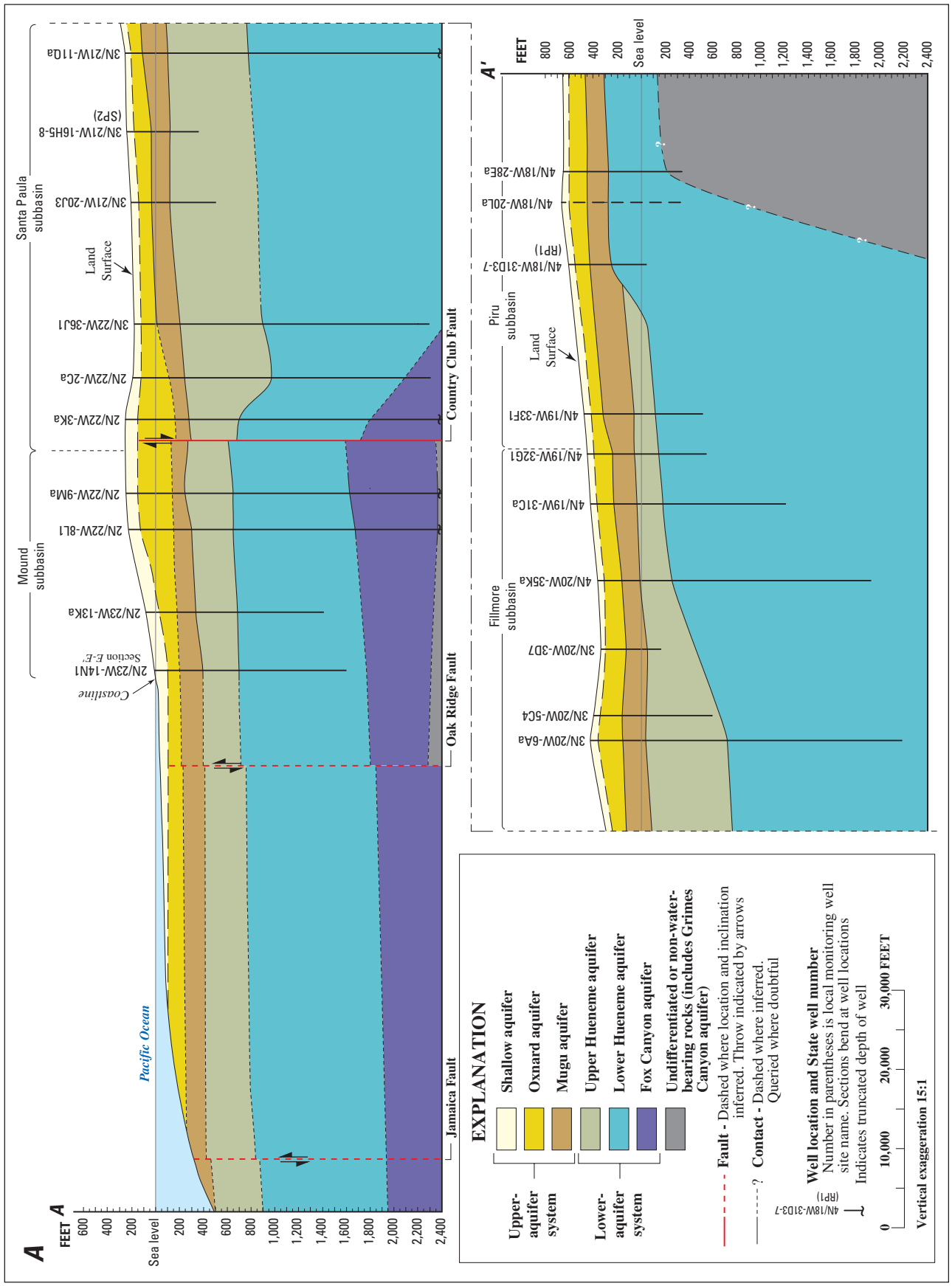

Figure 8. Hydrogeology of the Santa Clara–Calleguas ground-water basin, Ventura County, California. ***A***, Section *A–A'* Santa Clara River. ***B***, Section *B–B'*, Los Posas. ***C***, Section *C–C'*, Hueneme. ***D***, Section *D–D'*, Pleasant Valley. ***E***, Section *E–E'*, Coastal. (See figure 7A for location of sections.)

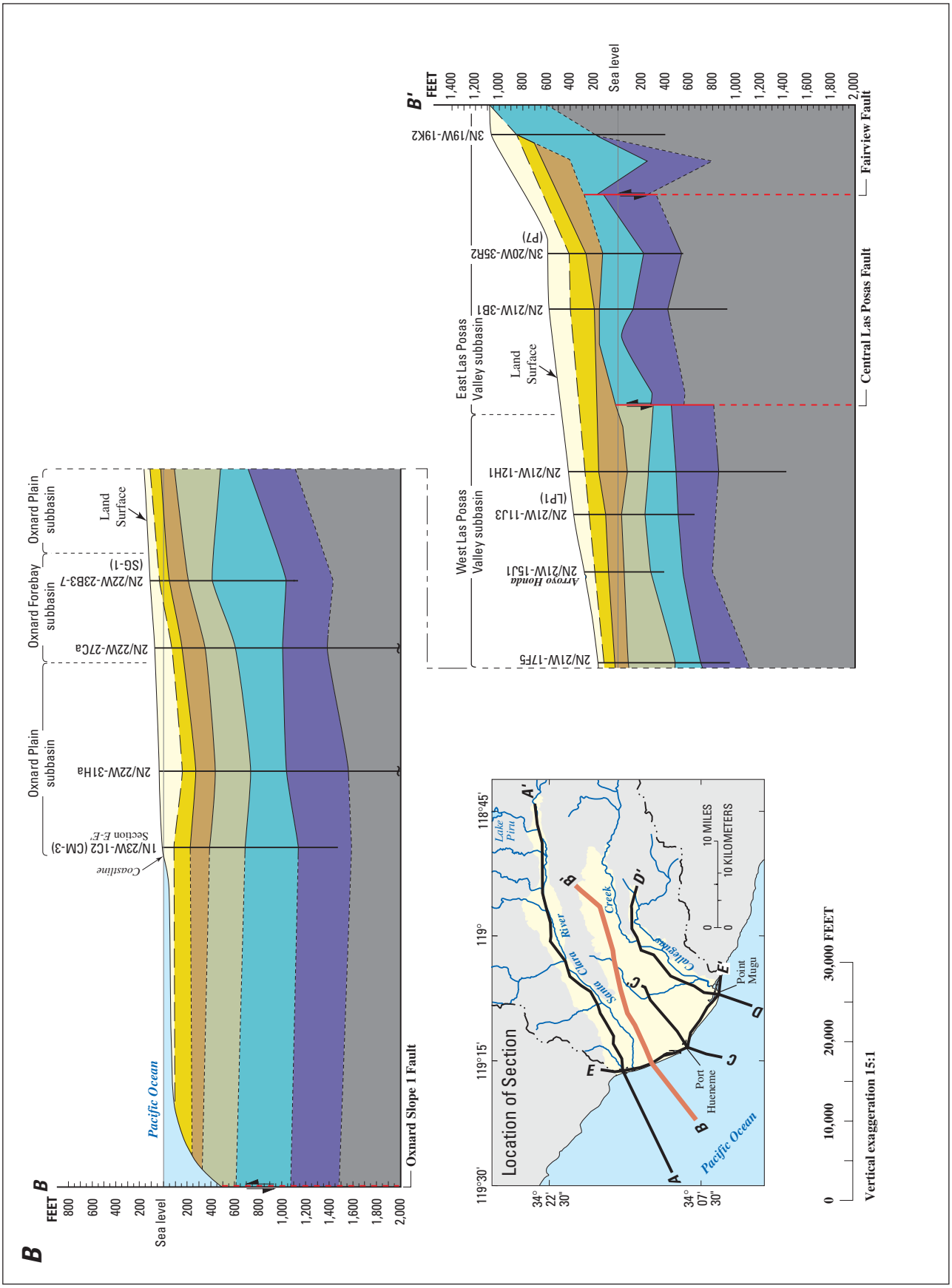

Figure 8—Continued.

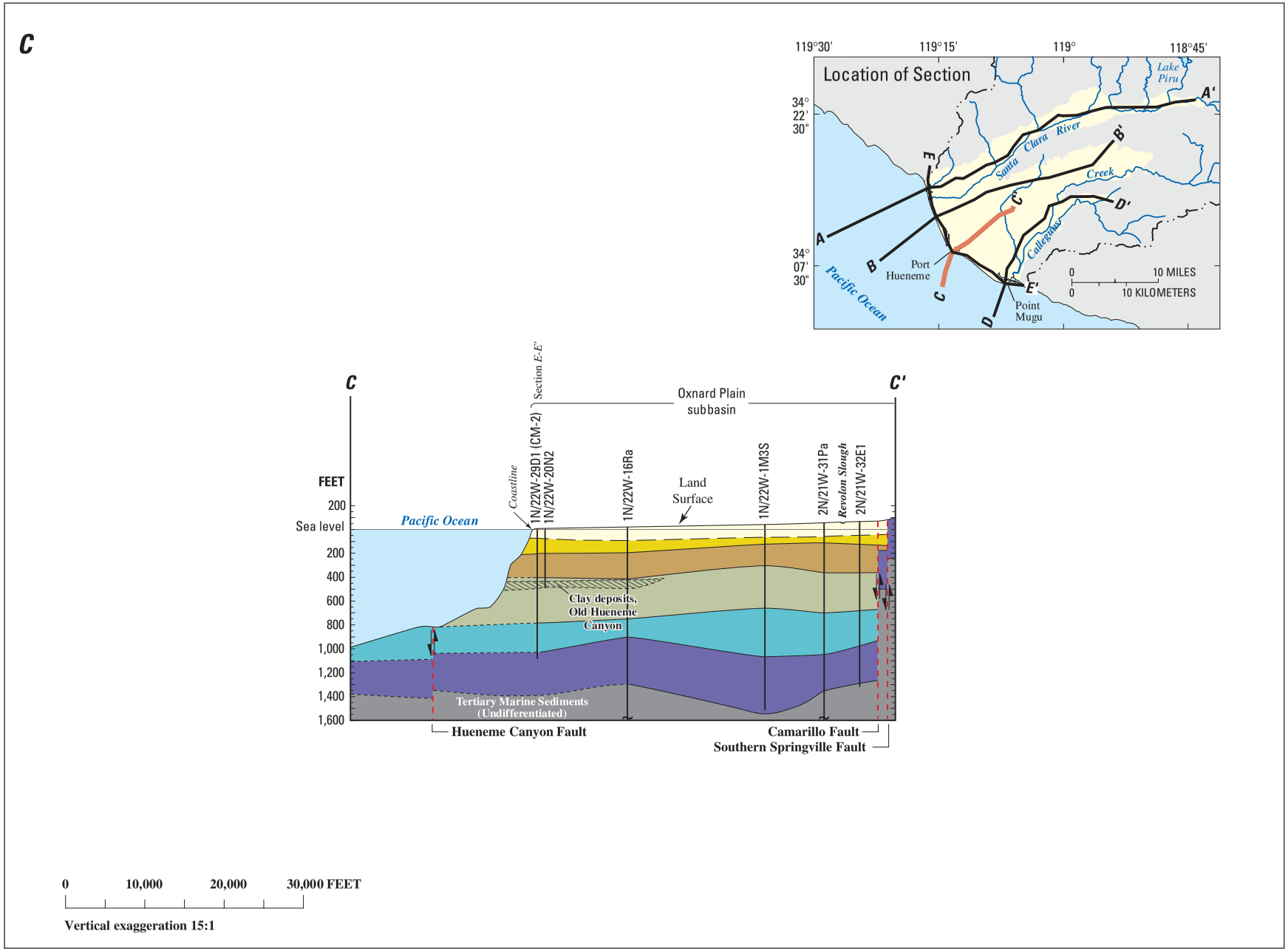

Figure 8—Continued.

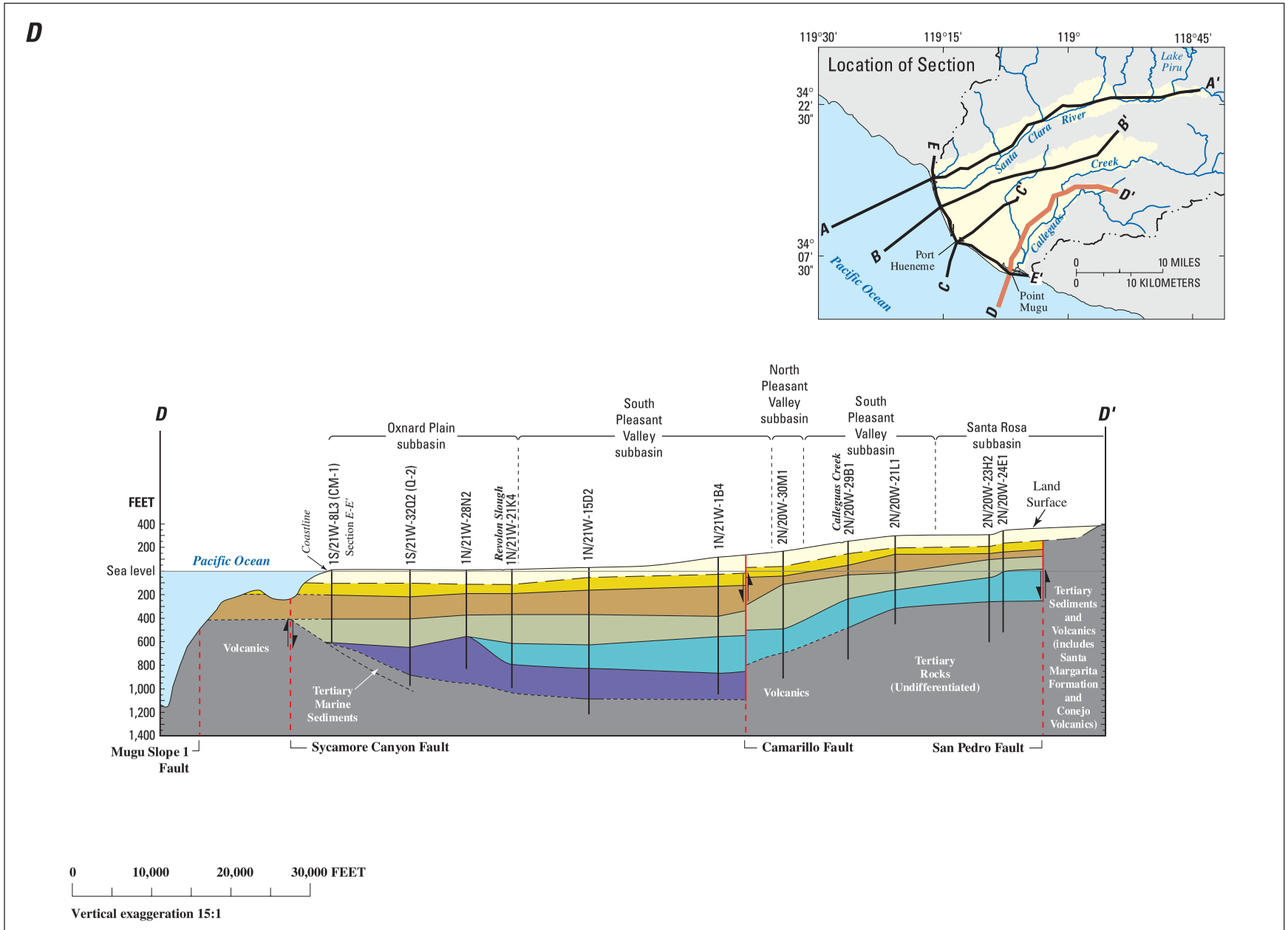

Figure 8—Continued.

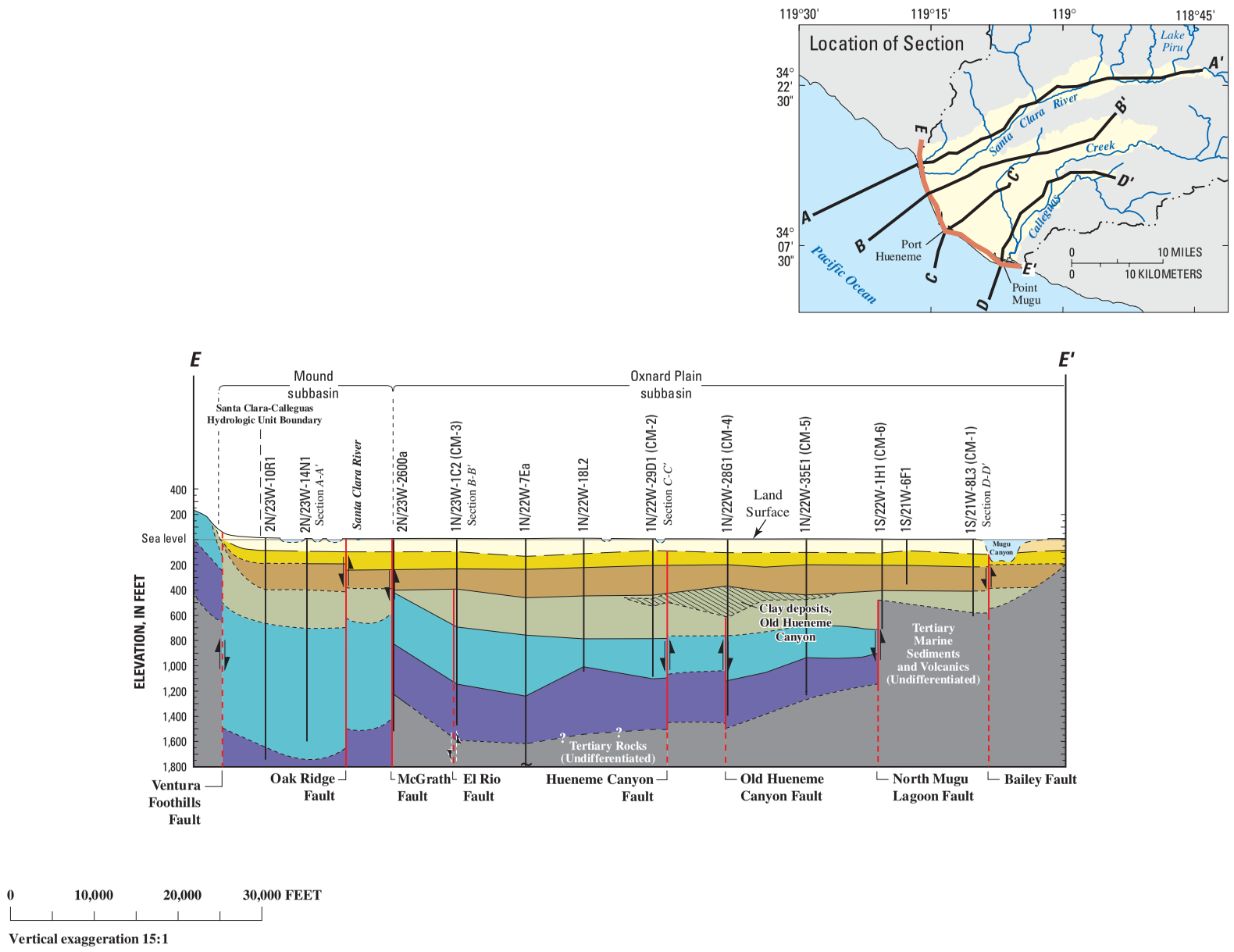

Figure 8—Continued.

Aquifer Systems

The water-bearing deposits were previously divided into six aquifers in the Santa Clara–Calleguas Basin within the two regional aquifer systems (Turner, 1975). Using geophysical and geochemical data collected as a part of the USGS RASA Program, the aquifer designations were realigned into seven major aquifers. The unconsolidated deposits of the late Pleistocene and Holocene epochs are grouped into the regional upper-aquifer system, which includes the Shallow, Oxnard, and Mugu aquifers (fig. 7*B*). The lower-aquifer system is composed of complexly faulted and folded unconsolidated deposits of the Pliocene and Pleistocene epochs and include the upper and lower Hueneme, Fox Canyon, and Grimes Canyon aquifers (fig. 7*B*). The lower aquifer extends to about 1,600 ft below sea level in the Oxnard Plain subbasin to more than 2,000 ft below sea level in the Mound subbasin (fig. 8 *A*,*E*). All these aquifers extend offshore within the continental shelf (fig. 8); however, the thickness, structure, and extent of the submarine outcrops vary across the basin for the upper- and lower-aquifer systems (figs. 7 and 8).

The onshore part of the Oxnard Plain is subdivided into a confined region and an unconfined region. The unconfined region includes the Oxnard Plain Forebay and the northeastern part of the Oxnard Plain. The confined region was subdivided into Northwest and South Oxnard Plain model subareas for the water-management analysis in this study (fig.1). The submarine shelf extends (fig. 7*A*) southwestward from the coastline and is subdivided along the McGrath Fault as an extension of the onshore separation between the Mound subbasin and the Oxnard Plain (figs. 1 and 7); these subbasins are hereinafter referred to as the "offshore Mound" and "offshore Oxnard Plain" subbasins. For the water-management analysis in this study, the offshore Oxnard Plain was subdivided into northern and southern regions separated by the Hueneme submarine canyon.

Upper-Aquifer System

Shallow Aquifer—The Shallow aquifer extends from land surface to a depth of 60 to 80 ft along the Santa Clara and the Arroyo Las Posas flood plains and throughout most of the Oxnard Plain and Pleasant Valley subbasins (figs. 7 and 8). Along the flood plain of the Santa Clara River, the shallow aquifer consists of predominantly sand and gravel and is an important source of ground water. During prolonged droughts, the Shallow aquifer becomes dewatered in the upper reaches of the Santa Clara River and Arroyo Las Posas. Beneath the Oxnard Plain and Pleasant Valley subbasins, the Shallow aquifer consists of fine-to-medium sand with interbedded clay layers and is referred to as the "semiperched aquifer"; the clay layers separate the Shallow aquifer from the underlying Oxnard aquifer. The Shallow aquifer occasionally becomes perched locally because of pumping from the Oxnard aquifer. Water quality is poor throughout most of the Oxnard Plain and Pleasant Valley subbasins and consequently few wells are perforated opposite this aquifer.

Oxnard Aquifer—The Oxnard aquifer lies at the base of the Holocene deposits and consists of sand and gravel deposited by the ancestral Santa Clara River and the Calleguas Creek and by their major tributaries. The coarse-grained basal deposits of the Holocene epoch are referred to as the "Oxnard aquifer" (Turner, 1975). The base of the aquifer ranges from about 150 to 250 ft below land surface throughout most of the Oxnard Plain subbasin (fig. 8). The basal deposits range in thickness from less than 10 to 200 ft and are a major source of water to wells in the Piru, Fillmore, Santa Paula, Oxnard Plain Forebay, and Oxnard Plain subbasins. Hydraulic conductivity in the Oxnard aquifer is about 190 ft/d near Port Hueneme (Neuman and Witherspoon, 1972). The Oxnard aquifer is relatively fine grained in the Mound, Pleasant Valley, Santa Rosa Valley, and Las Posas Valley subbasins; this aquifer is not considered an important source of ground water in these subbasins. Throughout most of East and West Las Posas Valley subbasins, the Oxnard aquifer is unsaturated.

In the Piru and Fillmore subbasins, there are few if any clay layers separating the Shallow and Oxnard aquifers; therefore, ground water can move freely between the two. In the Santa Paula subbasin, the Santa Clara River has migrated south of the ancestral river that deposited the sediments of the Oxnard aquifer and mostly overlies non-water-bearing rocks of Tertiary age. As a result, the Santa Clara River does not overlie the Oxnard aquifer throughout most of the Santa Paula subbasin.

In the Oxnard Plain Forebay subbasin, there are relatively few clay layers separating the Shallow and Oxnard aquifers. Alluvial fans derived from the mountains north of the Mound subbasin pushed the Santa Clara River south toward South Mountain. In the Oxnard Plain Forebay subbasin, clay layers were eroded by the Santa Clara River, and sand and gravel were deposited in their place; owing to the absence of clay, this subbasin is artificially recharged by surface spreading of water diverted from the Santa Clara River. The Oxnard aquifer is considered to be unconfined in the Oxnard Plain Forebay subbasin.

Throughout the Oxnard Plain and Pleasant Valley subbasins, the Shallow and Oxnard aquifers are separated by clay layers. These clay layers confine or partly confine the Oxnard aquifer throughout most of the Oxnard Plain and Pleasant Valley subbasins. Previous investigators (California Department of Water Resources, 1956; Turner, 1975) reported that the clay layers separating the Shallow and Oxnard aquifers in the Point Mugu area are thin or absent, allowing free interchange of water in this part of the subbasin. However, data, collected from several multiple-well monitoring sites constructed in the Point Mugu area as a part of this study (Densmore, 1996), indicate that relatively thick clay layers separate the Shallow and Oxnard aquifers.

Mugu aquifer—The Mugu aquifer (Turner, 1975) is composed of the basal part of the unnamed upper Pleistocene deposits. In the Piru, Fillmore, Santa Paula, Mound, Oxnard Plain Forebay, and Oxnard Plain subbasins, these deposits are similar to those of the underlying lower-aquifer system because the Santa Clara River was the primary source of sediment for both aquifers. The Mugu aquifer is differentiated from the lower-aquifer system because it is less indurated and relatively undisturbed. However, because of the similarities between these deposits, many investigators include the upper Pleistocene deposits in the lower-aquifer system. In the Pleasant Valley, Santa Rosa Valley, East Las Posas Valley, and West Las Posas Valley subbasins, the Mugu aquifer sediments were derived from South Mountain and the surrounding hills and are finer grained than sediments derived from the Santa Clara River.

Throughout most of the ground-water basin, the Mugu aquifer extends from about 200 to 400 ft below land surface (fig. 8) and consists of sand and gravel interbedded with silt and clay. The silt and clay layers retard the vertical movement of water through the Mugu aquifer and confine or partly confine the aquifer. Over most of the ground-water basin, the top of the aquifer is relatively flat; however, the base of the aquifer has a more irregular surface (Turner, 1975) owing to a regional uncomformity. This uncomformity, which is most pronounced in the Mound and the East Las Posas Valley subbasins (fig. 8*A*,*B*,*E*), is due to deformation during deposition of older alluvium that contains the Mugu aquifer.

Few production wells are perforated solely in the Mugu aquifer; most are also perforated in the overlying Oxnard aquifer or in the underlying lower-aquifer system. In general, wells that are perforated opposite both the Oxnard and Mugu aquifers, which are similar in thickness, obtain most of their water from the Oxnard aquifer because it is significantly more permeable. Hydraulic conductivities estimated from slug tests at the multiple-well monitoring sites constructed for this study range from less than 1 to 98 ft/d; most, however, are less than 25 ft/d (E.G. Reichard, U.S. Geological Survey, written commun., 1995). When individual wells at the same multiple-well monitoring site were tested, the estimated hydraulic conductivity of the Oxnard aquifer was almost always higher than that estimated for the Mugu aquifer.

In subbasins in which the Mugu aquifer is predominantly coarse-grained (the Piru, Fillmore, and Santa Paula subbasins), wells perforated in both the Mugu aquifer and the underlying lower-aquifer system obtain most of their water from the Mugu aquifer. This is shown by a wellbore flowmeter test completed on well 3N/21W–11J5 in the Santa Paula subbasin (see figure A5.1 in Appendix 5). Although this well is perforated predominantly in the lower-aquifer system, almost all the water yielded by the well is derived from the Mugu aquifer. As stated previously, the Mugu aquifer is less indurated than the lower-aquifer system, which would account for its greater water-yielding capacity. In the subbasins where the Mugu aquifer is predominantly fine grained, wells yield significant quantities of water from the aquifer only if they are perforated opposite the basal coarse-grained zone. This laterally extensive basal zone, which, as noted earlier, is due to a regional unconformity, yields water readily to wells. Many wells are not perforated opposite this zone, however, because its thickness is 20 ft or less throughout many of the subbasins. Results of the wellbore flowmeter test for well 1N/21W–15D2 (figure A5.1 in Appendix 5) in the Pleasant Valley subbasin show that the basal zone of the Mugu aquifer yields significantly more water per foot of aquifer penetrated than does the underlying lower-aquifer system.

Lower-Aquifer System

The lower-aquifer system consists of the folded and faulted Pleistocene continental and marine deposits of the Saugus, San Pedro, and Santa Barbara Formations as defined by Weber and others (1976) and the Saugus Formation and the Las Posas Sand as defined by Dibblee (1988, 1990a,b, 1991, 1992a,b,c,d) and by Dibblee and Ehrenspeck (1990). For this study, the unconsolidated deposits of the Saugus and the upper part of the San Pedro Formations as defined by Weber and others (1976) and the Saugus as defined by Dibblee were split into the "Upper Hueneme" and "Lower Hueneme" aquifers, respectively, for the entire Santa Clara–Calleguas Basin (fig. 7*B*). The lower part of the San Pedro Formation as defined by Weber and others (1976) and the upper part of the Las Posas Sand as defined by Dibblee are referred to as the "Fox Canyon aquifer" in the Las Posas, Pleasant Valley, and Oxnard Plain subbasins (Turner, 1975). The coarse-grained layers of the Santa Barbara Formation as defined by Weber and others (1976) are commonly referred to as the "Grimes Canyon aquifer" in the East Las Posas Valley subbasin and parts of the Pleasant Valley subbasins (Turner, 1975). In most of the other subbasins, the Santa Barbara Formation is of low permeability, yields poor-quality water, and is not considered an important source of water. Regional fault systems (figs. 7 and 8) segregate the lower-aquifer system into many parts and affect the flow of water between and within the subbasins.

Upper and Lower Hueneme Aquifers—The Hueneme aquifers constitute the upper part of the San Pedro Formation beneath the Oxnard Plain mapped by Weber and others (1976), and the Saugus Formation beneath the Santa Clara River Valley subbasins mapped by Dibblee (1988, 1990a,b, 1991, 1992a,b,c,d) and Dibblee and Ehrenspeck (1990). These aquifers consist of lenticular layers of sand, gravel, silt, and clay. The sediments constituting the aquifers have been subjected to considerable folding, faulting, and erosion since deposition. These deposits were divided into upper and lower aquifers based on data from electric logs which show a decrease in electrical resistivity at the contact between the aquifers. The decrease is attributed to the presence of more fine-grained deposits in the Lower Hueneme aquifer than in the Upper Hueneme. The Upper Hueneme aquifer reaches a maximum thickness of more than 700 ft (fig. 8*A*) and the Lower Hueneme aquifer reaches a thickness of more than 2,000 ft in the axis of the Santa Clara syncline in the Santa Paula, Fillmore, and Piru subbasins. In areas of the basin that have been uplifted since deposition (fig. 8*A*,*D*,*E*), much of the sediments constituting Hueneme aquifers have been removed by erosion.

In the Oxnard Plain subbasin, the Upper Hueneme aquifer is predominantly fine grained in two areas along the coast line between Port Hueneme and Point Mugu (Old Hueneme Canyon on figure 8*C*,*E*). These fine-grained deposits are more than 200 ft thick near the coast, and they extend about 3.5 mi inland. Turner (1975) attributed these deposits to a lagoonal or embayment depositional environment throughout most of the San Pedro Formation deposition. Inspection of lithologic and electrical logs collected during the drilling of the multiple-well monitoring sites constructed for this study indicates that these fine-grained deposits are ancestral submarine canyons (fig. 8*C*,*E*) that were backfilled during a rise in sea level. The submarine canyons were carved into the San Pedro Formation sometime prior to the deposition of the deposits of the upper Pleistocene. These backfilled ancestral submarine canyons are important hydrologic features because they are low permeable barriers to ground-water flow and may contribute to coastal subsidence (fig. 9). The hydraulic conductivity of the fine-grained deposits in the ancestral submarine canyon, estimated from a slug test at the CM-5 multiple-well monitoring site (fig. 8*E*), was 0.1 ft/d (E.G. Reichard, U.S. Geological Survey, written commun, 1995).

Fox Canyon Aquifer—The Fox Canyon aquifer constitutes the basal part of the San Pedro Formation mapped by Weber and others (1976). The aquifer consists of weakly indurated very fine- to medium-grained fossiliferous sand with occasional gravel and clay layers of shallow marine origin. As stated previously, Dibblee (1992a,b,c,d) mapped these deposits as a separate formation, which he designated as the Las Posas Sand. The marine deposition of the sediments of the Fox Canyon aquifer resulted in a relatively uniform series of layers, which can be correlated by the electric logs, over large areas of the ground-water basin (Turner, 1975). The Fox Canyon aquifer is identified on electric logs by zones of relatively high resistivity that are almost identical for thicknesses of 100 to more than 300 ft. In contrast, the overlying Lower Hueneme aquifer is characterized as a series of relatively high resistivity zones 10 to 100 ft in thickness separated by relatively low resistivity zones 10 to 20 ft in thickness. Most of the electric logs inspected show there was a significant shift in the spontaneous potential curve opposite the Fox Canyon aquifer, indicating a change in the aquifer mineralogy and (or) a change in the water quality of the aquifer.

Historically, very few wells tapped the Fox Canyon aquifer of the ground-water basin, except in the East and West Las Posas Valley and the Pleasant Valley subbasins. Because yield is significantly less in this aquifer than in the upper aquifer system, few water wells were perforated solely in the Fox Canyon aquifer. This limited testing of the hydraulic properties of the aquifer. For previous investigations, electric logs from petroleum wells were used to define the character and extent of the aquifer. High-resistivity zones on those logs, which indicate possible coarse-grained zones of good quality water, led to the belief that the Fox Canyon aquifer would be a major source of water to wells.

To help determine the hydraulic properties of the Fox Canyon aquifer, at least one piezometer at 13 of the 23 multiple-well monitoring sites constructed for this study was perforated opposite the aquifer. The lithologic and electric logs for these sites indicate relatively low permeability; the Fox Canyon aquifer consists of predominantly fine- to very fine-grained sand that is indurated to slightly indurated (Densmore, 1996); this is coincident with the high-resistivity zones on the electric logs and reflects the low dissolved-solids concentration of water in the aquifer and the induration of the aquifer sediments. The low permeabilities were confirmed by slug tests that indicate hydraulic conductivities ranging from 1 to 9 ft/d (E.G. Reichard, U.S. Geological Survey, written commun., 1995). These hydraulic conductivities are considerably lower than those of the overlying aquifers.

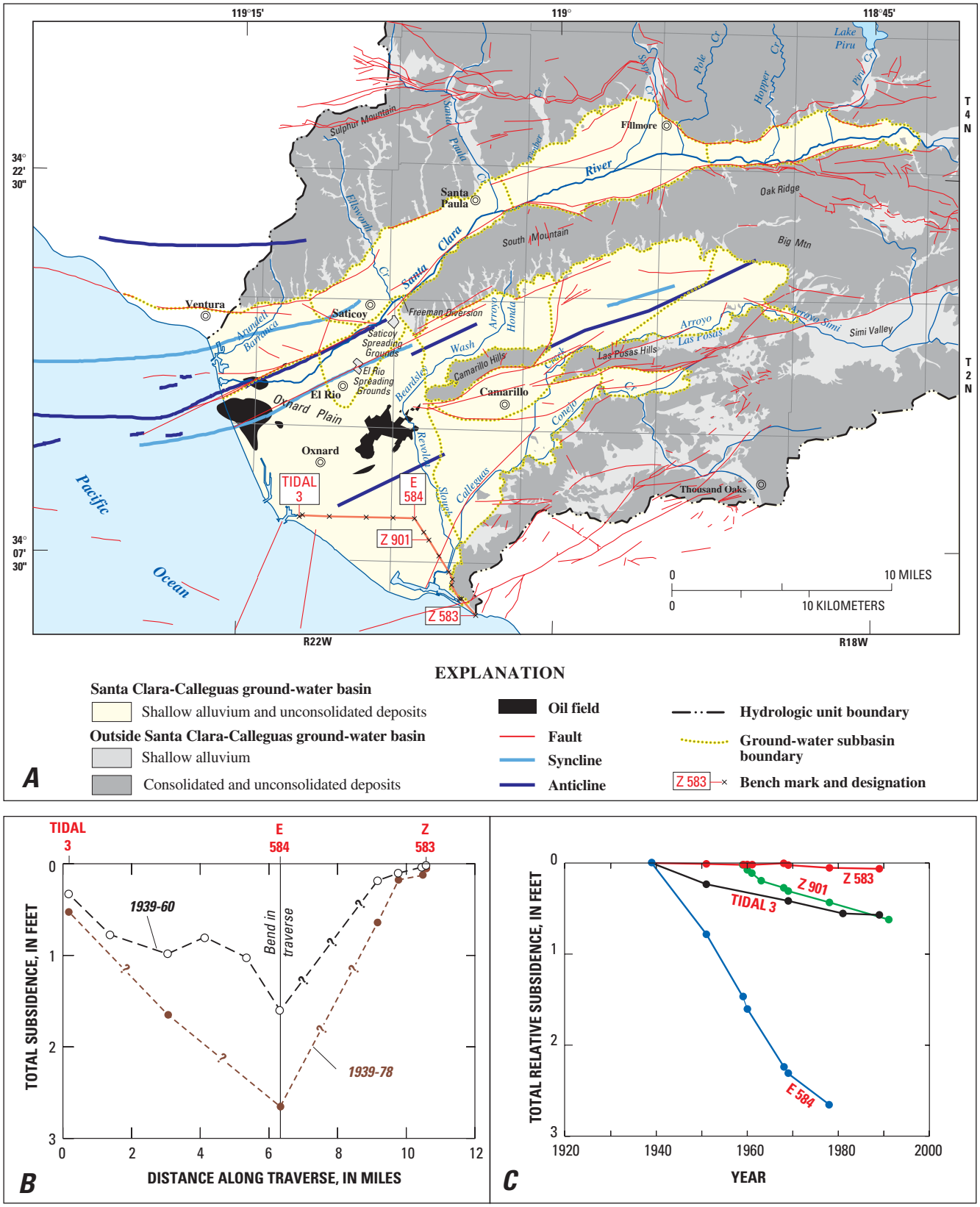

Figure 9. Subsidence in Oxnard Plain and Pleasant Valley, Santa Clara–Calleguas ground-water basin, Ventura County, California. ***A***, Geographic features. ***B***, Subsidence profile. ***C***, Subsidence of bench marks through time.

To determine the relative contribution of water from the Fox Canyon aquifer to wells perforated in the Fox Canyon and overlying aquifers, available flowmeter logs were inspected and additional logs were collected (see table 5 in the "Ground-Water Discharge" section). The flowmeter log collected at well 2N/22W-13N2 in the Oxnard Plain Forebay subbasin (in Appendix 5) shows that little, if any, water enters the wells from the Fox Canyon aquifer, and almost all the water pumped comes from the basal zone of the overlying Lower Hueneme aquifer. Flowmeter logs collected from wells in the Oxnard Plain and the Pleasant Valley subbasins indicate that, in most of the wells tested, the flow contribution from the Fox Canyon aquifer is less than the flow contribution from the overlying aquifers. Data from the flowmeter logs from the Pleasant Valley and the Oxnard Plain subbasins indicate that the Fox Canyon aquifer is a major source of water to wells perforated throughout the lower-aquifer system only if the overlying Lower Hueneme aquifer is absent or is predominantly fine grained. Based on well construction data, this may be the case throughout most of the East and West Las Posas Valley, Oxnard Plain, and Pleasant Valley subbasins.

Grimes Canyon Aquifer—The Santa Barbara Formation (Weber and others, 1976), which consists of non-water-bearing marine sandstone, siltstone, mudstone, and shale, underlies the Fox Canyon aquifer throughout most of the ground-water basin and is considered the base of the ground-water system throughout most of the basin. However, in parts of the ground-water basin, the upper part of the Santa Barbara Formation contains water-bearing deposits referred to as the "Grimes Canyon aquifer" (Turner, 1975).

In the East Las Posas Valley subbasin, the Grimes Canyon aquifer predominantly consists of layers of well-indurated sandstones and conglomerate with high resistivity as indicated by the electric logs, characteristic of well-indurated sandstone and conglomerate layers. Because the sediments are well indurated, the hydraulic conductivity of the aquifer is relatively low. However, the Grimes Canyon aquifer is an important source of water in the East Las Posas Valley subbasin where the overlying aquifers are absent or are unsaturated.

The Grimes Canyon aquifer is also present in the southeastern part of the Oxnard Plain subbasin and throughout most of the Pleasant Valley subbasins (Turner, 1975); many production wells tap this aquifer throughout the Pleasant Valley subbasin. Lithologic and electric logs collected from multiple-well monitoring sites constructed for the RASA study indicate that much of the deposits that contain the Grimes Canyon aquifer are relatively fine grained and water is relatively high in dissolved-solids (Densmore, 1996). Although deposits similar to those of the Grimes Canyon aquifer are present beneath the western part of the Oxnard Plain subbasin, few production wells tap these deposits owing to their greater depth in that part of the subbasin.

Ground-Water Recharge

Sources of recharge to the aquifer systems include streamflow infiltration, direct infiltration of precipitation on the valley floors of the subbasins and on bedrock outcrops in adjacent mountain fronts, artificial recharge of diverted streamflow and imported surface water, percolation of treated sewage effluent, and infiltration of excess irrigation water (irrigation return flow) in some agricultural areas. For previous studies, recharge was estimated using consumption and water-balance methods based on precipitation and streamflow data for various historical periods (Grunsky, 1925; California Department of Public Works, 1934; California State Water Resources Board, 1956; Mann and Associates, 1959; California Department of Water Resources, 1975).

Streamflow Infiltration

Streamflow infiltration is the largest component of ground-water recharge in the Santa Clara–Calleguas basin and includes gaged and ungaged streamflow. The Santa Clara River and the Calleguas Creek have been altered substantially by regulated flow; the construction of the Santa Felicia Dam (Lake Piru) transformed flow in the Santa Clara River system from predominantly winter and spring floodflows to significant summer and fall low flows.

Gaged Streamflow

Previous estimates of annual subbasin streamflow-infiltration rates are summarized in table 3. These reported estimates were aggregated into averages for the wet and dry periods used in this study (fig. 2*A*). The total estimated gaged streamflow infiltration reported by the California Department of Water Resources (1975) for 1937–67 ranged from 0 to 297,700 acre-ft annually (table 3). These estimates yield average wet-year and dry-year infiltration rates that are 67 and 57 percent of estimated runoff, respectively. The ratios of wet-year to dry-year infiltration for the Santa Clara River and for the total basin during the period were 2.0 and 2.7, respectively (table 3). For streamflows less than 250 ft^3/s (about 500 acre-ft/d), the rates of infiltration on the Santa Clara River were about 14 percent, and for several dry years (such as 1952 and 1958) the rates ranged from 50 to 70 percent (California Department of Water Resources, 1975, fig. 15).

Streamflow loss for the Santa Clara River for wet and dry seasonal flows less than 250 ft^3/s (about 500 acre-ft/d) was determined by subtracting downstream gaged streamflow (gaging station 11114000) from the sum of upstream gaged inflows (gaging stations 11108500, 11110000, 11110500, 713, 11113000, 11113500) (fig. 4). Similarly, the streamflow loss for Calleguas Creek was estimated as the difference between downstream streamflow (11106550) and gaged inflows (11106850 and 11106400) for flows less than 10 ft^3/s (20 acre-ft/d) (fig. 4). Seasonal streamflow losses in the Santa Clara River and the Calleguas Creek varied widely but generally show several patterns (fig. 10). Regression of seasonal streamflow loss in relation to total gaged streamflow indicates an overall loss of 35 percent for wet-year seasons (fig. 10*A*) and 52 percent for dry-year seasons (fig. 10*B*) for the Santa Clara River. Loss from the Calleguas Creek during low-flow conditions is generally either 0 percent during winter and fall seasons or 100 percent during spring and fall seasons (fig. 10*C*). During dry-year summers, 70 to 100 percent of the flow in the Santa Clara River is lost to ground-water recharge (fig. 10*B*). Streamflow loss is low for many of the wettest years, such as 1969 and 1984 (fig. 10*A*), which may indicate a significant contribution of ungaged inflow prior to or during periods with relatively low flow (less than 200 ft^3/s). The annual range of gaged streamflow loss in the Santa Clara River for 1956–93 varied from about 2,700 to 97,800 acre-ft/yr (table 3). On a climatic basis, total infiltration for the Santa Clara River was about 34,000 (22 percent of flow) and 25,100 (37 percent of flow) acre-ft/yr for wet- and dry-year periods during 1956–93, respectively; for the Calleguas Creek above Highway 101, it ranged from 0 to 6,100 acre-ft/yr for the period of record (1973–93) (table 3). The wide range of streamflow loss also was subject to the effects of additional inflow from treated municipal sewage between gaging stations of about 12 ft^3/s (8,700 acre-ft/yr) and irrigation return flow.

Streamflow infiltration along the Santa Clara River, estimated as part of a sediment-transport study, is 23 percent of flow per mile for flows less than 100 ft^3/s, 20 percent of flow per mile for flows from 100 to 500 ft^3/s, 6 percent of flow per mile for flows from 500 to 1,000 ft^3/s, and less than 2 percent of flow per mile for floodflows greater than 1,000 ft^3/s (Brownlie and Taylor, 1981).

Densmore and others (1992) estimated streamflow infiltration for a summer drought under conditions of controlled releases from Lake Piru. The controlled releases result in an increase in infiltration rate with increased channel width in Piru Creek when releases exceed 200 ft^3/s (Steve Bachman, United Water Conservation District, oral commun., 1996).

These various infiltration estimates collectively suggest that infiltration is dependent on antecedent conditions, which include antecedent ground-water levels; magnitude of the streamflow and related properties, such as channel width; and current and antecedent regulated flows.

Table 3. Summary of estimated ranges and averages of gaged and ungaged streamflow infiltration in the Santa Clara-Calleguas Basin, Ventura County, California

[Time periods are reported in water years except from this study. All estimates are in acre-feet per year. Numbers in parentheses are average infiltration values during dry and wet periods, respectively. —, no estimate was made]

Time period of estimate	Streamflow infiltration					Total infiltration		Basin total infiltration
	Gaged				Ungaged			
	Piru	Fillmore	Santa Paula	Montalvo Forebay of Oxnard Plain	Mountain-Front Recharge	Santa Clara River	Calleguas Creek	
1893 to [1]1932	—	—	—	—	1,400–56,200 [2] (11,500; 30,200)	12,300–138,900 (51,300; 65,000)	—	12,400–143,300 [1](62,500; 99,800)
1937 to [3]1951	6,800–68,600 (18,500; 38,400)	0–33,600 (0; 0)	0–16,200 (4,100; 9,300)	1,000–145,000 (23,600; 74,600)	—	—	—	—
1937 to [4]1957	6,400–68,300 (19,100; 36,100)	1,800–49,100 (20,500; 26,800)	4,200–24,400 (14,900; 15,700)	1,000–39,300 (12,100; 22,100)	—	—	—	—
1937 to [5]1967	—	—	—	—	3,600–190,000 (22,400; 80,300)	0–185,800 (26,400; 51,800)	—	0–297,700 (40,300; 108,600)
1956 to [6]1993	—	—	—	—	3,800–78,500 (13,200; 34,200)	2,700–97,800 (25,100; 34,000)	0–6,100	—

[1]Estimates from the California Department of Public Works (1934, table 59). For Santa Clara River, the net streamflow includes estimates of runoff from ungaged tributaries and valley-floor runoff.
[2]Estimates include only the Santa Clara River Valley.
[3]Estimates from the California State Water Resources Board (1956, tables 12–15).
[4]Estimates from Mann (1959), Plates 28–31
[5]Estimates from the California Department of Water Resources (1975, tables 23 and 24). For basin total the net streamflow includes estimates of runoff from ungaged tributaries.
[6]Estimates from this study. Streamflow leakage for Calleguas Creek does not include additional streamflow infiltration from treated waste water or irrigation returnflow.

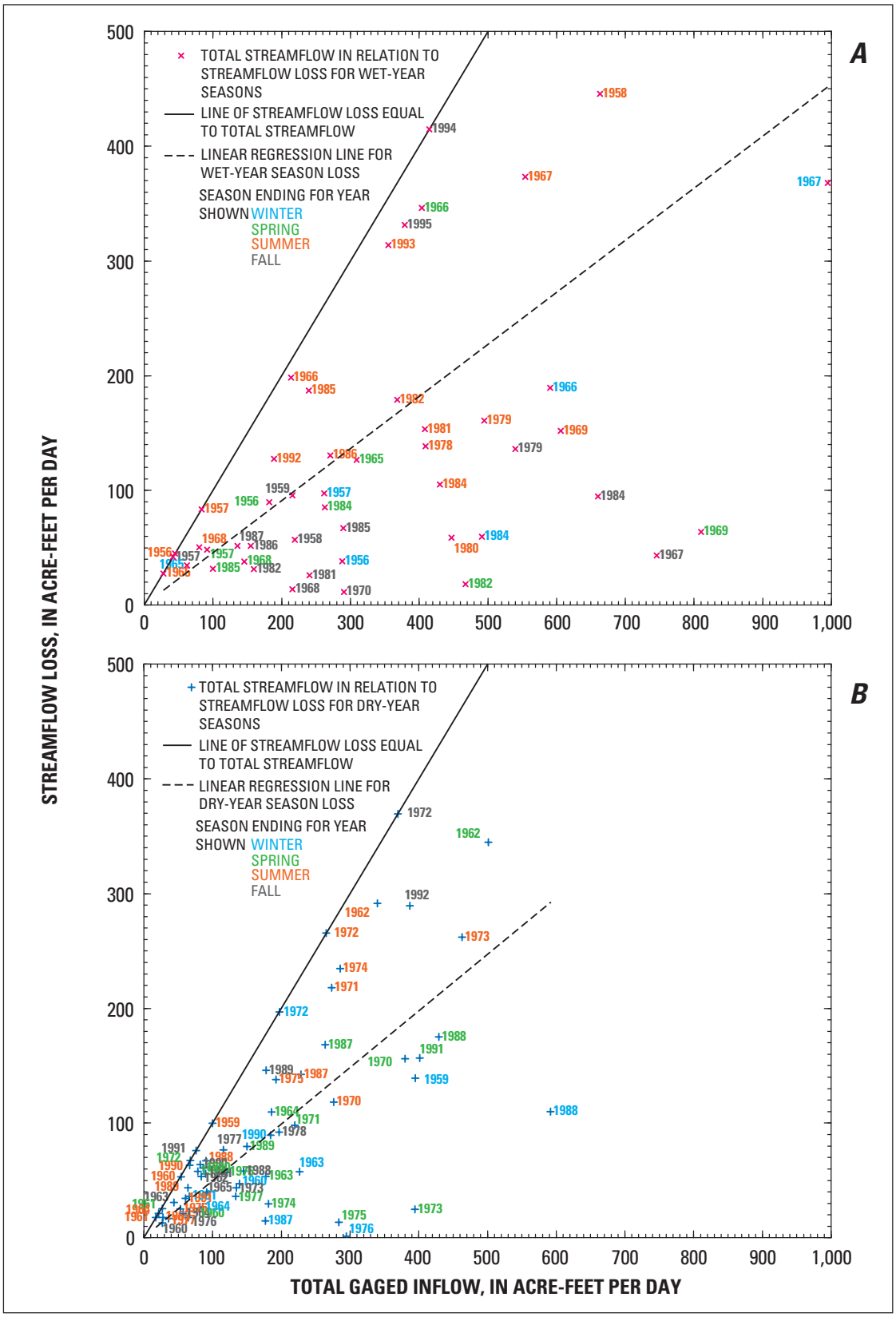

Figure 10. Estimated seasonal streamflow losses for gaged inflows in the Santa Clara River and Calleguas Creek and tributaries, Ventura County, California. ***A***, Santa Clara River streamflow in wet-years seasons. ***B***, Santa Clara River streamflow in dry-year seasons. ***C***, Calleguas Creek streamflow in wet-and dry-year seasons.

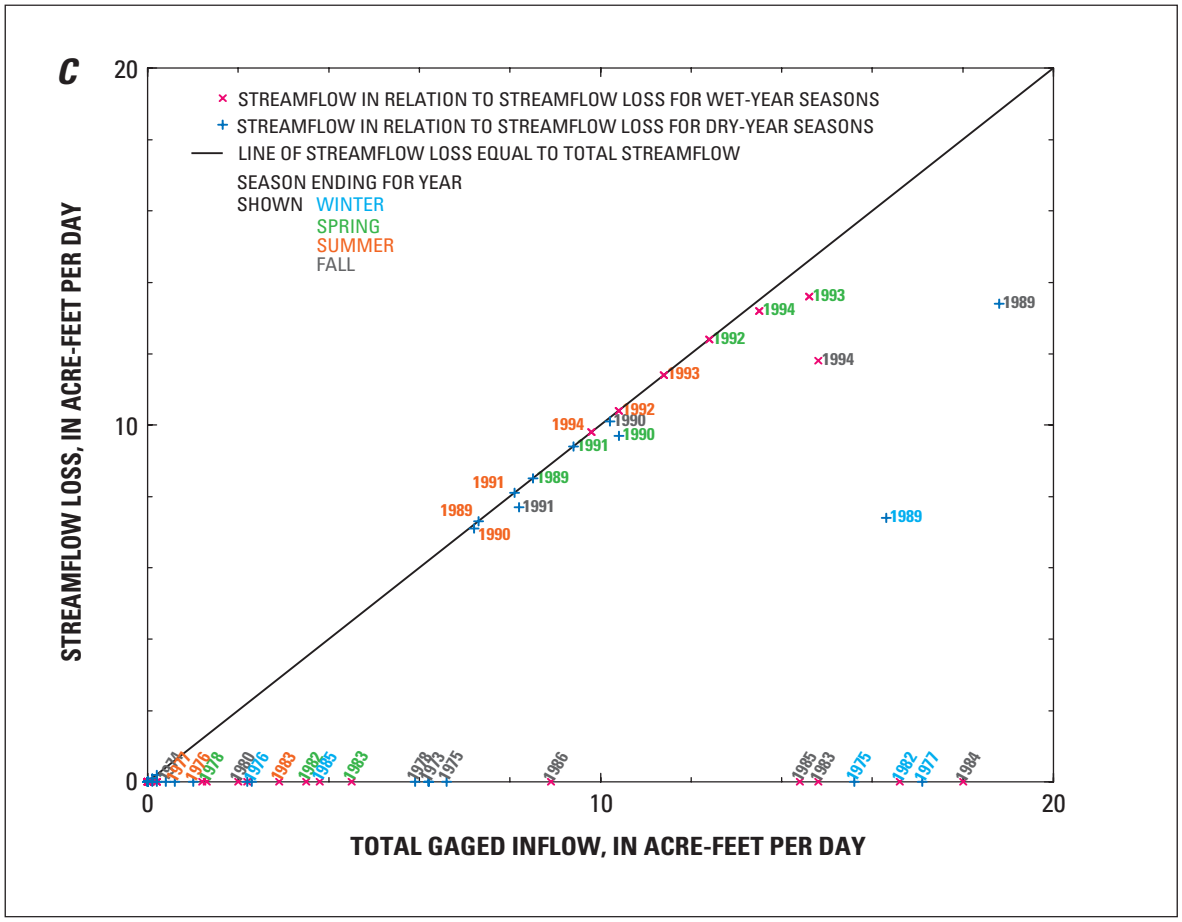

Figure 10—Continued.

Ungaged Streamflow

Infiltration of streamflow in ungaged drainage basins at the boundary of an alluvial aquifer system is referred to as "mountain-front recharge." Mountain-front recharge occurs along the arroyos and the small tributary stream channels of the 64 ungaged tributary drainage basins that drain into the ground-water subbasins from the surrounding mountain fronts of the Santa Clara–Calleguas Basin. This component of streamflow constitutes a small but significant contribution to streamflow and ground-water recharge, especially during wet years. For this study, it was assumed that the streamflow percolates into the alluvium and becomes ground-water recharge. This assumption may result in an overestimate of recharge during floodflows.

Previous estimates of mountain-front recharge range from 1,400 to 190,000 acre-ft/yr for 1893–1967 (table 3). In some wet years such as 1969, 1978, 1979, 1980, 1983, 1986, and 1993, measured outflow at the downstream gaging station at Montalvo (11114000) (fig. 4) on the Santa Clara River was greater than gaged inflow from the major tributaries. This difference can be attributed to the contribution of ungaged streamflow. Based on gaging-station data, this ungaged streamflow may have ranged from 39,800 to 479,800 acre-ft/yr for the Santa Clara River for 1956–93 and from 300 to 7,800 acre-ft/yr for Calleguas Creek for 1973–93 (the period of record).

For this study, mountain-front recharge was estimated by means of a modified rational method using gaged streamflow data from two small subdrainage basins, Hopper and Pole Creeks (fig. 4), referred to as "index" basins. The fraction of precipitation assumed to be mountain-front recharge was estimated as the ratio of total seasonal streamflow for each ungaged subdrainage basin to the average total seasonal precipitation for an index basin. To estimate mountain-front recharge, estimates of seasonal precipitation were required for each of the subdrainage basins for each wet year and dry year (fig. 3). It was assumed that most of the runoff from the ungaged drainage basins infiltrates near the mountain fronts and does not contribute significantly to mainstem streamflow.

The amount of recharge was estimated as the index-basin streamflow fraction of precipitation multiplied by the average total volume of seasonal precipitation (drainage area multiplied by kriged seasonal precipitation) for each of the 64 ungaged tributary subdrainage basins. Seasonal (winter, spring, summer, and fall) estimates for wet and dry years were made for all 64 subdrainage subbasins. The average percentages of precipitation that became mountain-front recharge during the period of record for the two index subdrainage basins, Pole and Hopper Creeks, were 4 and 7.5 percent, respectively. Estimates of mountain-front recharge ranged from about 3,800 to 78,500 acre-ft/yr for 1956–93 (table 3) and averaged 34,200 and 13,200 acre-ft/yr for wet- and dry-year periods, respectively. The estimates of seasonal mountain-front recharge ranged from zero for most of the Oxnard Plain to as much as 12,000 acre-ft per season for the Santa Clara River Valley subbasins (figs. 1 and *11A*).

Direct Infiltration

Recharge also occurs as direct infiltration of precipitation on the valley floors (hereinafter referred to as "valley-floor recharge") and as direct infiltration of precipitation on bedrock outcrops (hereinafter referred to as "bedrock recharge"). These components of recharge constitute a small but significant contribution to streamflow and ground-water recharge, especially during wet years.

Previous estimates of direct infiltration for water years 1894 through 1957 (California Department of Public Works, 1934; Mann and Associates, 1959; California Department of Water Resources, 1975) are summarized in table 4. The total estimated infiltration for the Santa Clara River Valley subbasins ranges from 0 to 90,800 acre-ft/yr (table 4) and averages 30,400 and 5,300 acre-ft/yr for wet-year and dry-year periods, respectively (Mann and Associates, 1959).

Direct infiltration was estimated as a percentage of precipitation and ranged from no infiltration in the confined parts of the Mound, Oxnard Plain, and North Pleasant Valley subbasins to as much as 6,238 acre-ft/yr in the unconfined Fillmore subbasin. The percentage of precipitation was based on the modified rational method in which the amount of potential recharge is the fraction of runoff from the index subdrainage basin multiplied by the total volume of precipitation for each ground-water subbasin. This method may overestimate potential recharge during periods of sustained rainfall when soil moisture is exceeded and overland runoff to stream channels occurs. Total estimated recharge as direct (valley-floor) infiltration ranges from 18,300 to 32,700 acre-ft/yr (fig. 11*A*, table 4) during dry- and wet-year periods, respectively; this estimate included an additional 2,200 acre-ft/yr of direct bedrock infiltration along the basin margins, which is described in a later section in the context of developing estimates of inflow for the subareas of the ground-water model.

Artificial Recharge

Artificial recharge is a major contributor to ground-water recharge in the Oxnard Plain Forebay and the Piru subbasins (fig. 11*A*). Artificial recharge was started in 1929 adjacent to Piru and Santa Paula Creeks and the Santa Clara River near Saticoy. The use of streamflows for recharge, as well as for agriculture, supplemented the growing use of the ground-water resources. Additional surface-water storage was provided by construction of Santa Felicia Dam on Piru Creek in the early 1950s. Major diversions along the Piru and Santa Paula Creeks and along the Santa Clara River at Saticoy and Freeman have been used for artificial recharge of the upper-aquifer system.

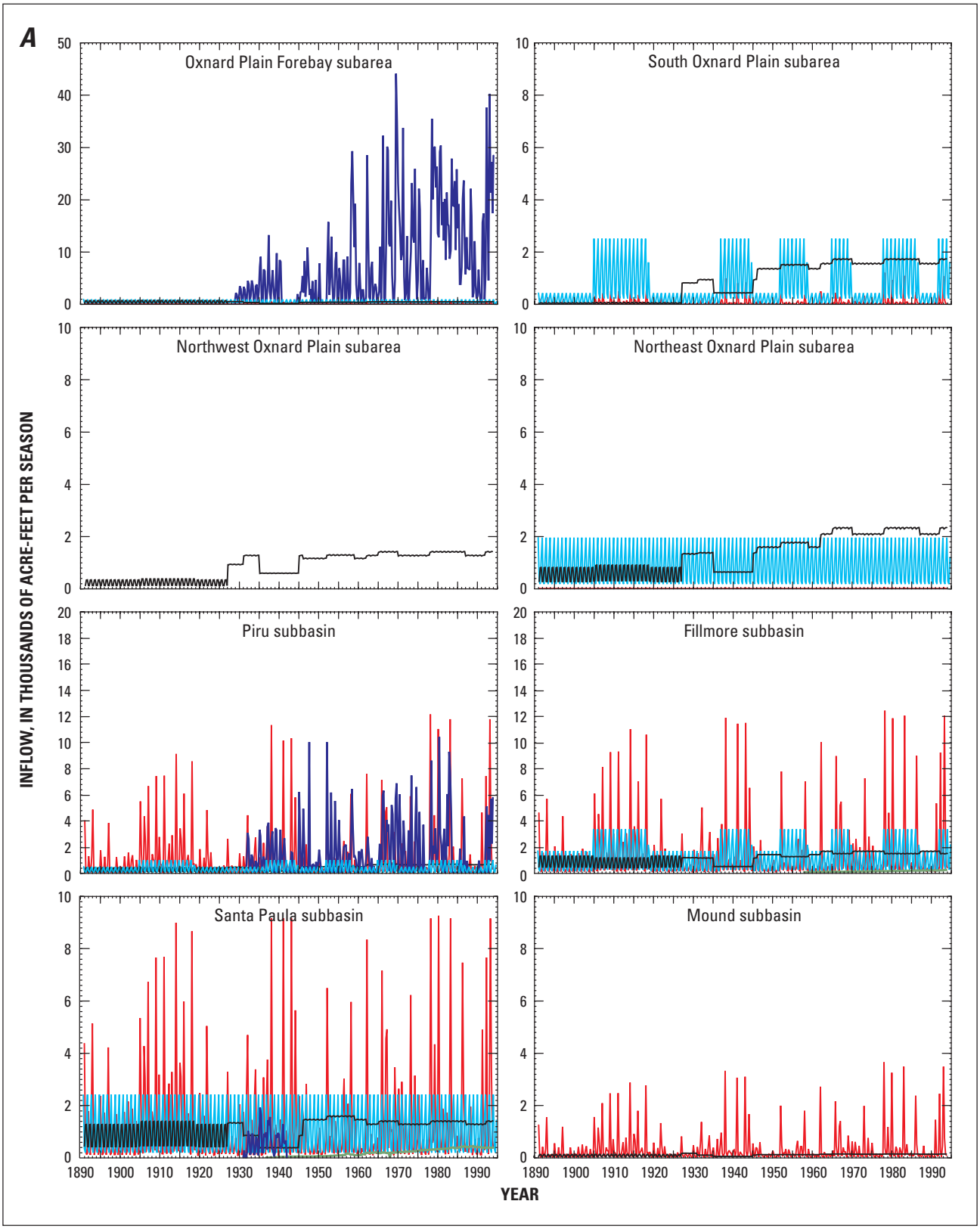

Figure 11. ***A***, Estimates of seasonal ground-water inflows to the subbasins and to the Oxnard Plain subareas of the Santa Clara–Calleguas ground-water basin, Ventura County, California, 1891–1993, and ***B***, Annual estimated and reported ground-water pumpage in the Santa Clara–Calleguas ground-water basin**,** Ventura County, California, 1891–1993.

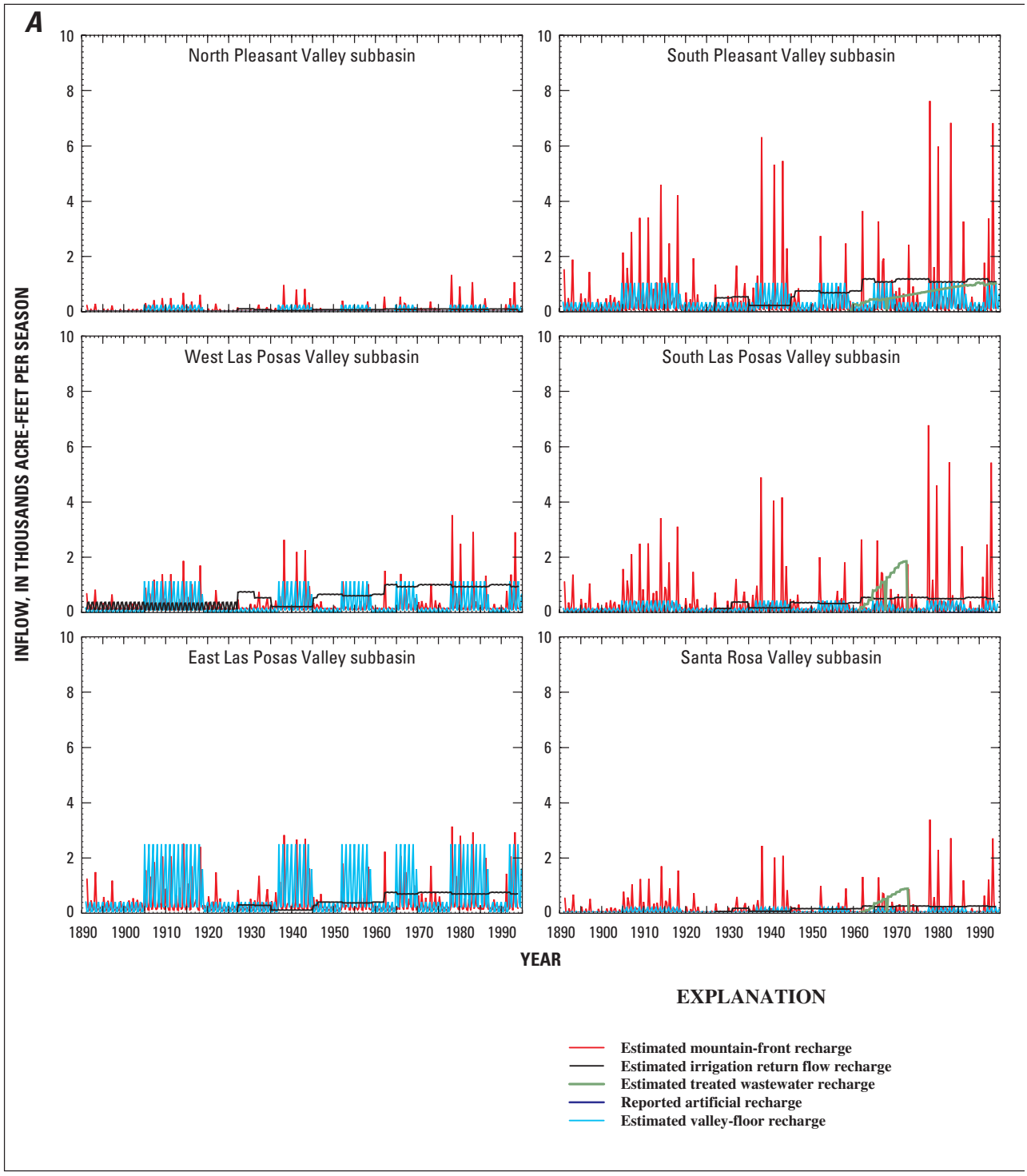

Figure 11—Continued.

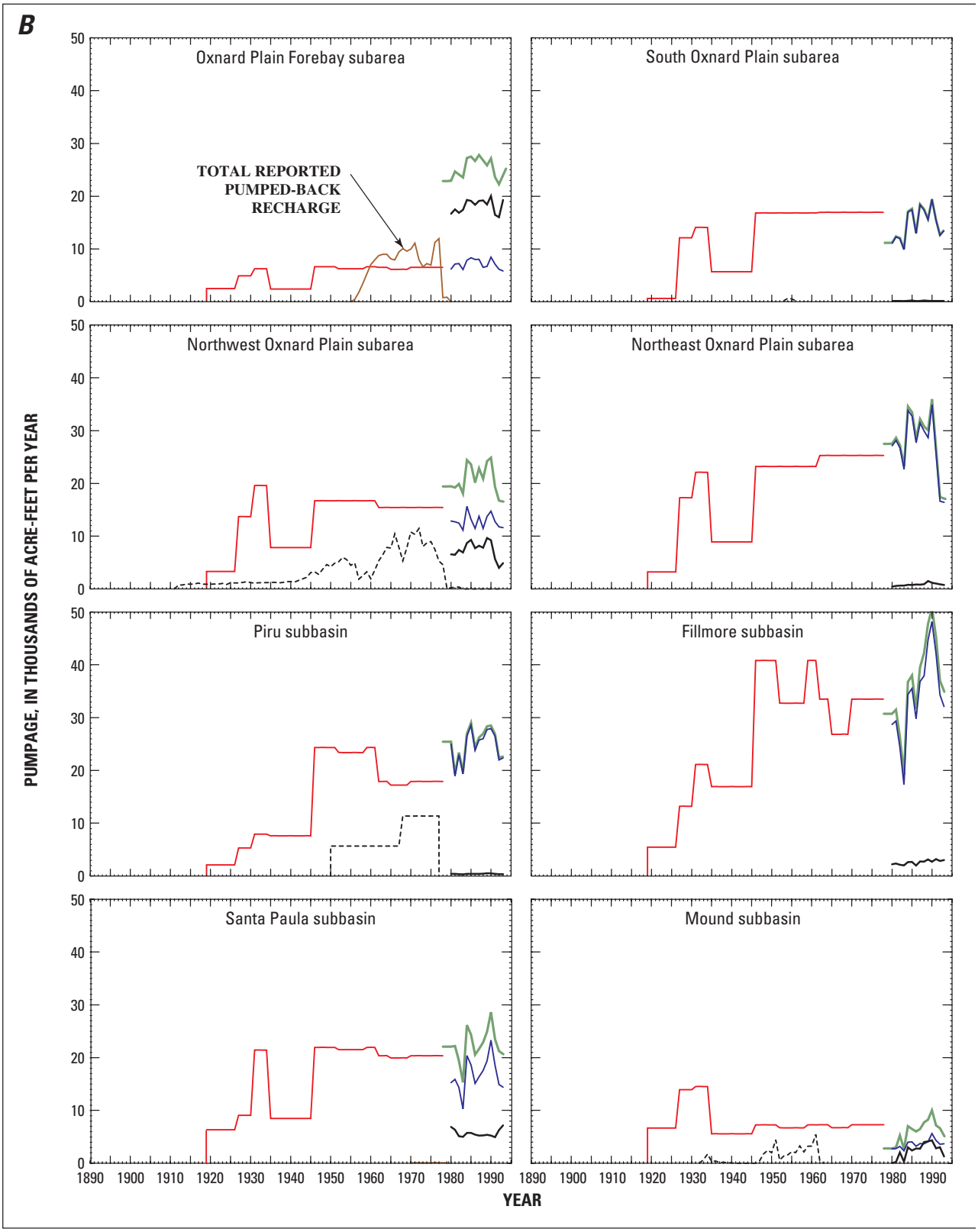

Figure 11—Continued.

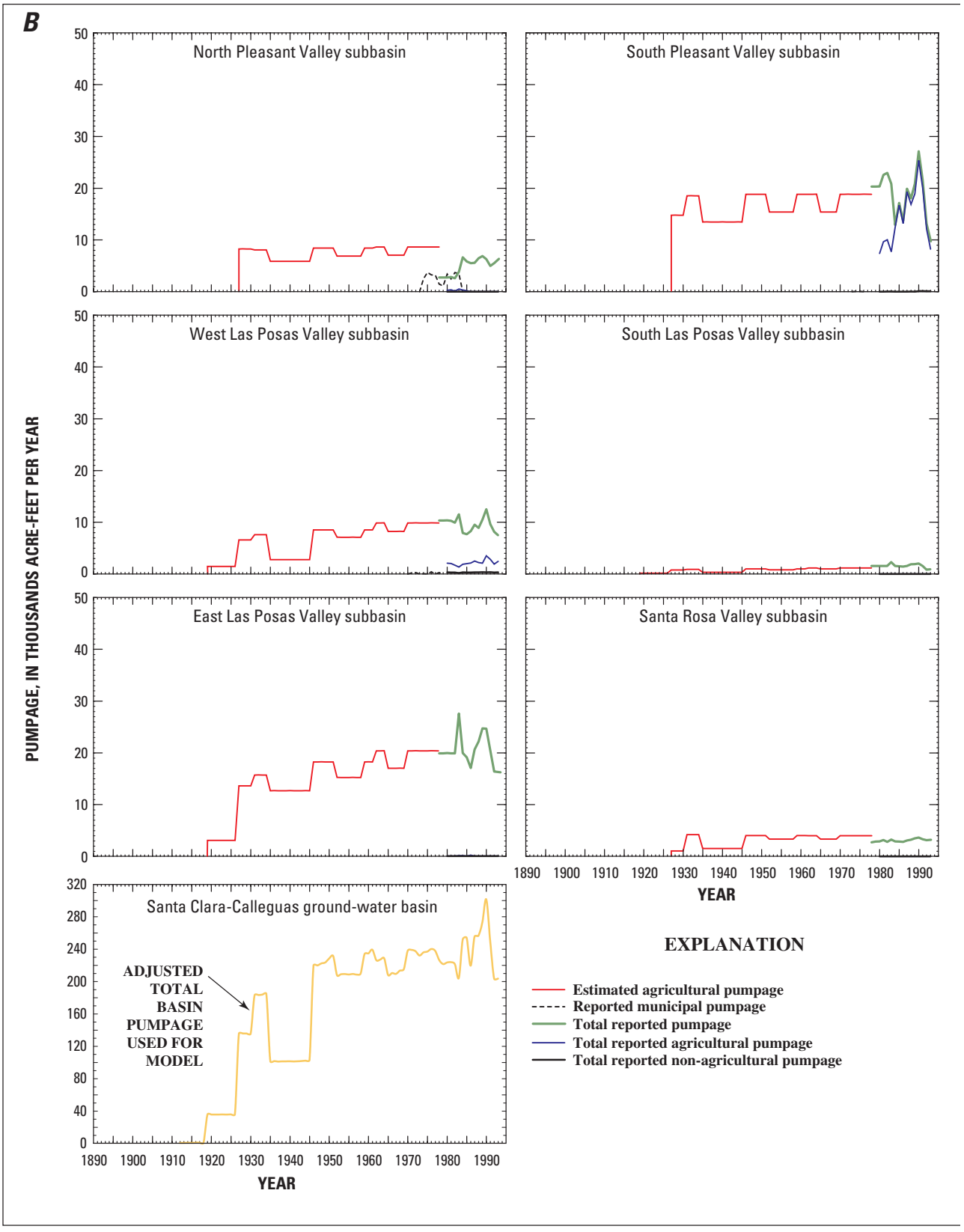

Figure11—Continued.

Table 4. Summary of selected estimates of ranges and averages of direct infiltration of precipitation in subbasins in the Santa Clara–Calleguas Basin, Ventura County, California

[All estimates in acre-feet per year. Numbers in parentheses indicate the average infiltration during dry and wet periods, respectively. —, no estimate made]

Period of record in water years	Piru	Fillmore	Santa Paula	Mound	Montalvo Forebay of Oxnard Plain	Oxnard Plain	East/South Las Posas	West Las Posas	Pleasant Valley/ Santa Rosa Valley	Total bedrock recharge	Total direct infiltration recharge
[1]1894 to 1932	0–11,300 (2,700; 6,600)	0– 21,200 (4,400; 11,800)	0–11,800 (2,300; 6,600)	0–4,500 (750; 2,200)	0–8,000 (1,600; 4,500)	—	—	0–5,400 (1,000; 3,000)	—	—	400–62,200 [2](12,900; 34,800)
[3]1937 to 1951	0–11,300 (0; 4,800)	0–29,800 (0; 11,700)	0–26,200 (0; 9,600)	—	0–9,500 (0; 0)	—	—	—	—	—	—
[4]1937 to 1957	[1]200–15,100 (1,100; 5,600)	[2]500–37,900 (2,800; 13,600)	[3]0–25,600 (900; 8,000)	—	[4]100–12,200 (500; 3,200)	—	—	—	—	—	—
[5]1937 to 1967	—	—	—	—	—	—	—	—	—	—	4,000–306,400 (20,200; 108,300)
[6]1891 to 1993	950–1,900	3,100–6,200	4,500	0	1,700	3,600	800–4,700 (570; 3,400)	350–2,100	640–2,400	2,200	18,300–32,700

[1]California Department of Public Works (1934, table 59). For the Santa Clara River, the net streamflow includes estimates of runoff from ungaged tributaries and valley-floor runoff.
[2]Includes only the Santa Clara River Valley and West Las Posas subbasins.
[3]California State Water Resources Board (1956, tables 12–15).
[4]Mann and Associates (1959, plates 28–31).
[5]California Department of Water Resources (1975, tables 3, 19, and 20). For basin total, the estimated recharge from direct infiltration of precipitation includes potential runoff.
[6]Final estimates from this study for valley-floor recharge. Period of record is in calendar years.

Artificial recharge began with offstream spreading-works to help provide an adequate and dependable water supply for agriculture. Spreading-works were operated by the Santa Clara Conservation District: Santa Clara River streamflow was diverted near Saticoy beginning in 1928–29; Piru Creek streamflow was diverted near Piru beginning in 1930–31; and Santa Paula Creek streamflow was diverted near Santa Paula beginning in water year 1931 (Freeman, 1968). The initial capacities of the diversions for the Saticoy, Piru, and Santa Paula spreading grounds (fig. 4) were 120, 60, and 25 ft^3/s, respectively (Freeman, 1968). These sites represent some of the earliest efforts to divert and artificially recharge shallow ground-water aquifers. The Saticoy and Piru spreading grounds have been in continuous operation since their construction more than 70 years ago. The Santa Paula diversion was operated for about 11 years (1930–41) (fig. 11*A*), recharging a total of 26,968 acre-ft.

The UWCD added additional spreading grounds at El Rio (fig. 4) in 1955 for diversions at Saticoy and added the Pleasant Valley pipeline and reservoir in 1957 for additional storage capacity. Earthen dikes were used to divert as much as 375 ft^3/s of streamflow from the Santa Clara River at Saticoy. However, between 1955 and 1983, there were 81 dike failures at the diversion (United Water Conservation District, 1983). The earthen dike and diversion was relocated about 1 mi upstream after the riverbed degraded during the large flood of 1969, but the dike remained prone to failures at streamflows greater than 1,600 ft^3/s. A concrete dike and diversion structure, called the Freeman Diversion, was constructed in 1991. It is more durable and provides a larger diversion capacity of 460 ft^3/s. Natural streamflow during winter and spring and controlled releases of combined imported water and natural streamflow from Lake Piru during summer and fall are diverted at the Freeman Diversion. About 2,500,000 acre-ft was artificially recharged along the Santa Clara River Valley of which 378,054 acre-ft was at Piru (October 1931–December 1993), 1,228,615 acre-ft at Saticoy (October 1928–December 1993), 868,408 acre-ft at El Rio (December 1955–December 1993), and 26,968 acre-ft at Santa Paula. Some of the surface water diverted at Saticoy and later at the Freeman Diversion was directly delivered by pipelines for irrigation. About 239,966 acre-ft of the diversions was delivered directly through the Pleasant Valley pipeline (September 1958–December 1993) from surface-water diversions, and an additional 4,161 acre-ft was delivered to John Lloyd Butler farms (March 1970–May 1991) for irrigation (Greg Middleton, United Water Conservation District, written commun., 1994).

Since the 1960s, most artificial recharge at El Rio has been pumped back for nearby irrigation or delivery by pipeline to adjacent subbasins. During October 1955–December 1977, about 389,600 acre-ft was recharged at El Rio and about 170,974 acre-ft was pumped back. Net recharge during this period was about 218,600 acre-ft and the pump-back rate was 44 percent. During July 1979–December 1993, about 411,300 acre-ft was recharged and about 231,400 acre-ft (44 percent) was pumped back at El Rio. The ratio of pumpage to recharge for the El Rio artificial storage and recovery system (ASR) for 1978–93 ranged from 0.38 in wet years to 1.5 in dry years.

Irrigation Return Flow

Deep percolation of excess applied irrigation water (hereinafter referred to as "irrigation return flow") is an additional source of artificial recharge to the ground-water system. However, areally extensive confining units retard the recharge of irrigation return flow to the upper-aquifer system throughout most of the Oxnard Plain and Mound subbasins. Irrigation return flow is redirected by drains throughout most of the southern part of the Oxnard Plain subbasin to streamflow that discharges to the Pacific Ocean through Revolon Slough (fig. 4). Increases in nitrate concentrations in ground water from wells in the upper-aquifer system (Izbicki and others, 1995; Izbicki and Martin, 1997) and related increases in ground-water levels may indicate that some irrigation return flows are infiltrating back to the upper-aquifer system in the Santa Clara River Valley and Las Posas Valley subbasins and in the Oxnard Plain Forebay and Santa Rosa Valley subbasins. The deep percolation of irrigation return flow within these subbasins consists of varying amounts of surface water and ground water. The amount of return flow was estimated based on a 70-percent irrigation efficiency of applied water (Blaney and Criddle, 1950, 1962) for the areas of irrigated agriculture estimated from five land-use maps. Estimates by Koczot (1996) were based on areas and crop types delineated from land-use maps for 1912 (Adams, 1913), 1927 (Grunsky, 1925; Koczot, 1996), 1932 (California Department of Public Works, 1934), 1950 (California Department of Public Works, 1950), and 1969 (California Department of Water Resources, 1970). The resulting annual estimates were about 17,900 acre-ft for 1912; 46,100 acre-ft for 1927; 45,700 acre-ft for 1932; 52,600 acre-ft for 1950; and 67,900 acre-ft for 1969. When the estimates for the Oxnard Plain and Mound subbasins are excluded, the annual estimates of irrigation return flow are reduced to about 11,800 acre-ft for 1912; 26,900 acre-ft for 1927; 22,400 acre-ft for 1932; 27,700 acre-ft for 1950; and 37,900 acre-ft for 1969 (Koczot, 1996).

Ground-Water Discharge

Discharge of water from the aquifer systems includes ground-water discharge as pumpage from wells, evapotranspiration along the river flood plains, and offshore flow along submarine outcrops. Some additional intermittent baseflow to rivers occurs at the subbasin boundaries, but the baseflow generally infiltrates again in the downstream subbasin and thus is not considered a loss to the ground-water flow system. During the wet periods, however, ground water discharges as stream baseflow to the Pacific Ocean; this base-flow component of discharge to the ocean was larger prior to the 1930s (Freeman, 1968).

Pumpage

The first wells were drilled on the Oxnard Plain in 1870 following the severe drought of 1853–64 and during a sustained dry climatic period (1840–83) (fig. 2). Although pumping occurred during the late 1800s and early 1900s, pumpage was minimal and therefore was not estimated for this report. These first artesian flowing wells typically were drilled to depths of 90 to 143 ft, and discharges were about 500 to 1,000 gal/min (Freeman, 1968). Many wells were completed during 1870–71 for irrigation of field crops. During the early development of the ground-water resources, the drilling of wells diminished the flow of the springs and the artesian wells. By 1912, as many as 42 pumping plants were operating north of the Santa Clara River, providing water for irrigation and domestic use (Freeman, 1968).

By 1920, a progressive lowering of water levels throughout the Santa Clara River Valley and the Oxnard Plain subbasins required the replacement of many centrifugal pumps with deep turbine pumps. By 1924, many of the previously undeveloped areas of the Santa Clara–Calleguas Basin were being used for agriculture (Grunsky, 1925). On the basis of a 1912 land-use map, estimated agricultural pumpage yields a basinwide average rate of withdrawal of about 33,500 acre-ft/yr, which results in a potential total withdrawal of about 267,700 acre-ft for the years 1919–26 of the dry-year period 1919–36 (fig. 2).

Ground water initially was developed predominantly for agricultural use. Agricultural ground-water pumpage was estimated indirectly from land-use maps for periods prior to the metering of pumpage; Koczot (1996) estimated pumpage using selected land-use maps and consumptive-use estimates for 1912, 1927, 1932, 1950, and 1969. Land-use maps were used instead of electrical power records because of the labor required to construct pumpage records for large timespans and because many wells were not powered by electricity. These land-use maps were used to delineate agricultural consumptive use which was used to estimate pumpage for periods prior to metering not represented by land-use maps. The 1912 land-use map was used for 1919–26; the 1927 map was used for 1927–30; the 1932 map was used for 1931–45; the 1950 map was used for 1946–61; and the 1969 map was used for 1962–77. These land-use time periods were based on a combination of factors including land use, climate, water levels, and historical events. The land-use pumpage estimates were used as initial agricultural pumpage for the simulation of ground-water flow but were adjusted for some periods during model calibration (fig. 11*B*). Municipal pumpage for the cities of Ventura, Camarillo, and Oxnard and for the Channel Islands Beach Community Services District (near Port Hueneme); pumpage for a fish hatchery in the southern end of the Piru subbasin; and pumpage of artificial recharge in the Oxnard Plain Forebay subbasin were estimated independently and combined with the agricultural pumpage for the total estimated pumpage prior to 1983.

Ground-water development continued to spread in the ground-water basin during the severe drought period of 1923–36, tapping deeper aquifers for agricultural supplies (fig. 2). As the surface-water resources became fully developed in the early 1930s, new ground-water development began to provide a significant proportion of the water resources. In the 1930s, the first deep wells were drilled in the Pleasant Valley and Las Posas Valley subbasins. Calculated agricultural pumpage, estimated from the 1927 land-use map, yields a basinwide average rate of withdrawal of about 128,400 acre-ft/yr for 1927 and an estimated total withdrawal of about 513,500 acre-ft for 1927–30. Calculated pumpage estimated from the 1932 land-use map is at about 174,000 acre-ft/yr, yielding an estimated total withdrawal of about 2,610,000 acre-ft for 1931–45. Estimates of agricultural pumpage, based on the 1950 land-use map, yield a basinwide average rate of pumpage of 180,000 acre-ft/yr and a total withdrawal of about 2,880,000 acre-ft for 1946–61.

By 1967, about 800 wells equipped with deep-well turbine pumps provided more than 90 percent of the water demand in the basin (Freeman, 1968). On the basis of 1969 land use, estimates of agricultural pumpage yield a basinwide average rate of withdrawal of about 201,700 acre-ft/yr, yielding an estimated total pumpage of 3,227,200 acre-ft for 1962–77.

Reported pumpage was compiled from the technical files of the FGMA and UWCD for July 1979–December 1993. These data generally were semiannual totals of user-reported agricultural, nonagricultural, and total pumpage. Early pumpage data were incomplete for the Las Posas Valley, Pleasant Valley, and Santa Rosa Valley subbasins. For these areas, 1984 FGMA reported pumpage was used to represent pumpage for 1978 through 1983. Estimated and reported total annual pumpage were combined for the entire Santa Clara–Calleguas Basin and range from 760 acre-ft for 1912 to as much as 301,400 acre-ft for 1990, which was during the last sustained drought.

Reporting of metered pumpage began in the 1980s; the total reported basinwide pumpage was 2,468,610 acre-ft during the 10-year period 1984–93 (Greg Middleton, United Water Conservation District, written commun., 1994). Of this reported total pumpage, 37 percent was from the Oxnard Plain subbasin, 37 percent from the upper Santa Clara River Valley subbasins, 13 percent from the Las Posas Valley subbasin, 9 percent from Pleasant Valley subbasin, 3 percent from the Mound subbasin, and 1 percent from the Santa Rosa Valley subbasin.

Evapotranspiration

Evapotranspiration (ET) from the regional ground-water flow system is restricted to the river flood plains, where ground water and streamflow infiltration are within the depths of the root zones of riparian vegetation. ET was not calculated for parts of the coastal areas of the Oxnard Plain subbasin where the Shallow aquifer is "semiperched."

Previous estimates of annual ET for the Santa Clara River Valley subbasins range from 11,700 acre-ft/yr for 1892–1932 (California Department of Public Works, 1934) to 13,724 acre-ft/yr for 1958–59 (Mann and Associates, 1959). The estimated average ET for the entire Santa Rosa Valley subbasin for 1972–83 is about 4,300 acre-ft/yr (Johnson and Yoon, 1987). Previous estimates of the ET rate vary widely, ranging from 1.1 ft/yr (California Department of Water Resources, 1974a,b) to 2.4 ft/yr (California Department of Public Works, 1934) to as much as 5.2 ft/yr (Mann and Associates, 1959).

The total area classified as land with riparian vegetation or as a flood plain was estimated from the five land-use maps (1912, 1927, 1932, 1950, 1969) compiled for the RASA study (Koczot, 1996; Predmore and others, 1997). A combination of riparian land distributions from the 1912, 1927, 1932, and 1950 maps of the Conejo Creek area yields an estimated total of 14,945 acres of riparian vegetation along the stream channels for predevelopment conditions in the basin. The 1932 land-use map for the entire basin indicates a total riparian area of 11,237 acres. The most detailed set of land-use maps (1950) for the entire basin yielded a reduction to 6,539 acres of riparian land by 1950. By 1969, the total was only 2,265 acres. The model, developed for this phase of the RASA study, was used to simulate the evapotranspiration along the flood plain of the Santa Clara River, Calleguas Creek, and its major tributaries.

Coastal Flow along Submarine Outcrops

Discharge from the regional ground-water flow systems probably occurs as lateral flow to the Pacific Ocean through outcrops that are exposed along the steep walls of the submarine canyons and that truncate the submarine shelf farther offshore. Because of the alternating layers of coarse- and fine-grained sedimentary deposits in these coastal aquifer systems, submarine leakage through the tops of the upper- and lower-aquifer systems that crop out along the submarine shelf probably is small. Outside of some folklore, there are no estimates or evidence, such as cold seeps, of submarine discharge in the Ventura area. However, the possibility of seawater intrusion along the coastal Oxnard Plain subbasin has long been recognized (Grunsky, 1925; California Department of Public Works, 1934; Freeman, 1968); geochemical evidence of seawater intrusion in the upper- and lower-aquifer systems (Izbicki, 1991, 1992, 1996a) indicates a hydraulic connection to the submarine outcrops of the aquifer systems (figs. 7 and 8). Coastal flow was estimated using the ground-water flow model developed for this study and is described later in the report (see Simulation of Ground-Water Flow).

Borehole electromagnetic-induction (EM) logs of monitoring wells installed as part of the RASA Program indicate that seawater intrusion occurs along multiple coarse-grained beds that are commonly, but not exclusively, the basal units of the seven major aquifers that compose the upper- and lower-aquifer systems (figure A5.2 in Appendix 5). These basal units commonly occur above regional unconformities that are related to the major sea-level changes during the Pleistocene epoch. Natural gamma and EM geophysical logs collectively indicate that the flow of seawater from the ocean occurs laterally through the submarine outcrops and remains confined to the most transmissive coarse-grained beds that are bounded by fine-grained layers (figure A5.2 in Appendix 5). A cross-sectional solute transport model developed for the Port Hueneme area supports the conceptual framework of lateral intrusion, with vertical intrusion impeded by shallow fine-grained confining units (Nishikawa, 1997). Seawater intrusion forms a relatively sharp interface with fresh ground water as it enters the basal coarse-grained beds of the aquifer systems laterally and remains stratified in the layered coastal alluvial-aquifer systems of the Santa Clara–Calleguas Basin.

Ground-Water Levels, Movement, and Occurrence

The largest source of discharge from the ground-water flow system in the Santa Clara–Calleguas Basin is pumpage. Pumpage has caused water-levels to decline below sea level (fig. 12) which has resulted in seawater intrusion and changes in ground-water quality, altered ground-water vertical-hydraulic gradients, reduced streamflow, reduced in ET, and caused land subsidence. Long-term hydrographs of water levels in production wells (figs. 13 and 14) and in the multiple-zone observation wells (fig. 15) show fluctuations driven by multiple-year to decadal changes in recharge and seasonal to multiple-year changes in pumpage.

Upper- and Lower-Aquifer-System Water Levels

Little information exists on predevelopment water levels in the upper- or lower-aquifer system during the periods of early ground-water development. In the 1870s, wells near the coast on the Oxnard Plain subbasin were reported to deliver water to the second floor of homes under the natural artesian pressures of the Oxnard aquifer (Freeman, 1968). Several early ground-water-level maps were constructed for parts of the basin (Adams, 1913; Grunsky, 1925), but the first map of the entire basin was completed for fall 1931 (California Department of Public Works, 1934), which was during a period of agricultural development and a severe drought (1923–36, fig. 2).

As the surface-water resources became fully used in the early 1930s, ground-water development began to provide a significant part of the water resources. If the conditions in 1931 represent, in part, conditions prior to major ground-water development, then ground water in all the aquifers initially moved from the landward recharge areas toward the west or southwest to the discharge areas along the submarine outcrops offshore in the Pacific Ocean (fig. 12*A*). By the 1930s, water levels had declined as a result of the 1927–1936 drought (figs. 12*A* and 13), changing from artesian-flowing conditions of the late 1800s to below or near land surface in most wells completed in the upper-aquifer system in the Oxnard Plain subbasin (fig. 13). The effects of ground-water development and overdraft first appeared in 1931 when water levels in wells in parts of the Oxnard Plain declined below sea level (Freeman, 1968). In the 1930s, the first deep wells were drilled in the Pleasant Valley and Las Posas Valley subbasins. Before development, water levels in the lower-aquifer system probably were higher, but the water-level patterns probably were similar to the patterns shown in figure 12*A* for 1931.Well owners in coastal areas began to recognize the connection between the ground-water reservoirs and the ocean when they observed that water-level changes in wells corresponded with the rising and falling phases of the ocean tides (Freeman, 1968). The Santa Clara Water Conservation District officially recognized the linkage between overdraft and seawater intrusion in their annual report of 1931 (Freeman, 1968).

Ground-water pumpage increased during the 1940s with the widespread use of the deep turbine pump. The effects of permanent overdraft were exemplified by the lack of recovery of water levels to historical levels after the spring of 1944, which marked the end of the wettest climatic period in the 103 years of historical rainfall record at Port Hueneme (fig. 2*A*). The effects of overdraft also were recognized landward in the Santa Clara River Valley when ground-water levels declined about 20 ft in the Fillmore subbasin (fig. 14). Water levels in the southern Oxnard Plain and Pleasant Valley were below sea level by 1946 (Freeman, 1968). In 1949, water-level altitudes were 30 ft below sea level in parts of the Oxnard Plain subbasin, and one of the first wells intruded by seawater was identified along the coast in the Silver Strand well field (north of Port Hueneme) (Freeman, 1968). The direction of subsurface flow within the upper aquifers near the coast has been landward since approximately 1947 (California Department of Water Resources, 1958).

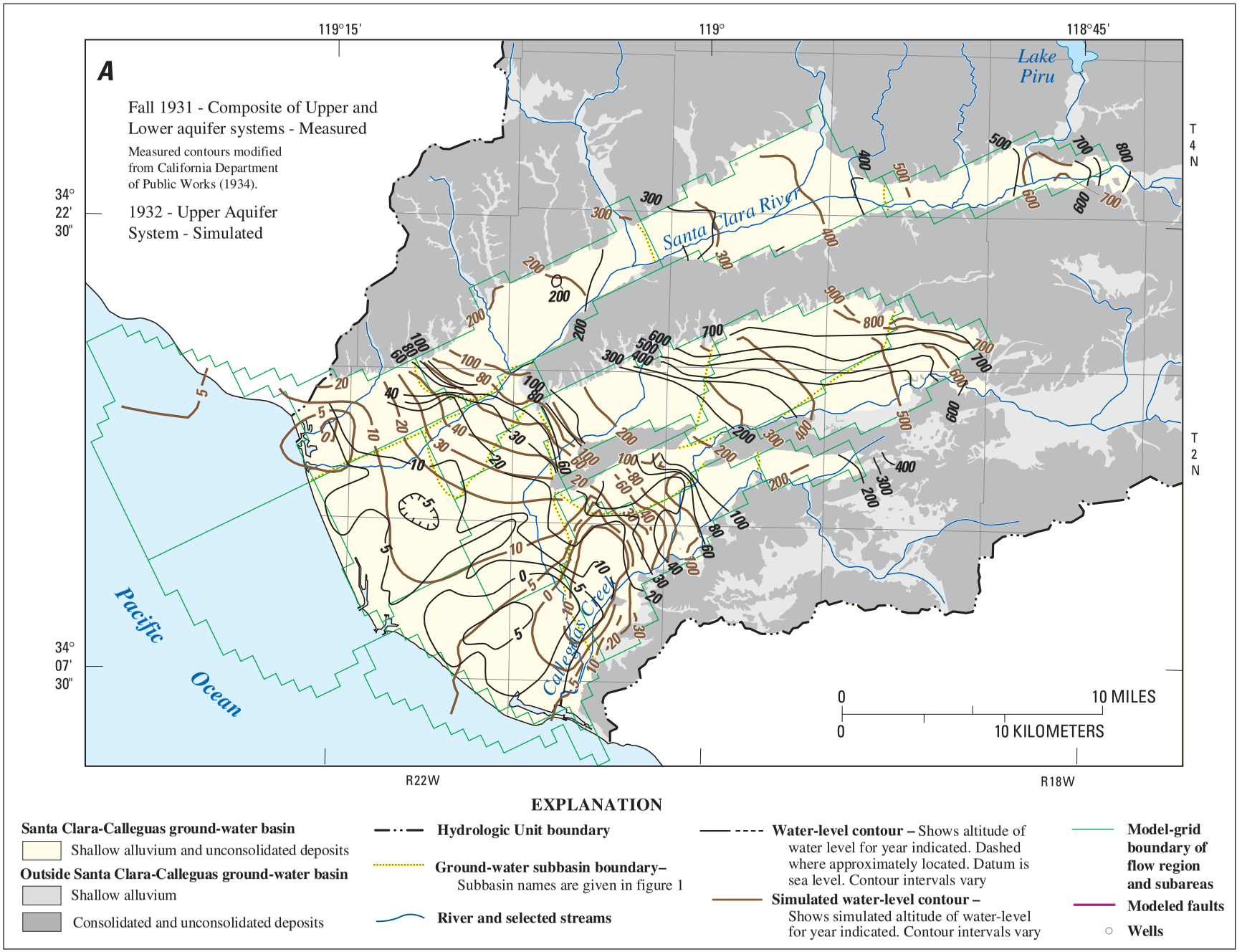

Figure 12. Ground-water level altitudes in the Santa Clara–Calleguas ground-water basin, Ventura County, California. ***A***, Fall 1932—Composite measured in upper- and lower-aquifer systems and simulated upper-aquifer system. ***B***, Spring 1993—lower-aquifer system. ***C***, Spring 1993—upper-aquifer system.

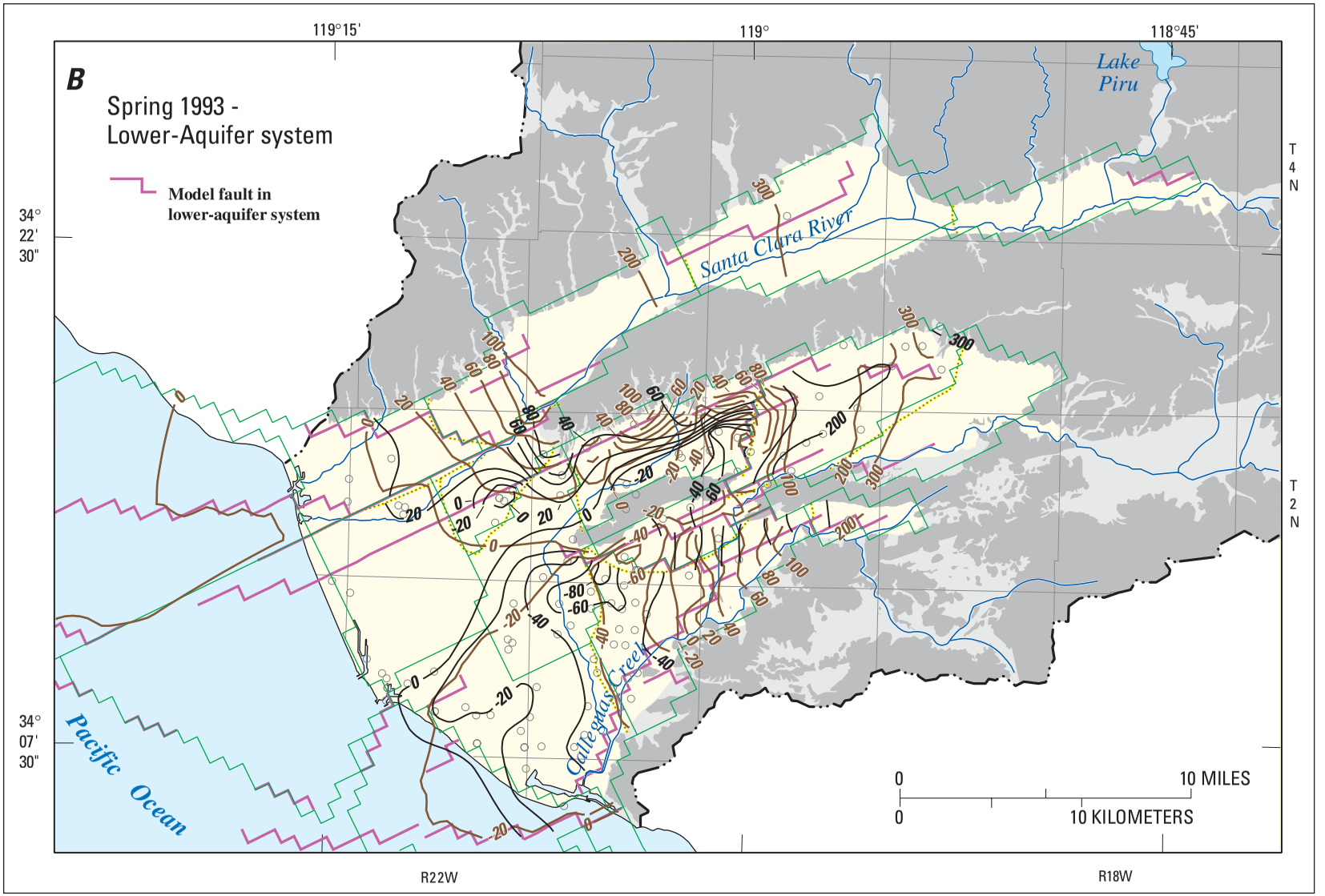

Figure 12—Continued.

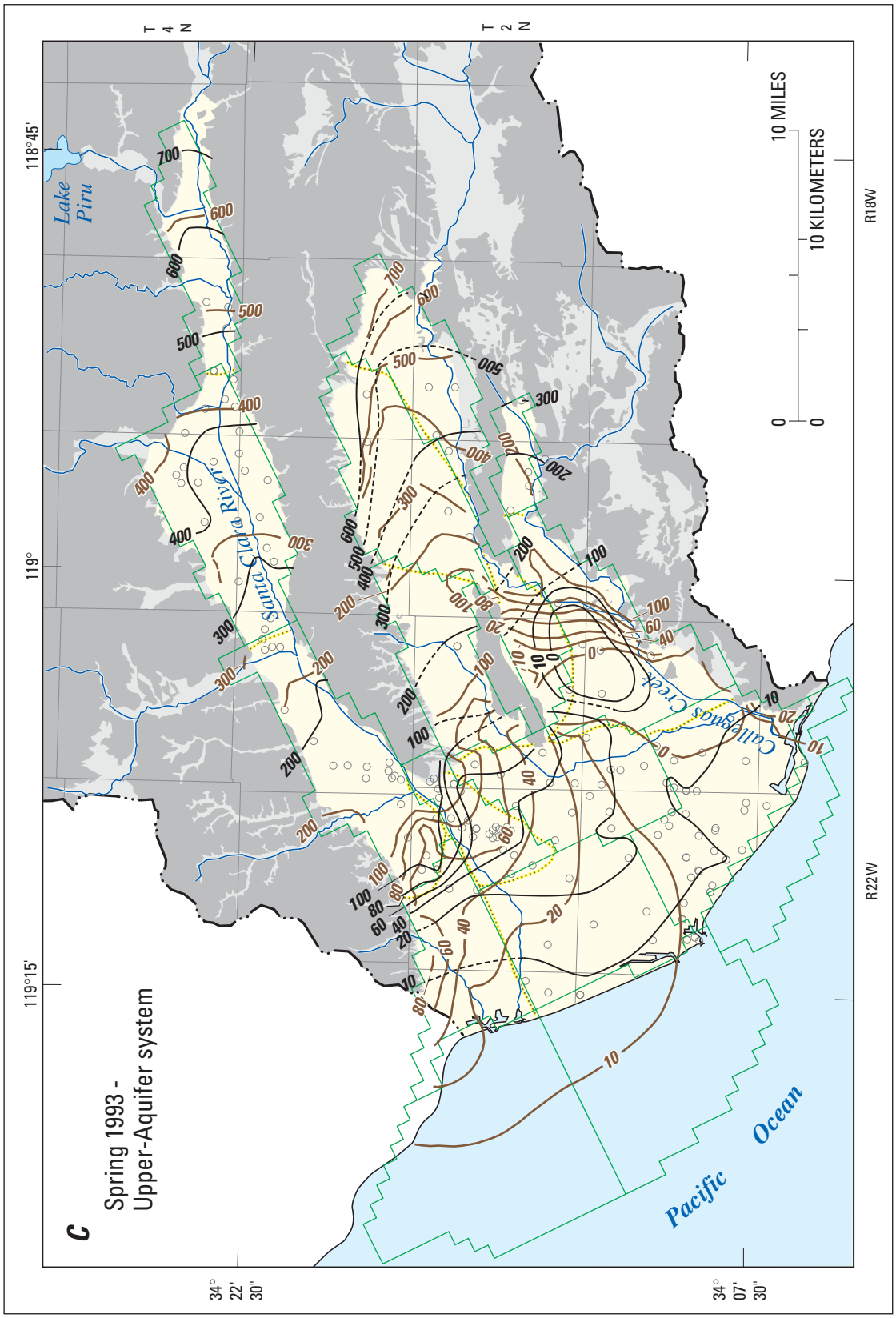

Figure 12—Continued.

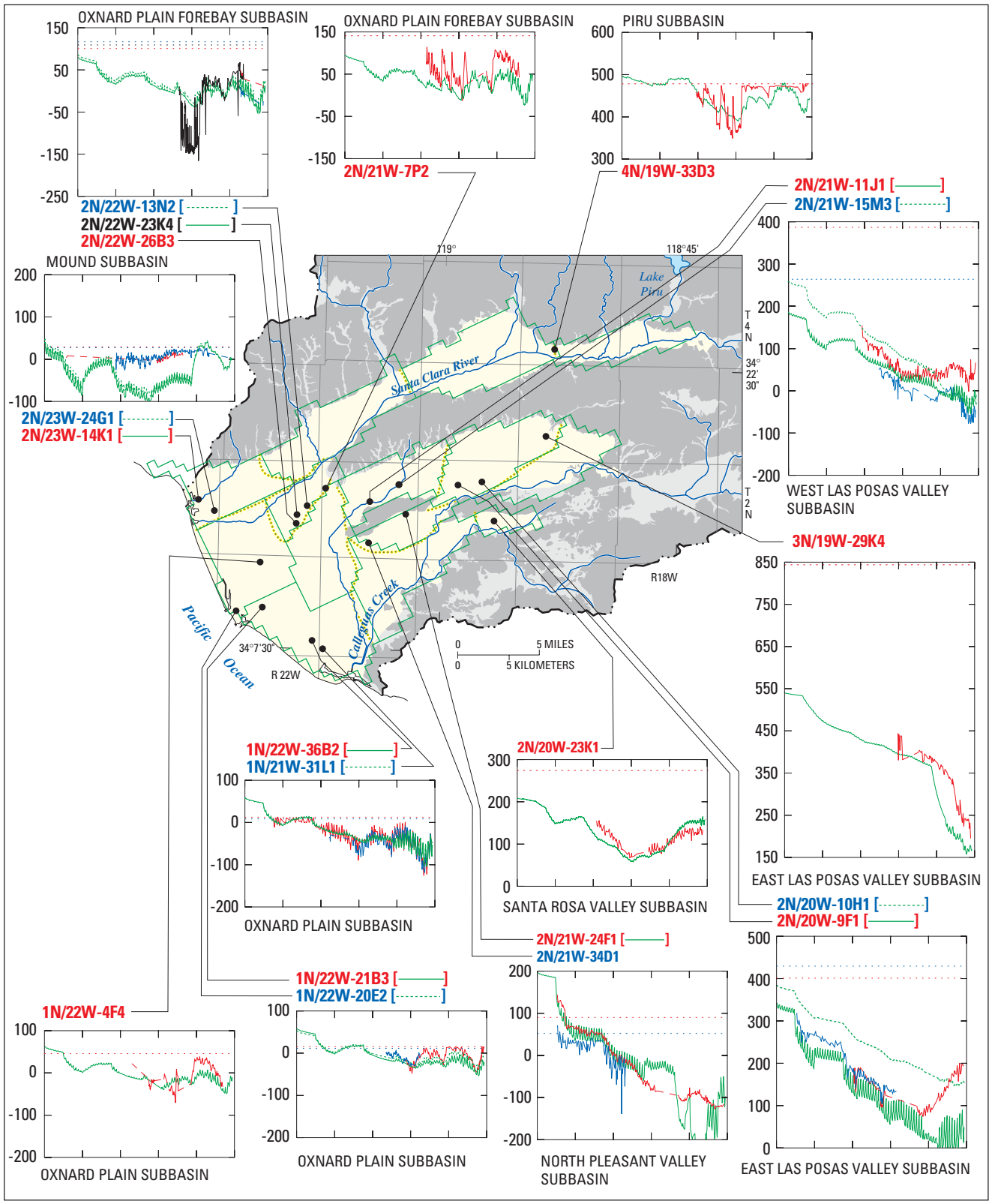

Figure 13. Measured and simulated water-level altitudes in wells completed in the lower-aquifer system of the Santa Clara–Calleguas ground-water basin, Ventura County, California.

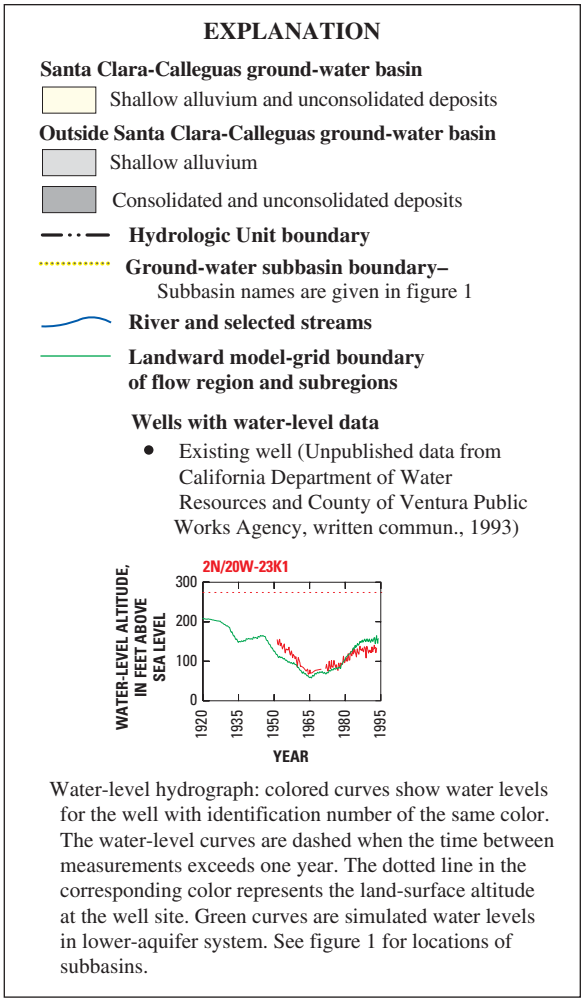

Figure 13—Continued.

When ground-water pumpage approached recorded maximum levels in 1951, which was at the end of a drought, water-level declines reached a new historical low in the upper-aquifer system (fig. 14) and levels began to decline significantly in the lower-aquifer system in the Oxnard Plain subbasin (fig. 13). By 1950, water levels had declined below sea level in the lower-aquifer system as far inland as the Pleasant Valley subbasin (fig. 13). Through 1950, water levels in most wells completed in the lower-aquifer system remained near land surface (fig. 13). Water levels in wells in the West and South Las Posas Valley subbasins indicate a water-level recovery in the upper-aquifer system beginning in the 1950s (fig. 14) related to increased irrigation return flow along Arroyo Simi and Beardsley Wash, importation of water which reduced local pumpage, discharge of pumped ground water into Arroyo Simi to control shallow ground-water levels, and discharge of treated municipal sewage into Arroyo Las Posas.

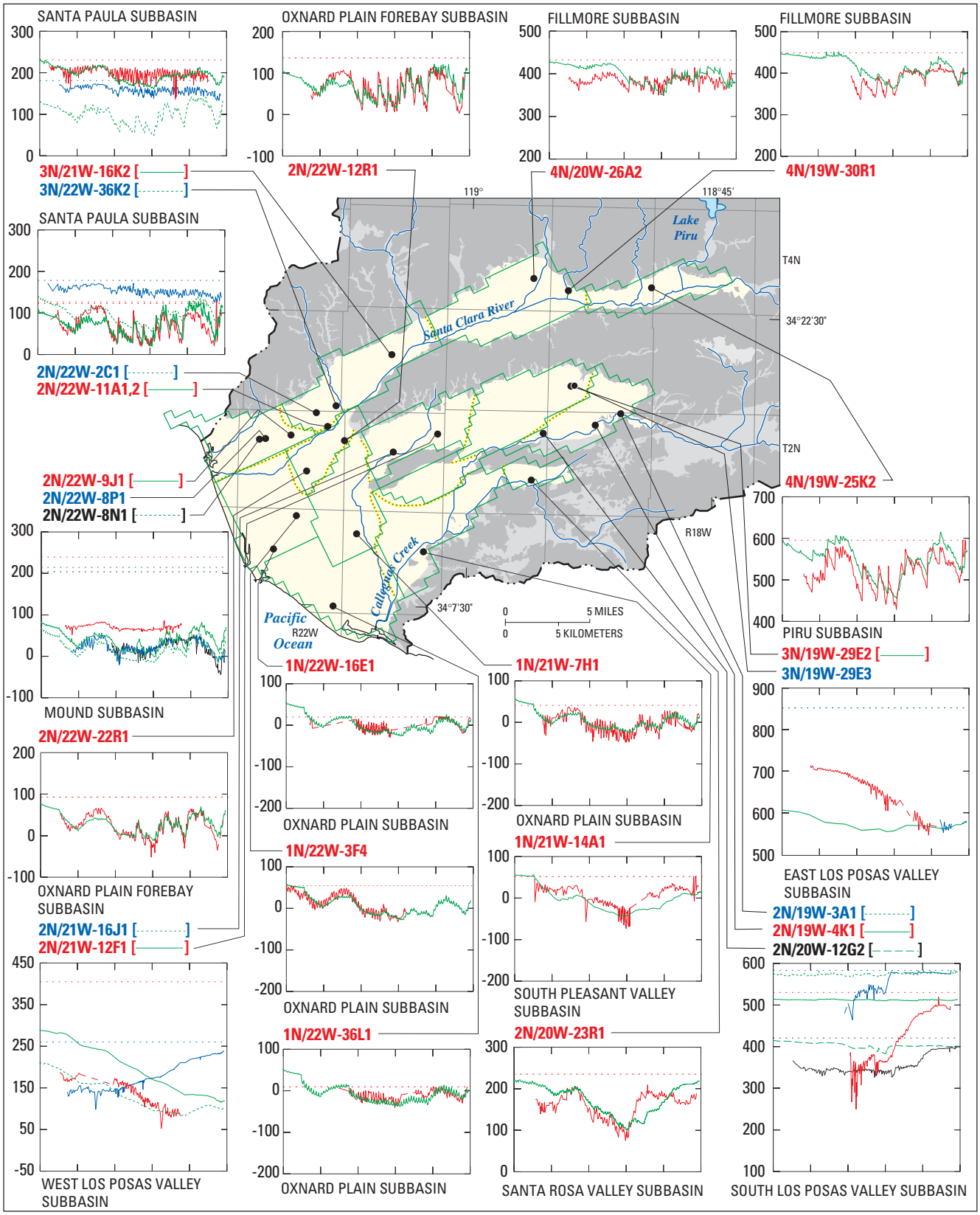

Figure 14. Measured and simulated water-level altitudes in wells completed in the upper-aquifer system of the Santa Clara–Calleguas ground-water basin, Ventura County, California.

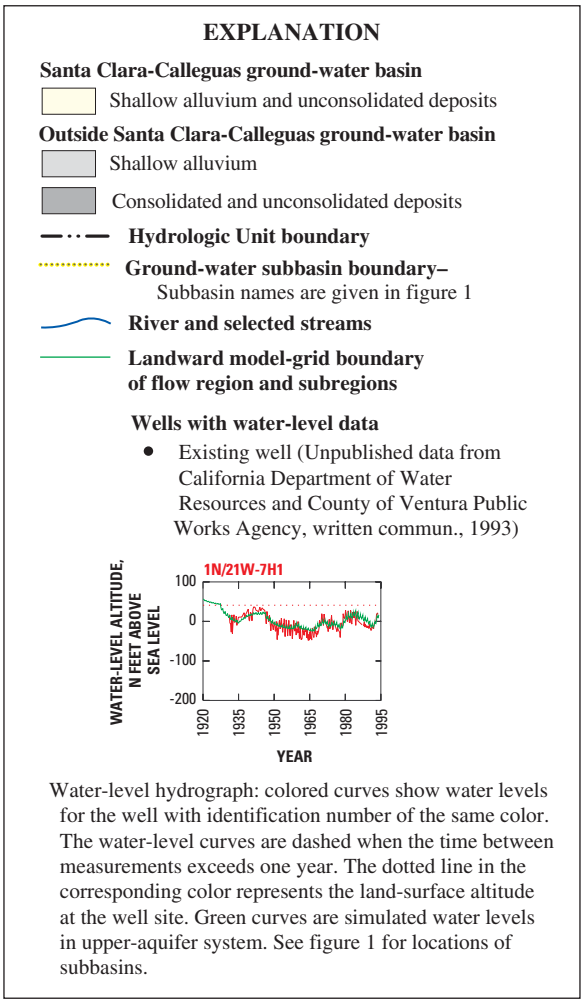

Figure 14—Continued,

The lowering of water levels continued in the upper- and lower-aquifer systems in the Oxnard Plain subbasin through the next dry period, 1959–64, furthering seawater intrusion (figs. 13 and 14). Water-level hydrographs (fig. 13) for many wells in the lower-aquifer system in the North Pleasant Valley and the Las Posas Valley subbasins indicate a monotonic decline through the 1950s and 1960s. Water levels started to recover in the Santa Rosa Valley subbasin beginning around 1965 because of decreased pumpage in the upper- and lower-aquifer systems and discharge of treated municipal sewage into Conejo Creek (figs. 13 and 14). The hydrographs of wells in the Mound subbasin and wells near the Hueneme submarine canyon (figs. 13 and 14) show little to no additional decline during these decades. By the late 1960s, thousands of acres of aquifer had been intruded by seawater in the Port Hueneme and Point Mugu areas, and coastal farmland had been lowered by land subsidence (see “Land Subsidence Effects”) owing to several decades of sustained overdraft.

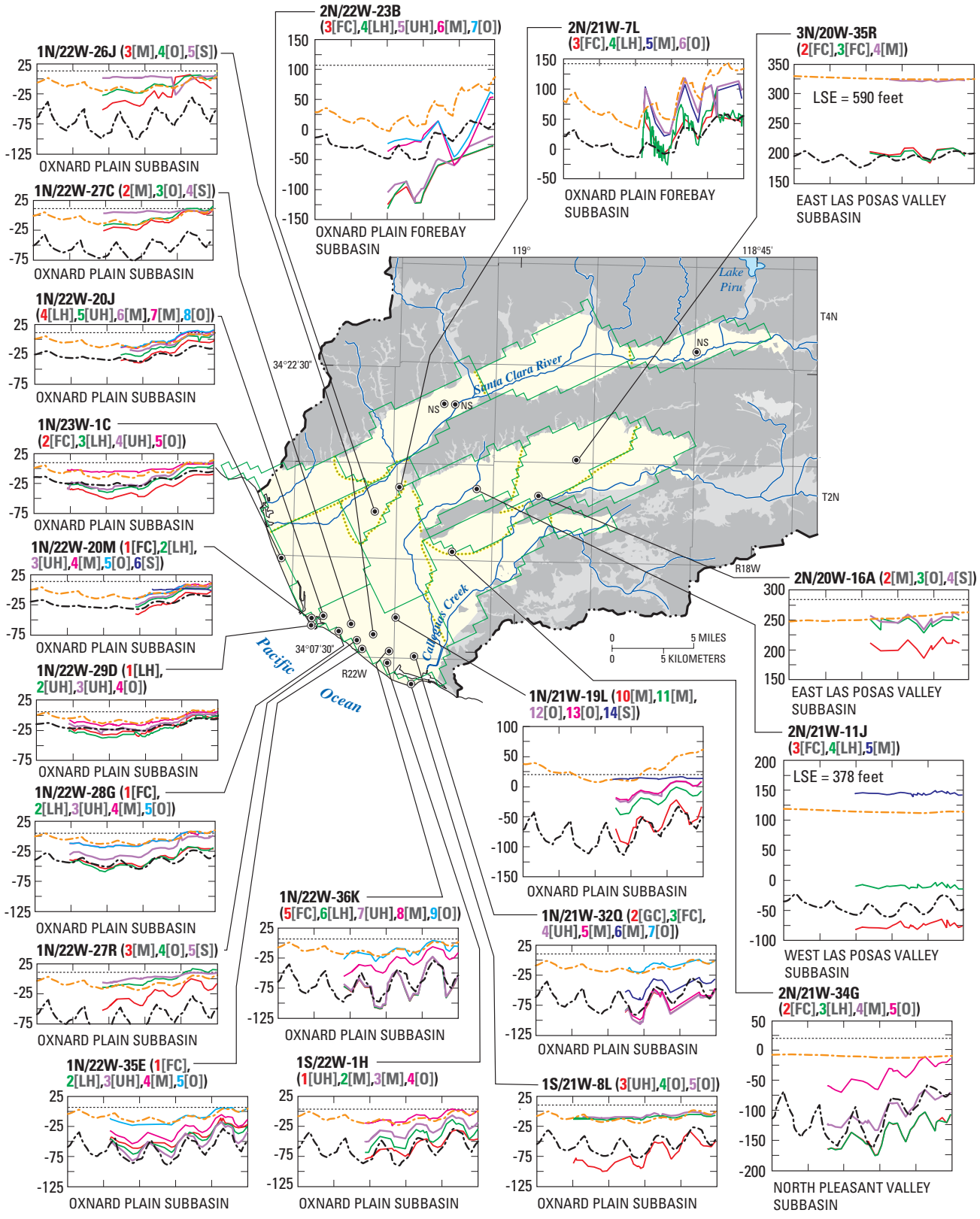

Figure 15. Measured and simulated water-level altitudes at sites with multiple wells of different depths completed in the Santa Clara–Calleguas ground-water basin, Ventura County, California.

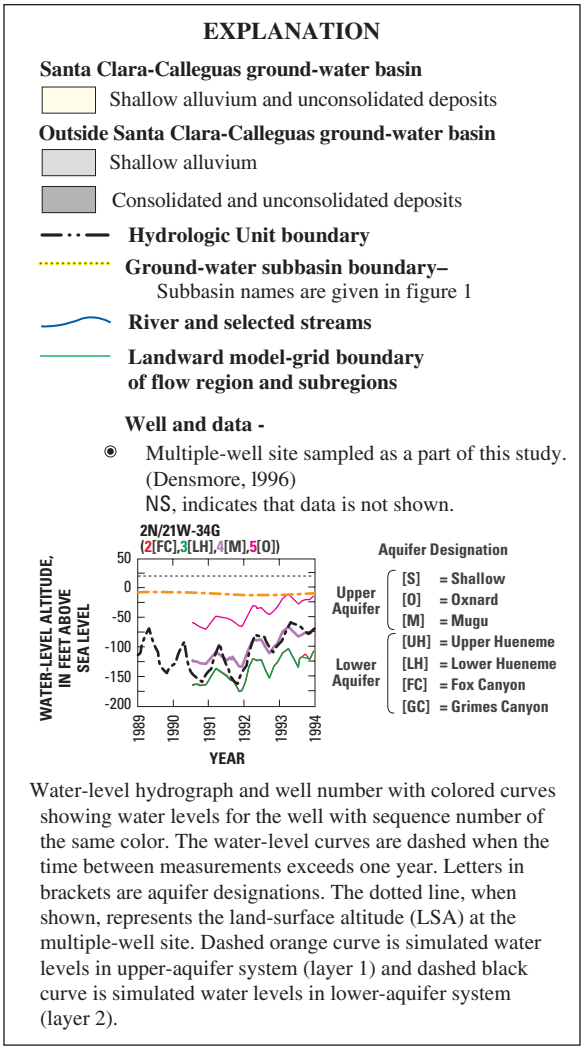

Water-level hydrograph and well number with colored curves showing water levels for the well with sequence number of the same color. The water-level curves are dashed when the time between measurements exceeds one year. Letters in brackets are aquifer designations. The dotted line, when shown, represents the land-surface altitude (LSA) at the multiple-well site. Dashed orange curve is simulated water levels in upper-aquifer system (layer 1) and dashed black curve is simulated water levels in lower-aquifer system (layer 2).

Figure 15—Continued.

Water levels in both aquifer systems in the Oxnard Plain subbasin partially recovered in the late 1960s owing to increased artificial recharge in the Oxnard Plain Forebay subbasin and natural recharge owing to a wetter climate. The water levels from wells in the upper-aquifer system in the Santa Clara River Valley subbasins also showed recovery during the late 1960s and early 1970s. The absence of wells completed in the lower-aquifer system in the upper Santa Clara River Valley subbasins precluded an assessment of the history or distribution of water levels there. Data from wells in the East Las Posas Valley subbasin indicate that water-levels began to recover in the late 1970s. This recovery was related to importation of water that reduced local pumpage, discharge of pumped ground water into Arroyo Simi to control shallow ground-water levels, and discharge of sewage effluent into Arroyo Las Posas. Similar water-level recoveries in the Santa Rosa Valley subbasin began in about 1965 (figs. 13 and 14) owing to decreased pumpage and discharge of sewage effluent into Conejo Creek and some water-level recovery near stream channels in shallower wells.

By the end of the most recent drought (1987–91), water levels were below sea level throughout the Oxnard Plain, Mound, and Pleasant Valley subbasins in both aquifer systems and below sea level in the lower-aquifer system throughout the West Las Posas Valley subbasin. In the inland subbasins, such as the South Pleasant Valley and West Las Posas Valley subbasins, water levels in many of the wells were near the historical lows in 1991 (figs. 13 and 14).

Beginning in 1992, which is the start of the most recent wet period, there was an increase in recharge owing to, in part, the increased capacity for artificial recharge at the Freeman Diversion and to a temporary reduction of pumpage from the coastal subbasins owing to increased surface-water supplies through pipeline deliveries, conservation practices, and new irrigation technology that increased irrigation efficiency. Pumpage was reduced because of a drilling moratorium established by the FGMA in 1983 on new wells completed in the upper-aquifer system in the Oxnard Plain. A comparison of the water-level maps for 1931 and 1993 indicates that by 1993 water levels had recovered in the upper-aquifer system and were greater than levels in 1931 (fig. 12*A*,*C*). Water levels in 1993 were about 5 ft higher near the coast, more than 20 ft higher in the Oxnard Plain Forebay than the 1931 levels, and above sea level throughout most of the Oxnard Plain. The water-level map for the lower-aquifer system shows that water levels were below sea level in the South Oxnard Plain subarea and Pleasant Valley subbasins (fig. 12*B*). Water-level data were not available for other inland subbasins for 1931; however, the hydrographs of long-term water levels indicate subdued fluctuations, or decline and recovery cycles (fig. 14), that may indicate that the shallower parts of the upper-aquifer system in these ground-water subbasins had recharged owing to increased streamflow during wet periods or increased discharge of treated sewage effluent.

Water-Level Differences Between Aquifers

Differences in water levels occur between the different aquifers (fig. 15) in the Santa Clara–Calleguas Basin. The water levels in the coastal Oxnard aquifer are lower than the water levels in the Shallow aquifer during dry-year periods and become higher than the water levels in the Shallow aquifer during recoveries (fig. 15) in wet-year periods. Large water-level differences occur between the Shallow and the underlying aquifers during the irrigation season, especially within the South Oxnard Plain subarea. These differences are primarily due to thick deposits of silt and clay in the Shallow aquifer that retard the movement of ground water between the Shallow and the Oxnard aquifers. Water levels for the RASA monitoring wells completed in the Shallow aquifer show little seasonal change owing to ground-water pumping or precipitation (fig. 15). Other shallow wells in the northern part of the Oxnard Plain subbasin show rises that are related to precipitation and declines that may be related to leakage (Neuman and Gardner, 1989, figs. 2 and 3). Previous investigators estimated that vertical leakage from the shallow semiperched system to the Oxnard aquifer ranges from 6,000 acre-ft/yr (California Department of Water Resources, 1971) to 20,000 acre-ft/yr (Mann and Associates, 1959).

Similarly, wells with depths of less than 50 ft completed in the Santa Clara River Valley subbasins also have higher water levels than those of nearby wells completed deeper in the upper-aquifer system. These elevated water levels may indicate some degree of hydraulic separation between the Shallow (recent alluvium) aquifer and the underlying aquifer along the Santa Clara River.

Except for those wells tapping the Shallow aquifer, water levels in wells in the coastal subareas and Santa Clara Valley subbasins indicate spring and summer declines followed by recovery during late fall and winter of each year. The seasonal fluctuations in wells in the upper-aquifer system are comparable with the changes in the wells in the lower-aquifer system north of the Hueneme submarine canyon. In the Oxnard Plain subbasin south of the Hueneme submarine canyon and in the Pleasant Valley subbasin, seasonal fluctuations in water levels are greater in the lower-aquifer system than in the upper-aquifer system. The smaller water-level differences and seasonal fluctuations near Port Hueneme are partly due to the source of water (seawater intrusion) along the near-shore submarine canyon outcrops, which tends to subdue the water-level fluctuations and changes in water levels between aquifers. In contrast, the larger water-level differences near Point Mugu are, in part, due to offshore faulting, which creates a barrier to ocean inflow for the lower-aquifer system. However, wells completed in the Mugu aquifer have water-level fluctuations that are similar to those of the lower-aquifer system. The similarity in seasonal fluctuations in the Mugu aquifer and the lower-aquifer system, in part, may be due to well-construction practices; well screens typically span the Mugu aquifer and parts of the lower-system aquifers. Flowmeter logs of wells screened opposite both the Mugu aquifer and the lower-aquifer system indicate a significant contribution from the Mugu aquifer (table 5). Water levels in the Pleasant Valley subbasin are about 50 ft lower in the Mugu-equivalent aquifer than water levels in the Oxnard-equivalent aquifer. This sustained water-level difference, along with water-level responses measured during short-term aquifer tests (Hanson and Nishikawa, 1996) and geophysical data (Densmore, 1996; Appendix 6), indicates that these aquifers are separated by fine-grained confining beds. The difference in water levels between the Oxnard aquifer and the lower-aquifer system increases during periods of pumping and decreases during seasonal periods of recovery.

Water levels in the lower-aquifer system were consistently more than 100 ft lower than water levels in the upper-aquifer system in the inland subbasins of Pleasant Valley, West Las Posas Valley, and East Las Posas Valley. For the inland Santa Clara River Valley subbasins, water-level differences in the Piru and Santa Paula subbasins were 10 to 25 ft lower for water levels in the lower-aquifer system than for levels in the upper-aquifer system.

Inter-Aquifer Flow

Flow between aquifers can be an important consideration in the management of water resources. Vertical water-level differences (figs. 13–15) indicate the potential for upward and downward flow between aquifers and aquifer systems. However, these differences can result in appreciable leakage only if a conductive pathway is present. Vertical flow between aquifers can occur as leakage through coarse-grained sedimentary layers, through and around fine-grained layers, and as vertical flow in and around well bores.

Vertical flow between the semiperched and the upper-aquifer systems also can occur through failed and abandoned wells (Stamos and others, 1992). Estimates of the number of abandoned and potentially failed wells range from 167 (Predmore, 1993) to 238 (Ventura County Resource Management Agency, Environmental Health Department, 1980) in the Oxnard Plain and as many as 1,215 wells throughout Ventura County (Predmore, 1993). Wellbore heat-pulse flowmeter tests in selected wells in the Oxnard Plain subbasin indicate that intraborehole flow rates of 3 to 11 gal/min may occur in some failed wells. This suggests a total maximum leakage of about 800 to 4,220 acre-ft/yr for periods when the hydraulic gradients are downward. The hydrographs for the multiple-observation well sites show that the heads in producing aquifers can vary seasonally and climatically (fig. 15). Thus, during wet-year periods or during periods of reduced pumpage, heads in the aquifer system can result in intraborehole discharge from the ground-water flow system to the overlying semiperched systems. Conversely, during dry-year periods or in areas of increased pumpage, heads in the semiperched system could be greater than heads in the underlying aquifers and could result in leakage as recharge to the ground-water system. For example, wellbore leakage of as much as 11 gal/min was measured with a heat-pulse flowmeter in failed monitoring well 1N/22W-27R2. However, detailed chemical sampling at nearby multiple-completion monitoring wells 1N/22W-27R3–5 (Izbicki, 1996a) indicates that the effects of this wellbore leakage were not areally extensive.

Vertical flow also can occur from the underlying marine sedimentary rocks or from brines related to oil deposits. Methane is reported to discharge from some production wells that are completed to depths just above the oil fields just west of Pleasant Valley in the Oxnard Plain subbasin (fig. 9). Geochemical data indicate that the amounts of leakage from deeper and older formations in the southern part of the Oxnard Plain and South Pleasant Valley subbasins probably are small (Izbicki, 1991, 1996a, figs. 3 and 5).

Source of Water to Wells

The relative contribution of water to wells completed in multiple aquifer systems is dependent on the local stratigraphy and on well construction. The vertical distribution of ground-water withdrawals from wells was estimated from flowmeter logs of 17 wells completed as part of the RASA Program and other studies (table 5, fig. 17*B* presented later in the "Model Boundaries" section, figure A5.1 in Appendix 5). Where wells are perforated across younger aquifers and older aquifers, most of the water is produced from the more transmissive younger aquifers [table 5, figure A5.1 in Appendix 5]. Combined with the stratigraphy, flowmeter logs indicate that the most productive and areally extensive water-bearing zones commonly occur as basal coarse-grained layers that overlie major regional unconformities. However, the relative contribution to any particular well from less productive aquifers may increase with increased pumping rates and decreased water levels in the more productive aquifers (table 5).

The most important aspects of well construction are the vertical extent of the well screen and the depth and location of the pump intake relative to the well screen. Wells that are screened across the basal layer of the upper-aquifer system can derive as much as 70 percent of the wellbore inflow from this relatively thin layer. Wells that are completed only in the lower-aquifer system can derive 100 percent of the wellbore inflow from the basal coarse-grained layer in the Hueneme aquifer (table 5). Flowmeter logs are not yet available for wells throughout most of the Oxnard Plain and Las Posas Valley subbasins; for wells in all the Piru, Fillmore, and Santa Rosa Valley subbasins; and for wells screened only in the upper-aquifer system.

Source, Movement, and Age of Ground Water

The source, movement, and age of ground water in the Santa Clara–Calleguas Basin can be inferred from the isotopic content of ground-water and surface-water samples. Based on deuterium isotope samples, most of the water in the upper- and lower-aquifer systems is derived from streamflow infiltration of high-altitude precipitation along the Santa Clara River that originated largely as runoff of precipitation falling at the higher altitudes of the surrounding mountains (Izbicki, 1996b, fig. 3). Isotopic data also suggest a local contribution of mountain-front recharge and direct infiltration of locally derived precipitation in the Las Posas and Pleasant Valleys and along the margins of the Santa Clara River Valley (Izbicki, 1996b). Although a large component of irrigation return flow may contribute to infiltration, no large areas of the Oxnard aquifer in the Oxnard Plain had an isotopic signature similar to that of evaporated waters. Analysis of ground-water samples for the hydrogen isotope tritium indicates that recent recharge (since 1952) has occurred largely in the Santa Clara River Valley subbasin, the Oxnard Plain Forebay subbasin, the northwestern part of the Oxnard Plain subbasin, and the South Las Posas Valley subbasin (Izbicki, 1996b, fig. 5). Tritium data also indicate that the artificial recharge from the Oxnard Plain Forebay subbasin has largely infiltrated the upper-aquifer system. Ages determined by carbon-14 analysis of ground-water samples indicate that water in the upper-aquifer system directly beneath the Saticoy spreading grounds is relatively young (less than 500 years old), but water in the lower-aquifer system beneath the El Rio spreading grounds ranges from 700 to more than 13,000 years old (Izbicki, 1996b, fig. 6). Samples from the lower-aquifer system near the coast range from about 7,000 to 23,000 years old (Izbicki, 1996b, fig. 6). Samples from wells in the Las Posas Valley and Pleasant Valley subbasins yielded ages of about 700 to 6,000 years old (Izbicki, 1996b, fig. 7). Collectively, these data indicate that the upper-aquifer system is recharged by streamflow infiltration and mountain-front recharge; the lower-aquifer system has received little recent water; and ground water moved relatively slowly under the hydraulic gradients present prior to water development.

Table 5. Summary of well-construction data and discharge rates and inflows from flowmeter logs of wells in selected subbasins of the Santa Clara–Calleguas Basin, Ventura County, California

[State well No.: See well-numbering diagram in text. Total depth of well and depth to top and bottom of well screen in feet below land surface. —, no data]

State well No.	Local well name	Subbasin	Total drilled depth (feet)	Well casing diameter (inches)	Depth to top of well screen (feet)	Depth to bottom of well screen (feet)	Year of flowmeter log	Well-test discharge rate (gal/min)	Inflow	
									Percent from upper/lower aquifer systems	Percent from Oxnard/Mugu/Hueneme/Fox Canyon/Grimes Canyon system
1N/21W-3K1	PVCWD-WELL#04	South Pleasant Valley	1,453	18	403	1,433	1980[1]	1,000	17/83	—/17/3/17/63
							1991	1500	30/70	—/30/21/11/38
1N/21W-3R1	PVCWD-WELL#01	South Pleasant Valley	1,033	18	443	1,013	1980[1]	4,000	9/91	—/9/91/0/—
							1991	1,414	54/46	—/54/46/0/—
1N/21W-4D4	PVCWD-WELL#03	Oxnard Plain	1,341	18	571	1,321	1980[1]	2,000	—/100	—/—/5/36/59
							1991	1,168	—/100	—/—/19/26/55
1N/21W-4K1	PVCWD-WELL#05	South Pleasant Valley	1,240	18	400	1,220	1980[1]	2,000	4/96	—/4/5/60/31
1N/21W-8R1	PVCWD-WELL#07	Oxnard Plain	1,383	18	603	1,363	1980[1]	2,500	—/100	—/—/0/28/72
							1991	1,128	—/100	—/—/0/21/79
1N/21W-10G1	PVCWD-WELL#06	South Pleasant Valley	1,020	18	420	1,000	1979[1]	3,150	—/100	—/—/34/53/0
							1992	2,000	—/100	—/10/27/37/26
1N/21W-15D2	PVCWD-WELL#08	South Pleasant Valley	1,103	18	383	1,083	1980[1]	4,000	17/83	—/17/20/58/5
							1991	1,121	40/60	—/40/30/23/7
1N/21W-21H2	PVCWD-WELL#10	South Pleasant Valley	883	18	503	863	1980[1]	2,500	—/100	—/—/49/51/—
1N/21W-22C1	PVCWD-WELL#09	South Pleasant Valley	1,023	18	443	1,003	1980[1]	4,000	—/100	—/—/25/53/22
							1991	1,440	—/100	—/—/19/37/44
1N/21W-28D1	PVCWD-WELL#11	Oxnard Plain	960	9	463	923	1980[1]	2,000	—/100	—/—/58/42/—
							1991	1,100	—/100	—/—/100/0/—
1N/21W-31L1	PTMUGU#03	Oxnard Plain	702	12	350	700	1991	407	12/88	—/12/88/—/—
1N/22W-3F5	OXNARD#20	Oxnard Plain	1,126	18	526	1,106	1984[2]	2,000	—/100	—/—/71/29/—

Table 5. Summary of well-construction data and discharge rates and inflows from flowmeter logs of wells in selected subbasins of the Santa Clara–Calleguas Basin, Ventura County, California—Continued

State well No.	Local well name	Subbasin	Total drilled depth (feet)	Well casing diameter (inches)	Depth to top of well screen (feet)	Depth to bottom of well screen (feet)	Year of flowmeter log	Well-test discharge rate (gal/min)	Inflow	
									Percent from upper/lower aquifer systems	Percent from Oxnard/Mugu/Hueneme/Fox Canyon/Grimes Canyon system
2N/20W-20M5	SAINT JOHNS#6	North Pleasant Valley	700	18	480	700	1992[3]	500	—/100	—/—/58/42/—
							1992[3]	1,000	—/100	—/—/58/42/—
							1992[3]	1,500	—/100	—/—/53/47/—
2N/21W-34G1	PVCWD-WELL#02	South Pleasant Valley	1,483	18	403	1,463	1980[1]	4,000	—/100	—/—/25/75/0
							1992	2,065	—/100	—/—/25/67/8
							1993	2,065	—/100	—/—/18/68/14
2N/22W-8F1	VICTORIA-WELL#2	Mound	1,190	18	580	1,180	1994[4]	1,906	50/50	—/50/50/—/—
							1994	2,485	44/56	—/44/56/—/—
							1994	4,015	33/67	—/33/67/—/—
2N/22W-13N2	ELRIO#12	Oxnard Forebay	1,112	18	752	1,092	1983[5]	1,960	—/100	—/—/100/—/—
3N/21W-11J5	SANTA PAULA#12	Santa Paula	700	16	260	700	1991	1,000	100/0	—/100/0/—/—
							1991	1,500	73/27	—/73/27/—/—
							1991	2,500	72/28	—/72/28/—/—

[1]Data from Pleasant Valley Water Conservation District (Lee Miller, written commun.,1991).
[2]Data from Geotechnical Consultants, Inc. (Ted Power, written commun, 1992).
[3]Data from Fugro-McClelland, Inc. (David Gardner, written commun., 1993).
[4]Data from Fugro-McClelland, Inc. (Curtiss Hopkins, written commun., 1994).
[5]Data from United Water Conservation District (Jim Gross, written commun., 1991).

Land-Subsidence Effects

Ground-water withdrawals, oil and gas production, and tectonic movement are three potential causes of land subsidence in the Oxnard Plain and adjacent subbasins (fig. 9) (Hanson, 1995). Ground-water levels in the Oxnard Plain subbasin have declined steadily since the first wells were completed in the 1870s. Ground water, however, has remained a primary source of water since the early 1900s. Oil and gas has been produced in the Santa Clara–Calleguas Basin since the 1920s and in the Oxnard Plain subbasin since the 1940s. The basin is a part of the tectonically active Transverse Ranges physiographic province. Ventura County has delineated a probable subsidence-hazard zone that includes parts of the Piru, Fillmore, Santa Paula, Mound, Oxnard Plain Forebay, Oxnard Plain, and Pleasant Valley subbasins (Ventura County Board of Supervisors, 1988).

Since the early 1900s, water-level declines in the upper- and lower-aquifer systems in the Oxnard Plain subbasin have ranged from about 50 to 100 ft. Water levels in wells at the multiple-well monitoring sites are lower in the lower-aquifer system than in the upper-aquifer system—by 20 ft near the Hueneme submarine canyon along the central coast and by about 80 ft near the Mugu submarine canyon along the southern coast of the Oxnard Plain subbasin. Because early pumpage data are unavailable for the Oxnard Plain subbasin, the total quantity of water withdrawn is unknown. However, reported pumpage data indicate that during 1979–91 about 822,000 acre-ft of ground water was withdrawn from the Oxnard Plain subbasin at a relatively constant rate. This pumpage has resulted in water-level declines that, in turn, have increased the effective stress on the aquifer-system sediments. An increase in the effective stress on aquifer sediments beyond their preconsolidation stress results in compaction and reduction of pore space and mechanically squeezes water from sediments.

More than 7,900 acre-ft of brines, 8,000 acre-ft of oil, and 72 million cubic feet of natural gas were withdrawn from oilfields in the Oxnard Plain subbasin (fig. 9) between 1943 and 1991 (Steven Fields, Operations Engineer, California Department of Conservation, Division of Oil and Gas, written commun., 1992). Pressure declines equivalent to more than 1,100 ft of water-level decline have occurred in the Oxnard oilfields since the onset of oil and gas production. These declines alone could potentially account for local subsidence of 1.5 to 2.0 ft (California Division of Oil and Gas, 1977).

Tectonic activity in the form of plate convergence and north-south crustal shortening has resulted in an average regional horizontal movement in the subbasins north of the Oxnard Plain of about 0.007 ft/yr over the past 200,000 years (Yeats, 1983). Vertical movement, as uplift north of the Oxnard Plain subbasin and as subsidence in the Oxnard Plain subbasin, has been caused by plate convergence and related earthquakes throughout the basin. For the southern edge of the Oxnard Plain subbasin (fig. 9*A*), elevation data from bench marks (BM) on bedrock (for example, BM Z 583) indicate that the 0.17 ft of subsidence that occurred during 1939–78 (at a rate of about 0.004 ft/yr) may be related to tectonic activity.

Data from a coastal leveling traverse near the southeastern edge of the Oxnard Plain (fig. 9*A*,*B*) indicate that as much as 1.6 ft of subsidence occurred during 1939–60 at BM E 584 (0.07 ft/yr) and an additional 1 ft occurred during 1960–78 (0.06 ft/yr). During 1960–92, 0.5 ft of subsidence (0.02 ft/yr) was measured at BM Z 901, which is southwest of BM E 584 and at the edge of the coastal Oxnard Plain. Bench-mark trajectories (fig. 9*C*) indicate that subsidence continues and may be driven by extreme water-level declines that occur during drought periods. Farther inland, where water-level and oilfield pressure declines are largest, greater subsidence might be expected.

Indirect evidence that subsidence may be related to ground-water withdrawals includes water-level declines greater than 100 ft, subsurface collapse of well casings in the South Pleasant Valley subbasin and South Oxnard Plain subarea, required repeated leveling of irrigated fields for proper drainage, degraded operation of drainage ditches in agricultural areas, and lowering of levees along the Calleguas Creek in the South Pleasant Valley subbasin. In the Las Posas Valley and South Pleasant Valley subbasins, water-level declines of 50 to 100 ft have occurred in the upper-aquifer system, and declines of about 25 to 300 ft or more have occurred in the lower-aquifer system since the early 1900s (figs. 13 and 14). Owing to large water-level declines, the area of probable subsidence may be larger than that delineated by Ventura County and may include the Las Posas Valley subbasin and the remainder of the Pleasant Valley subbasin. By 1992, total subsidence in the Oxnard Plain subbasin could exceed the 2.6 ft measured during 1939–78 along the coastal traverse. Although the amount of subsidence from various sources remains unknown, ground-water withdrawals and oil and gas production probably are major causes of subsidence in the Oxnard Plain subbasin, and tectonic activity probably is a minor cause.

Water released by compaction of layers of fine-grained deposits within the upper- and lower-aquifer systems can be a significant additional one-time source of water to adjacent producing coarse-grained layers in the aquifer systems. Geochemistry data (Izbicki, 1996a, fig. 3) and geophysical data (EM and natural gamma logs in Appendix 5) indicate that fine-grained beds may be a significant source of the poor-quality water in areas such as the South Oxnard Plain subarea in the coastal region between the Hueneme and Mugu submarine canyons where saline fine-grained layers and seasonal pumpage may collectively contribute to poor-quality water.

SIMULATION OF GROUND-WATER FLOW

A numerical ground-water flow model of the two regional aquifer systems (upper aquifers and lower aquifers) in the Santa Clara–Calleguas Basin was developed to simulate steady-state predevelopment conditions prior to 1891 and transient conditions for the development period January 1891–December 1993. The model simulations provided information concerning predevelopment hydrologic conditions and aquifer response to changes in pumpage and recharge through time. Simulations were made using the three-dimensional finite-difference ground-water flow model (MODFLOW) developed by McDonald and Harbaugh (1988). Additional packages were incorporated into the ground-water flow model to simulate the routing of streamflow (Prudic, 1989), land subsidence (Leake and Prudic, 1991), and faults as horizontal barriers to ground-water flow (Hsieh and Freckleton, 1993).

Transient simulations were calibrated for the period of historical systematic data collection, which generally spans from the 1920s through 1993. The most important period of the calibration spans the period of reported pumpage (1984–93). Simulation results and model calibration provided insight into the conceptual model of the regional flow system, and into the limitations and potential future refinements of the regional-scale model. The model also was used to analyze the distribution of flow and changes in storage during 1984–93, to project future ground-water flow, and to evaluate alternatives to future projected ground-water flow. The analysis allowed assessment of water-resources management alternatives and of the effect that implementation of selected alternatives and geologic controls might have on recharge, coastal landward flow (seawater intrusion), land subsidence, ground-water movement, and overall resource management under climatically varying conditions that affect supply and demand.

Model Framework

The orientation, areal and temporal discretization, vertical layering, areal extent, and internal structural boundaries constitute the framework of the numerical ground-water flow model developed for this study. The model is an extension and refinement of the previously developed regional models and, as such, represents the RASA Program contribution to the continuing effort to evaluate and manage the ground- and surface-water resources of the Santa Clara–Calleguas Basin. Model attributes and related data have been added to the Geographic Information System (GIS) completed by the RASA Program (Predmore and others, 1997). The metadata that describe and document these additional GIS coverages are summarized in Appendix 1. The flow of information used to estimate and assemble the input data for the Recharge Package, Streamflow Package, and Well Package of the ground-water model is summarized in the flowcharts in Appendix 6.

Previous Models

Previous models of the area include basinwide digital Theissan-Weber Polygon superposition simulations of historical transient hydraulic and water-quality conditions for 1950–67 (California Department of Water Resources, 1974a,b, 1975), and numerical subregional ground-water flow models of the lower-aquifer system in the East and West Las Posas Valley subareas (CH2M HILL, 1993) and the upper- and lower-aquifer systems in the Santa Rosa Valley subarea (Johnson and Yoon, 1987). More recently, Reichard (1995) completed an extended and enhanced digital model based on the original Theissan-Weber Polygon model. Reichard extended this model areally to include the offshore coastal areas; like the regional model, it simulates the upper- and lower-aquifer systems in the Oxnard Plain subareas, the lower-aquifer system in the Las Posas Valley and Pleasant Valley subareas, and the upper-aquifer system in the Santa Clara River Valley subareas. The model uses estimates of recharge and pumpage for the historical simulation period (1984–89), which is the base period used to evaluate the FGMA management goals. Reichard's model was used to simulate the flow of ground water and to generate response surfaces for use in an optimization model. In turn, the optimization model was used to test different ground-water and surface-water allocation schemes that would satisfy water demands and minimize coastal landward flow (seawater intrusion). Nishikawa (1997) completed a cross-sectional transport model of a vertical section through the Hueneme submarine canyon to test alternative conceptual models of seawater intrusion for predevelopment conditions and for 1929–93 developed conditions. A numerical wellbore hydraulic model of an aquifer test in the lower-aquifer system in the South Pleasant Valley subarea was completed to test alternative conceptual models of the vertical distribution of hydraulic properties (Hanson and Nishikawa, 1992, 1996).

Model Grid

The model grid is oriented at N. 27° W. and contains 60 rows and 100 columns discretized into square cells with sides 0.5 mi in length (figs. 7, 16, and A1.4). Average values of aquifer properties and initial hydraulic head are assigned to each cell; average initial hydraulic head for each cell is assigned at the center, or node, of each cell. The model contains two layers, one each for the upper- and lower-aquifer systems. The two model layers were made identical in areal extent everywhere in the landward part of the model domain (fig. 16). The top of the upper layer is aligned with the bottom of the fine-grained layers that separate the semiperched shallow aquifer from the upper-aquifer system throughout the Northwest and South Oxnard Plain subareas. The top of the upper layer is coincident with the land surface throughout the remainder of the upper layer. The bottom of the upper layer and the top of the lower layer are coincident with the bottom of the Mugu aquifer. This boundary generally occurs at a depth of 400 ft in the Oxnard Plain subareas. The bottom of the lower layer is coincident with the bottom of the Fox Canyon aquifer throughout most of the model area (figs. 7*A* and 8).

The model was extended offshore farther in the northwest corner of the lower layer than previous models (California Department of Water Resources, 1974a,b, 1975; Reichard, 1995). The areal extent of the layers was based on the outcrop areas on the geologic map (Weber and others, 1976) on land, and the seaward extent was based on bathymetry and submarine outcrops estimated from geology maps (Kennedy and others, 1987). The upper layer (upper-aquifer system) (fig. 16*A*) is an active flow region covering 374 mi^2, of which about 27 percent is offshore. The lower layer (lower-aquifer system) (fig. 16*B*) is an active flow region of 464.5 mi^2, of which about 41 percent is offshore.

Temporal Discretization

The model was used to simulate the period from January 1891 through December 1993. This 103-year historical simulation of ground-water and surface-water flow was temporally discretized into 3-month periods (stress periods) that represent the four seasons within a calendar year. For computational purposes, streamflow, recharge, and pumpage from wells are specified for each season of every year. Each season was discretized into 12 equal time steps to estimate flow and heads throughout the model.

Model Boundaries

The perimeter of the active flow region within the model represents the approximate limit of the ground-water flow system. The boundary is represented by a combination of no-flow, constant-flux, and general-head boundaries. Except where mountain-front recharge enters the model along the boundaries of the landward active flow region (fig. 17*A*), the landward model cells along this outer boundary of both model layers are represented as a no-flow boundary. No-flow boundaries occur where there is no flow of water between the active flow-region model cells and the adjacent areas. The bottom of the lower layer is also represented as a no-flow boundary; this layer generally is coincident with the base of the Fox Canyon aquifer except in the Santa Rosa Valley, East Las Posas, and parts of the Pleasant Valley subareas. These no-flow boundaries represent the contact with non-water-bearing rocks. Mountain-front recharge that enters along stream channels in the upper layer and at the outcrops of the Santa Barbara Formation outside of the active flow system in the lower layer are constant-flux boundaries (described later in this section). The constant-flux boundaries are specified flows that change with every season (stress period) of each year for the period of simulation.

The offshore boundary in both layers is represented as a strong source-sink boundary; this boundary is located at the geographic location of the seawater intrusion front identified by Greene and others (1978). This boundary is represented in the model as a general-head boundary simulating inflow (source) of water from outside the model area or discharge (sink) of water from the boundary model cells to outside the model area. Flow at this boundary is proportional to the hydraulic-head difference between the equivalent freshwater head of the ocean along the submarine outcrops and the head of the model cells that are coincident with the boundary (fig. 16). Flow at this boundary is also proportional to the hydraulic conductance. Hydraulic conductance was determined during model calibration and represents the impediment to flow at the seawater intrusion boundary in each layer. For the purposes of this report, coastal inflow along this boundary is termed coastal landward flow (a surrogate for seawater intrusion) and outflow is termed coastal seaward flow.

The coastal flow of water through the submarine canyon outcrops is, in part, dependent on the equivalent freshwater head of seawater and the location of the freshwater/seawater interface. On the basis of EM and natural gamma logs (figure A5.1 in Appendix 5), the intrusion and movement of seawater occurs largely along the coarse-grained basal layers above regional unconformities. Chloride-concentration data, geophysical logs, and cross-section transport modeling of the Hueneme submarine canyon (Nishikawa, 1997) indicate that seawater intrusion is characterized by a relatively sharp front restricted to selected coarse-grained layers. Simulation of the seawater-interface boundary in this model assumed a position of the interface that is between the submarine outcrop and the coast. The interface location for the current model was inferred from the location estimated by Green and others (1978) for the lower-aquifer system (fig. 16*B*), transport model simulations (Nishikawa, 1997), and geochemical data from coastal monitoring wells (Izbicki, 1996a). The limitations of this assumption are further discussed in the "Model Uncertainty, Sensitivity, and Limitations" section.

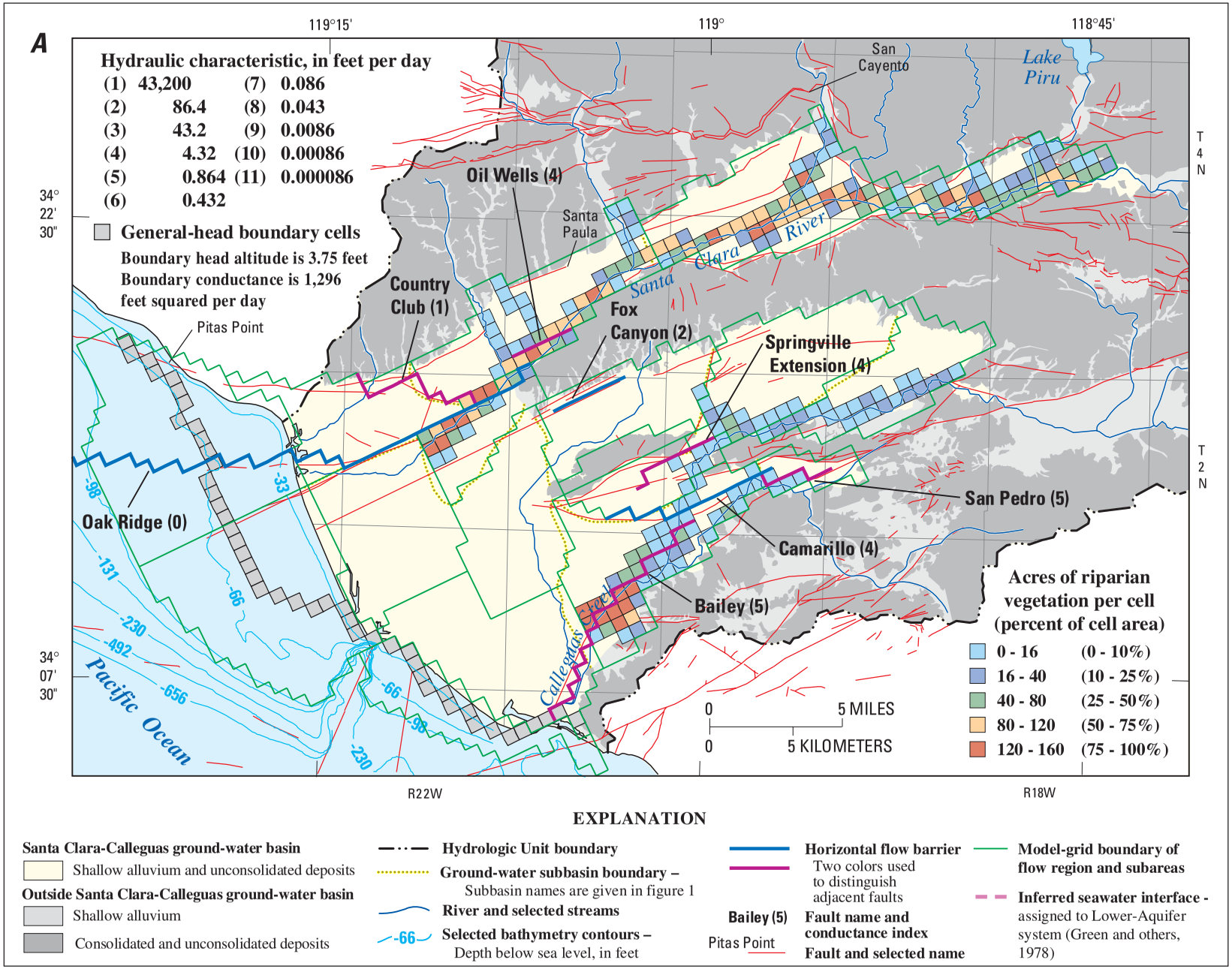

Figure 16. Location of model grid, location of general-head boundary cells with associated boundary head altitude and conductance, location of horizontal flow barriers and associated hydraulic characteristic, and location of evapotranspiration model cells and percent of riparian vegetation cover per cell in the Santa Clara-Calleguas ground -water basin, Ventura County, California. ***A***, Upper-aquifer system. ***B***, Lower-aquifer system.

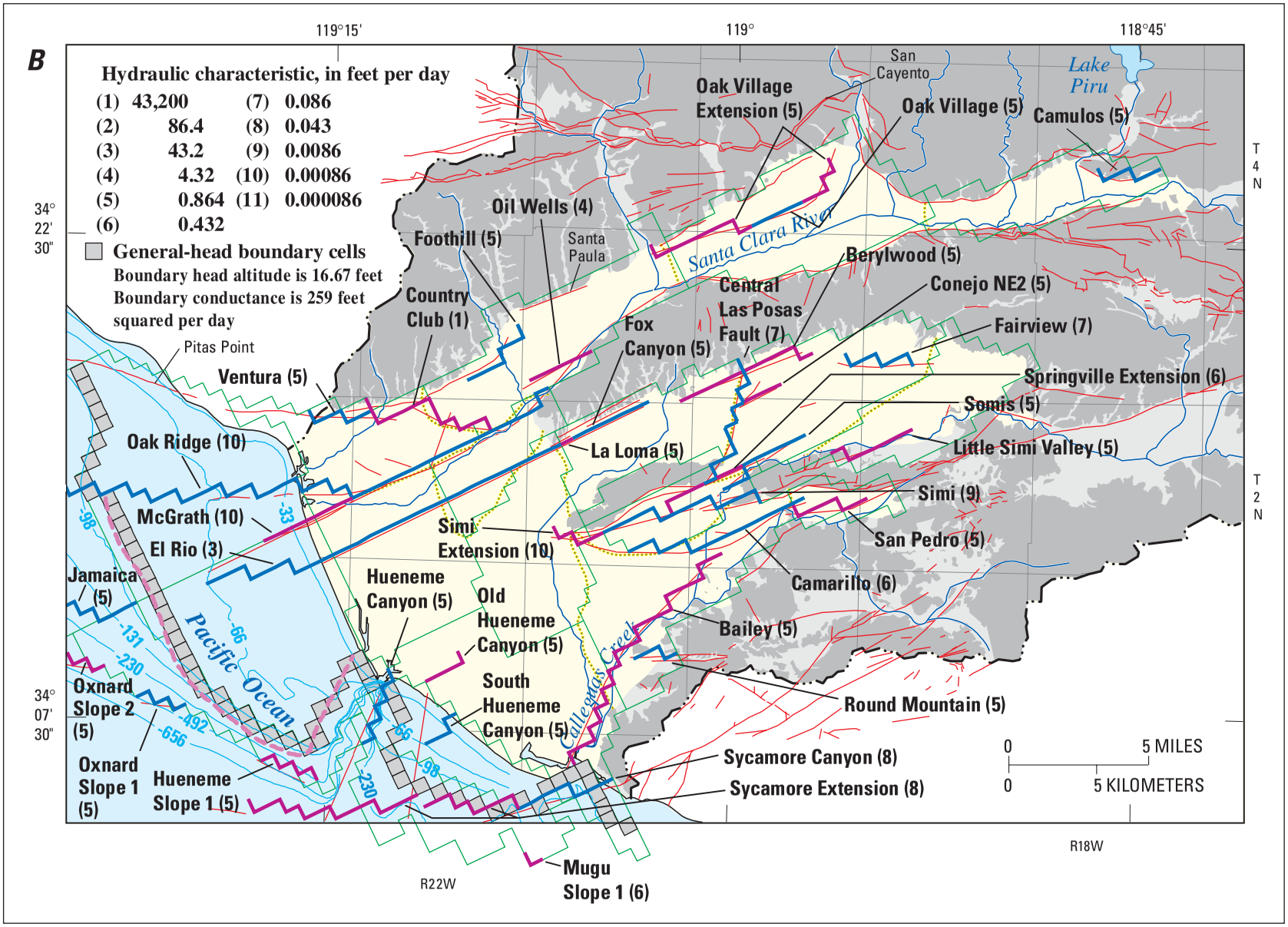

Figure 16—Continued.

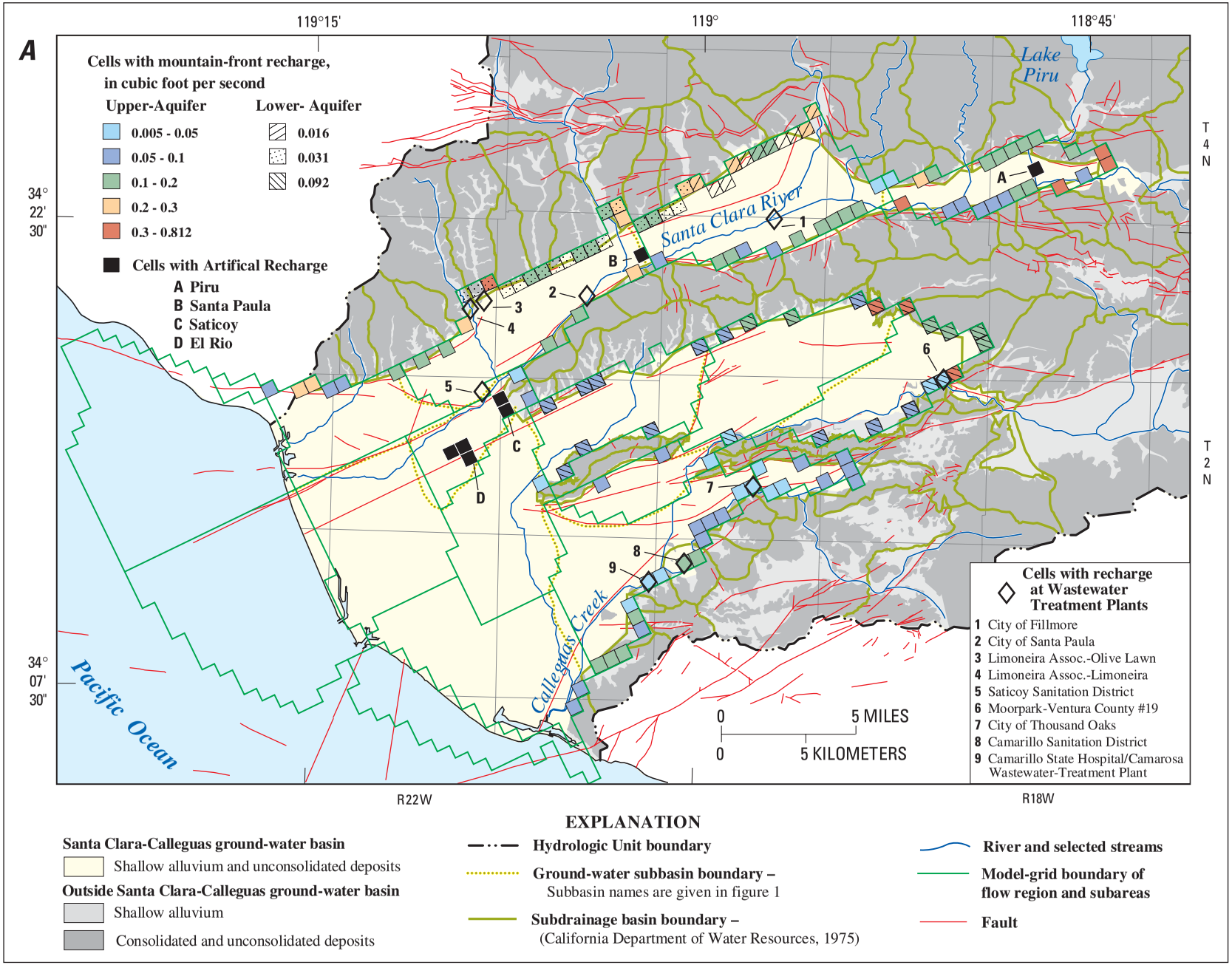

Figure 17. ***A***, Areal extent of model grid, location of model cells representing mountain-front, artificial, and treated wastewater recharge, and simulated rates of mountain-front recharge in the ground-water flow model of the Santa Clara–Calleguas ground-water basin, Ventura County, California.

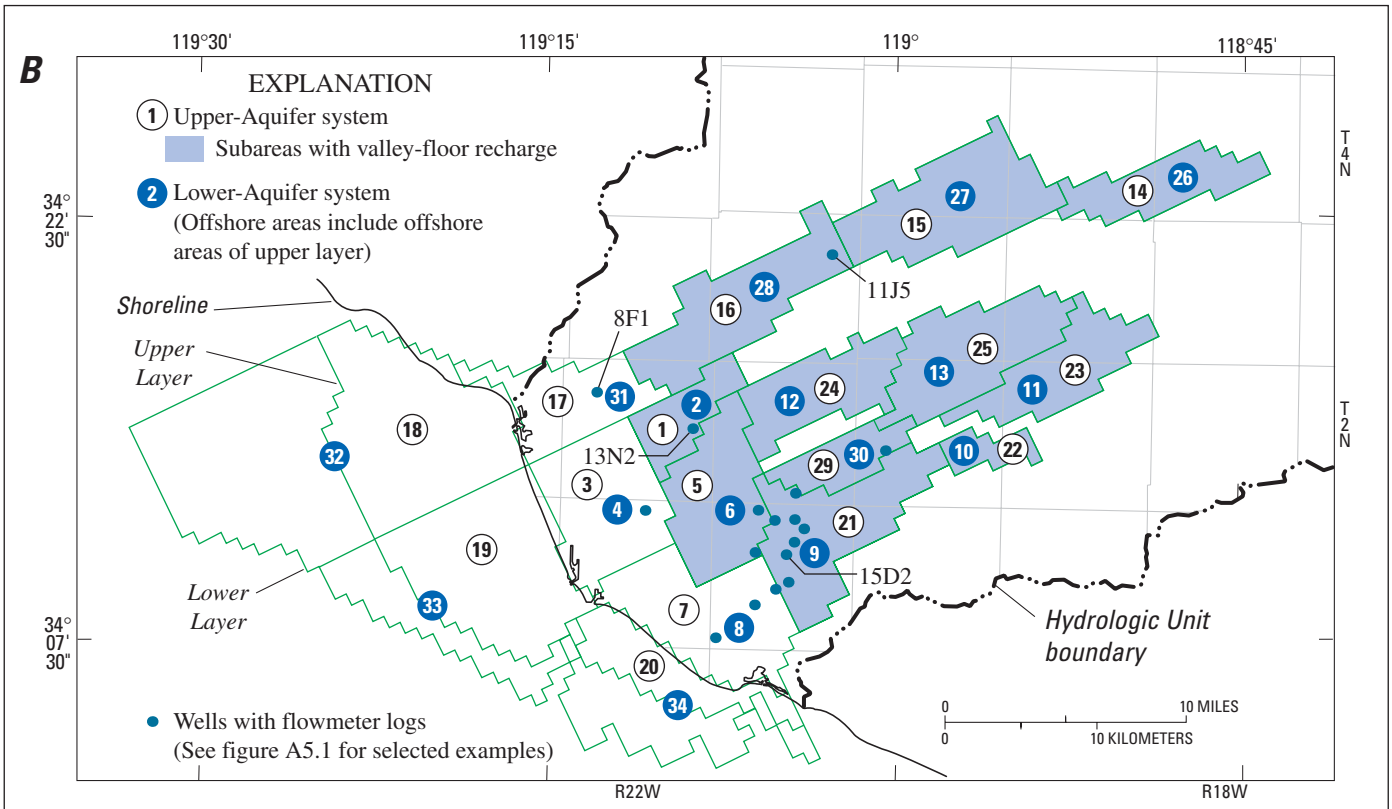

UPPER-AQUIFER SUBAREA		PERCENTAGE OF SEASONAL CLIMATIC PERIOD PRECIPITATION (WET/DRY)	ASSIGNED PERCENTAGE OF PUMPAGE FOR WELLS SPANNING BOTH MODEL LAYERS (UPPER/LOWER)	PERCENTAGE CHANGE IN AGRICULTURAL PUMPAGE FOR WET/DRY PERIODS	LOWER-AQUIFER SUBAREA	
NUMBER	NAME				NUMBER	NAME
1	Oxnard Plain Forebay	(30/30)	(100/0)	3	2	Oxnard Plain Forebay
3	Northwest Oxnard Plain	(0/0)	(90/10)	0	4	Northwest Oxnard Plain
5	Northeast Oxnard Plain	(30/30)	(90/10)	0	6	Northeast Oxnard Plain
7	South Oxnard Plain	(0/0)	(100/0)	0	8	South Oxnard Plain
14	Piru	(30/15)	(100/0)	2	26	Piru
15	Fillmore	(30/15)	(30/15)	11	27	Fillmore
16	Santa Paula	(30/30)	(70/30)	1	28	Santa Paula
17	Mound	(0/0)	(50/50)	4	31	Mound
18	Offshore Mound	(0/0)	(0/0)	--	32	Offshore Mound
19	Offshore North Oxnard Plain	(0/0)	(0/0)	--	33	Offshore North Oxnard Plain
20	Offshore South Oxnard Plain	(0/0)	(0/0)	--	34	Offshore South Oxnard Plain
21	South Pleasant Valley	(15/5)	(90/10)	10	9	South Pleasant Valley
22	Santa Rosa Valley	(15/5)	(100/0)	9	10	Santa Rosa Valley
23	South Las Posas Valley	(30/5)	(100/0)	9	11	South Las Posas Valley
24	West Las Posas Valley	(30/5)	(50/50)	9	12	West Las Posas Valley
25	East Las Posas Valley	(30/5)	(20/80)	9	13	East Las Posas Valley
29	North Pleasant Valley	(10/0)	(70/30)	10	30	North Pleasant Valley

Figure 17—Continued. ***B***, modeled subareas for the upper-and lower-aquifer systems, poercentage of infiltration for seasonal precipitation during wet and dry climatic periods, location of wells with flowmeter logs, and the related percentage of pumpage assigned to wells spanning the upper andlower layers.

The offshore boundary representing the density-dependent seawater interface was simplified with a general-head boundary simulation which may limit the accuracy of the model for the simulation of some small-scale features in the coastal areas. Since the actual location of the boundary through time along the entire coast is unknown, the location of the boundary was held stationary at an average location for all simulations. A general-head boundary represents the inflow or outflow of water in a model cell and is represented by boundary head and conductance to flow between the model cell and the boundary. Flow between the boundary and the aquifer is controlled by the boundary conductance and by the head gradient, which is calculated by the model as the difference between the aquifer head in the model cell and the specified boundary head. The boundary head that represents the equivalent freshwater head of seawater at the depth of outcrop was estimated to be equivalent to 3.75 ft at 46 cells in the upper model layer (fig. 16*A*) and 16.67 ft at 65 cells in the lower model layer (fig. 16*B*). The equivalent freshwater head at the upper-aquifer boundary was estimated by dividing the depth to the submarine outcrop (150 ft below sea level) by 40 (density ratio between saltwater and freshwater); this outcrop was assumed to represent the basal coarse-grained layer in the Oxnard aquifer. In a similar manner, the equivalent freshwater head for the lower-aquifer boundary was estimated by dividing the depth to the submarine outcrop (667 ft below sea level) by 40; this outcrop was assumed to represent the basal coarse-grained layer in the Hueneme aquifer that generally occurs at a depth from 400 to 800 ft below land surface.

Boundary conductances initially were based on aquifer transmissivity and were modified during model calibration. An initial uniform conductance of 4,320 ft^2/d was derived from the assumed values used in the extension of a model by Reichard (1995). The final distribution of conductances were 1,296 and 259 ft^2/d for the upper- and lower-aquifer systems, respectively (fig. 16 *A*,*B*).

Faults are simulated as barriers to ground-water flow and as such provide peripheral and internal boundaries to the ground-water flow system. The peripheral faults, however, were not simulated as faults because they are coincident with no-flow boundaries. The offshore Pitas Point and onshore Ventura, Foothill, Santa Paula, and San Cayento (thrust) Faults form the northern boundary of the ground-water flow system along the northern side of the Santa Clara River Valley subareas (fig. 16). The Oak Ridge Fault and South Mountain form the southern boundary of the ground-water flow system for the Mound (coastal) subarea and the inland subareas of the Santa Clara River Valley, respectively.

Internal faults are represented as a horizontal-flow barrier (Hsieh and Freckleton, 1993), across which the flow of water is proportional to a fault hydraulic characteristic determined during model calibration. The hydraulic characteristic is defined as the transmissivity of the fault divided by the fault width for confined aquifers. All faults in the lower-aquifer system and a subset of these faults in the upper-aquifer system were simulated as flow barriers (fig. 16). The most notable boundary occurs at the intersection of the Oak Ridge and Country Club (left-lateral reverse) Faults (fig. 16*A*) where the springs at Saticoy seeped ground water to the surface under predevelopment conditions. Ground-water level differences as great as 100 ft are reported across the Country Club Fault (Turner, 1975); data collected in the spring of 1992 suggest water-level differences of about 10 to 40 ft across this fault (Law/Crandall Inc., 1993).

Other faults at the subbasin boundaries acting as potential barriers to ground-water flow in the lower-aquifer system include a previously unmapped fault (hereinafter referred to the “Central Las Posas Fault”), which separates the lower-aquifer system between the West and East Las Posas Valley subbasins, and the extension of the Springville Fault, which separates the South Las Posas Valley and North Pleasant Valley subbasins (fig. 16*B*). The Camulos Fault, which forms the northeastern boundary of the Piru subbasin, also was included as a potential barrier to ground-water flow in the lower-aquifer system because of the extension of the ground-water model to the flanks of the mountain front. The Ventura Fault, which is aligned with the Pitas Point Fault (fig. 16) near the northwestern boundary in the Mound subbasin, also was included as a potential interior boundary to ground-water flow in the lower-aquifer system (fig. 16*B*).

Offshore faults of Pliocene to Miocene (?) age, mapped by Green and others (1978) and Kennedy and others (1987), were included as barriers to ground-water flow in the lower-aquifer system (fig. 16*B*). Some of these offshore faults (figs. 7, 9, and 16) are curvilinear and generally are subparallel to the submarine shelf; their northwest trend is typical of structures of the southern Coast Ranges Province. Other offshore faults trend west to southwest and are subparallel to the axes of the anticlines, synclines, and submarine canyons (figs. 7, 9, and 16) typical of structures of the Transverse Ranges Province. The northwest-trending faults included in the lower-aquifer system are an extension of the Sycamore Fault and minor fault traces, hereinafter referred to as "Hueneme slope 1," "Mugu slope 1," "Oxnard slope 1," and "Oxnard slope 2" (fig. 16*B*). Offshore faults subparallel to the fold structures include extensions of the McGrath-Jamaica, Bailey, and El Rio Faults, and smaller faults coincident with the submarine canyons, hereinafter referred to as the "Hueneme Canyon," "Old Hueneme Canyon," and "South Hueneme Canyon" (fig. 16*B*).

Estimates of the hydraulic characteristics of faults were not available from aquifer tests or other field data. An initial uniform hydraulic characteristic of 0.09 ft/d was used to simulate faults as horizontal-flow barriers in the lower-aquifer system. The final distribution was derived by fitting simulated water-level changes near faults and water-level differences across faults to measured data; the distribution ranges from 43,200 to 8.6×10^{-5} ft/d (figs. 16*A* and *B*). On the basis of subsurface stratigraphy, mapping, and trenching (California Department of Water Resources, 1954; California State Water Resources Board, 1956; Weber and others, 1976; Jakes, 1979; Dahlen and others, 1990; Association of Engineering Geologists, 1991; Dahlen, 1992), selected faults were simulated to extend into the upper-aquifer system of the model for this study (fig. 16*B*). These faults include Oil Wells, Country Club, Camarillo, Fox Canyon, Springville Extension, Oak Ridge, San Pedro, and Bailey Faults.

Streamflow Routing and Ground-Water/Surface-Water Interactions

Streamflow was simulated using the streamflow-routing package developed by Prudic (1989). As the numerical model routes the streamflow from the inflow locations through the stream network to the outflow locations, the model simulates streamflow infiltration to the ground-water flow system, ground-water discharge to the streams, streamflow diversions, and discharge of streamflow to the ocean. To simulate streamflow routing, each cell containing a reach of stream channel is assigned a segment number and a reach number within the segment. The network of streams and diversions contains 233 model cells (reaches) that are grouped into 30 segments (fig. 18*A*). The segments are groups of model cells that are coincident with the stream channels and represent the major parts of the river systems, which are divided at the points of confluence (fig. 18*B*). Streamflow entering the headwater segment of each stream and major tributary (fig. 18*B*) is specified for every season for the entire historical simulation period. The Santa Clara River and Calleguas Creek stream segments were linked at the confluence with their major tributaries and are shown in figure 18*B*. The altitude of the stage of the stream and streambed conductance for every reach of each segment and the altitudes of the top and base of the streambed are specified for each model cell.

For this study, streamflow infiltration was calculated using measured and estimated streamflow and the streamflow-routing program component of the ground-water flow model. Streamflow routing required construction of streamflow records for the major rivers and tributaries in the basin for January 1891 to the period of the continuous gaged streamflow record. Streamflow was estimated using regression equations with seasonal precipitation for wet and dry climatic periods (described later in Appendix 4, tables A4.1–A4.4). Precipitation data from three coastal, one intermontane, and two mountain precipitation stations were normalized and then used to produce "wet-day" nonlinear regression estimates of seasonal streamflow (Duell, 1992). Because precipitation data were available for coastal stations only for 1891–1905, an additional set of nonlinear relations was estimated for streamflow reconstruction for this early period of water-resources development. Correlations between precipitation and streamflow were better for the wettest periods (wet winters) than for the driest periods (dry summers). Most of the natural streamflow occurs during wet winters. Between 51 and 84 percent of the variance in natural streamflow during wet winters was estimated using the nonlinear relations between precipitation and gaged streamflow data.

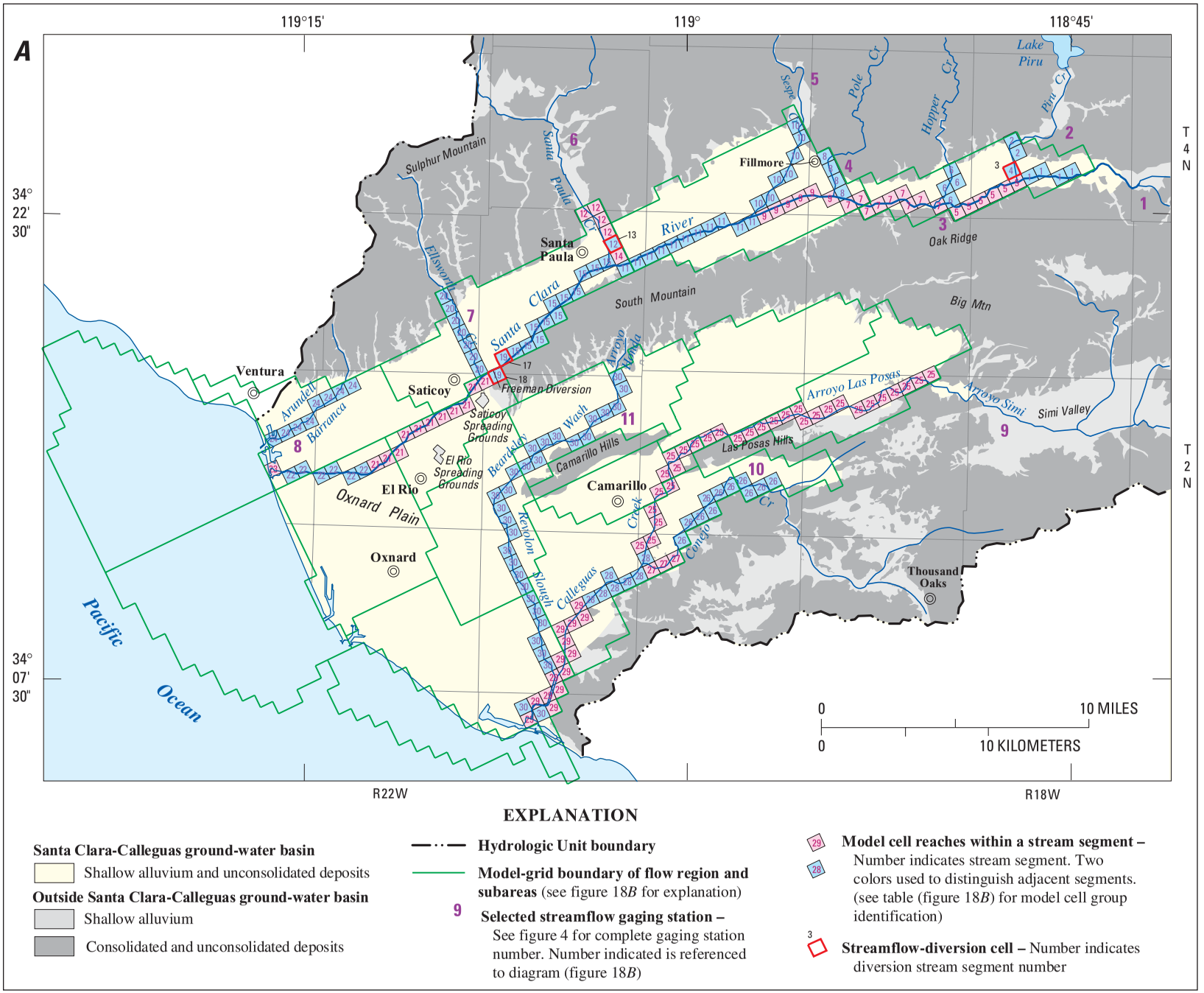

Figure 18 Streamflow network as simulated in the numerical model of the Santa Clara–Calleguas ground-water basin, Ventura County, California. ***A***, Stream reaches and related gaging stations used for inflow and for calibrations of simulated streamflow. ***B***, Schematic routing diagram of simulated streamflow network and streambed conductance for stream segments.

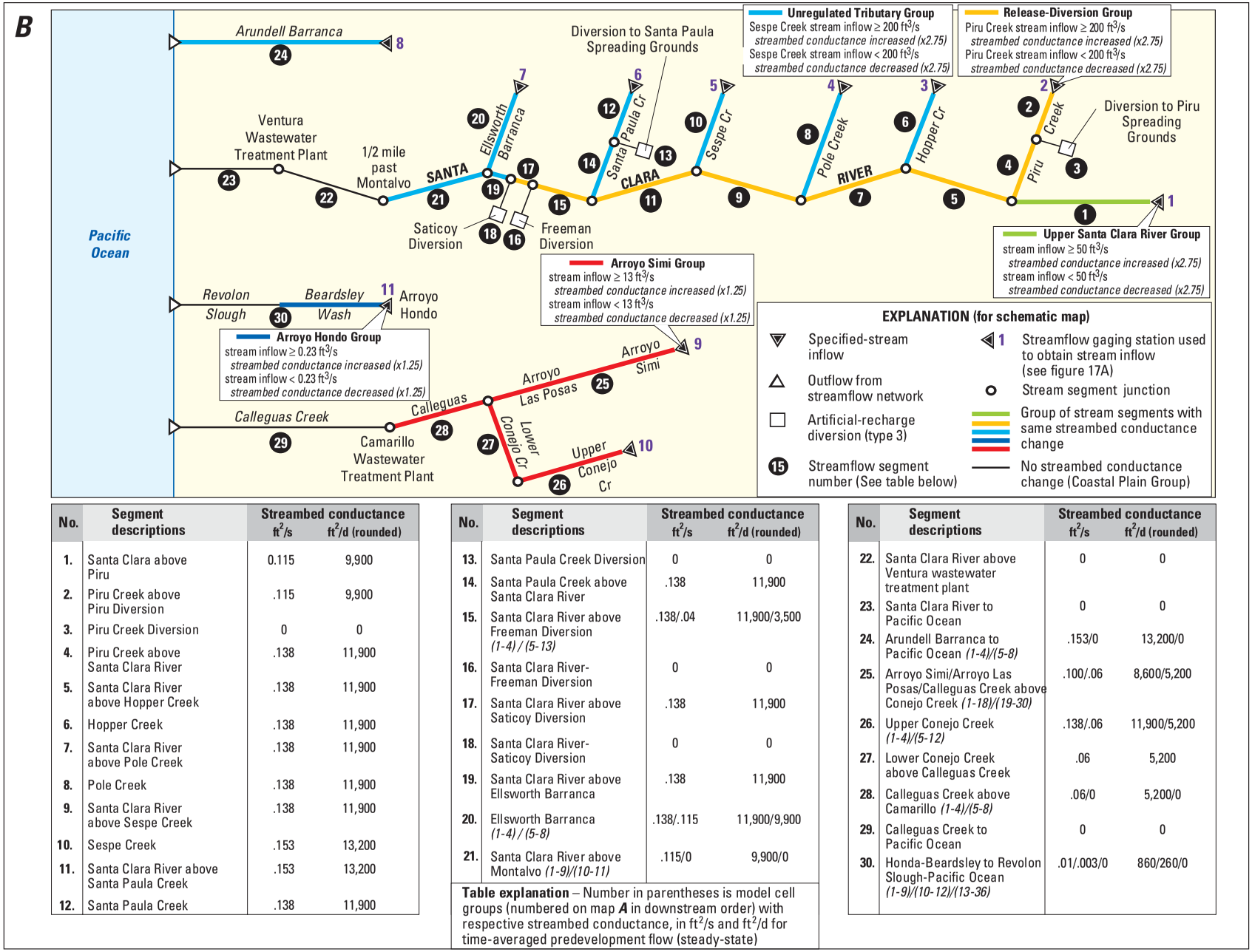

No.	Segment descriptions	Streambed conductance ft²/s	Streambed conductance ft²/d (rounded)
1.	Santa Clara above Piru	0.115	9,900
2.	Piru Creek above Piru Diversion	.115	9,900
3.	Piru Creek Diversion	0	0
4.	Piru Creek above Santa Clara River	.138	11,900
5.	Santa Clara River above Hopper Creek	.138	11,900
6.	Hopper Creek	.138	11,900
7.	Santa Clara River above Pole Creek	.138	11,900
8.	Pole Creek	.138	11,900
9.	Santa Clara River above Sespe Creek	.138	11,900
10.	Sespe Creek	.153	13,200
11.	Santa Clara River above Santa Paula Creek	.153	13,200
12.	Santa Paula Creek	.138	11,900

No.	Segment descriptions	Streambed conductance ft²/s	Streambed conductance ft²/d (rounded)
13.	Santa Paula Creek Diversion	0	0
14.	Santa Paula Creek above Santa Clara River	.138	11,900
15.	Santa Clara River above Freeman Diversion *(1-4) / (5-13)*	.138/.04	11,900/3,500
16.	Santa Clara River-Freeman Diversion	0	0
17.	Santa Clara River above Saticoy Diversion	.138	11,900
18.	Santa Clara River-Saticoy Diversion	0	0
19.	Santa Clara River above Ellsworth Barranca	.138	11,900
20.	Ellsworth Barranca *(1-4) / (5-8)*	.138/.115	11,900/9,900
21.	Santa Clara River above Montalvo *(1-9)/(10-11)*	.115/0	9,900/0

Table explanation – Number in parentheses is model cell groups (numbered on map ***A*** in downstream order) with respective streambed conductance, in ft²/s and ft²/d for time-averaged predevelopment flow (steady-state)

No.	Segment descriptions	Streambed conductance ft²/s	Streambed conductance ft²/d (rounded)
22.	Santa Clara River above Ventura wastewater treatment plant	0	0
23.	Santa Clara River to Pacific Ocean	0	0
24.	Arundell Barranca to Pacific Ocean *(1-4)/(5-8)*	.153/0	13,200/0
25.	Arroyo Simi/Arroyo Las Posas/Calleguas Creek above Conejo Creek *(1-18)/(19-30)*	.100/.06	8,600/5,200
26.	Upper Conejo Creek *(1-4)/(5-12)*	.138/.06	11,900/5,200
27.	Lower Conejo Creek above Calleguas Creek	.06	5,200
28.	Calleguas Creek above Camarillo *(1-4)/(5-8)*	.06/0	5,200/0
29.	Calleguas Creek to Pacific Ocean	0	0
30.	Honda-Beardsley to Revolon Slough-Pacific Ocean *(1-9)/(10-12)/(13-36)*	.01/.003/0	860/260/0

Figure 18—Continued.

The streamflow network represents gaged inflow along the Santa Clara River and tributaries, the Calleguas Creek and tributaries, Arroyo Hondo, and Arundell Barranca. Measured and estimated seasonal streamflow was used to simulate streamflow from 11 inflow points on the Santa Clara River, Piru Creek, Hopper Creek, Pole Creek, Sespe Creek, Santa Paula Creek, Ellsworth Barranca, Arrundell Barranca, Arroyo Hondo, Arroyo Simi, and Upper Conejo Creek (fig. 18*B*). Seasonal inflow rates were specified as the total seasonal flow volume divided by the number of days in the season for the period of record of each inflow site. For the period prior to historical records, nonlinear regressions of flow as a function of precipitation were used to estimate wet- and dry-period seasonal flows for the Santa Clara River, Piru, Hopper, Pole, Sespe, and Santa Paula Creeks and Arroyo Simi (Appendix 4, table A4.1–A4.4). Streamflow estimates for Ellsworth and Arrundell Barrancas, Arroyo Hondo, and Conejo Creek were based on seasonal ratios of gaged runoff to precipitation (modified rational method) for Pole and Hopper Creeks. The modified rational method was used for the period prior to the period for which streamflow-gaging data are available because there was no period of unregulated gaged streamflow that could be used to establish regression relations between streamflow and precipitation. Streamflow between the segments is the simulated streamflow routed from all upstream segments connected to a given segment. The simulation of predevelopment conditions used time-averaged streamflow estimates based on the geometric means and median streamflow values for the gaged streamflow (table 2) and the geometric-mean values of long-term runoff for ungaged tributaries.

The diversions at Piru, Santa Paula, and Saticoy and at the Freeman Diversion, which provide surface water for irrigation and artificial recharge, were simulated as losses from the stream network (fig. 18 *A*,*B*). The streamflow-routing package of this model was altered to offer additional types of diversion (Appendix 2). The modified diversion type used for all four simulated diversions is referred to as an "artificial recharge diversion" [type 3 (Appendix 2)]; it will accept all streamflow available up to the specified amount of diversion. The seasonal amounts of diversion were based on the UWCD's reported total monthly diversions (Greg Middleton, United Water Conservation District, written commun., 1993).

Streamflow stages for all the reaches were estimated from relations between stream stage and streamflow at the inflow-gaging stations. The stream stage was held constant for all reaches in all segments for all simulations. Stream stage was initially estimated using extrapolated gaged height at the estimated predevelopment flow, which ranged from 0.3 to 4.5 ft for the steady-state flow rate at the inflow-gaging stations. However, stream stages were simplified and finally held to a constant value of 2.5 ft above the top of the streambed for all simulation periods and for all river reaches. The altitude of the top of the streambed was estimated from the arithmetic average of land-surface altitudes for the entire extent of the stream channel in each reach, which was estimated from digital altitude model data, 1:24,000-scale topographic maps, and gaging-station altitudes. The altitude of the base of the streambed was assumed to be 10 ft below the altitude of the top of the streambed for all the reaches for all time periods.

As water flows down the channels of the Santa Clara River and Calleguas Creek and their tributaries, some of the water infiltrates through the streambed and becomes ground-water recharge. In a few places, however, shallow ground water discharges to streams. In the model, this vertical flow between the stream and the aquifer is controlled by the streambed conductance and a vertical gradient that is driven by the difference between the specified stream stage and the simulated ground-water level. Stream stage for each stream reach was specified and was not changed for the entire simulation time. Streambed conductance initially was estimated as the product of the assumed channel width, channel length, and vertical hydraulic conductivity of the streambed deposits divided by the streambed thickness. Streambed conductance also can be estimated as the product of the streamflow and the fraction of streamflow loss divided by the streambed thickness. Although the actual stream channel width and streambed thickness vary spatially and with flow within many of the model cells, the streambed conductances were simplified into groups of segments with the same streambed conductance values (fig. 18*B*).

Initial estimates of streambed conductance were based on streamflow-loss estimates made in the early 1930s (California Department of Public Works, 1934) and in 1991 (Densmore and others, 1992); however, these direct estimates of streamflow losses vary widely—from 1 to 100 percent. Various mass-balance estimates for the Santa Clara River (Taylor and others, 1977; Dal Pozzo, 1992; Law/Crandall Inc., 1993) also have been made; these estimates also vary widely, ranging from 0 to 100 percent, with an average loss of about 22 percent. A water-balance approach yielded an estimate of streambed hydraulic conductivity of about 2 ft/d for the Santa Paula subarea (Law/Crandall Inc., 1993). The simulation of streamflow in the Santa Rosa Valley subarea model used vertical hydraulic conductivities of 3 ft/d for Arroyo Conejo and Conejo Creek and 1 ft/d for Arroyo Simi and an assumed streambed thickness of 1 ft (Johnson and Yoon, 1987). The assumed width is 50 ft, and the assumed streambed length was assumed to be the length of the cell (2,640 ft). Using values from Johnson and Yoon (1987), estimated streambed conductance is 13,200 ft^2/d for Arroyo Simi and 39,600 ft^2/d for Conejo Creek.

For the regional-scale model, the stream channel width initially was assumed to range from 50 to 200 ft, the length of the reach was assumed to be the length of the cell (2,640 ft), and the streambed thickness was assumed to be 10 ft. The streambed conductances were then put into six groups: the coastal plain group for which segments and reaches were set to a streambed conductance of zero, the upper Santa Clara River group, the release-diversion group, the unregulated tributary group, the Arroyo Simi group, and the Arroyo Hondo group (fig. 18*B*). Streambed conductances for each group were increased and decreased from the predevelopment values and were changed on the basis of threshold values of stream inflows (fig. 18*B*). Results of model calibration indicate that the three groups of streambed conductances for the Santa Clara River system were increased when streamflows were greater than the flow threshold and decreased when they were less than the flow threshold by a factor of 2.75 with respect to conductances used to simulate time-averaged predevelopment conditions. The Arroyo Hondo and Arroyo Simi groups were increased when streamflows were greater than the flow threshold and decreased when streamflows were less than the flow threshold by a factor of 1.25 with respect to conductances used to simulate time-averaged predevelopment conditions. This change in conductance is believed to reflect the change in channel width and is similar to the factors of 1.2 to 2.0 used for the simulation of the streamflow routing of the Little Humboldt River, Nevada (Prudic and Herman, 1996). The final distribution of streambed conductances ranges from 0 to 13,200 ft^2/d (fig. 18*B*) for time-averaged predevelopment conditions. These final values are the product of model calibration for time-averaged predevelopment (steady-state) conditions and of comparisons of the streamflow hydrographs for historical downstream streamflow and diversions.

Mountain-Front Recharge

Natural recharge along the model boundaries, mountain-front recharge, was simulated as a constant-flux inflow for each season (fig. 17*A*,*B*). Mountain-front recharge was simulated as a seasonally varying estimate of runoff specified as infiltration at the mountain front for 64 ungaged surface-water subdrainage basins (California Department of Water Resources, 1975, plate 2) that surround and drain into the 12 ground-water subbasins of the Santa Clara–Calleguas Basin (figs. 1 and 17*A*). The average for total wet- and dry-seasonal precipitation was estimated for each ungaged subdrainage basin. The modified rational method was used to estimate the seasonal runoff for each of the 412 seasons in the simulated historical period January 1891–December 1993. The ratio of runoff from Pole or Hopper Creeks to the total seasonal precipitation for these two index subdrainage basins ranged from 0 to 7, but most of the ratios were less than 0.25. These ratios were comparable to the fraction of precipitation as ground-water recharge estimated from detailed water-balance studies completed by Blaney (California Department of Public Works, 1934) for water years 1928–32. Blaney estimated annual fractions of rainfall penetration ranging from 0.01 to 0.17 for dry years and from 0.06 to 0.34 for wet years. Using the modified rational method, estimated ratios greater than 1 would result in a runoff total that is greater than the average precipitation. On the basis of previous infiltration studies in the Santa Clara–Calleguas Basin (California Department of Public Works, 1934; Taylor and others, 1977; Densmore and others, 1992), most fractions of runoff that infiltrate are less than 0.9. The ratios selected for estimating recharge were from Pole Creek for winter and fall seasons and from Hopper Creek for spring and summer seasons. When any ratio exceeded 0.9, the ratio from the other index subarea was used. When both ratios exceeded 0.9, the ratios were replaced with the geometric mean of ratios less than or equal to 0.9 for that respective wet or dry climatic season. The estimated mountain-front recharge for each subdrainage basin was then equally distributed to one or more cells that are coincident with the stream channels at the model boundary (fig. 17*A*). The resulting recharge estimates for an individual cell was reduced to 3.4 ft^3/s if the estimated recharge value exceeded that amount. This value was determined from streamflow seepage measurements of low flows on Santa Paula Creek (Dal Pozo, 1992).

The estimated total time-averaged mountain-front recharge rate used for the steady-state simulation of predevelopment conditions was 12,500 acre-ft/yr. The constant rate of recharge for the steady-state simulation, which was based on the geometric-mean ratios, was used to estimate the time-averaged runoff from each mountain-front subdrainage basin. The estimated total time-varying mountain-front recharge rate used for transient-state simulation of historical conditions ranged from 6,000 acre-ft/yr in 1923 to 80,600 acre-ft/yr in 1993. Mountain-front recharge was simulated as injection wells, with a constant rate of recharge per season, for 119 model cells in the uppermost active layer that coincide with the stream channels in the ungaged-tributary drainage basins (fig. 17*A*).

Additional recharge as direct infiltration on the outcrops of the San Pedro Formation (fig. 7*A*) was estimated based on wet-period average winter precipitation for 54 model cells that coincide with the San Pedro Formation in the Fillmore, Santa Paula, and Las Posas Valley subareas (figs. 7*A* and 17*A*). The recharge rate representing deep infiltration over the outcrops was estimated using the modified equation developed by the Santa Barbara County Water Agency (1977):

$$\text{Recharge} = (P_{wet} - 17 \text{ inches})/1.55,$$

where

Recharge is average recharge rate, in inches per year, and P_{wet} is wet-period total annual precipitation of 20.75 in. for outcrops surrounding the Las Posas Valley subareas and 21.25 in. for outcrops on the north side of the Santa Clara River Valley subareas.

This method assumes uniform temporal and areal distributions of rainfall without regard to the intensity of individual storms. The resulting recharge rate is reduced by the fraction of wet years (32 years) in the total period of historical simulation (103 years). The resulting estimates for a constant average recharge were 470 acre-ft/yr for East Las Posas Valley subarea, 740 acre-ft/yr for South Las Posas Valley subarea, 400 acre-ft/yr for West Las Posas Valley subarea, 240 acre-ft/yr for Fillmore subarea, and 320 acre-ft/yr for Santa Paula subarea. Thus, the long-term average recharge to the lower-aquifer system for a total bedrock recharge was about 2,200 acre-ft/yr (table 4).

Valley-Floor Recharge

Direct infiltration of precipitation on the valley floors, hereinafter referred to as "valley-floor recharge," was simulated using the model recharge package and was distributed equally to all cells in each valley floor of the Piru, Fillmore, Santa Paula, Las Posas Valley (East, West, and South), Pleasant Valley (North and South), Oxnard Plain Forebay, and Santa Rosa Valley, and the Northeast Oxnard Plain subareas (fig. 17*B*). The estimated total time-averaged recharge rate used for the steady-state simulation of predevelopment conditions was 4,800 acre-ft/yr, which is based on the geometric-mean ratios of runoff to precipitation at Pole and Hopper Creeks. The total time-varying valley-floor recharge used for the transient-state simulation of historical conditions was varied seasonally using the same percentages of infiltration of irrigation based on model calibration (fig. 17*B*). The recharge rates ranged from 18,300 acre-ft/yr for dry-year periods to 32,700 acre-ft/yr for wet-year periods (table 4).

Artificial Recharge

Recharge of infiltration of diverted streamflow, discharge of treated sewage effluent, and irrigation return flow were simulated as a constant-flux inflow using the MODFLOW well package. No artificial recharge was applied to predevelopment (steady-state) conditions. For developed (transient-state) conditions, infiltration of diverted streamflow was applied for the period 1928–93, infiltration of irrigation was applied for the period 1891–1993, and infiltration of treated sewage effluent was applied for the period 1936–93.

Recharge of diverted streamflow was simulated at the artificial-recharge spreading grounds (basins) operated by the UWCD in the Piru and Santa Paula subareas and in the Oxnard Plain Forebay subarea (figs. 4 and 18*A*). The quantity of artificial recharge simulated in the model (fig. 11*A*) was based on reported annual and seasonal amounts of recharge (United Water Conservation District, 1986, plate 5a,b; Greg Middleton, United Water Conservation District, written commun., 1993).

Recharge of treated sewage effluent was simulated as constant-flux inflows using the MODFLOW well package. This recharge was based on reported and extrapolated annual amounts of treated sewage discharge (California Department of Water Resources, 1975; W.D. Jesena, California Regional Water Quality Control Board, written commun., 1991; E.G. Reichard, U.S. Geological Survey, written commun., 1993; Mitri Muna, Ventura County Waterworks, written commun., 1995) and was assigned to nine model cells (fig. 17*A*) at a rate reduced to 74 percent (Farnsworth and others, 1982) of the reported or interpolated annual rate of discharge to account for the free-water surface evaporation while in percolation ponds and streambeds. The treated sewage effluent represents discharge from the city of Fillmore during 1958–93, the city of Santa Paula during 1937–93, the Limoneira Association at Olive Lawn Farm and Limoneira Farm during 1975–93, the Saticoy Sanitation District during 1960–93, the Camarillo Sanitation District during 1959–93, the city of Thousand Oaks during 1962–72, the Camarillo State Hospital during 1960–80, the Camarosa wastewater-treatment plant during 1981–93, and the Moorpark-Ventura County wastewater-treatment plant No. 19 during 1973–93. Additional sewage effluent discharged from the city of Thousand Oaks Hill Canyon Plant is represented as streamflow during 1973–93. Treated sewage effluent from the percolation ponds near the Santa Clara River which was used by the city of Piru during 1975–93 was not included because of the small volumes of discharge (Charles Rogers, city of Piru, oral commun., 1995). Total treated-sewage effluent that becomes ground-water recharge was applied at a constant rate for all four seasons of every year; the rate increased from 20 acre-ft/yr in 1936 to 9,000 acre-ft/yr in 1993 (fig. 11*A*).

Irrigation return flow was estimated as a percentage of the total applied water and included ground-water and surface-water components for many of the subareas. This recharge was simulated as a constant-flux inflow using the MODFLOW well package for the uppermost layer of the model. Irrigation return flow was estimated for each of the land-use periods and held constant for the same periods used to estimate ground-water pumpage (fig. 11*A*,*B*). The irrigation return flow was applied over a 245-day growing period prior to 1927 and applied uniformly for the entire year for the remainder of the simulation period. It was applied over the entire year because infiltration through the unsaturated zone tends to extend the period of infiltration. The 1969 land-use map was used to estimate the distribution of irrigation return flow for the period of reported pumpage, 1973–93. The assumed infiltration ranged from 5 to 30 percent of applied irrigation water for all subareas and was varied for wet- and dry-year periods (fig. 17*B*). The percentage of irrigation return flow was estimated during model calibration. Irrigation return flow ranged from less than a few hundred acre-feet per season for the Mound and North Peasant Valley subareas to about 1,400 acre-ft per season for the Santa Paula subarea (fig. 11). Total irrigation return flow ranged from 14,600 acre-ft/yr for the 1890s to 51,500 acre-ft/yr for the drought period 1987–91.

Other Sources of Recharge

Other sources of recharge include flow of water along some fault zones from older (Miocene age) marine sedimentary rocks and brines related to oil deposits. Some of these potential sources of water may yield water of poor quality or water of different chemical composition. Water-chemistry data indicate that the amount of leakage from the deeper, older formations in the South Oxnard Plain subarea and the South Pleasant Valley subarea probably is small (Izbicki, 1991, 1996a); therefore, it was not included in the current regional simulations.

Another source of potential recharge is leakage of the semiperched water to the upper-aquifer system. Leakage of semiperched ground water may enter the upper- and lower-aquifer systems through failed and abandoned wells. Because the initial water-chemistry data indicate a potentially small effect and because water-level hydrographs indicate a potentially complicated relation, this element was not included in the current regional simulation. Any potential leakage through intraborehole flow or failed wells was included collectively and simulated in the irrigation-return-flow component.

Natural Discharge

Natural discharge is simulated as seaward coastal flow through submarine outcrops and as evapotranspiration (ET) along the flood plains of the Santa Clara River and Calleguas Creek. The coastal flow of water to the ocean was determined through model simulation and calibration; it is described in the "Model Boundaries" section.

ET by riparian vegetation (phreatophytes) and evaporation from bare soil were simulated at 306 model cells of layer 1 (upper-aquifer system) (fig. 16*A*) using the MODFLOW evapotranspiration package. Using previous estimates (California Department of Public Works, 1934), a maximum ET rate of 2.4 ft/yr was assumed when the water table is at land surface, and ET was assumed to decrease linearly to zero when the water table reaches a depth of 10 ft or more below land surface. The ET rate was multiplied by the ratio of riparian vegetation area to total model-cell area to account for the riparian vegetation density in each model cell. The weighting factor is the number of acres of riparian vegetation, estimated from the 1912, 1927, 1932, and 1950 land-use maps, for each cell divided by the total number of acres (160) in a model cell. The composite ET rates and the model cells with the potential for ET in 1912, 1927, 1932, and 1950 (Conejo Creek area) were used for the predevelopment and historical simulation for 1891–1926. The ET surface remained the same for the remainder of the simulation periods, but the ET rates were updated to reflect changing ET acreage. Thus, acreage for riparian vegetation was updated using the 1932 acreage for 1927–46 and the 1950 acreage for the remainder of the simulation period.

Pumpage

The simulation of ground-water withdrawal from wells as pumpage required a compilation of historical estimates that include indirect estimates of agricultural pumpage based on land use (1891–1977), reported municipal pumpage (1914–77), and metered agricultural and municipal pumpage (1978–93) reported to and compiled by the UWCD and the FGMA. Estimated pumpage ranged from 34,800 acre-ft for the drought years of the 1920s to a maximum pumpage of 301,400 acre-ft for the 1990 drought year. Estimated pumpage is shown in figure 11*B* for the period of simulation. The annual and biannual pumpage estimates were temporally distributed for model input to the seasonal intervals on a well-by-well basis. The initial vertical distribution of pumpage between aquifer systems was based on well construction (Predmore and others, 1997) and wellbore flowmeter studies completed as part of the RASA studies (table 5). For wells completed only in the upper-aquifer system, all water was derived from the upper model layer, and for wells completed only in the lower-aquifer system, all water was derived from the lower model layer. For wells that were completed in both the upper- and lower-aquifer systems, a percentage of total well pumpage was assigned to the upper and lower layers on the basis of wellbore flowmeter data, slug tests, and model calibration (fig. 17*B*). Pumpage from wells with no construction data was distributed using these same assumed percentages of pumpage. The distribution of pumpage from the upper- and lower-aquifer systems, estimated from the land-use map for agricultural pumpage, also used these same percentages for all the subareas.

Indirect estimates of agricultural pumpage were compiled for five land-use periods that span from 1912 to 1977 (Koczot, 1996). The compilation was based on land-use maps for 1912, 1932, 1950, and 1969 and on a mosaic of areal photos from 1927 (Predmore and others, 1997). The distribution of estimated agricultural pumpage was based on well locations reported in 1987 and on percentages of pumpage within each subarea. The estimates of agricultural pumpage were distributed over time on the basis of major changes in crop types and climatic periods. Because the growing periods of the various crop types spanned an 8-month period, pumpage was estimated and distributed using a 245-day growing season (Koczot, 1996) spanning March through October for the period 1912–26. The growing season was extended to 275 days, spanning from March through November for the period 1927–77. The extension of the growing period was based on inspection of water-level hydrographs and the wider variety of truck and orchard crops introduced during this period. The magnitude of pumpage was reduced during wet climatic periods and increased during dry climatic periods. The percentage change in agricultural pumpage was based on the ratios of wet-year to average-annual reported pumpage for each subarea and dry-year to average-annual reported pumpage (fig. 17*B*). The reported municipal pumpage for the cities of Ventura, Camarillo, and Oxnard and the Channel Island Community Services District; pumpage for the fish hatchery in the southern end of the Piru subarea; and pumpage of artificial recharge in the Oxnard Plain Forebay were estimated independently and combined with agricultural pumpage for input to the ground-water flow model for the period of simulation prior to 1983 (fig. 11*B*).

Regional management of ground-water resources was implemented by the State of California in 1983 with the creation of the Fox Canyon Groundwater Management Agency (FGMA) for controlling seawater intrusion. The FGMA jurisdiction covers part of the Santa Clara–Calleguas Basin and includes the Oxnard Plain, Oxnard Plain Forebay, Pleasant Valley, and Las Posas Valley subareas (figure 26 presented later in the section "Analysis of Ground-Water Flow"). Reported pumpage was compiled from the technical files of the FGMA and the UWCD for the period July 1979–December 1993. These data generally consist of semiannual totals of user-reported agricultural, nonagricultural (municipal, industrial, and domestic), and total pumpage. Agricultural pumpage was distributed based on a 275-day growing period and the nonagricultural pumpage was distributed equally over seasonal periods of the flow model. Pumpage for 1980, which was based on water-level hydrographs and on climate data, was used for the period 1978 through 1980. When only total pumpage was reported, that pumpage was assumed to be for agricultural use. Early pumpage data were incomplete for the Las Posas Valley, the eastern part of the Pleasant Valley, and the Santa Rosa Valley subareas. For these areas, 1984 FGMA-reported pumpage was used to represent pumpage for 1978 through 1983. Total reported annual pumpage ranged from as little as 850 acre-ft in the South Las Posas Valley subarea during 1992 to as much as 107,300 acre-ft in the Oxnard Plain and Oxnard Plain Forebay subareas during 1990.

Hydraulic Properties

Estimates of transmissivities and storage coefficients for both model layers and estimates of coefficients of vertical leakance between layers are required to simulate the flow of ground water. Estimates of the horizontal conductance of faults are required to simulate potential barriers to ground-water flow, and the vertical conductance of streambeds is required to simulate the flow of water between shallow ground water and streamflow. The average values for these parameters are used in the model and represent the hydraulic properties which are the spatial averages over individual model cells. They generally are held constant through time. Except for fault hydraulic characteristics, vertical conductances of the streambed, subsidence parameters, and areas where model layers were extended, the initial estimates for all the model parameters were derived largely from the spatial estimates used in previous ground-water flow models of the basin (California Department of Water Resources, 1974a,b, 1975; Johnson and Yoon, 1987; CH2M HILL, 1993; Reichard, 1995).

Transmissivity

Transmissivity is the product of the hydraulic conductivity and saturated thickness of the aquifers; therefore, transmissivity values may be affected by changes in saturated thickness. Transmissivity throughout much of the modeled area is associated with the basal coarse-grained layers of the aquifers that remain saturated; many parts of the aquifers are confined or show water-level changes that are a relatively small percentage of the saturated thickness. Because the effective saturated thickness is relatively constant over most of the model area, this model uses constant transmissivities for the entire period of simulation. Transmissivities estimated from specific-capacity tests were used to simulate ground-water flow using the Theissan-Weber Polygon model (California Department of Water Resources, 1975). Estimates for the upper-aquifer system range from 650 ft^2/d along the northern edge of the Santa Paula subarea to more than 53,000 ft^2/d in the northern Oxnard Plain and 67,000 ft^2/d north of the Mugu submarine canyon (California Department of Water Resources, 1975, pl. 8). Estimates for the lower-aquifer system range from about 1,300 ft^2/d near Moorpark to 53,000 ft^2/d north of Port Hueneme (California Department of Water Resources, 1975, pl. 8). The coastal estimates from the Theissan-Weber Polygon model were extended as constant values to the adjacent offshore regions by Reichard (1995, fig. 10).

The current model modified these estimated transmissivities and used additional estimates beyond the areal extent of the previous models for the upper-aquifer system (layer 1) in the Las Posas Valley, Pleasant Valley, and Santa Rosa Valley subareas and for the lower layer in the Santa Clara River Valley subareas (fig. 17*B* and 19*A*). The estimated transmissivities for the upper-aquifer system (layer 1) ranged from 1.3 ft^2/d for the Las Posas Valley subarea to about 73,800 ft^2/d for the Oxnard Plain Forebay (fig. 19*A*); the estimated transmissivities for the lower-aquifer system (layer 2) ranged from about 38 to 26,500 ft^2/d. A constant transmissivity of about 4,700 ft^2/d was assigned to the lower-aquifer system (layer 2) for the offshore part of the Mound subarea on the basis of the estimated thicknesses and the hydraulic conductivities used onshore (fig. 19*A*).

The final estimates of transmissivities in the calibrated model for both model layers were refined for each subarea using the sum of transmissivities for the aggregate thicknesses of the coarse-grained and fine-grained deposits in each model cell (fig. 20). The transmissivity of the coarse-grained deposits was determined as the product of the thickness of the coarse-grained deposits (estimated from resistivity logs) and a geometric-mean hydraulic conductivity (estimated from slug tests). The transmissivity of the fine-grained deposits is the product of the thickness of fine-grained deposits and an assumed hydraulic conductivity of 0.1 ft/d.

Some of the transmissivities from previous regional models for the upper-aquifer system were reestimated using estimates of a geometric-mean hydraulic conductivity from the slug tests and the aggregate thicknesses of the coarse- and fine-grained deposits (fig. 20*A*). Transmissivity estimates were made using a hydraulic conductivity of 35.1 ft/d for the coarse-grained deposits in the Piru and Santa Paula subareas; these values were based on slug-test values that range from 18 to 88 ft/d in monitoring wells completed in these subareas (E.G. Reichard, U.S. Geological Survey, written commun., 1995).

Transmissivities for the upper-aquifer systems (layer 1) of the Las Posas Valley, Santa Rosa Valley, and Pleasant Valley subareas were needed to extend the upper model layer of the previous models for all the subareas (figs. 17*B* and 19*A*). The transmissivities of the coarse-grained deposits of the East Las Posas Valley subarea were estimated using a geometric-mean hydraulic conductivity of 0.3 ft/d, which was based on slug-test values that range from 0.21 to 0.47 ft/d in monitoring wells completed in this subarea. Transmissivities of the coarse-grained deposits of the West Las Posas Valley subarea were estimated using a geometric-mean hydraulic conductivity of 0.19 ft/d, which was based on slug-test values that range from 0.14 to 0.27 ft/d in monitoring wells completed near Arroyo Hondo. Transmissivities of the coarse-grained deposits of the South Las Posas Valley subarea were estimated using a geometric-mean hydraulic conductivity of 1.58 ft/d, which was based on slug-test values that range from 0.48 to 3.49 ft/d in monitoring wells completed in the subarea. The transmissivities of the coarse-grained deposits of the Santa Rosa Valley subarea (fig. 20) were based on two sets of hydraulic conductivities: A reported value of 80 ft/d for the Saugus Formation (Johnson and Yoon, 1987) was used to represent the upper and lower aquifers on the west side of the San Pedro Fault; reported values of 150 and 120 ft/d for the alluvium and the Santa Margarita Formation, respectively, were used for the east side of the San Pedro Fault (Johnson and Yoon, 1987). Transmissivity for the Pleasant Valley subarea was estimated using a geometric-mean hydraulic conductivity of 8.8 ft/d for the coarse-grained deposits, which is based on slug-test values that range from 0.13 to 11.8 ft/d in monitoring wells in this subarea.

Estimates of hydraulic conductivities for the lower-aquifer system (layer 2) deposits range from 1 to 8 ft/d for monitoring wells completed in the northern part of the Oxnard Plain subarea and from 5.5 to 44 ft/d for monitoring wells completed in the Piru and Santa Paula subbasins (E.G. Reichard, U.S. Geological Survey, written commun., 1992). Transmissivities for the coarse-grained deposits within layer 2 of the Santa Clara River Valley subareas were estimated using a geometric-mean hydraulic conductivity of 15.4 ft/d.

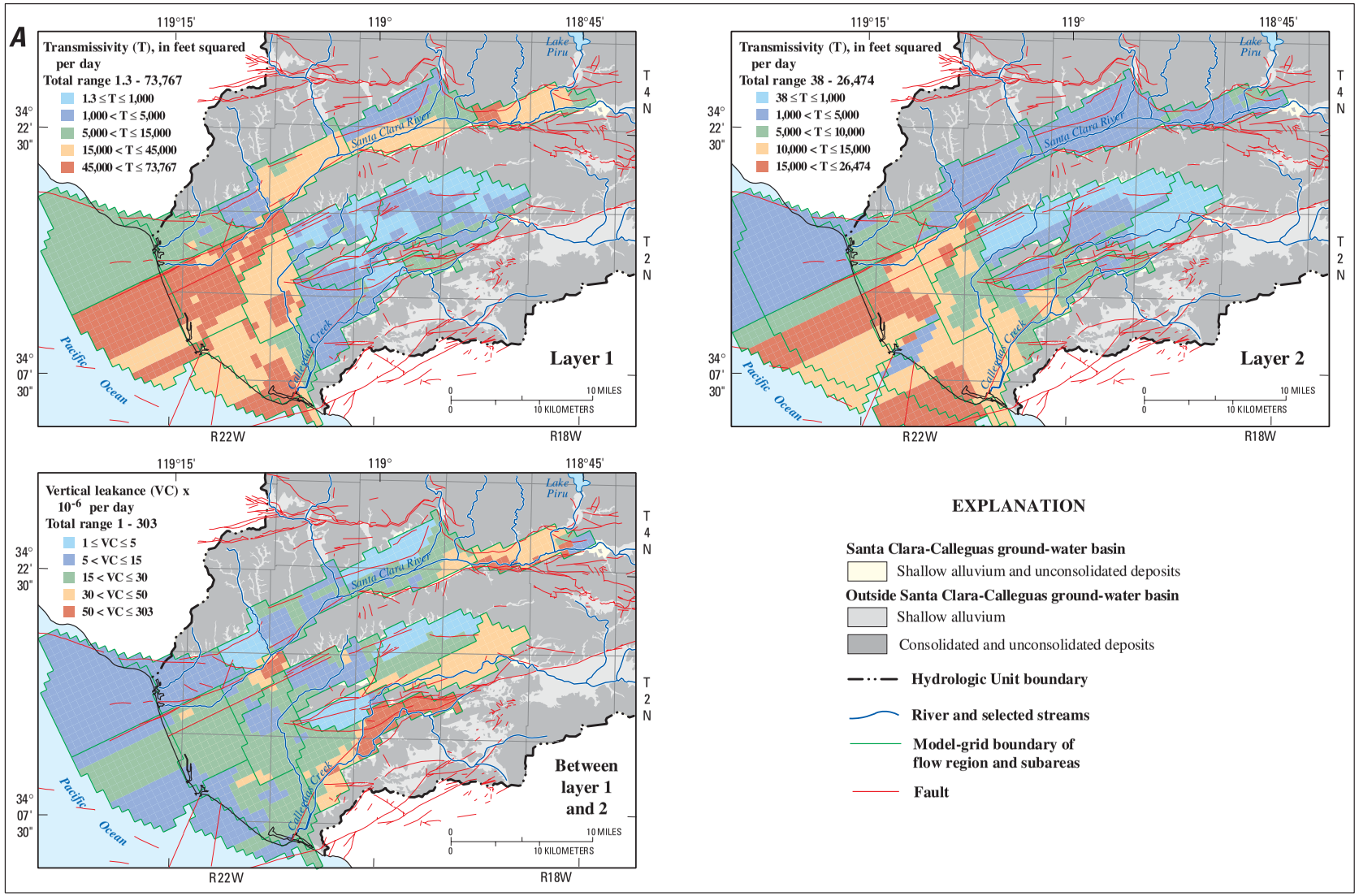

Figure 19. Distribution of hydraulic properties in layers 1 and 2 of the model of the Santa Clara–Calleguas ground-water basin, Ventura County, California. ***A***, Distribution of transmissivity in model layers 1 and 2, and vertical leakance between model layers 1 and 2. ***B***, Storage coefficient for model layers 1 and 2.

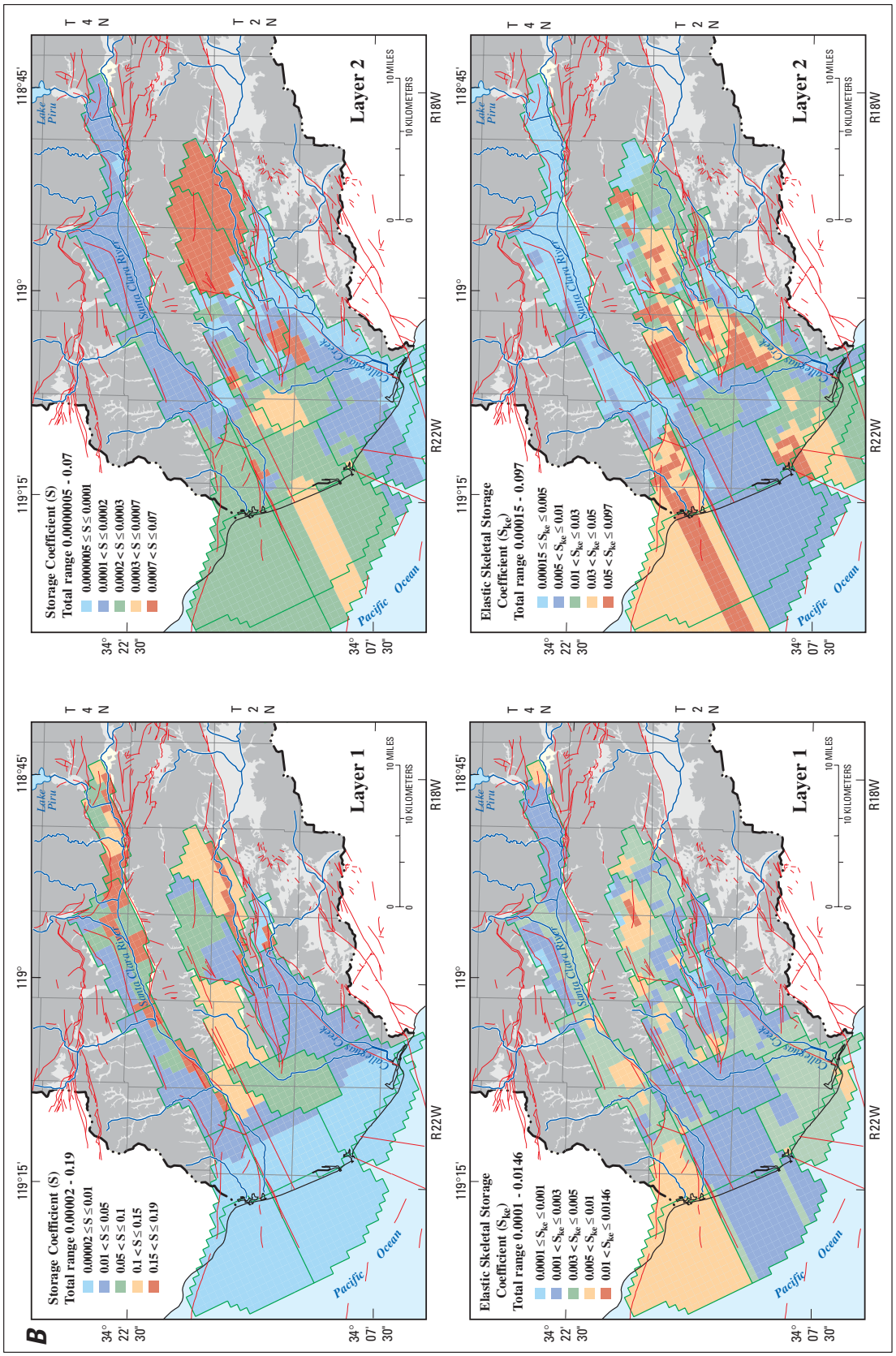

Figure 19—Continued.

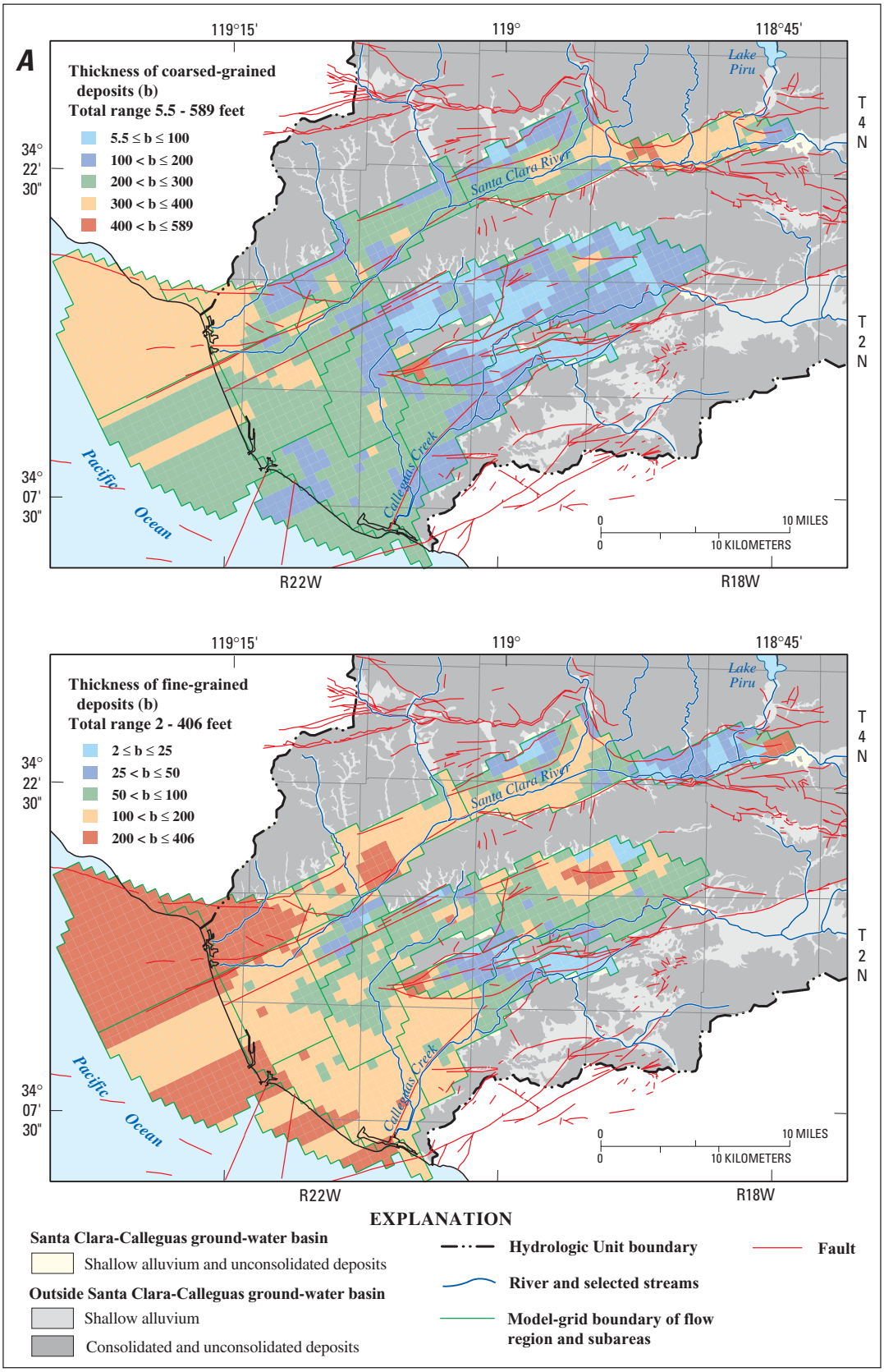

Figure 20. Distribution of estimated total thickness of coarse-grained and fine-grained interbeds used to estimate hydraulic properties and storage properties for the model of the Santa Clara–Calleguas ground-water basin, Ventura County, California. ***A***, Upper-aquifer system (model layer 1). ***B***, Lower-aquifer system model (layer 2).

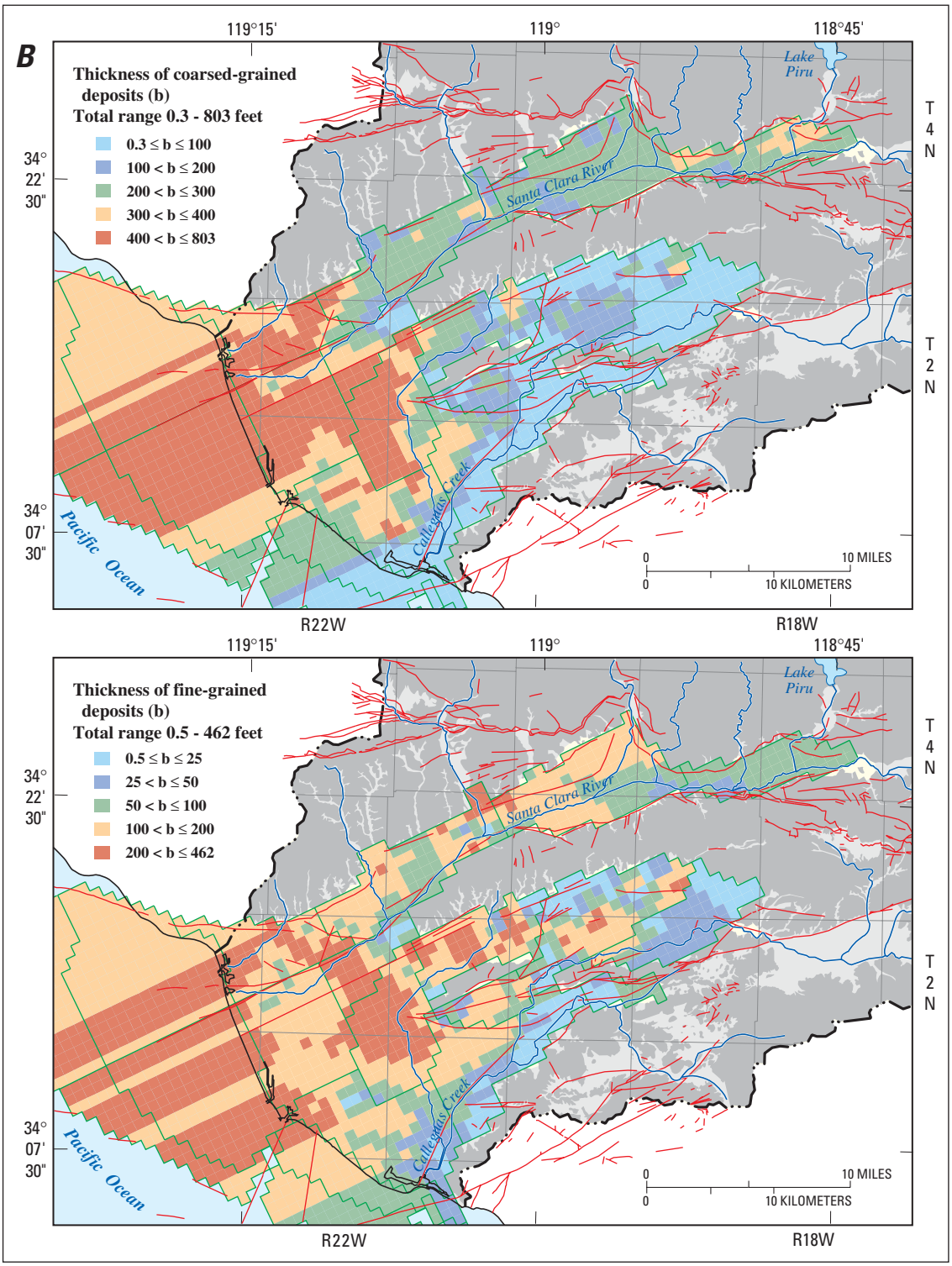

Figure 20—Continued.

Storage Properties

The hydraulic properties used to simulate the changes in storage of water within the aquifer systems consist of three components (Hanson, 1989). The first two components are specific yield and the elastic storage coefficient of the aquifer system, and the third component is the inelastic storage coefficient, which governs the irreversible release of water from the inelastic compaction of the fine-grained deposits. The specific yield and the elastic storage coefficients represent and govern the reversible release and uptake of water from storage. The elastic and inelastic storage coefficient represents the sum of storage owing to the compressibility of water and to the compressibility of the matrix or the skeleton of the aquifer system.

Storage owing to the compressibility of water was estimated as the product of the compressibility and the specific weight of water, the porosity, and the total thicknesses of the coarse- and fine-grained deposits in the aquifer (fig. 20). The assumed porosities were 35 and 25 percent for fine- and coarse-grained deposits, respectively; they were estimated from transport modeling of seawater intrusion along the Hueneme submarine canyon (Tracy Nishikawa, U.S. Geological Survey, written commun., 1994) and range from 1.8×10^{-5} to 2.5×10^{-4} for the upper-aquifer system (layer 1) and from less than 1×10^{-6} to 4.5×10^{-4} for the lower-aquifer system (layer 2). The ranges were specified within MODFLOW as the aquifer-system storage coefficients.

The upper-aquifer system (layer 1) was simulated as unconfined in the Santa Clara Valley, the Las Posas Valley, parts of the Santa Rosa Valley subareas, the Oxnard Plain Forebay subarea, and the Northeast Oxnard Plain subareas (fig. 19*B*). In the remainder of the Oxnard Plain and the Mound subareas, the upper-aquifer system was simulated as confined. Storage coefficients, estimated from specific yields from previous models, range from 0.01 to 0.19 in the Santa Clara River subareas; the estimate was 0.12 along Conejo Creek in the Santa Rosa Valley subarea. The storage coefficients (specific yields) were assumed to range from 0.02 to 0.19 in the Las Posas Valley subareas (fig. 19*B*).

The elastic and inelastic skeletal storage coefficients were simulated using the interbed storage package (Leake and Prudic, 1991). The elastic skeletal storage coefficient of the coarse-grained deposits was estimated from the difference between an estimated aquifer specific storage and the specific storage representing the compressibility of water (Hanson, 1989). Specific storage is the ratio of the storage coefficient to the thickness of the sediments, in this case the aggregate thickness of the coarse-grained deposits. Reported values for aquifer specific storage determined from local aquifer tests in the upper- and lower-aquifer systems range from 1.2×10^{-6} to 2×10^{-6} ft^{-1} (Neuman and Witherspoon, 1972; Hanson and Nishikawa, 1996). An initial elastic specific storage of 3×10^{-6} ft^{-1} was assumed from other reported values for alluvial sediments (Ireland and others, 1984; Hanson, 1989). The aquifer elastic skeletal storage coefficient was estimated as the product of the aquifer skeletal specific storage and the aggregate cell-by-cell thickness of the coarse-grained deposits for each model layer (fig. 20). In a similar manner, the elastic skeletal storage coefficient of the fine-grained deposits was estimated from the difference between a specific storage for the fine-grained deposits and the specific storage representing the compressibility of water (Hanson, 1989). The elastic storage coefficient for the fine-grained deposits was estimated as the product of the elastic skeletal specific storage of the fine-grained deposits and the aggregate cell-by-cell thickness of fine-grained deposits for each model layer (fig. 20). The composite aquifer-system elastic skeletal storage coefficient was the sum of the elastic skeletal storage coefficients for the coarse-grained and fine-grained deposits for each cell in each model layer (fig. 19*B*).

The third component of storage, owing to the inelastic compaction of the fine-grained deposits, was estimated as the product of the inelastic specific storage and the aggregate cell-by-cell thickness of the fine-grained deposits for each model layer (fig. 20). An initial inelastic skeletal specific storage of 2×10^{-4} ft^{-1} was based on the estimates from a consolidation test performed on the cores of fine-grained deposits from the Oxnard and Mugu aquifers (California Department of Water Resources, 1971, figs. VI–12 and VI–13) and aquifer-test analyses (Neuman and Witherspoon, 1972; Neuman and Gardner, 1989); these estimated range from 1.3×10^{-4} to 4.3×10^{-4} ft^{-1}.

The transition from elastic to inelastic storage is controlled by the preconsolidation stress—the maximum previous load that has been put on each sedimentary layer. The preconsolidation-stress threshold, expressed in terms of equivalent hydraulic head, can range from 50 ft of water-level decline in some well-sorted, fine-grained deposits that have had minimal sedimentary loading or lithification to more than 150 ft of water-level decline in some lithified, compressed, poorly sorted, or coarse-grained deposits (Holzer, 1981). The transition from elastic to inelastic storage was estimated to be 150 ft of water-level decline from predevelopment conditions throughout the lower-aquifer system and 100 ft of water-level decline throughout the upper-aquifer system, with the exception of 50 ft of water-level decline in the upper-aquifer system in the South Oxnard Plain subarea. These estimates were based, in part, on consolidation tests (California Department of Water Resources, 1971), water-level hydrographs (figs. 13 and 14), subsidence trajectories (fig. 9*C*), and lithologic data (Densmore, 1996).

Vertical Leakance

Vertical leakance controls vertical flow between the upper- and lower-aquifer systems. Vertical leakance was calculated for this model (fig. 19A) as the estimated vertical hydraulic conductivity divided by the combined half-thicknesses of each adjacent model layer for the estimated fine-grained deposits (fig. 20) in the upper- and lower-aquifer systems (McDonald and Harbaugh, 1988, eq. 5). Estimates of vertical leakance of flow between the upper and lower aquifers used in previous regional models range from less than 9×10^{-6} to 0.002 (ft/d)/ft for the Oxnard Plain subarea (California Department of Water Resources, 1975; Reichard, 1995, fig. 12). A subregional model developed for the Santa Rosa Valley subarea (Johnson and Yoon, 1987) yielded estimates that range from 1.5×10^{-3} (ft/d)/ft between the alluvium and the underlying Santa Margarita Formation to 3×10^{-5} (ft/d)/ft between the Santa Margarita and Saugus Formations and the underlying Conejo Volcanics. A subregional model developed for Las Posas Valley (CH2M HILL, 1993) used a uniform value of vertical hydraulic conductivity of 0.05 ft/d to simulate flow across the aquitards separating the Fox Canyon and Grimes Canyon aquifers in the Las Posas Valley subareas. Published values of vertical hydraulic conductivity range from 0.01 to 1×10^{-4} ft/d for the Oxnard Plain subarea (California Department of Water Resources, 1975; Neuman and Gardner, 1989) and from 24. to 6×10^{-4} ft/d for the Pleasant Valley subarea (Hanson and Nishikawa, 1996).

The initial estimates of vertical leakance were from previous ground-water flow models. For the extensions of the two model layers, the initial values used were 1×10^{-6} (ft/d)/ft for the Mound, the Santa Clara River Valley, the Pleasant Valley, and the Santa Rosa Valley subareas and for the offshore regions, and 1×10^{-5} (ft/d)/ft for the Las Posas Valley subareas. These are largely assumed values. The final distribution of vertical leakance was based on fitting simulated head differences to those measured at multiple-well completion sites (fig. 15). All vertical leakance values were held constant for the period of simulation.

Model Calibration

Calibration of the transient-state simulations was done for 1891–1993 and was based on matching water levels (fig. 13, 14, 15, and 21) and streamflows (fig. 22). Predevelopment conditions (steady-state) were used as the initial conditions for the transient-state calibration. The long period of transient simulation was required because features of development, such as coastal landward flow (seawater intrusion) and subsidence, are dependent on the initial state of the aquifer systems.

Calibration Summary

Calibration was achieved through trial-and-error adjustments to recharge, hydraulic properties, and pumpage to achieve a good fit within each subarea over the historical period of record. These adjustments were made as systematically as possible, starting with recharge and streamflow, then hydraulic properties, and finally indirect agricultural pumpage estimates. Calibration and model development began using the extended model developed by Reichard (1995).

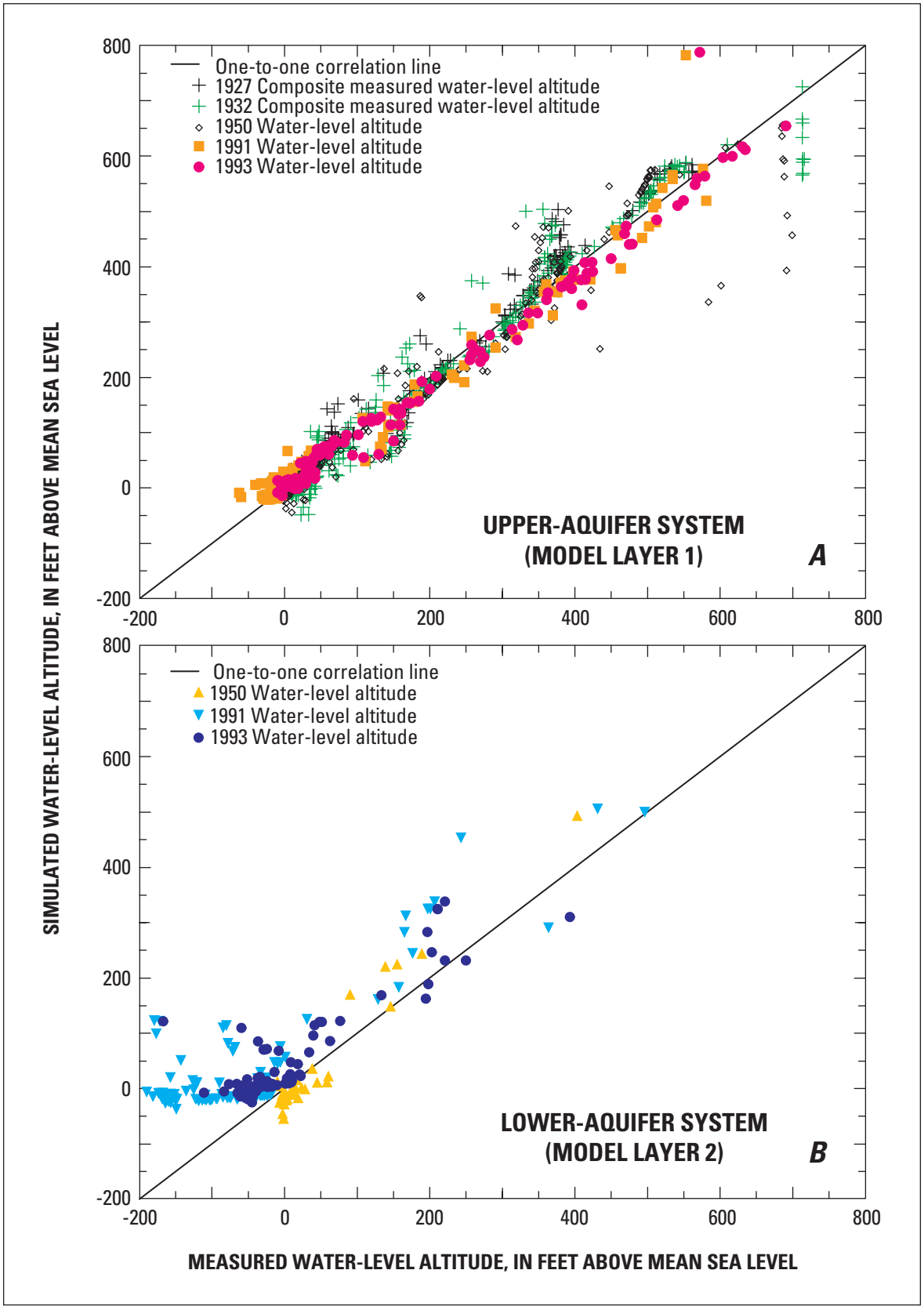

Figure 21. Relation between measured and simulated water-level altitudes for selected years for the transient simulation of developed conditions (1927, 1932, 1950, 1991, and 1993) in the Santa Clara–Calleguas ground-water basin, Ventura County, California. ***A***, Upper-aquifer system (model layer 1). ***B***, Lower-aquifer system (model layer 2). ***C***, Oxnard Plain.

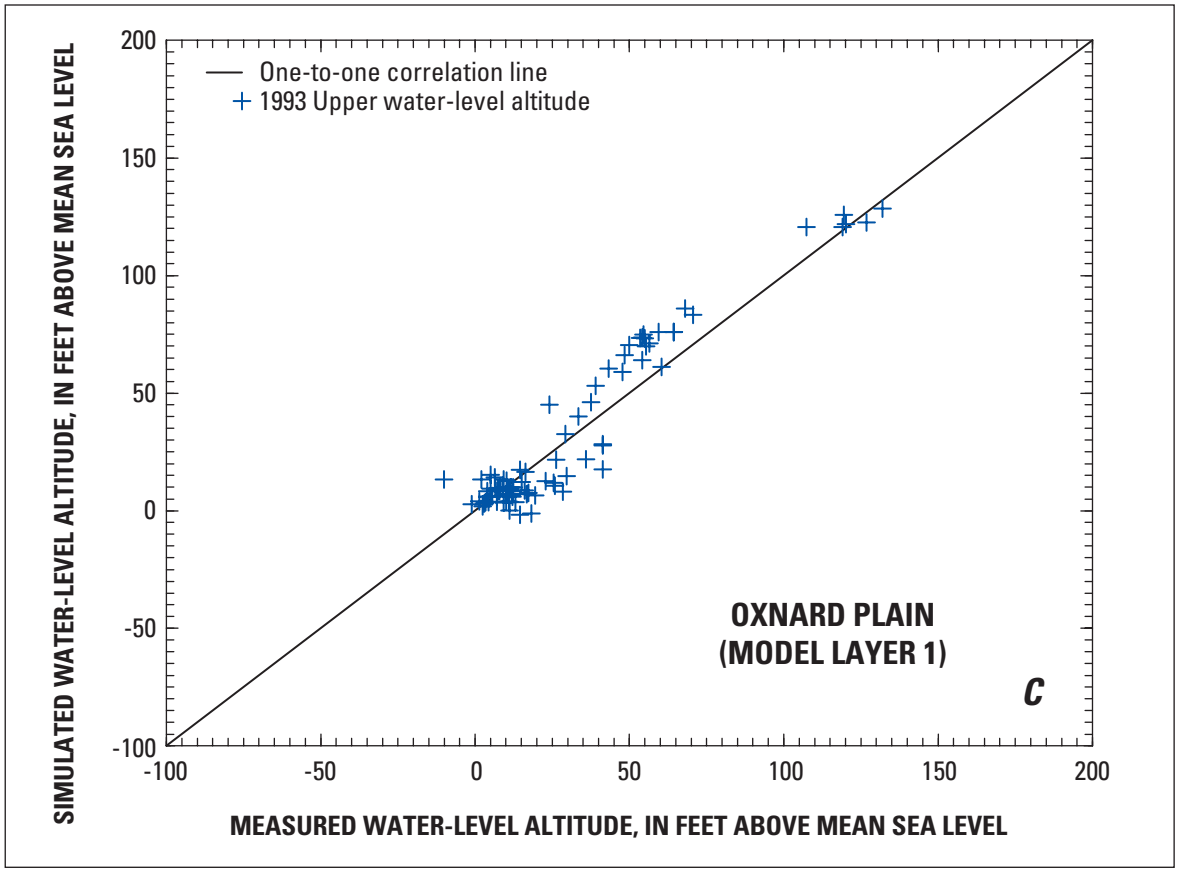

Figure 21—Continued.

Predevelopment Initial Conditions

Calibrating the model was an iterative process between the steady-state and transient-state simulations. The steady-state simulation provided initial conditions for the transient-state calibration. After each transient-state calibration, the updated model parameters were used to simulate updated steady-state conditions prior to additional calibration. The steady-state conditions were dependent on recharge (streamflow, mountain-front recharge, and valley-floor recharge) and discharge (streamflow and ET) from the aquifer system, transmissivity, vertical leakance between layers, fault hydraulic characteristic, and general-head boundary conductance. Because water levels are constant under steady-state conditions, storage is not required to simulate steady-state conditions. Initial recharge was based on the long-term seasonal geometric-mean ratios of runoff to wet-period winter precipitation. Streamflows were simulated as median streamflows. The composite ET rates and the model cells with the potential for ET for the years 1912, 1927, 1932, and 1950 (Conejo Creek area) were used for the predevelopment simulation (fig. 23). The initial hydraulic properties were based on Reichard's (1995) values and were adjusted during transient-state calibration. Few data were available for comparison of steady-state conditions. However, the simulated initial conditions are considered adequate if water levels are 40 to 50 ft above sea level near the coast along the Oxnard Plain subareas. This requirement was based on a report of early hydraulic conditions (Freeman, 1968).

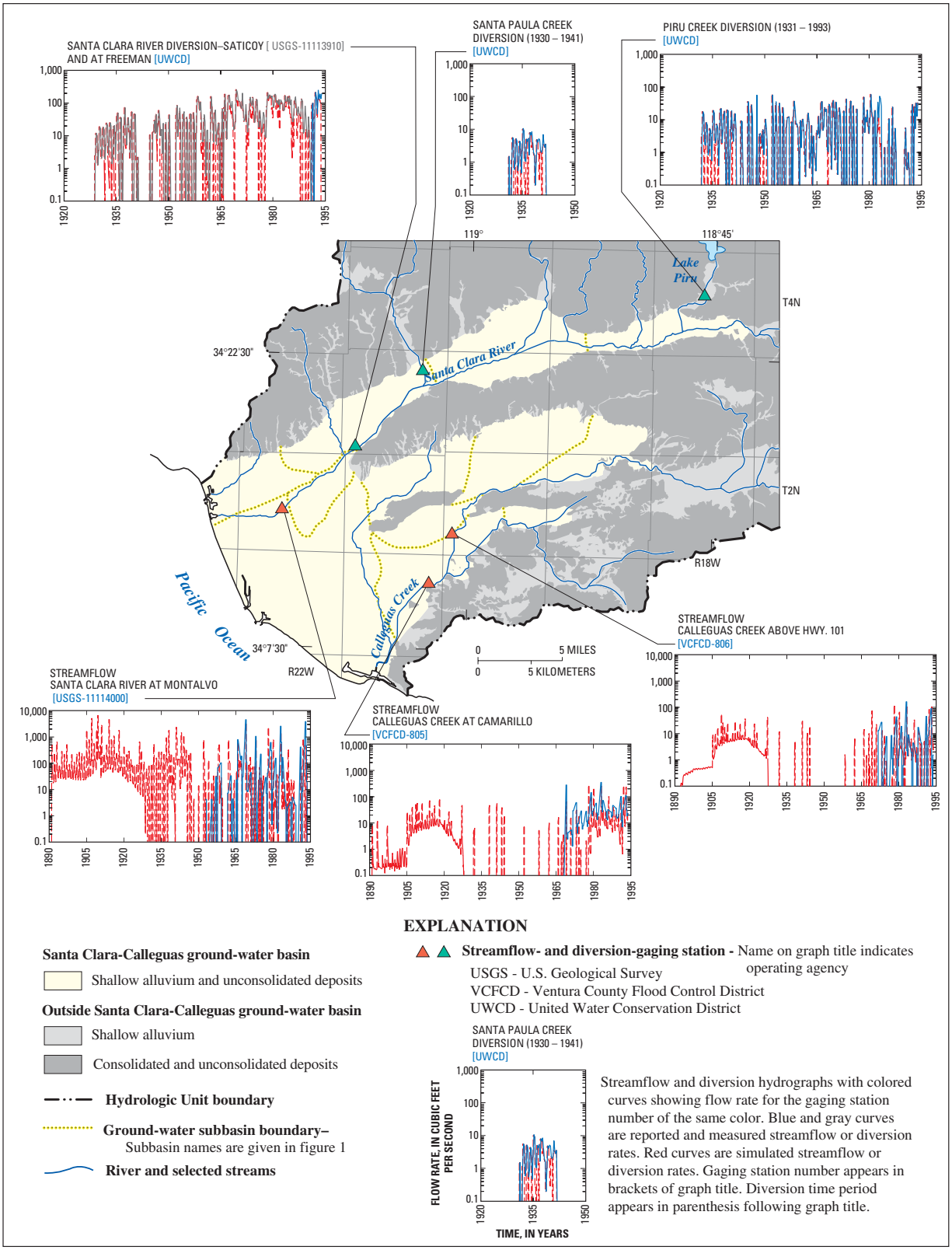

Figure 22. Measured and simulated seasonal streamflows or diversion rates for the Santa Clara–Calleguas ground-water basin, Ventura County, California.

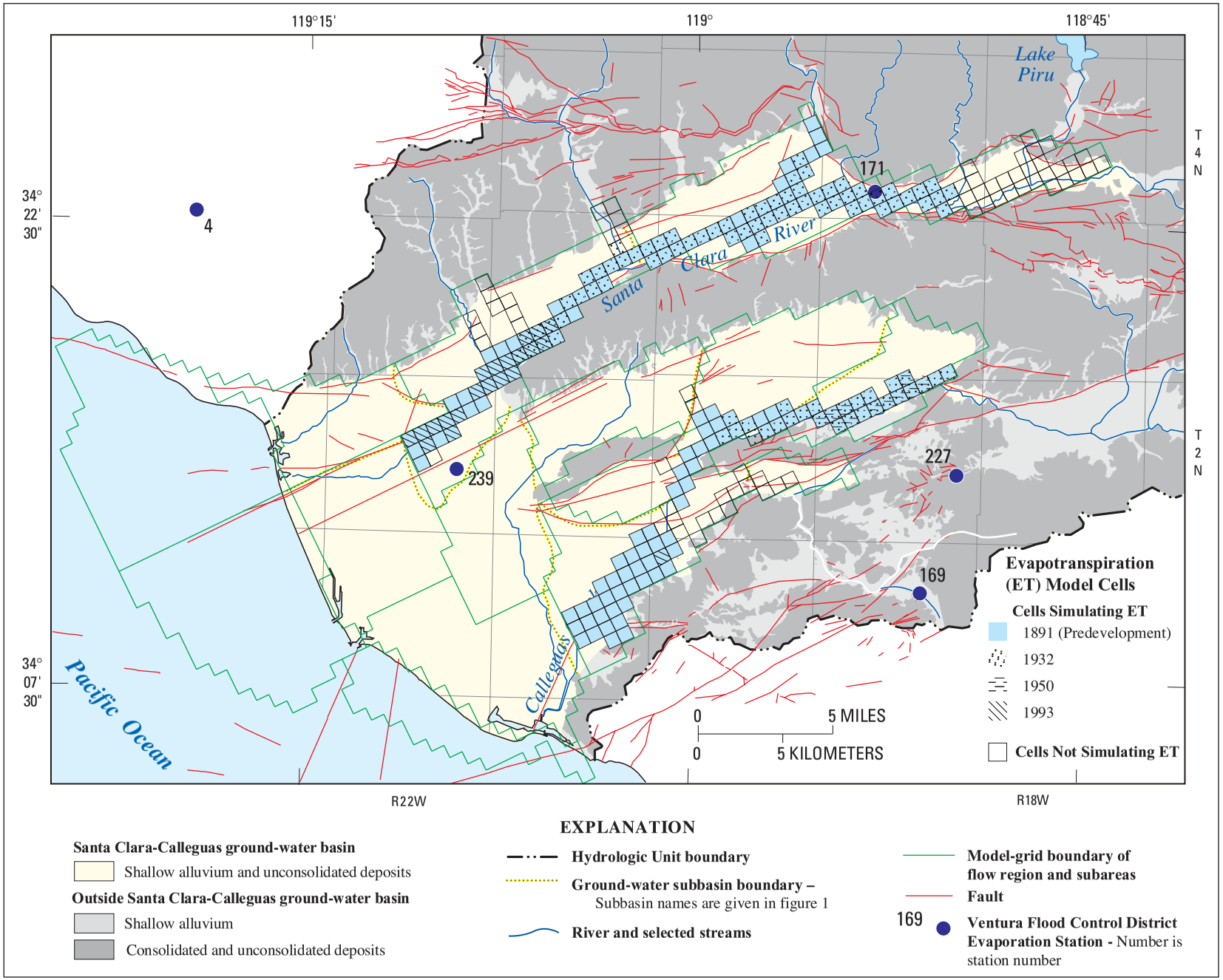

Figure 23. Model cells with simulated evapotranspiration in 1891 (predevelopment), 1932, 1950, and 1993 in the upper layer of the model of the Santa Clara-Calleguas ground-water basin, Ventura County, California.

Transient-State Calibration Parameters

Transient-state conditions were dependent on recharge (streamflow, mountain-front recharge, valley-floor recharge, and artificial recharge) to and discharge (pumpage, streamflow, and ET) from the aquifer system and on transmissivity, storage, vertical leakance between layers, fault hydraulic characteristics, and general-head boundary conductance. Because of the large head differences within some parts of the aquifer systems, water-level maps were used for comparisons but are considered less reliable than time-series data. Estimates of spatial fit were made for selected times of the transient simulation (fig. 21). Calibration was primarily based on temporal comparisons, instead of spatial comparisons, using long-term water-level hydrographs (figs. 13, 14, and 15), streamflow hydrographs (fig. 22) and time-series of bench-mark land-surface altitudes (subsidence trajectories) (fig. 9).

Recharge was adjusted to reduce the overestimation of mountain-front recharge, valley-floor infiltration, and streamflow infiltration. The modified rational method of estimating infiltration tended to overestimate the water available during the wettest seasons; therefore, the upper limit of runoff available for mountain-front recharge was limited to less than 90 percent of average precipitation.

Simulated streamflow infiltration initially was too large when floodflows or intermittent flows were spread over an entire season, and it did not reflect the observed and measured changes in streamflow during low-flow and high-flow conditions. The flow-dependent changes in streambed conductance are believed to be related mostly to changes in channel width. Grouping and varying streambed conductance with flow were critical for accurately depicting water-level declines and recoveries in wells during wet and dry periods (figs. 13 and 14). Grouping and varying streambed conductance for the dry periods helped to simulate a more accurate depiction of the conveyance (delivery) of controlled releases from Lake Piru that are routed down the Santa Clara River and are simulated as the total reported diversions at Piru, Santa Paula, Saticoy, and Freeman (fig. 22). Segments of the streamflow network in the coastal plain (segments 22, 23, 29, and part of 30) (fig. 18*B*) are not in direct connection with the upper-aquifer system and therefore were assigned a streambed conductance of zero. This allowed the simulated water levels for predevelopment conditions and the recovery periods for development conditions to rebound to the measured water levels (figs. 13 and 14). Streamflow was increased from about 1.5 to 14 ft^3/s for Arroyo Simi to account for treated-sewage effluent discharged between 1964 and 1993. On the basis of streamflow data from the hydrographs for Calleguas Creek at Camarillo (fig. 22, VCFCD station 805), the initial discharge (1964–79) was estimated to start at 1.5 ft^3/s and increase linearly to 10 ft^3/s.

The hydraulic properties estimated by Reichard (1995) were adjusted during model calibration; they include transmissivity, storage properties, and vertical leakance. The initial estimates were described earlier (see section on “Hydraulic Properties”). The only change to the storage properties was the transformation of Reichard’s (1995) initial estimates to cell-by-cell estimates, as was described earlier. Additional calibration also was done for fault hydraulic characteristics and offshore general-head boundary conductance. These properties were adjusted for the period of reported pumpage largely on the basis of the water levels in the hydrographs.

Transmissivity values were reduced by a factor of 0.55 for the lower layer of the Port Hueneme area and were increased by a factor of 1.5 for the lower layer of the East Las Posas Valley subarea (figs.17*B* and 19*A*) compared with the values used by Reichard (1995). The decrease in transmissivities in the lower layer brought the values closer to those in the transport model of the Port Hueneme area (Nishikawa, 1997) and to those estimated from aquifer tests completed in the East Las Posas Valley area (CH2M HILL, 1992). The transmissivities of the aquifer layer underlying the major streams and tributaries also were increased during model calibration.

Adjustments in vertical leakance were made on the basis of water-level differences at multiple-well observation sites and, for some areas, on the basis of data from the hydrographs of selected production wells. Recall that the vertical leakances were calculated as the estimated vertical hydraulic conductivity divided by the combined half-thicknesses of the estimated fine-grained deposits in the upper- and lower-aquifer systems (McDonald and Harbaugh, 1988, eq. 51). Cell-by-cell estimates for the West Las Posas Valley subarea were based on a vertical hydraulic conductivity of 0.0005 ft/d. Cell-by-cell estimates for the Forebay region of the Oxnard Plain were based on a vertical hydraulic conductivity of 0.001 ft/d for all but five cells in the Saticoy area, for which a value of 0.01 ft/d was used. The final distribution of vertical leakances ranged from 1×10^{-7} to 3.03×10^{-5} (ft/d)/ft (fig. 19*A*). Cell-by-cell estimates initially were made for all the subareas, but the estimates did not improve model fit for the East and South Las Posas Valley subareas. For these two subareas, estimates were not based on the thickness of the fine-grained deposits; the final calibrated vertical leakances align with the underlying syncline-anticline structures within the lower-aquifer system (figs. 9 and 20).

Although pumpage was the largest stress in the model, some uncertainty remained about the accuracy of the land-use estimates of pumpage. Some adjustments in the magnitude and distribution of the pumpage estimated from land use were made during the calibration of the flow model in order to have the model enter the final 10-years of reported pumpage at the correct water-level altitudes. These changes were largely based on the measured temporal variations in ground-water levels in the subareas and on the magnitude and changes of pumpage for the 1983–93 period of reported pumpage. Changes to land-use estimates of historical pumpage include elimination of pumpage from the Santa Clara River Valley subareas and the Oxnard Plain Forebay subarea for 1891–1918 so that the first significant ground-water pumpage began with the dry period of 1919–36. The 1950 and 1969 estimates of the land-use-based pumpage also had to be modified for selected subareas. The changes in the 1950 estimate of agricultural pumpage applied over the period 1946–61 ranged from a 34-percent reduction in pumpage for the Mound subbasin to an approximate 300-percent increase for the Piru subbasin; the changes in the 1969 estimate applied over the period 1962–77 ranged from a 34-percent reduction for the Mound subarea to an approximate 100-percent increase in the North and South Pleasant Valley and the Piru subareas. These changes brought the estimated historical agricultural pumpage into alignment with the reported agricultural pumpage (fig. 11*B*) and improved the alignment between the measured and simulated ground-water levels and the land-use changes in various subareas for these two periods. Pumpage was reduced to 40 percent of the 1932 estimate for the years 1935–45, which span the post-Great Depression and World War II period, as well as a severe drought that was followed by one of the wettest periods on record (fig. 2). This reduction was the only way to achieve the record water-level recoveries that have been equaled only during predevelopment conditions and more recently during 1993. These adjustments did not affect calibration of hydraulic properties or recharge during the period of reported pumpage.

The percentage of pumpage between layers was changed during model calibration. The final vertical distribution of pumpage between the model layers for wells spanning both model layers is summarized in figure 7*B* for all the subareas.

The general-head boundaries that initially were placed at the submarine outcrops were moved landward to better represent the average location of the freshwater-saltwater interface. The values of the boundary heads were aligned with the top of the basal coarse-grained layers in the Oxnard and Hueneme aquifers for the upper- and lower-aquifer systems, respectively. The boundary conductances were grouped into several coastal subreaches with different values, grouping the conductances, however, did not improve model fit. The final configuration consisted of a single value for each model layer, which was the simplest approach without additional data and was adequate for matching water levels along the coast. The flows at the general-head boundaries were monitored to verify that simulated outflow was occurring during wet periods when recovery of water levels exceeded the specified heads of the seawater at the general-head boundary. To be consistent, the model should simulate coastal landward flow (seawater intrusion) during the major droughts when water levels decline below the heads of the denser seawater. The current model is consistent with the concept of the wet-period outflow, as shown by the outflows of 1984–93 (figure 25*B* in the section "Transient-State Model Comparisons"), and with the concept of coastal landward flow (seawater intrusion) during droughts, such as the drought of 1987–91.

Transient-State Model Comparisons

Calibration and goodness-of-fit of the transient-state model were determined by comparing simulated values with measured values for ground-water levels, streamflow, and land subsidence. The simulated water levels were compared with water-level maps for 1932 and 1993 (fig. 12) and correlated with the water-level data for 1927, 1932, 1950, 1991, and 1993 (fig. 21) and the water-level hydrographs of selected production wells (figs. 13 and 14) and multiple-well observation sites (fig. 15). A comparison of simulated streamflow was made for the downstream gaging stations and the streamflow-diversion sites (fig. 22). The spatial distribution of potential ET, based on riparian vegetation, and the spatial distribution of simulated ET for predevelopment and developed conditions in 1932, 1950, and 1993 were also compared (fig. 23). Measured and simulated subsidence for selected bench marks (fig. 24) were used to compare the potential effects of water-level declines on simulated subsidence in the South Oxnard Plain subarea. And, finally, selected comparisons of ground-water flows were used to confirm that flows within the model (fig. 25) were conceptually consistent with the framework provided by geohydrologic and geochemical analyses.

The best and primary comparison period is the 10-year period of reported pumpage, 1984–93, which represents one dry period and parts of two wet periods (fig. 2*A*). Within this period is a 4-year period (1990–93) for which measured water levels and water-level differences between aquifer systems measured at the multiple-well monitoring sites (fig. 15) can be compared with model results.

The model generally matched the measured water-level, streamflow, and bench-mark data for the calibration period (figs. 12, 13–15, 21; 22, and 24, respectively). Comparisons of the simulated and measured water levels estimated from land-use maps have some uncertainty because the measured ground-water levels reflect a wide variety of screened intervals in wells, and the "synoptic" measured water levels reflect water levels measured over spans of several months over a season (fig. 12*A*,*B*). The model slightly overestimates historical water-level altitudes for the early period of development (fig. 12*A*). The correlation diagram on figure 12*A* shows no systematic discrepancies between measured and simulated water levels in the upper-aquifer system. Measured minus simulated water levels have a mean error (ME) for the upper aquifer system of –22.8 ft and a root mean square error (RMSE) of 35.2 ft for 1927 (number of comparison wells: N = 169), and a ME of 7.29 ft and a RMSE of 42.2 ft for 1932 (N = 354). A comparison of the measured and simulated water levels for 1932 (fig. 12*A*) indicate similar patterns. Water-level differences between simulated and measured data range from less than 5 ft near the coast to about 40 ft in the Forebay, and they are less than 20 to 40 ft in the Santa Clara River Valley and Pleasant Valley subareas.

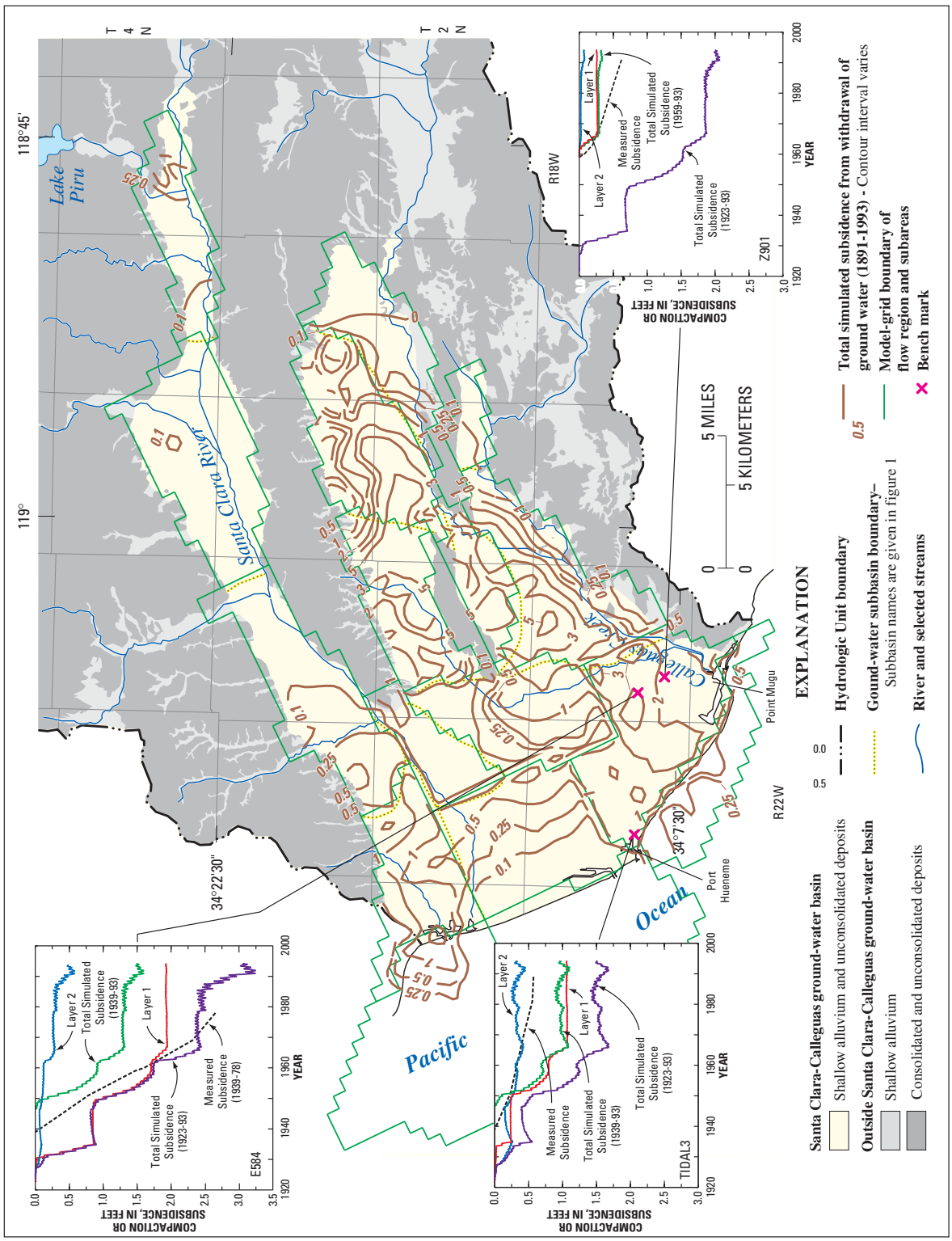

Figure 24. Simulated compaction owing to withdrawal of ground water, 1891–1993, in the Santa Clara–Calleguas ground-water basin, Ventura County, California, and locations of selected bench marks and related measured and simulated bench-mark trajectories.

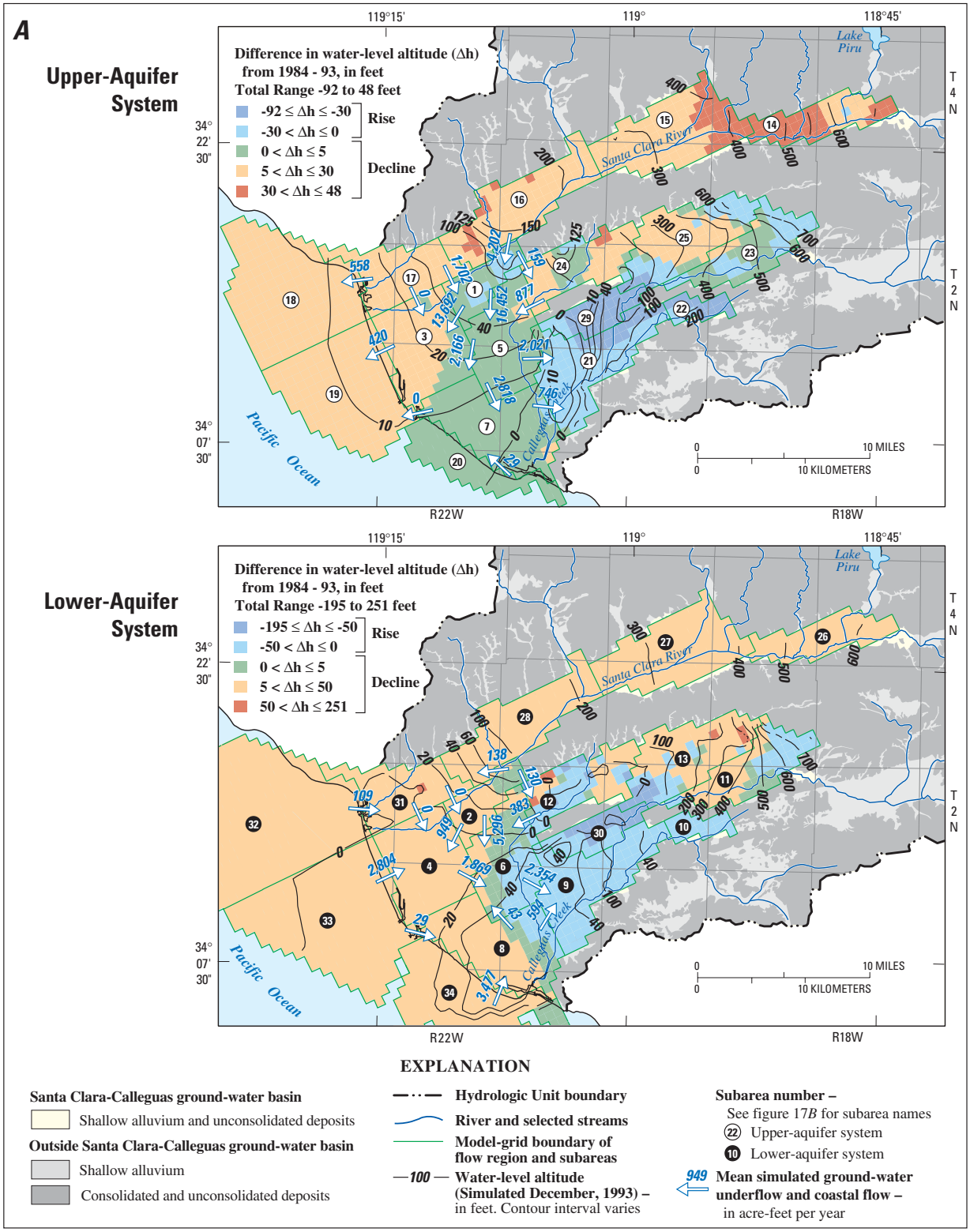

Figure 25. ***A***, Simulated water-altitudes (December 1992), decline in ground-water levels from 1984 to 1994, and mean ground-water flow in the Santa Clara–Calleguas ground-water basin, Ventura County, California. ***B***, Cumulative changes in ground-water storage and ground-water flow for selected subareas during 1984–93. ***C***, Hydrologic budgets for predevelopment conditions. ***D***, Hydrologic budgets for 1984–93 period.

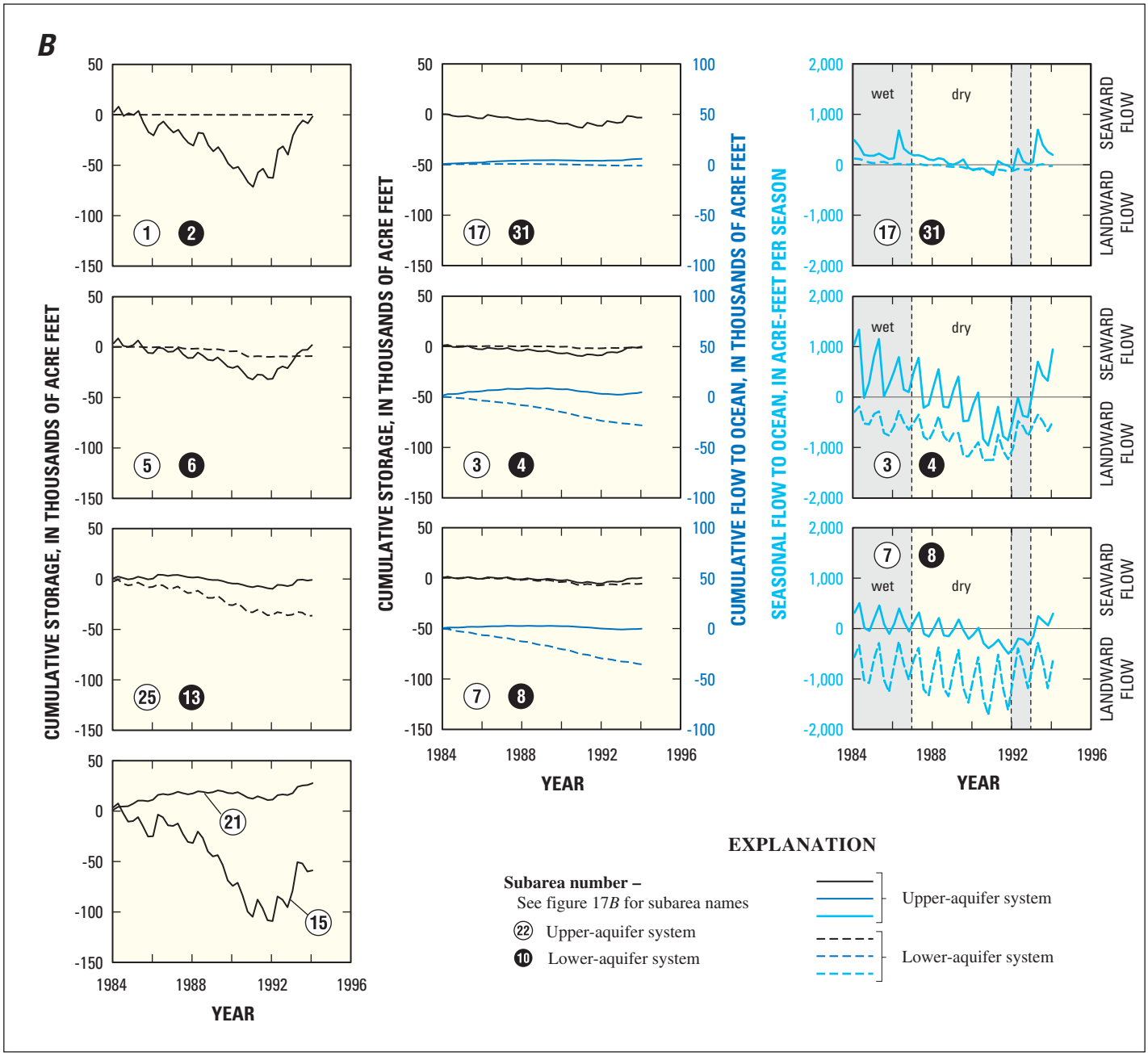

Figure 25—Continued.

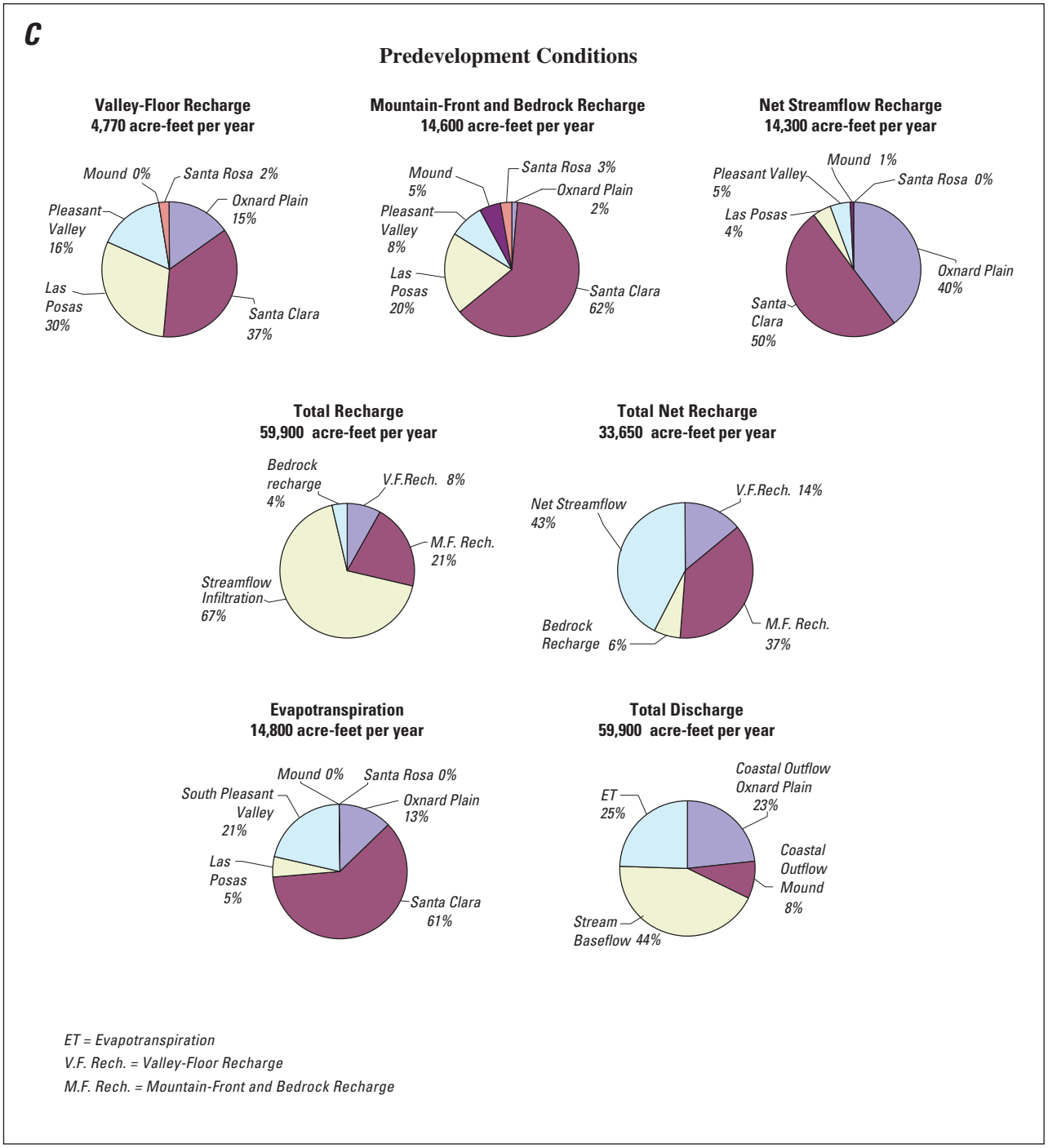

Figure 25—Continued.

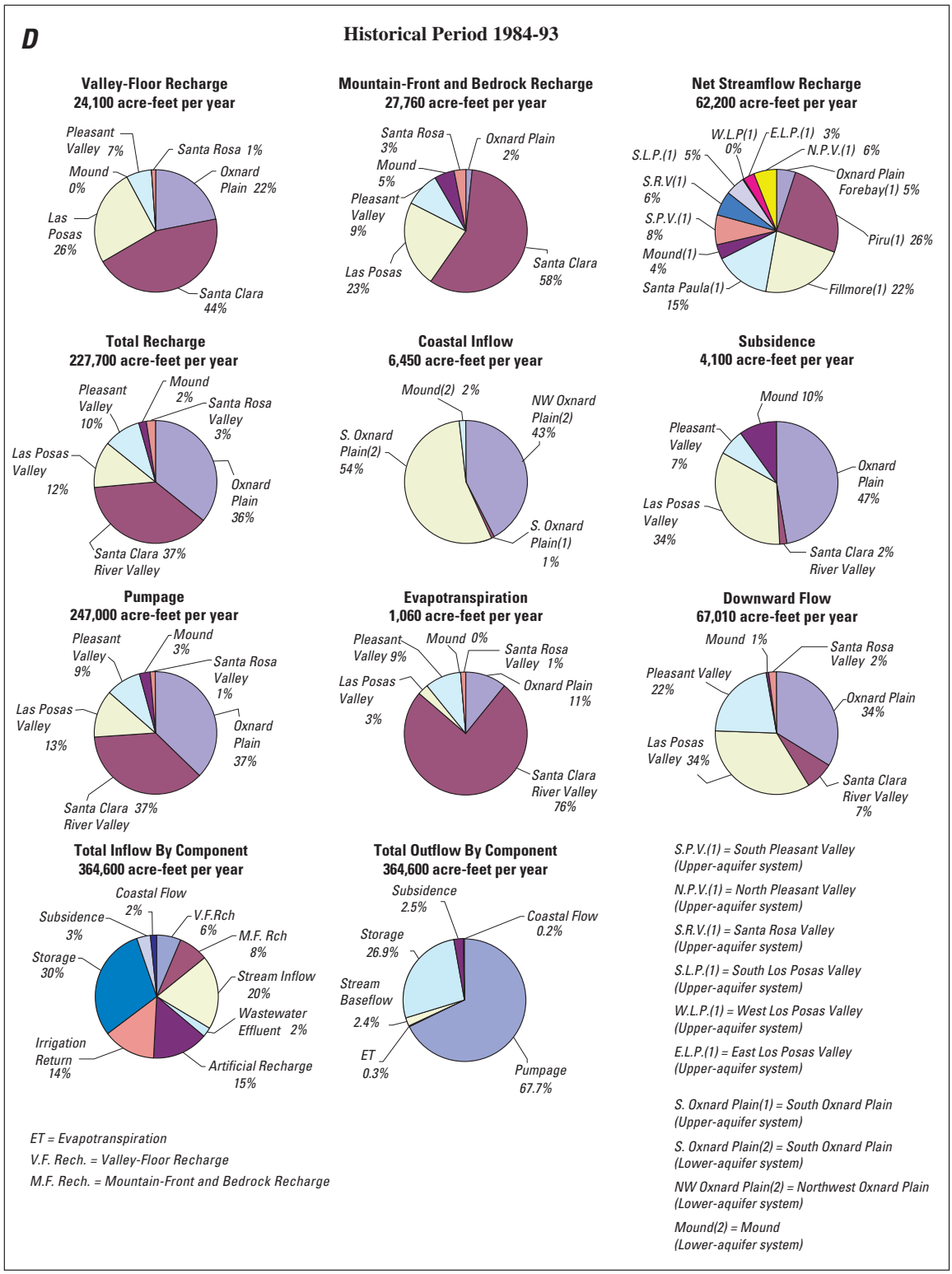

Figure 25—Continued.

The simulated water levels were lower than the measured water levels for 1950, the first period of substantial ground-water development in both aquifer systems [ME and RMSE are 9.95 and 52.7 ft, respectively, for the upper-aquifer system (N = 297) (fig. 21*A*), and 8.39 and 39.3 ft, respectively, for the lower-aquifer system (N = 31) (fig. 21*B*)]. The simulated water levels for the 1987–91 drought were lower than the measured water levels in the upper-aquifer system [ME and RMSE are 1.96 ft and 26.1 ft, respectively, (N = 130) (fig. 21*A*)] and higher than the measured water levels in the lower-aquifer system [ME and RMSE are –89.8 ft and 110.4 ft, respectively (N = 101) (fig. 21*B*)]. The differences between the measured and simulated water levels in the lower-aquifer system are, in part, due to the many wells used for the calibration which are completed solely in the Fox Canyon or Grimes Canyon aquifer in parts of the Pleasant Valley and Las Posas Valley subareas. These aquifers were not simulated as separate aquifer layers in the current model and therefore the simulation represents the average water level for the entire lower aquifer system. The Fox Canyon and Grimes Canyon aquifers are relatively low-permeability aquifers; pumpage from these aquifers resulted in large water-level declines. The overlying Hueneme aquifer is relatively more permeable; pumpage from this aquifer resulted in smaller water-level declines. Measured water levels for the multiple-well monitoring sites indicate water-level differences within the lower-aquifer system of as much as 75 ft between the Hueneme aquifer and the Fox Canyon and Grimes aquifers (fig. 15). The model was calibrated to the Hueneme aquifer and would have required additional layers to simulate the water-level differences for the lower aquifers. Some water-level measurements also may have been affected by pumping, which resulted in measured water levels being lower than the simulated levels. Another reason for the water-level differences may be that instantaneous water-level measurements were compared with simulated water levels controlled by average seasonal pumpage.

Measured water levels for the 1992–93 wet-period recovered; the simulated water levels were lower than the measured water levels for the upper-aquifer system [ME and RMSE are 9.68 ft and 20.5 ft, respectively (N = 161) (fig. 21*A*)] and higher than the measured water levels in the lower-aquifer system [ME and RMSE are –42.3 ft and 66.9 ft, respectively (N = 94) (fig. 21*B*)]. When the comparison was restricted to the upper-aquifer system of the Oxnard Plain for spring 1993, the simulated water levels were only slightly lower than the measured water levels [ME and RMSE are 1.61 ft and 10.7 ft, respectively (N = 90) (fig. 21*C*)].

In general, the long-term water-level hydrographs (figs. 13 and 14) indicate that the match between measured and simulated water-level altitudes is good for the entire period of simulation, especially those for the Oxnard Plain subbasin. However, some hydrographs show large discrepancies between the simulated and measured water levels; examples of these discrepancies can be seen on the hydrographs of wells along Beardsley Wash, such as well 2N/21W-16J1 in the West Las Posas Valley subarea and wells along the Santa Clara River, wells 2N/22W-2C1 and 3N/22W-36K2 in the Santa Paula subarea, well 2N/22W-9J1 in the Mound subarea, and well 3N/19W-29E2 in the East Las Posas Valley subarea (fig. 14). A comparison of the short-term hydrographs for the RASA multiple-well monitoring sites shows good agreement between the simulated and measured water levels (fig. 15). The simulated water-level differences between the upper and lower layers closely match the measured seasonal and multiple-year patterns of water-level differences (fig. 15). This indicates that the collective estimates of vertical leakance, vertical distribution of pumpage, and recharge are reasonable.

Water-level differences between wells across faults were calibrated by adjusting fault hydraulic characteristics; for example, the water-level differences between well 2N/20W-23K1 (fig. 13) and well 2N/20W-23R1 (fig.14) across the San Pedro (Bailey) Fault in the Santa Rosa Valley subarea.

Seasonal water-level variations in the upper-aquifer system are controlled largely by streamflow infiltration and related streambed conductance; these factors, when combined with seasonally and climatically variable pumpage, resulted in water-level fluctuations of tens to a hundred feet in wells in the Santa Clara River Valley subareas [wells 4N/19W-25K2, 30R1; 22N/22W-11A1,2 (fig. 14)]. Water-level fluctuations in the Oxnard Plain Forebay subareas include the effects of artificial recharge and pumping back artificially recharged water [wells 2N/22W-12R1, 22R1 (fig. 14); wells 2N/22W-23B3–7, 2N/21W-7L3–6 (fig. 15)].

Simulated streamflows for Montalvo and for the Piru, Santa Paula, Saticoy, and Freeman diversions closely match measured streamflow along the Santa Clara River system. Simulated streamflows also match many of the historical high flow events (figs. 2*B* and 22); however, they overestimate low streamflow conditions (less than 10 ft^3/s) for some dry-year periods at Montalvo on the Santa Clara River (fig. 22). The simulations underestimated the diversions for some dry-year periods when flows were less than 2 to 10 ft^3/s at Saticoy and less than 2 ft^3/s at the Santa Paula and Piru diversions (fig. 22). Simulated streamflows for Camarillo and above Highway 101 in Calleguas Creek match measured streamflow; the simulated streamflow is intermittent in character after the onset of ground-water development in the late 1920s (fig. 22).

Simulation results indicate that land subsidence started as early as the 1920s and continued through 1984–93, the period when water levels declined below the water levels of the 1950s and 1960s. Results also indicate that preconsolidation may vary considerably and that subsidence occurred primarily during dry-year periods when seasonal and multiple-year water-level declines exceeded past declines in the South Oxnard Plain, Las Posas Valley, and Pleasant Valley subareas (figs. 24 and 25*B*). Subsidence started in the upper-aquifer system in the South Oxnard Plain subarea during the early period of development (1939–60) (fig. 24). Subsidence has continued, in part, because of the development of the lower-aquifer system, which has contributed most of the subsidence in recent decades (1959–93) (fig. 24).

Simulated subsidence generally matches total measured subsidence in the South Oxnard Plain subarea (fig. 24). The time-series comparisons of subsidence from bench-mark measurements are similar in trend but underestimate subsidence at BM Z 901 near Point Mugu and overestimate subsidence at BM TIDAL 3 near Port Hueneme (fig. 24). The extent of subsidence generally is not well known for areas outside the South Oxnard Plain subarea but may be overestimated for parts of the Pleasant and Las Posas Valley subareas. Field inspections throughout West and East Las Posas subareas did not reveal any surface expressions of land subsidence that would be expected for the amount of simulated subsidence. This overestimation may be caused by overestimation of inelastic skeletal specific storage, overestimation of the aggregate thickness of fine-grained material that is actually subject to loading from water-level declines, and a lack of separate model layers within the lower-aquifer system for the Pleasant and Las Posas Valley subareas. A detailed land survey or Interferometric Synthetic Aperture Radar (InSAR) imagery analysis would be needed to resolve this issue.

Model Uncertainty, Sensitivity, and Limitations

Numerical models of ground-water flow are useful tools for assessing the response of an aquifer system to changing natural and human-induced stresses. Regional-scale models are especially useful for assessing many of the components in the hydrologic cycle and the collective effect of ground-water development in separate subareas of a regional ground-water system. Models, however, are only an approximation of actual systems and typically are based on average and estimated conditions. The reliability or certainty with which a model can simulate aquifer response is directly related to the accuracy of the input data, the amount of detail that can be simulated at the scale of the model, and the model discretization of time and space. Hence, the regional models can be useful for simulating subregional and regional performance of a flow system and for providing boundary information for more detailed local-scale models even though the results of the regional model for a local scale may not be appropriate for site-specific problems such as the performance at a particular well.

The certainty of a model is inversely related to the duration, magnitude, and distribution of simulated inflows and outflows. Thus, better time-varying estimates of pumpage, recharge, irrigation return flow, streamflow, and coastal landward flow (seawater intrusion) could improve simulation of historical development. Additionally, the trial-and-error calibration process is inexact, and this problem is compounded by uncertainty of the variables and by sensitivity of the aquifer-parameter and boundary-condition estimates. Uncertainty in model attributes results in a broader range of possible aquifer-parameter and boundary-condition estimates used to constrain calibration of the ground-water flow model. Uncertainty in water levels in wells, streamflows, and altitudes of bench marks used for model comparison during calibration can affect the degree of fit achieved. Sensitivity to changes in model parameters and boundary conditions during calibration also can affect the degree of fit and the possible range of values used to simulate historical ground-water flow.

An exhaustive analysis of the uncertainty and sensitivity of every model parameter and boundary condition is beyond the purpose and scope of this report. However, a summary can yield insight into the capabilities and limitations of the model, and specific insight into its performance with respect to ground-water management. The combination of the uncertainty in the model-input and comparison data and the sensitivity of the model to changes in model input yield a qualitative measure of the importance of various model attributes. For example, uncertainties in the measurement of streamflows may contribute to uncertainties in the simulation of streamflows and affect the comparison between measured and simulated streamflows. Based on gaging-station ratings, inaccuracy in streamflow measurements can range from 5 to 20 percent. For high flows, this inaccuracy may result in an uncertainty of hundreds to thousands of acre-feet in potential recharge for some wet years. Other sources of uncertainty include estimates of precipitation, which may have estimation errors (kriging errors) ranging from 5 to 10 percent which can result in thousands of acre-feet of uncertainty for wet-year seasons; estimates of irrigation return flow, which may have estimation errors ranging from 10 to 20 percent owing to the uncertainty and the variability of the estimates of applied water and irrigation efficiency (Koczot, 1996); and errors in the assignment of percentages of pumpage for wells completed across both aquifer systems, which may range from 10 to 20 percent.

Additional uncertainties also may exist with respect to boundary conditions such as the average location of the seawater front, which is represented by the general-head boundary cells; horizontal-flow barriers, some of which may be of inferred extent; and the conductance of some faults. The importance of some faults remains uncertain; for example, faults whose traces generally are parallel to the hydraulic gradient, such as the Oak Ridge and McGrath Faults in the upper-aquifer system, or faults that are adjacent to a spatial contrast in transmissivity, such as the Country Club Fault. Considerable testing of these boundaries was done during model calibration; the resulting estimates for boundary locations and conductance satisfy the conceptual framework and the measured comparison data.

The simulated ground-water levels in the regional model were most sensitive to the location of the freshwater–saltwater interface, the amount of recharge and irrigation return flow applied to the Oxnard Plain, the vertical distribution of pumpage, the variation in streambed conductance, and the conductance of faults at subarea boundaries where the hydraulic gradient is approximately perpendicular to the fault trace. The model also was sensitive to estimates of vertical conductivity in areas where there are large differences between heads in the two aquifer systems. For the most part, a group of model parameters, such as the vertical distribution of pumpage; vertical leakance; general-head boundary conductance; and irrigation return flow controlled the goodness-of-fit for the Oxnard Plain. The model was relatively insensitive to ET, valley-floor infiltration, and some aquifer parameters such as transmissivity. As in most models, changes in water levels and ground-water flow were most sensitive to changes in the recharge and discharge boundary conditions near basin margins. Changes in pumpage, vertical leakance, and storage properties were more important to changes in head and ground-water flow in areas away from basin margins. Pumpage, and its vertical distribution, was the most sensitive parameter in this regional ground-water flow model. As in previous simulations of regional subsidence (Hanson, 1989; Hanson and Benedict, 1994), matching the timing and the amount of land subsidence was most sensitive to changes in the initial preconsolidation stress thresholds.

This current model adequately reproduces long-term historical changes in flows and in ground-water levels on a regional scale, but the ability of the model to simulate the specific water-level histories of some wells is limited because the aquifers were grouped into only two layers. Because the ocean boundary greatly simplifies the mobile freshwater–saltwater interface, the simulation of coastal inflow and outflow is only a crude approximation of the actual process of seawater intrusion; therefore, caution should be taken in using this model to simulate relatively small-scale flows near the coast. Inflows and outflows over seasonal time periods were combined in the model; this may have had some effect on the ability of the model to simulate rapidly changing streamflow conditions during natural floodflows or during releases from Lake Piru in low-flow summer and fall months. The complex processes of irrigation return flow and related vertical leakage to the upper-aquifer system in the Oxnard Plain were further simplified by the exclusion of the semiperched system. The exclusion of the shallow fluvial deposits as a separate layer precluded the assessment of some ground-water/surface-water exchanges along the Santa Clara River and Calleguas Creek. However, even with these significant limitations, this model provides a framework for assessing regional water-resources management issues and a basis for further model development and refinement. This model also can be used to assess future water-supply projects and the relative importance of various flow components on a regional scale.

ANALYSIS OF GROUND-WATER FLOW

The calibrated ground-water flow model was used to analyze the distribution and magnitude of ground-water flow within the entire Santa Clara–Calleguas Basin. The flow analysis in this report includes a summary of flow under predevelopment and historical conditions, the period of reported pumpage 1984–93, projected future ground-water flow conditions in relation to planned water-supply projects, and projected future ground-water flow conditions for possible alternative water-supply projects. Formulation of planned future and alternative future water-supply projects was done jointly by the FGMA, the UWCD, and the CMWD.

The summaries of the flow analysis are grouped into categories of recharge, coastal flow, inland flow, and subsidence. These summaries describe the major inflow and outflow components driving the changes in supply and the effects of ground-water overdraft (demand). For budgetary-flow analysis, the regional ground-water flow system was divided into 34 subareas (fig. 17*B*) that represent the upper- and lower-aquifer systems in the 12 landward subbasins and offshore subareas of the Santa Clara–Calleguas Basin (fig. 1). Total flows, relative percentages of flow, and mean flows for the simulation period were used for the analysis of the long-term ground-water conditions. The mean flows were based on the flows from the last time step of every season; therefore, the mean flows of head-dependent boundary conditions used to describe flows closely approximate but may not equal the average total flow over a simulation period. The mean flows should be considered with some caution because they may not adequately represent the true variability or the cumulative magnitude of a particular flow component. Net flow represents the difference between ground-water inflow and outflow for a particular boundary flow, such as coastal flow accross subarea boundaries.

The basin is partially under the management authority of the FGMA; other water purveyors include the UWCD and the CMWD water districts—all of which provide water and water-related services to different parts of the basin (fig. 26). The Oxnard Plain subbasin is subdivided into four model subareas: the Oxnard Plain Forebay, the Northwest Oxnard Plain, the Northeast Oxnard Plain, and the South Oxnard Plain (fig. 17*B*). These subareas are roughly in alignment with surface-water pipeline service areas and are coincident with the areal extent of the fluvial deposits within the two river drainages that cross the Oxnard Plain. The offshore part of the model is subdivided into three subareas that represent extensions of the Mound subbasin (Offshore Mound subarea), the northwestern Oxnard Plain north of the Hueneme submarine canyon (Offshore North Oxnard Plain), and the southern Oxnard Plain south of the Hueneme submarine canyon (Offshore South Oxnard Plain) (fig. 17*B*). For the purposes of this discussion, the Santa Clara River Valley consists of the Piru, Fillmore, Santa Paula, and Mound subareas, and the non-FGMA area consists of these same subareas plus the Santa Rosa Valley subarea. The FGMA areas are composed of the Oxnard Plain model subareas, referred to as the coastal FGMA subareas, and the Pleasant Valley and the Las Posas Valley model subareas, referred to as the inland FGMA subareas (fig. 17*B*).

Total flows, relative percentages of flow, and mean flows for the simulation period were used to analyze long-term ground-water conditions. Mean flows were based on flows from the last time step of every season. Therefore, mean flows of head-dependent boundary conditions, used to describe flows, closely approximate but may not exactly equal the average total flow over a simulation period. Because the regional model does not simulate transport or density-dependent flow, the summaries on coastal landward flow (seawater intrusion) (fig. 25*B*) are meant to give some regional approximation of potential flow along the coastal boundary of the regional aquifer system. Thus, using the reference to seawater intrusion implies that gradients above the equivalent freshwater head at the approximate average location of the seawater interface represent the inflow of seawater into the coarse-grained layers of the aquifer systems. Without density-dependent or transport modeling, such as that described by Nishikawa (1997), or some surrogate for advective flow, such as particle tracking, the reference to outflow at the coast could include moving the seawater front seaward or actually discharging freshwater into the ocean.

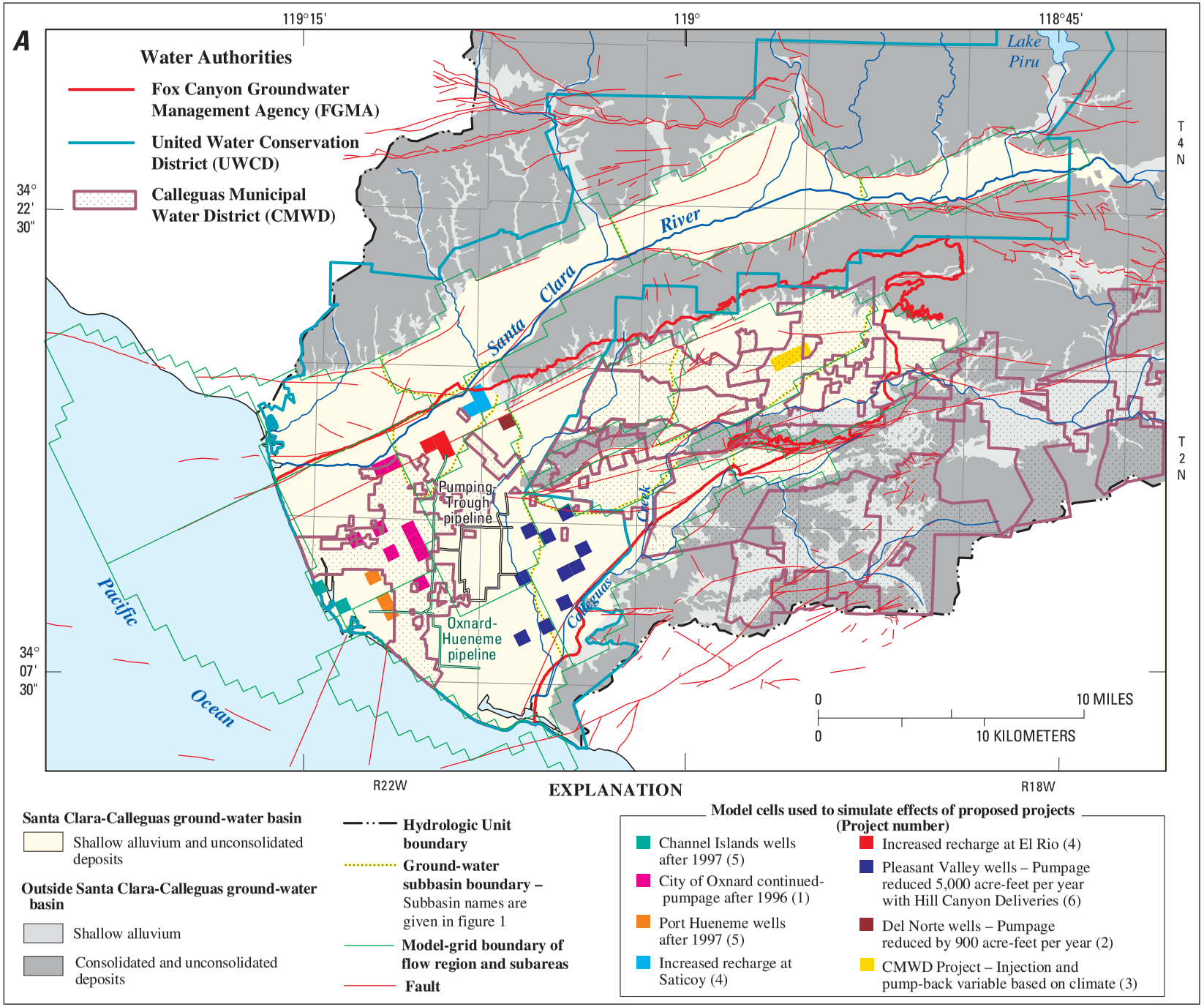

Figure 26. Location of model cells used to simulate (***A***) proposed water-supply projects for the existing management plan, Santa Clara–Calleguas ground-water basin, Ventura County, California.

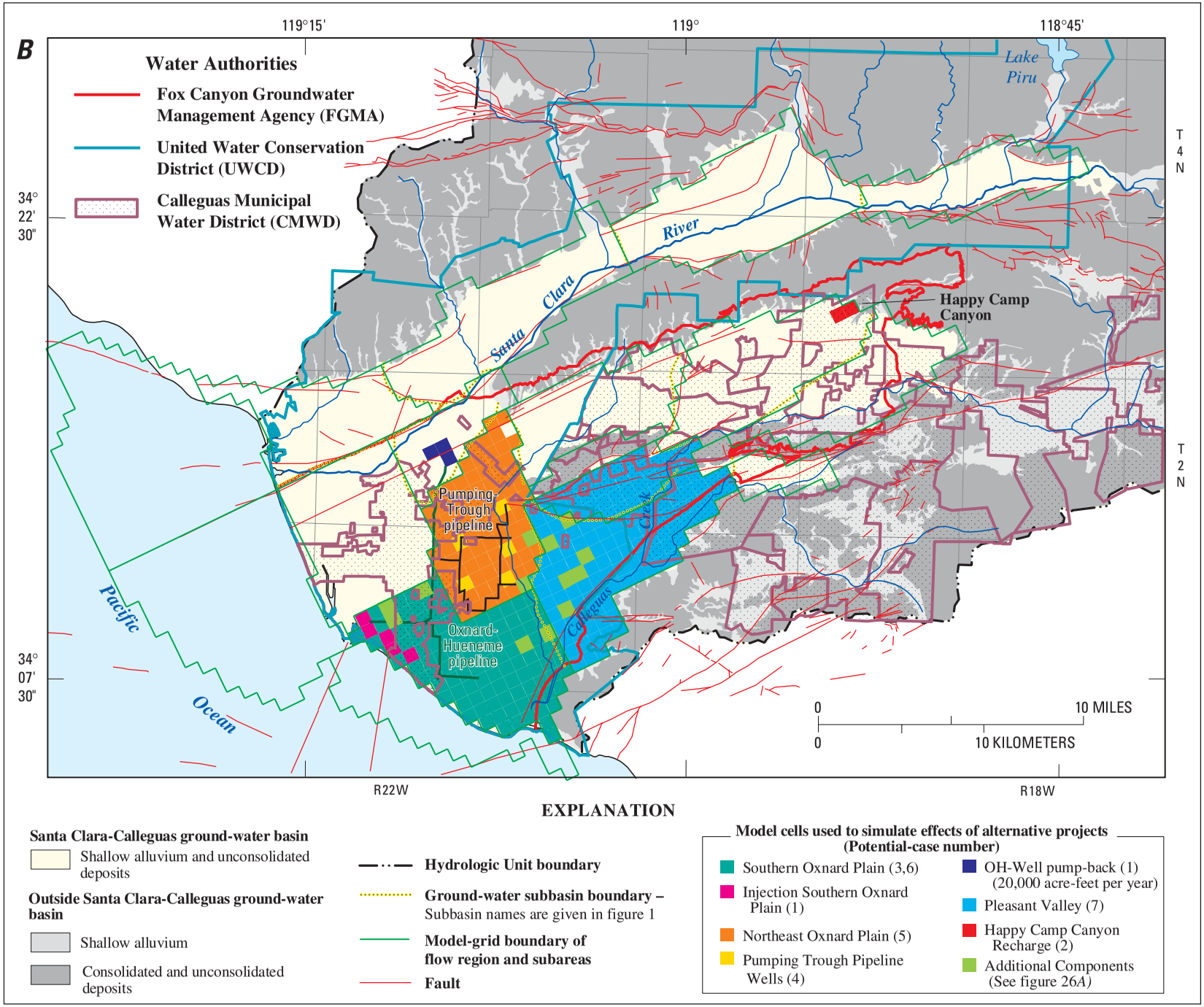

Figure 26—Continued. (***B***) alternative water-supply projects in the model of the Santa Clara–Calleguas ground-water basin, Ventura County, California.

Predevelopment Ground-Water Flow

Simulated water levels for predevelopment conditions were about 40 and 50 ft above land surface in the upper- and lower-aquifer systems along the coast, respectively, which is consistent with early reports of artesian water levels during 1870–90. The total simulated recharge for predevelopment conditions was 59,900 acre-ft/yr, and the total net recharge was 33,650 acre-ft/yr. Streamflow accounted for 68 percent of the total recharge and nonstreamflow recharge accounted for 32 percent (fig. 25*C*). Simulated streamflow resulted in 40,600 acre-ft/yr of infiltration and 26,300 acre-ft/yr of ground-water discharge back into the stream channels for a net streamflow recharge of about 14,300 acre-ft/yr (table 6). Net streamflow recharge was largest in the Piru (32 percent) and Fillmore (22 percent) subareas and the Oxnard Plain Forebay (18 percent). Ground-water discharge to the Santa Clara River was largest in the Fillmore subarea (41 percent) and was concentrated near the narrow boundary with the Santa Paula subarea. Streamflow discharge also occurs in the Piru subarea at the narrow boundary with the Fillmore subarea and in the Santa Paula and South Las Posas Valley subareas. Total mean nonstreamflow recharge for the entire regional flow system was about 19,400 acre-ft/yr (table 6) of which about 4,800 acre-ft/yr is valley-floor recharge and about 14,600 acre-ft/yr is mountain-front and bedrock recharge (fig. 25*C*).

Total simulated natural discharge was 59,900 acre-ft/yr (fig. 25*C*) and the total net discharge, which equals net recharge, was about 33,650 acre-ft/yr. Coastal outflow accounts for about 18,900 acre-ft/yr which is 31 percent of the total discharge (fig. 25*C*) and 56 percent of the net discharge. ET accounts for about 14,800 acre-ft/yr which is 25 percent of the total discharge (fig. 25*C*) and 44 percent of the net discharge. The largest amounts of ground-water discharge as ET occur in the Fillmore (38 percent), South Pleasant Valley (21 percent), and Santa Paula subareas (17 percent).

Net underflow from the Santa Clara River Valley subareas to the Oxnard Plain subareas was simulated as about 6,890 acre-ft/yr for time-averaged predevelopment conditions. A net downward leakage between aquifer systems of about 450 acre-ft/yr was simulated for the entire Oxnard Plain subareas. The largest downward flow, about 1,330 acre-ft/yr, was simulated in the Oxnard Plain Forebay. This relatively small net leakage includes downward leakage in the Oxnard Plain Forebay and strictly upward leakage in the South Oxnard Plain subarea and most of the Northeast and Northwest Oxnard Plain subareas, which is consistent with the upward vertical head gradient in these areas.

Historical Ground-Water Flow, 1984–93

The analysis of historical ground-water flow was restricted to 1984–93, the period when estimates of pumpage were the most complete and were largely based on reported values of metered pumpage. This period contains an equal number of wet and dry years; 3 wet years, followed by 5 dry years, followed by 2 wet years. This period also was one of increasing ground-water management related actions: increasing streamflow diversions for artificial recharge at the Freeman Diversion, increasing discharges of treated sewage effluent, and increasing pumpage. As a result of these increases in supply and demand, there was an increase in recharge, seawater intrusion, subsidence, leakage between aquifers, and ground-water flow between subareas, as well as reduced ET and a reduction in ground water in storage. The policies of the FGMA resulted in a moratorium on new wells in the upper-aquifer system in the northwestern part of the Oxnard Plain subareas and on the drilling of new wells and increased pumpage in the lower-aquifer system (Rick Farnsworth, Fox Canyon Ground-Water Management Agency, oral commun., 1991). This has resulted in additional seawater intrusion in the lower aquifer system and additional subsidence.

Summary of Ground-Water Conditions

The total simulated pumpage for 1984–93 is 2,468,600 acre-ft, which is an average of about 247,000 acre-ft/yr. About 37 percent of the pumpage was from the Oxnard Plain subareas, 37 percent from the Santa Clara River Valley subareas, 13 percent from the Las Posas Valley subareas, 9 percent from the Pleasant Valley subareas, 3 percent from the Mound subarea, and 1 percent from the Santa Rosa Valley subarea (fig. 25*D*). The distribution of pumpage for the ground-water management area is 59 percent for the FGMA-managed areas and 41 percent for the non-FGMA-managed areas.

Overall, pumpage during the 1984–93 sequence of wet and dry years resulted in overdraft of the ground-water flow system. The combination of water from storage, coastal landward flow (seawater intrusion), and subsidence represents an estimated 23,830 acre-ft/yr of average overdraft for the 1984–93 period, which is about 10 percent of the average annual pumpage. Of the total overdraft, 60 percent is from aquifer storage depletion, 31 percent is from coastal landward flow (seawater intrusion), and 17 percent is from subsidence. The mean rate of water extracted from aquifer storage is 14,260 acre-ft/yr. Results of the model simulations indicate that a relatively large contribution of aquifer storage is from the lower-aquifer system (layer 2) of the Oxnard Plain subarea and of the inland FGMA-managed subareas, and from the upper-aquifer system in the Santa Clara River Valley subareas. The contribution of ground water from subsidence (interbed storage) was about 4,100 acre-ft/yr (table 6) and represent about 17 percent of the average annual overdraft (23,830 acre-ft/yr). Recall that water derived from subsidence is, in part, a one-time source of water because the inelastic component of interbed storage is irreversible. Simulation results show that most of water derived from subsidence is from the Oxnard Plain subareas (47 percent) and the Las Posas Valley subareas (34 percent) (fig. 25*D*).

Ground-water pumpage resulted in a decrease in ET and stream baseflow in the inland subareas. Both ET and stream baseflow remain concentrated at the basin narrows of the Santa Clara River Valley and the Las Posas Valley subareas. Most of the simulated ET occurs in the Santa Clara Valley subareas (76 percent or 810 acre-ft/yr) (fig. 25*D*). The simulated ET for 1984–93 averaged 1,060 acre-ft/yr and is 7 percent of the simulated annual ET for the predevelopment period. Baseflow averaged about 8,250 acre-ft/yr for the period 1984–93 and is about 13 percent of the total streamflow infiltration and about 33 percent of the simulated predevelopment baseflow.

Recharge

Hydrological, geophysical, and geochemical data and ground-water simulations indicate that the upper-aquifer system is the recipient of most of the natural and artificial recharge and, thus, is a relatively more dynamic flow system than is the lower-aquifer system. Simulated total recharge (natural and artificial) for 1984–93 was 228,500 acre-ft/yr, which is about 93 percent of the average pumpage for this period. Most of the recharge occurred in the upper-aquifer system of the Santa Clara River Valley and the Oxnard Plain Forebay subareas. The total simulated natural recharge was about 114,100 acre-ft/yr: 27,800 acre-ft/yr of mountain-front and bedrock recharge, 24,100 acre-ft/yr of valley-floor recharge, and 62,200 acre-ft/yr of net streamflow infiltration. The distributions of natural recharge show that most of the mountain-front and bedrock recharge occurs in the Santa Clara River Valley subareas, most of the streamflow recharge occurs in the Piru and Fillmore subareas, and most of the valley-floor infiltration occurs in the Santa Clara subareas (fig. 25*D*). Simulated natural recharge and streamflow infiltration were 21 and 25 percent, respectively, of the total pumpage for 1984–93. The model simulated 54,400 acre-ft/yr of artificial recharge; 51,000 acre-ft/yr of irrigation return flow; and 9,000 acre-ft/yr of treated sewage effluent. About 93 percent of the total distribution of artificial recharge occurs in the Oxnard Plain Forebay and 7 percent occurs in the Piru subarea. Simulated irrigation return flow is greatest in the Oxnard Plain, and infiltration of treated sewage effluent is greatest in the Pleasant Valley subareas.

A comparison of the 1984–93 conditions with predevelopment conditions indicated a large increase in the rate of valley-floor recharge and streamflow recharge (fig. 25*C*,*D*). The largest increases were in the Santa Clara River Valley subareas. The net streamflow recharge increased from 14,300 acre-ft/yr to 62,200 acre-ft/yr.

Coastal Flow

Net coastal landward flow occurred in both aquifer systems throughout the Oxnard Plain subareas during parts of the 1984–93 period (fig. 22A,B). The total simulated net seaward flow in the upper-aquifer system (layer 1) was 9,500 acre-ft, which is considerably less than the seaward flow simulated for steady-state conditions. Flow was seaward in 1984 but reversed to landward in 1985; landward flow increased during the 1987–91 dry-year period (fig. 25*B*). By the end of 1993, the measured and simulated water levels had recovered and were above the equivalent freshwater head in the upper-aquifer system of the submarine outcrops (fig. 25*A*) resulting in seaward flow and artesian conditions and flowing wells in parts of the Oxnard Plain subareas. This change in coastal flow in the upper-aquifer system is supported by reduced chloride concentrations and reduced EM conductivities in many of the coastal monitoring wells (figure A5.2 in Appendix 5).

The simulated total coastal landward flow for 1984–93 was 64,200 acre-ft; the landward flow was due to declining water levels in the lower-aquifer system (fig. 25*A,B)*. This sustained coastal landward flow (fig. 25*B*) is supported by increased chloride concentrations and increased EM conductivities in many of the coastal monitoring wells (figure A5.2 in Appendix 5).

The model simulations indicate that total coastal landward flow occurs during seasonal and climatic cycles and during periods of long-term storage depletion (fig. 25*B*). Simulated coastal landward flow began in the lower-aquifer system of the South Oxnard Plain subarea in about 1928, in the Northwest Oxnard Plain subarea in about 1930, and in the Mound subarea as early as 1919. Coastal flow was landward in the upper-aquifer system during the droughts of the 1930s and from the mid-1940s through the last drought (1987–91), and was seaward during the intervening wet periods. Coastal flow was consistently landward in the lower-aquifer system of the south Oxnard Plain subarea for the entire period 1928–94. The general timing of the simulated coastal landward flow is consistent with observed increases in salinity, which were due to seawater intrusion into the water-supply wells. The earliest documented seawater intrusion in the upper aquifer occurred in the Oxnard Plain subareas during 1930–40 followed by increases in seawater intrusion between 1946 and the late 1970s.

Of the total simulated coastal landward flow, about 54 percent entered the South Oxnard Plain subarea, most of which entered the lower-aquifer system (fig. 25*D*). The mean net coastal seaward flow was about 950 acre-ft/yr for the upper-aquifer system and the mean net coastal landward flow (seawater intrusion) was about 6,420 acre-ft/yr for the lower-aquifer system (table 6). Seawater intrusion, however, has a cumulative effect, contributing to long-term overdraft and loss of storage for potable water. The long-term simulation of coastal landward flow indicates that seawater intrusion started as early as the summer of 1927; by 1932, about 1,957 acre-ft/yr was intruding the offshore parts of the upper-aquifer system. This is consistent with the early accounts of increased salinity in some of the shallow coastal wells. Model simulations show that the total coastal landward flow during 1984–93 was about 12 percent of the 526,600 acre-ft of total coastal landward flow (seawater intrusion) simulated for the summer of 1927 through the winter of 1993.

Flow Between Subareas and Aquifer Systems

The direction and mean flow for the simulated historical period 1984–93 are shown in figure 25*A*. Faults are an important factor in the distribution of ground-water and water levels in the lower-aquifer system and, to a lesser extent, in the upper-aquifer system. For the upper-aquifer system, ground-water underflow to the Oxnard Plain subareas averaged about 4,200 acre-ft/yr of inflow from the Santa Paula subarea and about 2,770 acre-ft/yr of outflow into the South Pleasant Valley subarea (fig. 25*A*). For the lower-aquifer system, the simulated flow averaged less than 140 acre-ft/yr out of the Oxnard Plain Forebay toward the Santa Paula subarea and about 3,000 acre-ft/yr into the region of lower water levels in the South Pleasant Valley subarea (fig. 25*A*).

Table 6. Summary of simulated ground–water flow components for the Santa Clara–Calleguas Basin, Ventura County, California

[All flows in acre–feet per year. The precision of the numbers do not reflect the variable accuracy of the estimates. FGMA, Fox Canyon Ground–water Management Agency]

Simulation case and time period[1]	1) Total–mean nonstreamflow recharge[2] 2) Mean spreading grounds recharge[3] 3) Las Posas recharge[4]	Mean ground–water inflow to Oxnard Plain from adjacent subbasins[5]: 1) Santa Clara River Valley 2) West Las Posas 3) South Pleasant Valley	Mean–net streamflow recharge[6]	Mean coastal flow[7] 1) Layer 1 2) Layer 2	Mean vertical flow between aquifer systems in Oxnard Plain[8]	Mean evapotrans-piration	Mean pumpage[9] 1) FGMA area 2) Outside FGMA area 3) Total Basin area	Mean flow from interbed storage (subsidence)	Mean change in aquifer storage[10]
Predevelopment (time–averaged)	1) 19,400 2) 0 3) 0	1) 6,900 2) 2,180 3) 1,720	14,300	1) –16,000 2) –2,900	450	14,800	1) 0 2) 0 3) 0	0	0
Reported pumpage period: 1984–1993	1) 166,000 2) 54,400 3) 0	1) 5,770 2) 1,260 3) 5,720	62,200	1) –950 2) 6,420	22,700	1,060	1) 146,000 2) 101,000 3) 247,000	4,100	14,260
Base–Case 1: 1994–2017	1) 179,000 2) 63,500 3) 3,750	1) 2,900 2) –80 3) –2,740	58,700	1) –3,970 2) 4,770	20,900	950	1) 141,000 2) 100,000 3) 241,000	1,500	2,700
Base–Case 2: 1994–2017	1) 179,000 2) 63,500 3) 3,750	1) 2,540 2) 20 3) –1,840	56,000	1) –5,750 2) 3,420	18,600	1,030	1) 129,000 2) 100,000 3) 229,000	420	–2,400
Base–Case 3: 1994–2017	1) 179,000 2) 63,500 3) 3,750	1) 2,000 2) 30 3) –1,360	50,300	1) –9,430 2) 2,130	17,400	1,180	1) 113,600 2) 99,700 3) 213,000	–330	–7,000
Base–Case 4: 1994–2037	1) 159,000 2) 55,300 3) 3,750	1) 3,490 2) –110 3) –2,500	80,800	1) –2,680 2) 4,950	20,500	2,030	1) 140,000 2) 100,000 3) 240,000	1,070	–1,750
Potential–Case 1: 1994–2017	1) 194,000 2) 63,500 3) 3,750	1) 3,500 2) –100 3) –2,950	60,600	1) –8,000 2) 4,900	20,700	900	1) 140,000 2) 101,000 3) 241,000	1,500	950
Potential–Case 2: 1994–2017	1) 190,000 2) 63,500 3) 3,750	1) 2,900 2) 80 3) –2,740	58,600	1) –3,970 2) 4,770	20,900	950	1) 141,000 2) 100,000 3) 241,000	1,500	–8,500
Potential–Case 3: 1994–2017	1) 179,000 2) 63,500 3) 3,750	1) 2,540 2) 290 3) –4,580	56,100	1) –7,330 2) 2,470	17,800	1,030	1) 129,000 2) 100,000 3) 229,000	790	–420

Table 6. Summary of simulated ground–water flow components for the Santa Clara–Calleguas Basin, Ventura County, California

Simulation case and time period[1]	1) Total–mean nonstreamflow recharge[2] 2) Mean spreading grounds recharge[3] 3) Las Posas recharge[4]	Mean ground–water inflow to Oxnard Plain from adjacent subbasins[5]: 1) Santa Clara River Valley 2) West Las Posas 3) South Pleasant Valley	Mean–net streamflow recharge[6]	Mean coastal flow[7] 1) Layer 1 2) Layer 2	Mean vertical flow between aquifer systems in Oxnard Plain[8]	Mean evapotrans-piration	Mean pumpage[9] 1) FGMA area 2) Outside FGMA area 3) Total Basin area	Mean flow from interbed storage (subsidence)	Mean change in aquifer storage[10]
Potential–Case 4:	1) 179,000	1) 2,910	58,700	1) –3,640	19,600	950	1) 141,000	1,360	–40
1994–2017	2) 63,500	2) 80		2) 4,480			2) 100,000		
	3) 3,750	3) –2,880					3) 241,000		
Potential–Case 5:	1) 179,000	1) 3,000	58,700	1) –2,880	14,800	950	1) 141,000	1,250	3,130
1994–2017	(2) 63,500	2) 110		2) 3,590			2) 100,000		
	3) 3,750	3) –3,380					3) 241,000		
Potential–Case 6:	1) 179,000	1) 2,910	58,500	1) –2,220	16,600	950	1) 141,000	1,270	2,800
1994–2017	2) 63,500	2) 80		2) 3,180			2) 100,000		
	3) 3,750	3) –3,260					3) 241,000		
Potential–Case 7:	1) 179,000	1) 2,860	57,900	1) –3,950	18,100	970	1) 141,000	1,070	4,650
1994–2017	2) 63,500	2) 110		2) 4,040			2) 100,000		
	3) 3,750	3) –1,600					3) 241,000		

[1] All time periods are in calendar years and all simulated mean flows are in acre-feet per year.

[2] Recharge includes mountain-front recharge, valley-floor infiltration, bedrock infiltration, irrigation returnflow, sewage effluent, and artificial recharge.

[3] Spreading-grounds recharge is the sum of infiltration of surface spreading at the Piru, El Rio, and Saticoy spreading grounds operated by United Water Conservation District.

[4] Number is the additional potential recharge at the aquifer storage and recovery facility planned for operation by Calleguas Municipal Water District in the East Las Posas subarea in the lower-aquifer system.

[5] Simulated mean underflow to the Oxnard Plain subareas with top number net underflow from Santa Clara Valley subareas, middle number is mean underflow from West Las Posas subarea, and bottom number is mean underflow from the South Pleasant Valley subarea.

[6] Total net mean streamflow loss to all simulated rivers and tributaries.

[7] Mean coastal flow is the total flow between all coastal subareas and the adjacent offshore subareas and is used in this study as a surrogate for seawater intrusion for the total time period simulated. A positive number is coastal landward flow (seawater intrusion) from offshore subareas and a negative number is coastal seaward flow to offshore subareas.

[8] Total net mean flow from upper-aquifer system (model layer 1) to lower-aquifer system. Positive number is downward flow and negative number is upward flow.

[9] Top number indicates simulated mean pumpage for FGMA area, middle number is pumpage outside of GMA areas, and bottom number is pumpage in total Santa Clara–Calleguas Basin.

[10] Mean change in storage is the total for the upper- and the lower-aquifer system divided by the number of years for the period of simulation for the entire model. Positive number indicates water coming from ground-water storage and negative number indicates water returning to ground-water storage.

The simulated flow across the Oak Ridge and McGrath Faults from the Mound and Santa Paula to the Oxnard Plain subareas for 1984–93 was about 5,800 acre-ft/yr, of which about 73 percent flowed to the upper-aquifer system, in the narrow swath of the Santa Clara River flood plain where the fault was not simulated. Almost no flow occurred across the Oak Ridge and McGrath Faults into the lower-aquifer system. The simulated mean flow across the Country Club Fault from the Santa Paula subarea to the Mound subarea was about 4,200 acre-ft/yr, resulting in a net inflow to the Mound subarea of about 2,500 acre-ft/yr. Three other fault-related flow barriers between the subareas control underflow: the Central Las Posas Fault, the extension of the Springville Fault and the Somis Fault, and the Camarillo Fault. The Central Las Posas Fault controls flow between the East and West Las Posas Valley subarea; the simulated mean flow across this fault toward the West Las Posas Valley subarea was 920 acre-ft/yr. The extension of the Springville Fault and the Somis Fault control flow between the East Las Posas Valley and North Pleasant Valley subareas; the simulated mean flow toward North Pleasant Valley subarea was 1,500 acre-ft/yr in the lower-aquifer system and about 196 acre-ft/yr in the upper-aquifer system. The Camarillo Fault controls flow between the North and South Pleasant Valley subareas; the simulated mean flow across this fault from the South to the North Pleasant Valley subareas was 3,600 acre-ft/yr (figs. 12 and 16). Coastal and offshore faults, such as the Bailey Fault and the extension of the Sycamore Fault, are effective barriers that have contributed to water-level declines of more than 100 ft below sea level at the coast and prevent seawater intrusion into the lower-aquifer system in the southern Oxnard Plain near Mugu submarine canyon (fig. 16). The Hueneme Canyon, the Old Hueneme Canyon, and the South Hueneme Canyon Faults reduce flow along the southern exposures of the submarine canyons and retard the northwestern propagation of water-level declines caused by pumping in the lower-aquifer system of the South Oxnard Plain subarea (figs. 16 and 25*A*).

The simulated downward flow from the upper- to the lower-aquifer system during 1984–93 for groups of subareas (fig. 25*D*) averaged about 67,000 acre-ft/yr. The downward flow was greatest in the Las Posas Valley (34 percent, or 22,800 acre-ft/yr), Oxnard Plain (34 percent, or 22,700 acre-ft/yr), and Pleasant Valley (22 percent, or 14,700 acre-ft/yr) subareas (fig. 25*D*). The simulated average downward flow in the Oxnard Plain is similar to previous estimates (Mann and Associates, 1959; California Department of Water Resources, 1971). The downward flow between aquifer systems increased during the dry years owing to increases in water-level differences (fig. 15). Water-level differences between the upper- and lower-aquifer systems were more than 100 ft in the East and West Las Posas Valley and the Pleasant Valley subareas, more than 30 ft in the Oxnard Plain subareas, and more than 10 ft in the Santa Clara River Valley subareas.

Land Subsidence

Simulation results indicate that the total quantity of water derived from subsidence during 1984–93 was 35,700 acre-ft, for an average net rate of subsidence of 3,570 acre-ft/yr. The largest contributions were from the Oxnard Plain (47 percent) and the Las Posas Valley (34 percent) subareas; smaller contributions were from the Mound subarea (10 percent), the Pleasant Valley subareas (7 percent), and the Santa Clara River Valley subareas (2 percent) (fig. 25*D*). Water derived from compaction is about 20 percent of the mean annual overdraft, which is comparable to previous regional estimates (Hanson and Benedict, 1994).

Simulation results for the 1984–96 period show that 96 percent of the water was derived from compaction of the lower-aquifer system. This may reflect, in part, the additional development of ground water from the lower-aquifer system and, in part, the moratorium of the 1980s on new wells in the upper-aquifer system throughout the Oxnard Plain subareas. Collectively, these resulted in increased water-level declines in the lower-aquifer system during the 1987–91 drought. Thus, overdraft appears to have a significant effect on subsidence in the coastal regional-aquifer systems. Overdraft and land subsidence will continue during dry-year periods when water levels drop below previous maximum declines.

Projected Future Ground-Water Flow for Existing Management Plan

The model was used to assess future ground-water conditions based on the implementation of proposed water-supply projects included in the existing management plan for the Santa Clara–Calleguas ground-water basin. These plans assume the current water demands plus the addition of proposed water-supply projects. Testing of projects included assessing long-term conditions of the ground and surface water through periods of climatic extremes; for example, the ability to recharge aquifers during wet periods and to arrest seawater intrusion and subsidence during dry periods.

Using the model to cycle the average water demand through a wet and dry period, simulated natural and artificial recharge were varied to reflect the changing and extreme conditions typical of the southern California coast. Two approaches were used to estimate future recharge, streamflow, and climate-related water-demand: a 24-year projection (1994–2017) using historical estimates of recharge and measured streamflow, and a 44-year spectral projection (1994–2037) of future precipitation.

The primary approach used to project future ground-water flow was to simulate the 24-year period 1994–2017. The historical inflow conditions for 1970–93 were used for these simulations; this period cycles through a combination of 13 dry and 11 wet years (fig. 2*A*). This record was used to simulate the extremes in recharge, streamflow, and pumping demand that may be typical of future interdecadal climate variation. The 1970–93 data series, although not a correlated projection of probable future conditions, does capture the complete variation of recent climate, recharge, and streamflow and the beginning of regulated streamflow (1970) in the Santa Clara–Calleguas Basin.

The alternative approach to project future ground-water flow was to simulate recharge, streamflow, and climate-related demand based on spectral estimates of future precipitation. For this approach, precipitation was estimated for the next 50 years (see Appendix 3 for a description of this approach). The first 44 years, 1994–2037, represent a total of 21 wet years and 23 dry years. The precipitation estimates are an autocorrelated series of probable future conditions that include three climatic cycles of intradecadal (2.9 and 5.3 yr) to decadal (22 yr) length; they represent 60 percent of the variation of typical changes in rainfall. The 44-year period approximately represents two decadal cycles of climate variability. The advantages of the spectral approach are a longer period of projection and a seamless transition from historical climatic and aquifer conditions to probable future conditions of supply and demand (Hanson and Dettinger, 1996). The spectral approach uses a moving autocorrelation with historical rainfall data that closely approximates rainfall for the years 1994–96 (figure A3.3 in Appendix 3). The autocorrelation with historical data provides a seamless transition with high correlation for about the first 7 years into the future and decreasing correlation further into the future.

The simulations for both projection approaches included adjusting average ground-water pumpage on a well-by-well basis for the period of reported pumpage (1984–93), estimating irrigation return flow from the 1969 land-use distribution, and varying recharge and streamflow climatically. Average pumpage and irrigation return flow were adjusted climatically using ratios of wet or dry pumpage to average historical reported pumpage for each subarea. The following six proposed water-supply projects (fig. 26*B*) were included in assessing the potential for continued overdraft conditions:

(1) Cessation of pumping of well in the city of Oxnard from July 1995 through December 1996, and a restart of pumping in January 1997;

(2) UWCD surface-water deliveries of 900 acre-ft/yr to Del Norte in lieu of pumpage from the upper-aquifer system starting in January 1997;

(3) CMWD aquifer storage and recovery (ASR) project in the East Las Posas Valley subarea from January 1997 to December 2001, using a proposed injection rate of 5,000 acre-ft/yr for wet years, 1,250 acre-ft/yr for average years, and a pump-back recovery of 2,500 acre-ft/y for dry years. In 2002, the proposed injection rate was increased to 10,000 acre-ft/yr for wet years; 2,500 acre-ft/yr for average years; and a pump-back recovery of stored water of 5,000 acre-ft/yr for dry years;

(4) Increased artificial recharge by the UWCD at El Rio and Saticoy based on the projected increased capacity of the Freeman Diversion (Steve Bachman, United Water Conservation District, written commun., 1996). With the addition of the Rose pit near Saticoy, the projected artificial recharge ranges from 0 to 127,900 acre-ft/yr. The spectral approach used estimates ranging from 6,000 to 92,000 acre-ft/yr;

(5) Reduced average pumpage from the lower-aquifer system by the city of Port Hueneme, the Channel Islands Beach Community Services District, and the U.S. Navy base at Port Hueneme for a combined reduction of as much as 1,000 acre-ft/yr in lieu of new deliveries of imported water from the State water project starting in January 1997;

(6) Reduced pumpage by the PVCWD in lieu of 5,000 acre-ft/yr of new surface-water deliveries from the city of Thousand Oaks Hill Canyon wastewater-treatment plant starting in January 1998.

Four simulations, referred to as "base-cases 1–4," were used to project future ground-water conditions. Base-case 1 represents the adjusted 1984–93 mean annual pumpage for the six proposed water-supply projects listed above for the 24-year period (1994–2017). Two additional base-case scenarios were simulated to address the existing FGMA ordinance 5.5 (Fox Canyon Groundwater Management Agency, 1997) of a rolling cut back in pumpage (base-case 2) and the step cut-back reduction of pumping which began in the early to middle 1990s (base-case 3). These two cut-back simulations are based on average pumpage throughout the entire Santa Clara–Calleguas Basin for 1984–89. These two base-case projections used the 24-year period of projection and the same historical period of recharge, streamflow, and climate-related demand conditions. Base-case 4 is the simulation of future ground-water flow for the extended 44-year period; this simulation is based on the spectral estimate of precipitation and uses the same adjusted mean pumpage for 1984–93 that was used for base-case 1.

The mean historical pumpage for 1984–93 for the six hypothetical projects yielded a mean adjusted pumpage of about 241,000 acre-ft/yr for base-case 1 for the 24-year period and 240,000 acre-ft/yr for base-case 4 for the 44-year period (table 6). This represents about 59 percent (141,000 acre-ft/yr) of the total pumpage in the FGMA area and 41 percent (100,000 acre-ft/yr) in non-FGMA areas for base-case 1 (table 6). The total adjusted mean pumpage for base-case 1 for the FGMA area was about 6,000 acre-ft/yr less than the total mean pumpage for the FGMA area for the 1984–93 period.

Simulation of the rolling cut-back (base-case 2) scenario shows the potential effect of the FGMA Ordinance 5.5 (Fox Canyon Groundwater Management Agency, 1997) and represents the 25-percent total cut back in pumpage as a 5-percent rolling cut back every 5 years through the 2010. This is equivalent to a 5-percent cut back in average pumpage for 1994, a 10-percent cut back in average pumpage for the years 1995–99, a 15-percent cut back in average pumpage for the years 2000–2004, a 20-percent cut back in average pumpage for the years 2005–2009, and a 25-percent cut back in average pumpage for the years 2010–2017. Total average pumpage with climatic variation in demand was about 229,000 acre-ft/yr, of which 56 percent is for the FGMA area of the basin and 44 percent is for the non-FGMA areas of the basin (table 6). The total adjusted average pumpage for base-case 2 is about 18,000 acre-ft/yr less than that for the 1984–93 period for the entire modeled area. Most of the reduction was in the FGMA area and represents an average 12-percent reduction in pumpage in the FGMA area for the 24-year period.

The simulation of the step cut-back (base-case 3) scenario represents the potential effect of continuing the apparent reduction in pumping that occurred in the mid-1990s. The reduction is based on the estimated total pumpage of about 100,000 acre-ft for 1996 for the FGMA area, which represents a 37-percent cut back from the average pumpage for 1984–89. This 37-percent reduction was applied uniformly to all pumpage within the FGMA boundaries for the entire projection period; it was not applied to pumpage in the Piru, Fillmore, Santa Paula, and Mound subareas or in the eastern part of the Santa Rosa Valley subarea, areas that are outside the FGMA area. The projected climatic variations increased overall demands on pumpage and added an average additional 13,600 acre-ft/yr to the reduced pumpage rate in the FGMA area. Total mean pumpage for base-case 3 is about 213,000 acre-ft/yr, of which about 53 percent is for the FGMA area of the basin and 47 percent is for non-FGMA area (table 6). Total mean pumpage is about 34,000 acre-ft/yr less than that for the 1984–93 period for the entire modeled area.

Summary of Projected Ground-Water Conditions

Differences in ground-water levels and changes in ground-water storage between 1994 and 2017, the end of the projected period, are shown in figure 27 for the four base-case simulations. The water-level-change maps (fig. 27*A–D*) indicate a continued decline in the Oxnard Plain subarea, the Santa Clara River Valley subareas, and the East and West Las Posas Valley subareas for base-case 1; the declines are as much as 67 ft in the upper aquifer system (fig. *27A*). The rolling cut-back (base-case 2) and the step cut-back (base-case 3) projections progressively show decreased declines and increased recoveries (fig. 27*B*,*C*). Total ground-water storage change ranges from a withdrawal from storage of about 65,200 acre-ft (2,700 acre-ft/yr) for base-case 1 to a return of water to storage of about 168,100 acre-ft (7,000 acre-ft/yr) for base-case 3 (table 6). The large withdrawals of water from storage in the Oxnard Plain subareas were coincident with the withdrawals in the Oxnard Plain Forebay and the Northeast Oxnard Plain subareas. The changes in storage during the projection period were as much as 60,000 acre-ft during dry-year periods in the Oxnard Plain Forebay and Fillmore subareas (fig. 27*E*). In the step cut-back and rolling cut-back simulations, the storage changes were reduced for the Oxnard Plain Forebay but were comparable for the Piru, Fillmore, and Santa Paula subareas (fig. 27*A*,*B*,*C*,*E*). The cut backs did not affect the magnitude of pumpage in these Santa Clara River Valley subareas because they were outside the FGMA area (fig. 26). The step cut-back projection (base-case 3) resulted in the largest reduction of coastal landward flow (seawater intrusion) in the lower-aquifer system and the largest increase of coastal seaward flow in the upper-aquifer system because the pumpage reductions were applied for the entire projection period (fig. 27*E*). This is illustrated by the hydrographs of supply well 1N/22W-3F4 for the city of Oxnard which show that the simulated water levels for the step cut-back projection (base-case 3) are always higher than those for the rolling cut-back projection (base-case 2) (fig. 27*F*). The higher hydraulic head near the coast results in less coastal landward flow (seawater intrusion).

A comparison of model results between the spectral projection for base-case 4 and the historical hydrology projection for base-case 1 indicates differences in the amount of water-level declines, changes in storage, cumulative coastal landward flow (seawater intrusion), and the timing of wet and dry periods. The spectral projection for base-case 4 indicates that water-level declines and losses in storage were comparable to those of base-case 1 at the end of the 44-year spectral projection period 1994–2037 (fig. 27*A*, *D*, and *E*). However, the major cycles of water-level declines and storage losses were opposite in phase during 2017 and occurred earlier in the projection period of base-case 4 (fig. 27*A*,*D*). For example, the difference in water levels in supply well 1N/22W-3F4 for the city of Oxnard was as much as 80 ft between base-cases 1 and 4 during periods when the projections were out of phase (fig. 27*F*). Projections of base-case 4 show significantly more coastal landward flow (seawater intrusion) by 2017 (fig. 27*D*) than was projected in base-case 1 (fig. 27*A*). The comparison of base-cases 1 and 4 shows the importance of the range of possible wet and dry periods and the sequence of events that may affect the state of the system and the management of the water resources.

Recharge

The historical inflow conditions for the base-case 1–3 projections are similar and consist of recharge of about 179,000 acre-ft/yr, of which about 63,500 acre-ft/yr was artificial recharge from the UWCD spreading grounds in Piru subarea and in the Oxnard Plain Forebay (table 6). Recharge of diverted streamflow from the spreading grounds was about 9,000 acre-ft/yr more than the average historical recharge for 1984–93; the projected increase in recharge was due to the increased capacity of the Freeman Diversion. This increase in recharge, however, did not stop water-level declines throughout most of the Santa Clara River Valley and the Oxnard Plain subareas (fig. 27*A*).

The simulation of the proposed CMWD ASR project (base-case 3) in the East Las Posas Valley subarea for the injection of 3,750 acre-ft/yr added about 90,000 acre-ft of net imported water to ground-water storage in the lower-aquifer system (table 6) during 1994–2017. An additional 25,000 acre-ft of injected water was pumped back during dry years or years with average precipitation. Water-level rises relative to 1993 simulated conditions were more than 30 ft in most of the lower-aquifer system for all base-case projections (fig. 27*A–D*). Water-level rises in the lower-aquifer system reduced downward vertical leakage, which contributed to water-level rises in the upper-aquifer system for all the base-case projections.

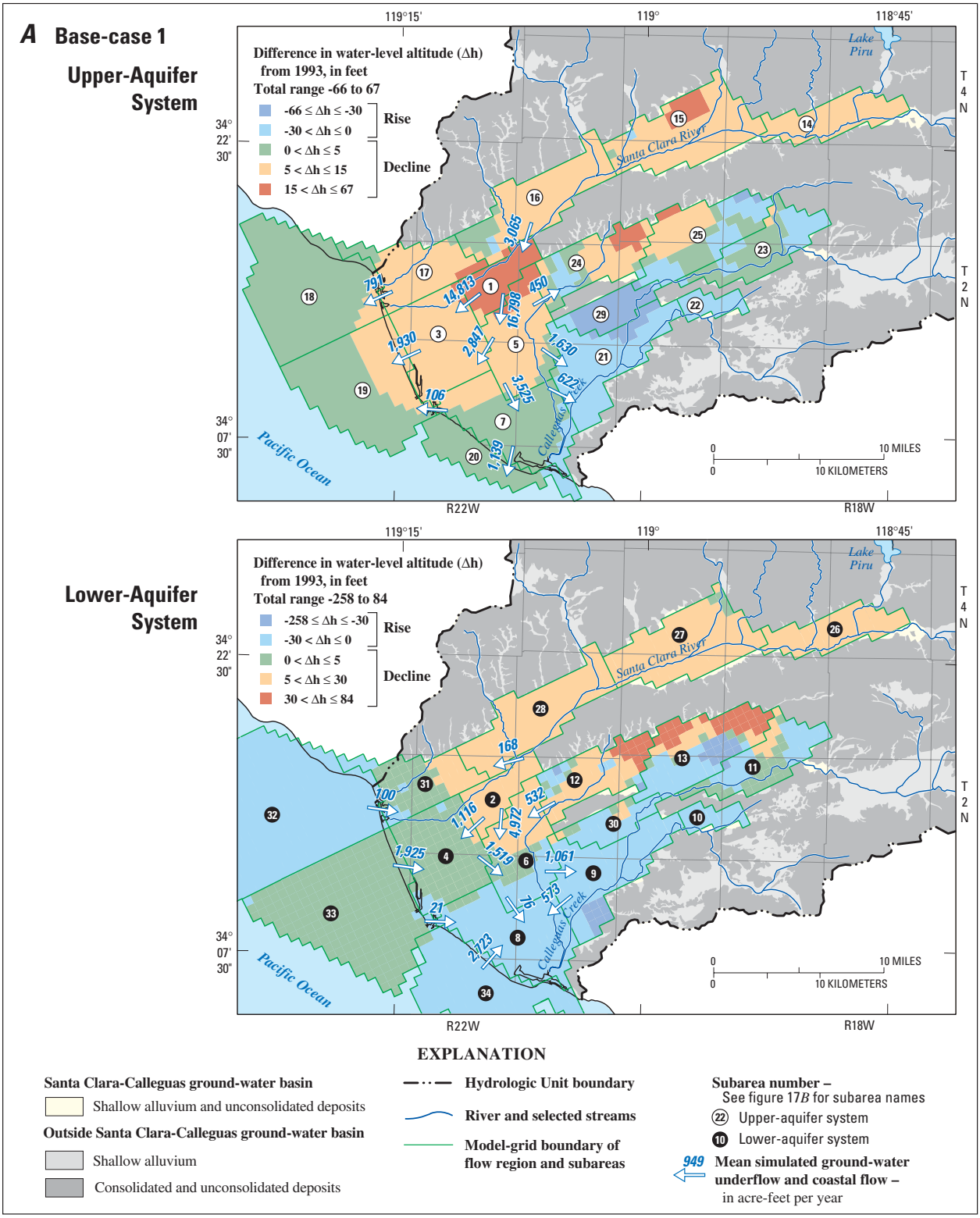

Figure 27. Simulated differences in ground-water levels from 1993 to 2017 for proposed water-supply projects in the existing management plan for the Santa Clara–Calleguas ground-water basin, Ventura County, California. ***A***, Historical reported pumpage averaged over the period 1984–1993 and estimated or measured historical recharge, streamflow, and diversion data (base-case 1).

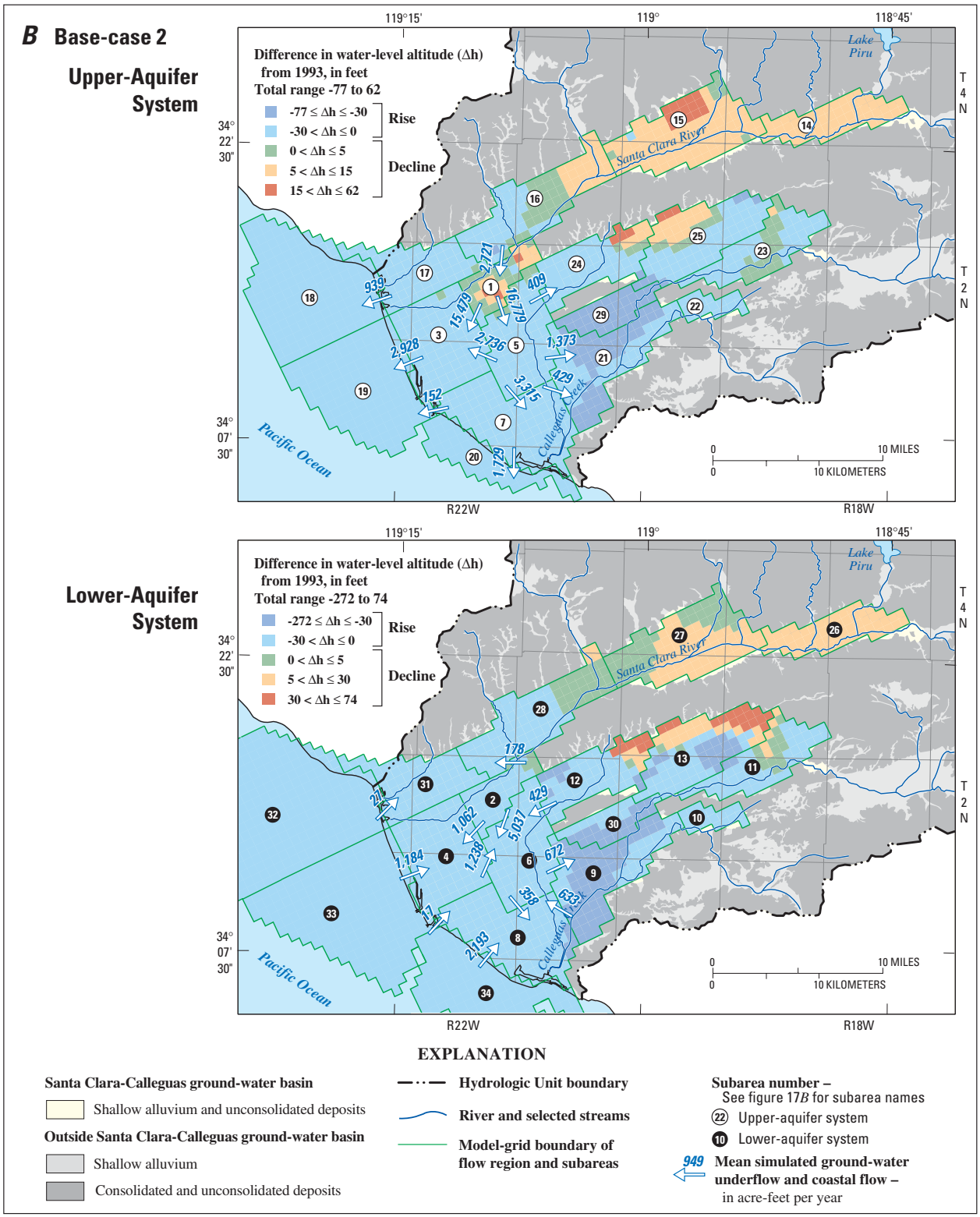

Figure 27—Continued. ***B***, Rolling cut back in pumpage and estimated or measured historical recharge, streamflow, and diversion data (base-case 2)

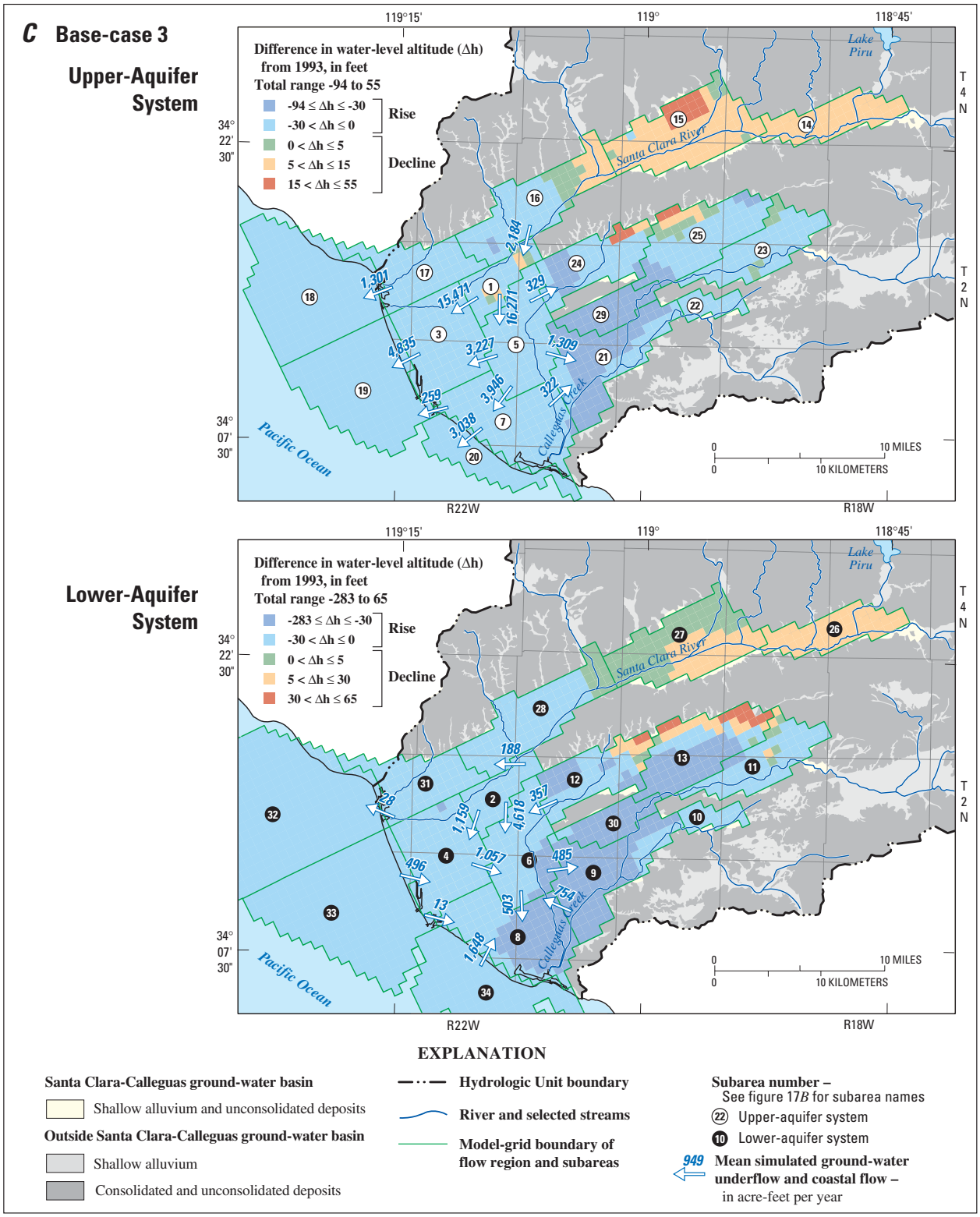

Figure 27—Continued. ***C***, Step cut-back reduction in pumpage and estimated or measured historical recharge, streamflow, and diversions data (base-case 3).

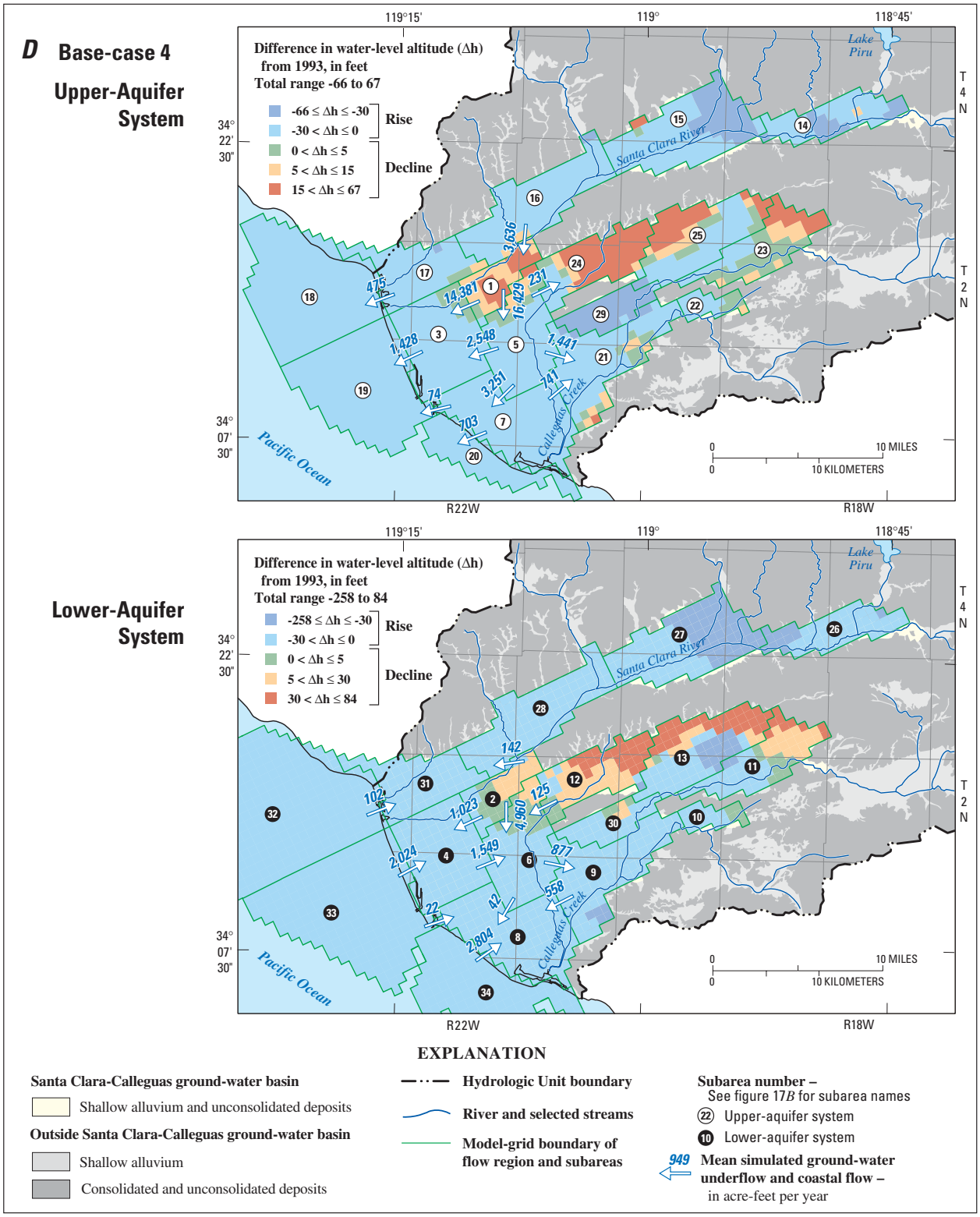

Figure 27—Continued. ***D***, Historical reported pumpage averaged over the period 1984–1993 and spectral-based estimates of recharge, streamflow, and diversions (base-case 4).

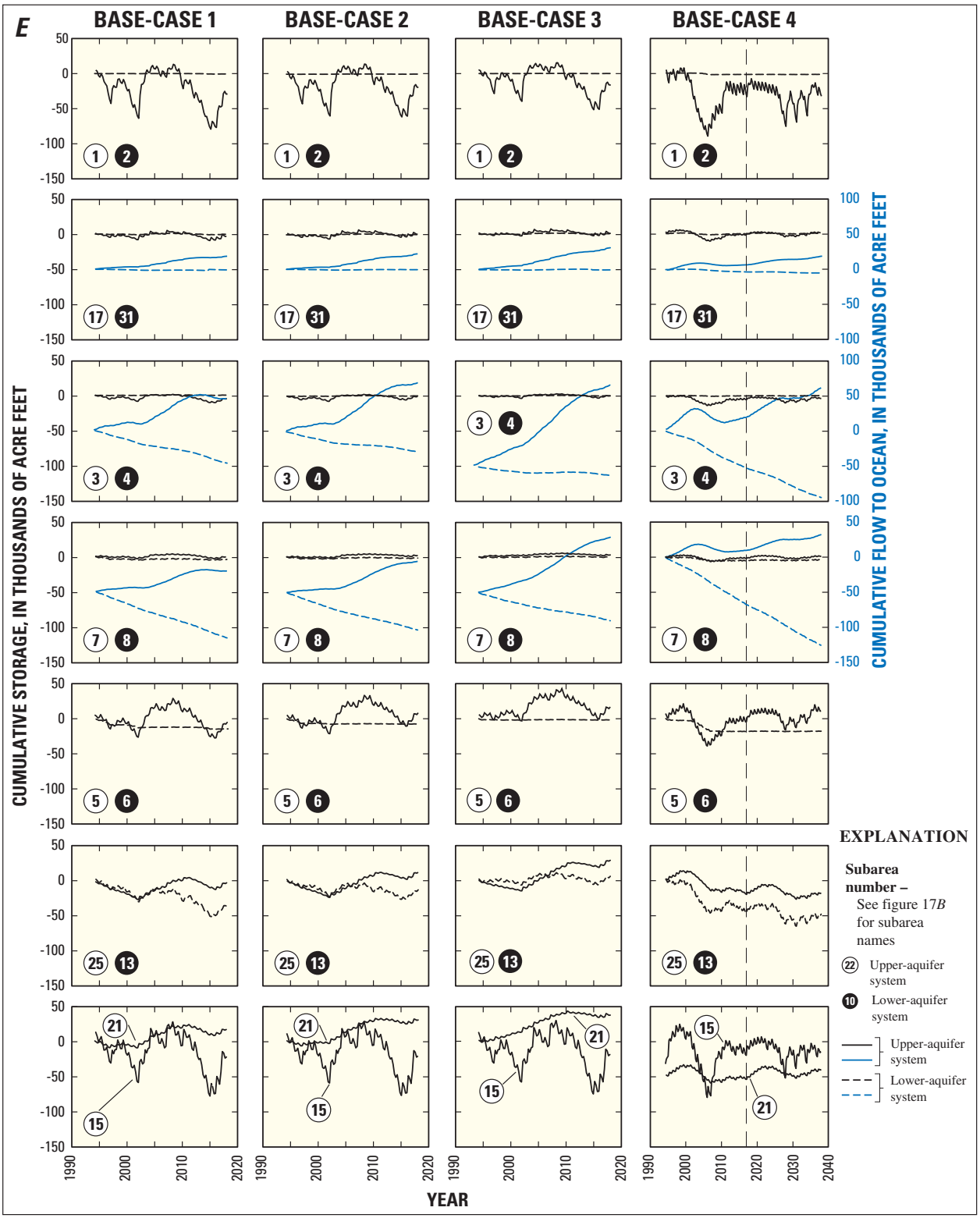

Figure 27—Continued. ***E***, Cumulative changes in ground-water storage and ground-water flow for selected subareas during 1993–2037.

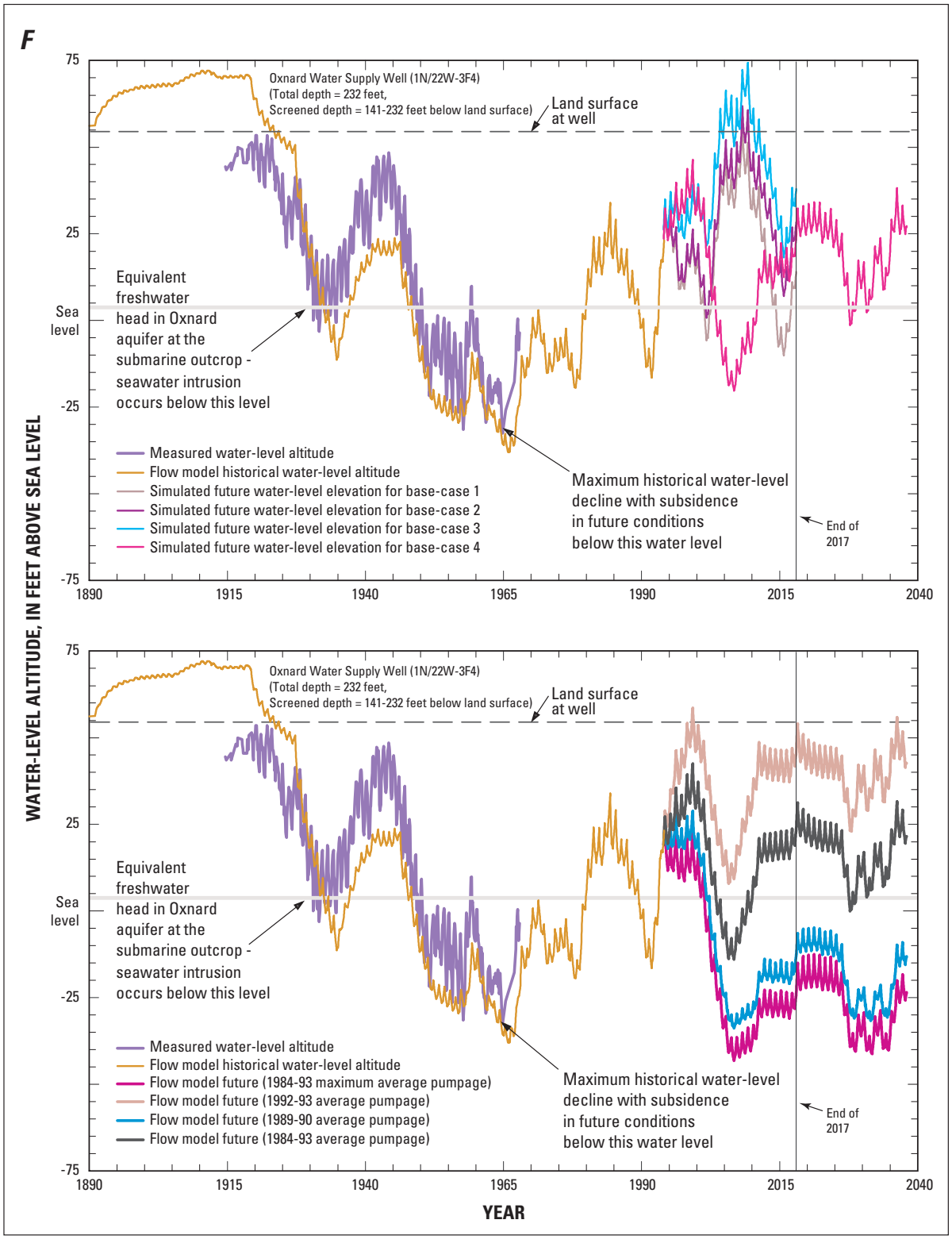

Figure 27.—Continued. ***F***, Water-level altitudes for the city of Oxnard public-supply well (1N/22W-3F4). Upper hydrograph generated from historical and spectral simulation data; lower hydrograph generated from spectral simulation data.

The mean streamflow recharge rates were similar for the base-case 1–3 projections, ranging from about 59,000 acre-ft/yr for continued historical demand (base-case 1) to about 50,000 acre-ft/yr (a rate reduced by about 11,000 acre-ft/yr) for the step cut back of FGMA pumpage (base-case 3). Mean streamflow recharge for base-case 1 was about 3,000 acre-ft/yr less than that for the historical period 1984–93. Although the simulated water-level declines were reduced in the western part of the Santa Paula subarea for the rolling (base-case 2) and step cut-back projections (base-case 3) (fig. 27*A*,*B*,*C*), the streamflow recharge was similar to base-case 1 because most of the recharge occurred in the Piru and Fillmore subareas and the eastern part of the Santa Paula subarea (fig. 27*A*,*B*,*C*). The mean recharge for the spectral 44-year projection (base-case 4) was about 80,800 acre-ft/yr, which is about 19,000 acre-ft/yr higher than the historical projections (table 6). This difference was largely due to the projection of a severe and prolonged drought spanning 1999 through 2006. The projected drought caused water levels to decline below streambeds resulting in greater streamflow recharge. The larger streamflow recharge may also have been due to the use of regression estimates (Appendix 4) of future streamflow which do not completely capture the extremes of streamflow. Changes in streamflow recharge had little effect on ground-water discharge. ET was simulated at about 1,000 acre-ft/yr and was similar for the three historically based projections, but was about twice this rate for the spectral projection.

Coastal Flow

The simulation of coastal flow yielded one of the largest differences among the base-case scenarios. All the base-case simulations indicated some coastal landward flow (seawater intrusion) into the upper-aquifer system during dry years but a cumulative coastal seaward flow along the coast, and coastal landward flow (seawater intrusion) into the lower-aquifer system for the entire period (table 6). The projection of historical average pumpage for the six hypothetical ground-water/surface-water projects (base-case 1) resulted in about 95,300 acre-ft of coastal seaward flow from the upper-aquifer system and about 114,500 acre-ft of coastal landward flow (seawater intrusion) to the lower-aquifer system. This was almost 10 times the total coastal seaward flow simulated for the historical period (1984–93), even though the simulation period was only 2.4 times longer. The largest mean coastal seaward flow in the upper-aquifer system occurred in the Northwest and South Oxnard Plain subareas, and the largest coastal landward flow occurred in the lower-aquifer system in the South Oxnard Plain subarea (fig. 27). The reductions in pumpage increased the total simulated coastal seaward flow by about 43,000 acre-ft for base-case 2 and about 131,000 acre-ft for base-case 3 while reducing coastal landward flow (seawater intrusion) in the lower-aquifer system only about 32,400 acre-ft for base-case 2 and about 63,400 acre-ft for base-case 3 relative to the projection of historical average pumpage with selected projects (table 6).

Flow Between Subareas and Aquifer Systems

The mean horizontal ground-water underflow to and from subareas surrounding the Oxnard Plain subareas are shown in figure 27, and the total mean downward flow between aquifer systems is given in table 6. More than 20,000 acre-ft/yr of underflow entered the Northwest and South subareas from the inland subareas of the Oxnard Plain for base-case 1 (fig. 27*A*). Even larger subregional underflows were indicated for the cut-back projections for base-cases 2 and 3 (fig. 27*B*,*C*). Changes in horizontal flow of ground water as underflow to the Oxnard Plain subareas were directly proportional to the reductions in pumpage in the FGMA area, ranging from about 9,850 acre-ft/yr for base-case 1 to about 10,720 acre-ft/yr for base-case 3 (table 6). The largest components of underflow were from the Santa Clara River Valley and the Pleasant Valley subareas. These flow rates are small relative to coastal landward flow (seawater intrusion), water derived from storage, and downward flow between aquifers, but are important locally near subarea boundaries (fig. 27, table 6). The mean rate of underflow for the base-case 1 projection was about half the rate simulated for 1984–93 (table 6). Ground water was flowing from the Oxnard Plain subareas and adjacent inland subareas toward the Pleasant Valley subareas in both aquifer systems during the 1984–93 period (fig. 25). Yet, the base-case projections simulated flow of water toward Pleasant Valley in the upper-aquifer system, flow from the Northeast Oxnard Plain subarea in the lower-aquifer system, and a reversal of flow toward the South Oxnard Plain subarea. The rate of underflow from the Santa Clara River Valley subareas was similar to that for base-case 1, for the rolling cut-back (base-case 2), and was almost half that for the step cut-back (base-case 3). The direction of mean underflow from the South Pleasant Valley subarea was reversed for both cut-back projections (fig. 27*B*,*C*, table 6). About 1,800 and 1,400 acre-ft/yr of underflow left the Oxnard Plain subarea to the South Pleasant Valley subarea for base-case 2 and for three projections, respectively (fig. 27*B*,*C*, table 6). Similarly, the direction of net underflow was reversed in the upper-aquifer system toward the West Las Posas Valley subarea. The net inflow to the Oxnard Plain subareas for the historical period of pumpage was a net flow of about 900 acre-ft/yr (fig. 25*A*), and the net mean inflow toward the West Las Posas Valley subarea for base-cases 1–3 was less than 500 acre-ft/yr (fig. 27 *A–C*, table 6). The spectral-based projection (base-case 4) was similar to the base-case 1 projection, that is, there was a large underflow component from the Santa Clara River Valley subareas but a net mean flow toward the Pleasant Valley and Las Posas Valley subareas (fig. 27*D*, table 6).

Mean downward flow between aquifer systems in the Oxnard Plain subareas changed directly with changes in potential pumpage in the FGMA area, but it varied only between about 17,400 acre-ft/yr and 20,900 acre-ft/yr for the four base-case projections (table 6). Net water-level declines reversed to water-level recoveries throughout most of the subareas in the FGMA areas, as well as the adjacent Mound and Santa Paula subareas, for the cut-back projections (base-cases 2 and 3) (figs. 25, 26, 27*B*,*C*).

Land-Subsidence

The water derived from aquifer-system compaction also was reduced and was proportional to the cut backs in pumpage and related water-level recoveries. The total amount of water derived from storage owing to the compaction of fine-grained deposits was about 36,400 acre-ft (1,500 acre-ft/yr) for base-case 1; the amount was reduced to about 10,000 acre-ft (420 acre-ft/yr) for base-case 2 and was reversed to about 8,000 acre-ft (330 acre-ft/yr) returning to storage in the fine-grained deposits for base-case 3 (table 6). For the spectral analyses, the total amount of water from compaction was about 47,250 acre-ft for the entire 44-year period. The larger amount simulated for the spectral analysis relative to base-case 1 is due to the prolonged drought estimated by the spectral precipitation method. The simulated subsidence, which was driven by this extended drought, resulted in potential subsidence of about 1 ft throughout most of the Northeast Oxnard Plain subarea, the northeastern part of the South Oxnard Plain subarea, and the West and East Las Posas Valley subareas.

The base-case projections generally produced water-level recoveries or modest water-level declines that generally were less than previous maximum declines (figs. 25 and 27). However, as much as an additional 1 ft of subsidence was simulated in the Northeast Oxnard Plain subarea, the northern part of the South Oxnard Plain subarea, the West Las Posas Valley subarea, and the western part of the East Las Posas Valley subarea during the early dry-year period for base-case 1. Simulated subsidence for the rolling cut-back (base-case 2) projection was reduced to a smaller areal extent and generally from about 0.5 ft (base-case 1) to 0.1 ft throughout most of the South and Northeast Oxnard Plain subareas. Simulated subsidence was further reduced for the step cut-back in pumpage for the FGMA areas for base-case 3. However, about 1 ft of subsidence persisted in the base-case 3 simulation in the northeastern part of the Oxnard Plain subareas and the South Pleasant Valley subarea and in the East Las Posas Valley and North Pleasant Valley subareas. The extended drought simulated in the early part of the 44-year projection of base-case 4 produced water-level declines in most of the Oxnard Plain Forebay subarea (fig. 27*D*) and, to a lesser extent, in the remainder of the Oxnard Plain subareas and the inland subareas in the FGMA areas (fig. 26), which resulted in additional subsidence.

Projected Future Ground-Water Flow for Alternative Water-Supply Projects

The analysis of future ground-water flow for alternative water-supply projects was simulated for the same 24-year period used for the analysis of the proposed projects for the existing management plan. The simulations included well-by-well average ground-water pumpage for the 1984–93 period, irrigation return flow estimated using the 1969 land-use distribution, and climatically varying recharge, streamflow, and pumpage. Each projection of future ground-water flow that includes potential alternative projects also includes the proposed projects described in the previous section.

Each of these potential future projects was simulated individually, but they include the base-case 1 set of projects and assumptions. These seven alternative water-supply projects were proposed to help manage the effects of increasing demand and variable supply on seawater intrusion, subsidence, increased withdrawal from storage, and vertical and lateral flow between subareas and aquifer systems.

The model cells used to simulate the alternative water-supply projects (referred to as potential cases 1–7) are shown in figures 26 *A*,*B*. The simulated differences in ground-water levels and the cumulative changes in ground-water storage, coastal flow, and mean ground-water underflow in and out of the Oxnard Plain are shown in figure 28. In general, reductions in water derived from subsidence in the alternative water-supply projects were proportional to the cut backs in pumpage and related water-level recoveries. The potential-case projections resulted in water-level recoveries or modest water-level declines that generally were less than historical maximum declines (fig. 27). However, an increase in subsidence was simulated in the FGMA areas and in the Fillmore subarea during the early dry-year period for all seven alternative water-supply projects (potential cases 1–7). Selected details for each alternative water-supply project (potential case) are presented below.

Potential Case 1—Seawater Barrier and Increased Pumpage in the Oxnard Plain Forebay

For potential case 1, pumpage by the city of Oxnard was reduced by 4,000 acre-ft/yr. The reduced pumpage was supplanted with CMWD deliveries, and a seawater-intrusion barrier project was implemented by injecting 20,000 acre-ft/yr of imported water and reclaimed sewage into the upper-aquifer system along the South Oxnard Plain subarea from Port Hueneme to just south of the wastewater treatment plant. Ground water that had been historically pumped from the lower-aquifer system from the El Rio-OH wells was pumped from the upper-aquifer system in the Oxnard Plain Forebay. This offset the injection of effluent and imported water and reduced the pumpage stress on the lower-aquifer system. These projects collectively started in the year 2000.

Results of potential case 1 show that the simulated seawater-barrier injection stopped coastal landward flow (seawater intrusion) in the upper-aquifer system but did not reduce the coastal landward flow (seawater intrusion) in the lower-aquifer system. The rates of coastal landward flow (seawater intrusion) in the lower-aquifer system were comparable to those simulated for base-case 1 (figs. 27*A* and 28*A*; table 6). Injecting water into the upper-aquifer system to form a seawater-intrusion barrier for the South Oxnard Plain subarea south of the Hueneme submarine canyon (fig. 1) produced water-level rises as great as 30 ft (fig. 28*A*) that resulted in heads as much as 20 ft above sea level (add water-level changes from fig. 28*A* to water-level elevations from fig. 25*A*). For this case, more water was pumped from storage in the Oxnard Plain Forebay without increasing coastal landward flow (seawater intrusion) in the upper-aquifer system. However, this additional pumpage produced a small amount of additional subsidence. A 24-percent increase in net underflow from the Santa Clara River Valley subareas to the Oxnard Plain subarea was simulated for this case with the increase of 20,000 acre-ft/yr of pumpage in the Oxnard Plain Forebay at the OH wells (figs. 26*B* and 28*A*). In addition, the pumpage reduced the net ground-water underflow away from the Oxnard Plain Forebay to the Northeast and Northwest Oxnard Plain model subareas by about 11,000 acre-ft/yr in the upper-aquifer system compared with the net underflow in base-case 1 (figs. 27*A* and 28*B*). As in the base-case 1 projection, as much as an additional foot of subsidence was simulated in the northeast Oxnard Plain subarea, the northern part of the South Oxnard Plain subarea, the West Las Posas Valley subarea, and the western part of the East Las Posas Valley subarea during the early dry-year period for potential case 1. Subsidence of a few tenths of a foot was further extended across the Oxnard Plain Forebay subarea owing to the additional 20,000 acre-ft/yr of pump-back pumpage, and the extent of subsidence in the South Oxnard Plain subarea along the coast was reduced owing to the 20,000 acre-ft/yr injection project in the upper-aquifer system.

Potential Case 2—Artificial Recharge in Happy Camp Canyon

For potential case 2, additional recharge of 15,000 acre-ft/yr was added as surface-spreading to the upper-aquifer system at the mouth of Happy Camp Canyon along the northeast border of the East Las Posas Valley subarea beginning in 2000. The projected additional recharge contributed about 204,000 acre-ft of water going into storage but resulted in simulated water levels being significantly above land surface (not feasible) in the upper-aquifer system in the East Las Posas Valley subarea (figs. 27*A* and 28*B*, table 6). Although this case resulted in simulated water levels that were above land surface in the East Las Posas Valley subarea, essentially no changes were simulated in the hydrologic conditions in the Oxnard Plain, Pleasant Valley, or Santa Clara River Valley subareas. The simulated water-level rise above land surface at the mouth of Happy Camp Canyon may, in part, be due to the hydraulic properties and layering used in the model.

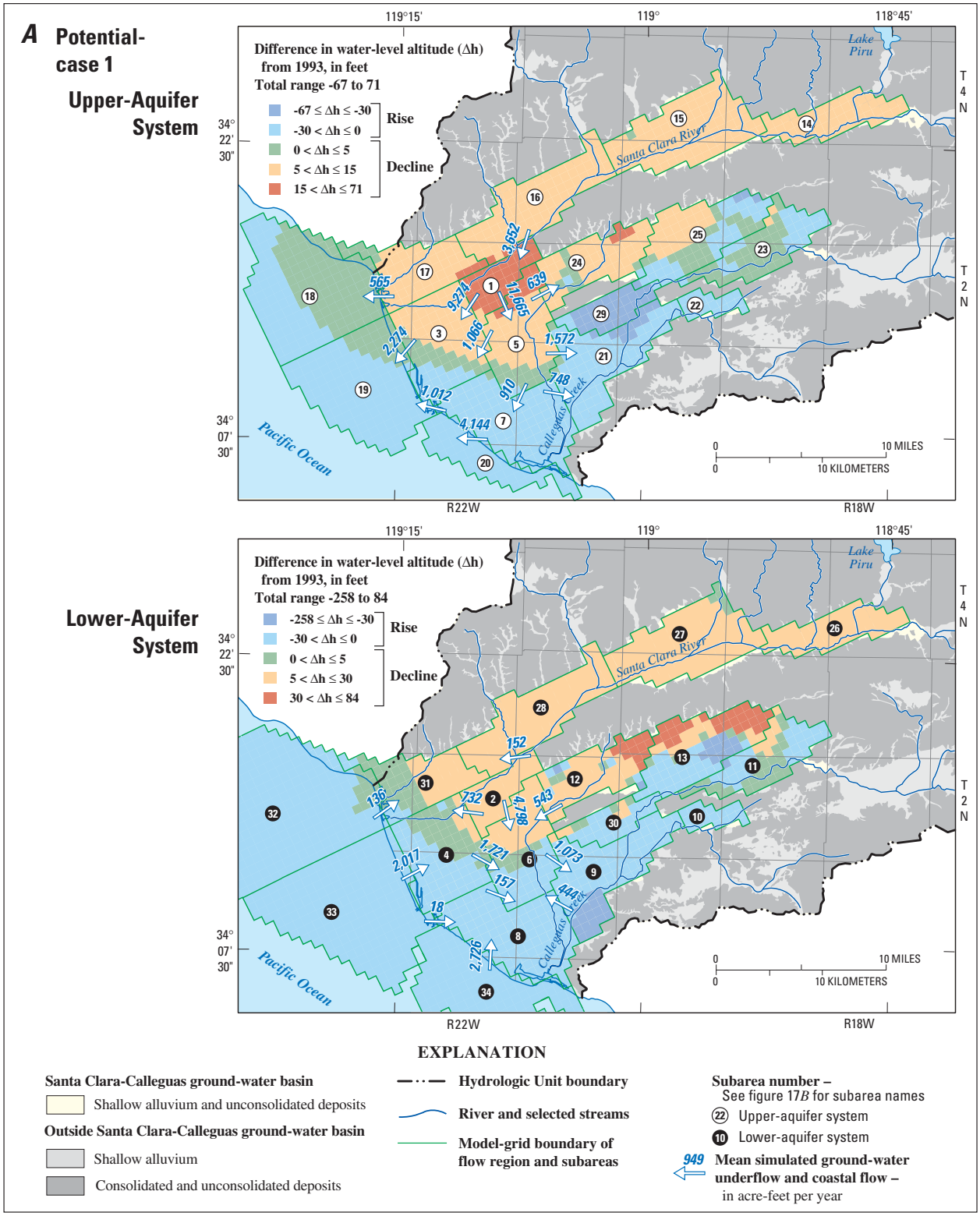

Figure 28. Simulated differences in ground-water levels from 1993 to 2017 for alternative water-supply projects using the base-case 1 set of projects and assumptions in the Santa Clara–Calleguas ground-water basin, Ventura County, California. ***A***, Seawater intrusion barrier project in the southern Oxnard Plain subregion and equal pump-back from the Oxnard Forebay in the upper-aquifer system (potential case 1).

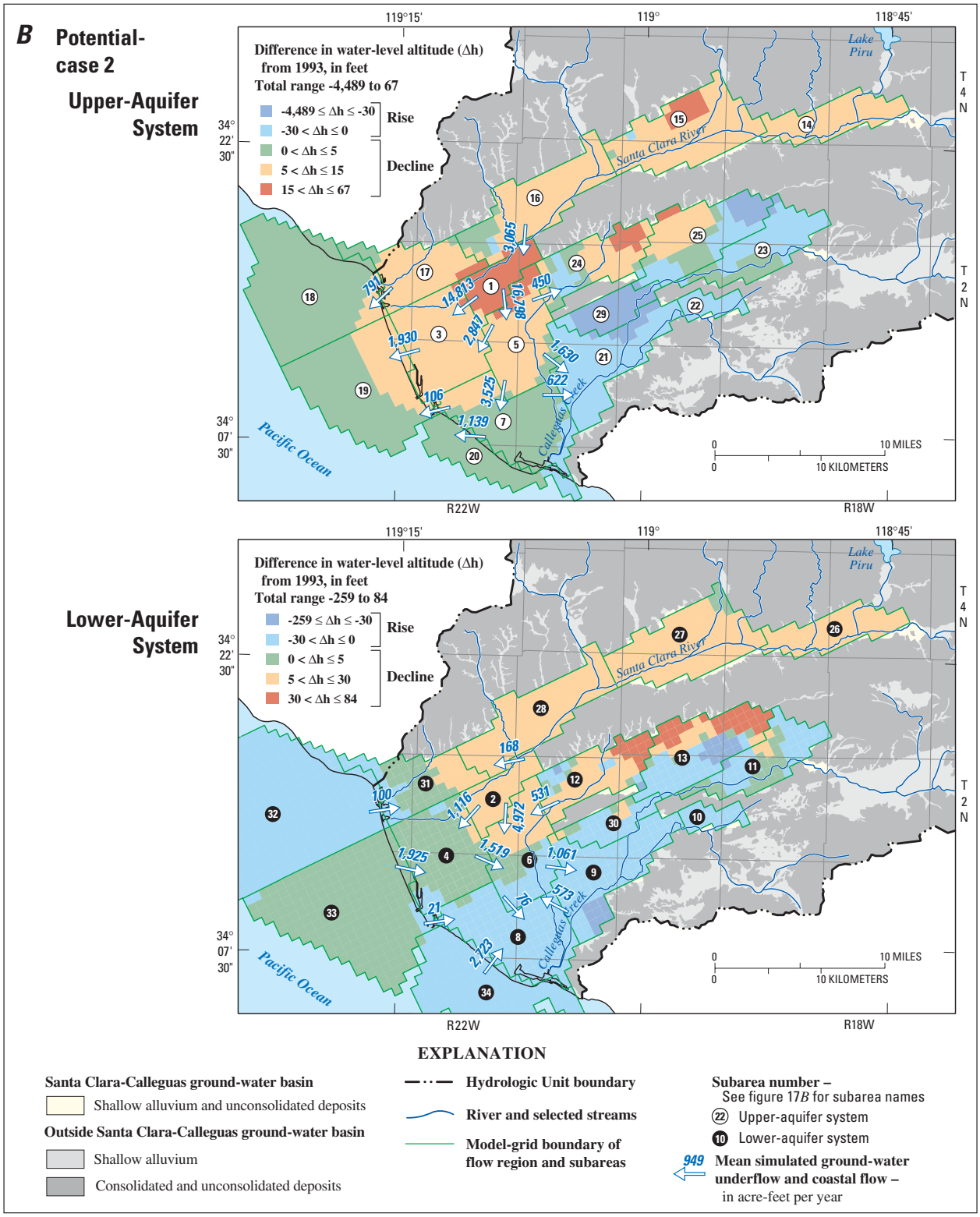

Figure 28—Continued. ***B***, Additional artificial recharge added at mouth of Happy Camp Canyon, East Los Posas subarea (potential case 2).

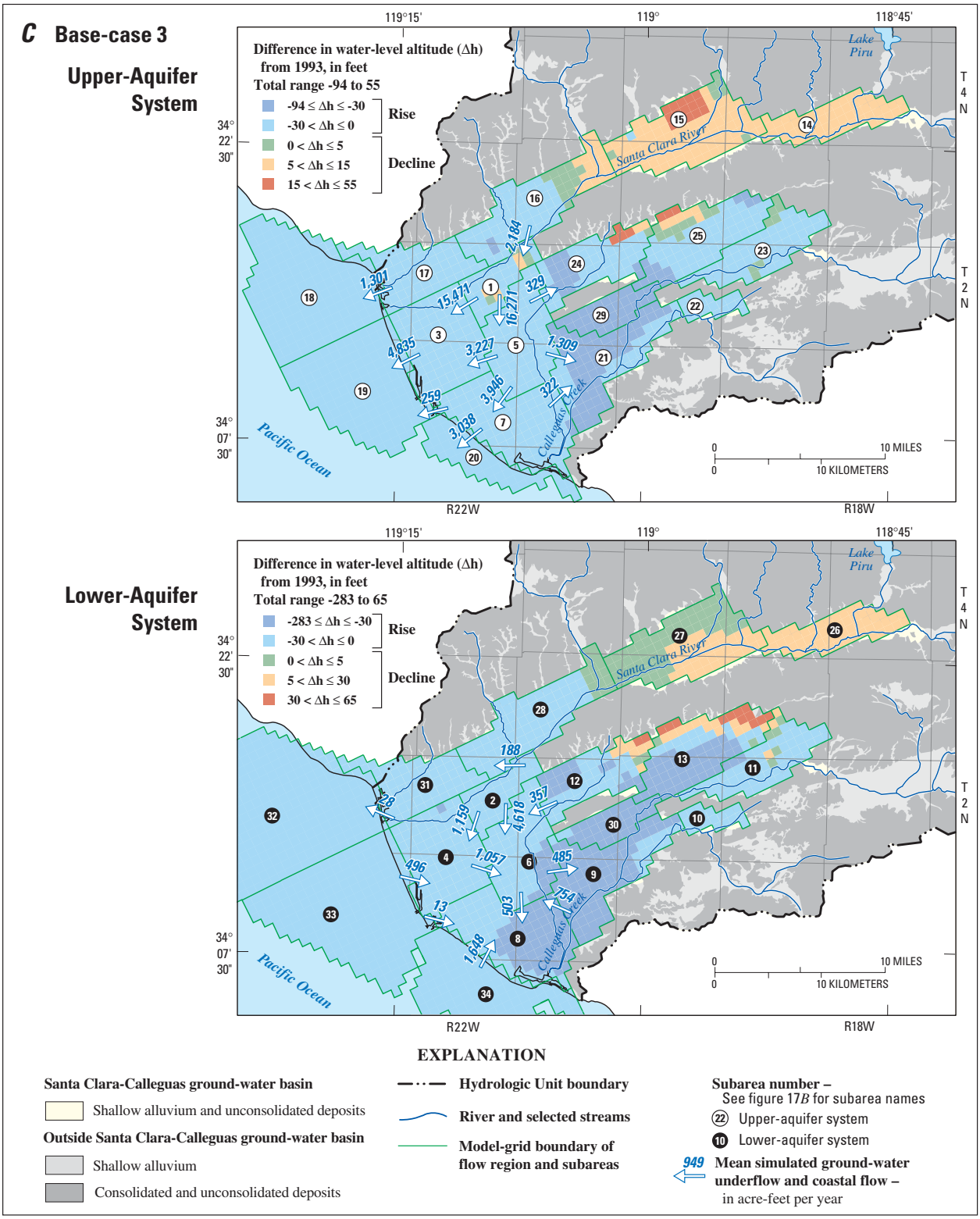

Figure 28—Continued. ***C***, Cessation of pumpage in the southern Oxnard Plain subregion (potential case 3).

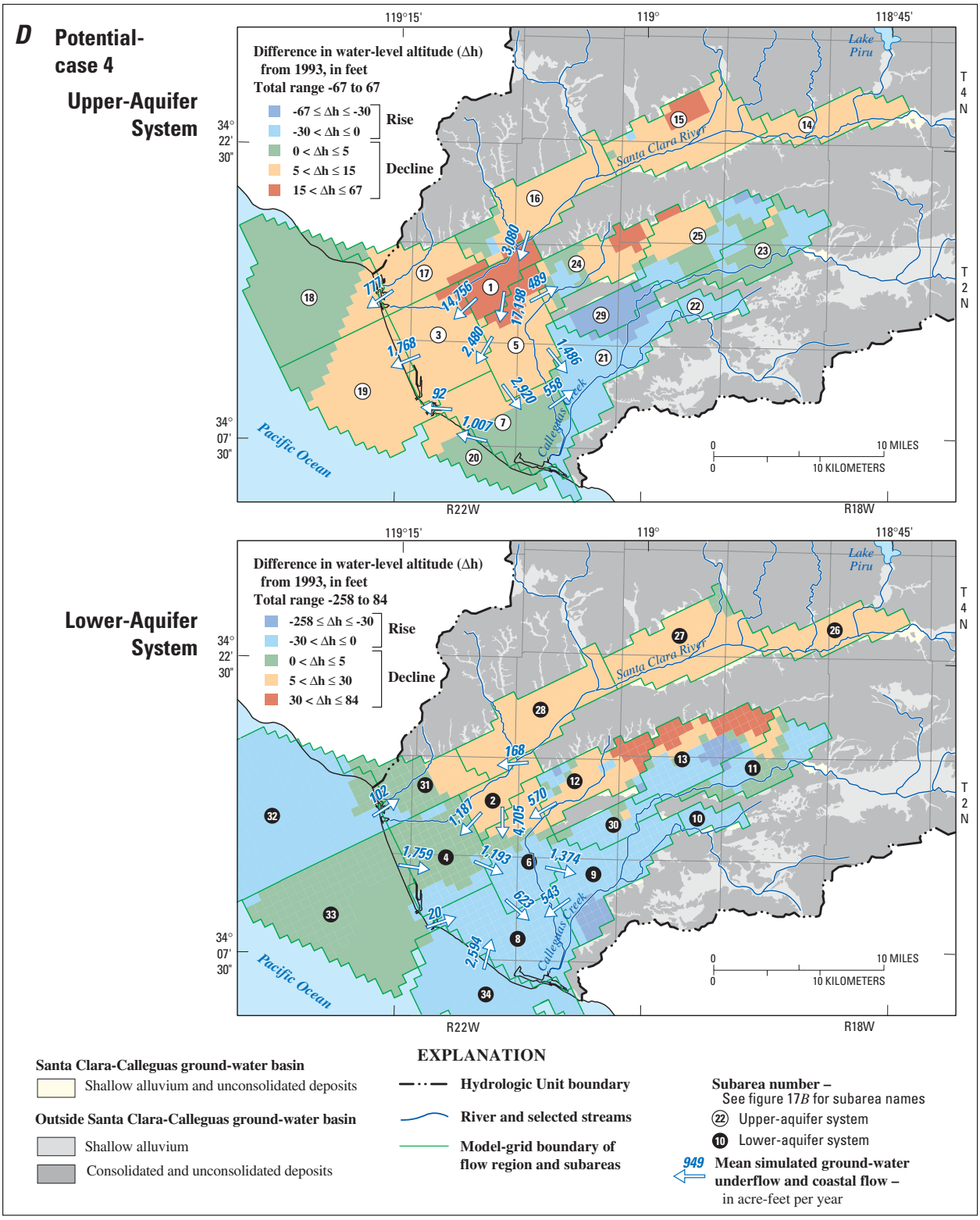

Figure 28—Continued. ***D***, Shifting pumpage from the Pumping-Trough Pipeline (PTP) wells from the lower- to upper-aquifer system (potential case 4).

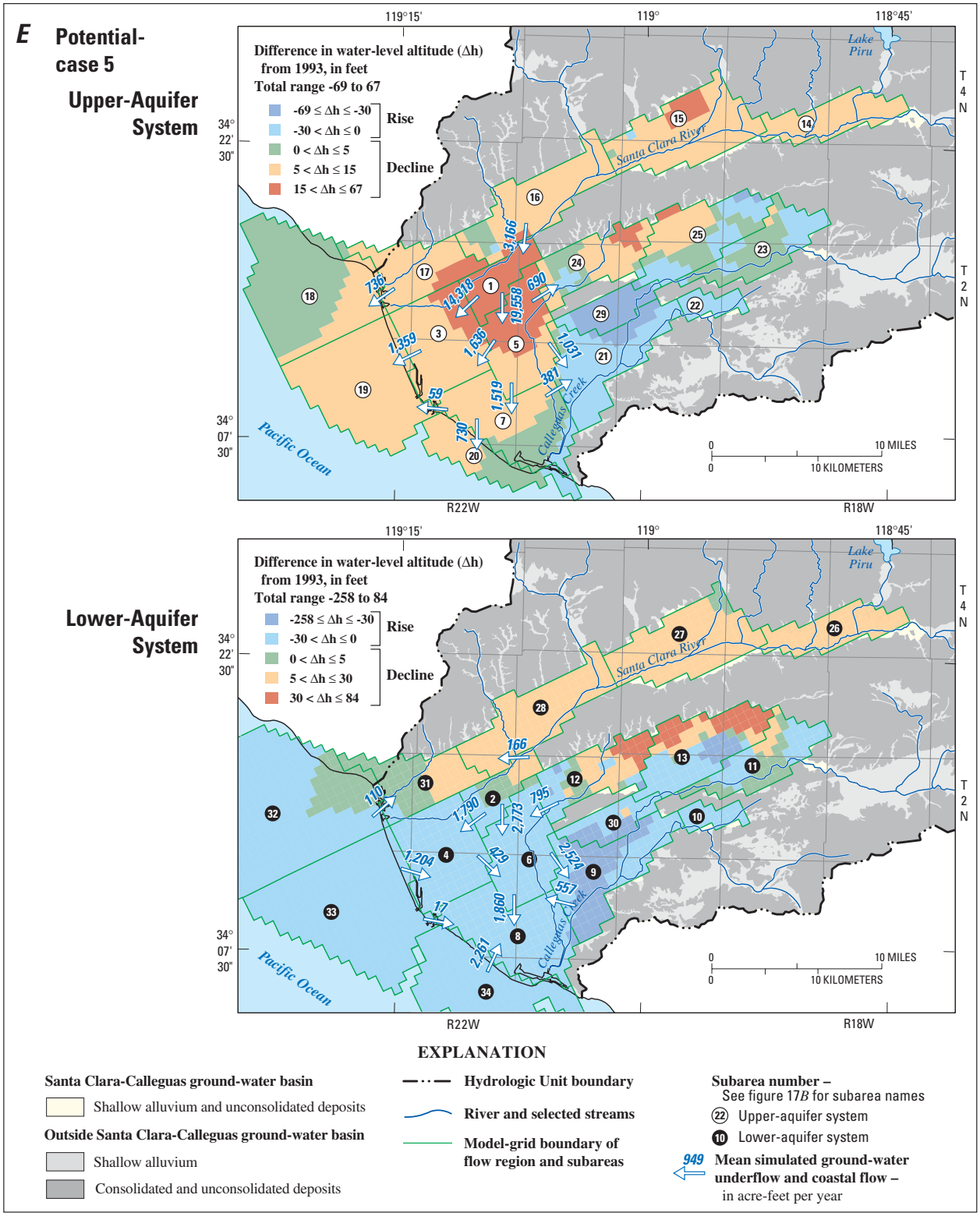

Figure 28—Continued. ***E***, Shifting pumpage from the lower- to upper-aquifer system in the northeastern Oxnard Plain subarea (potential case 5).

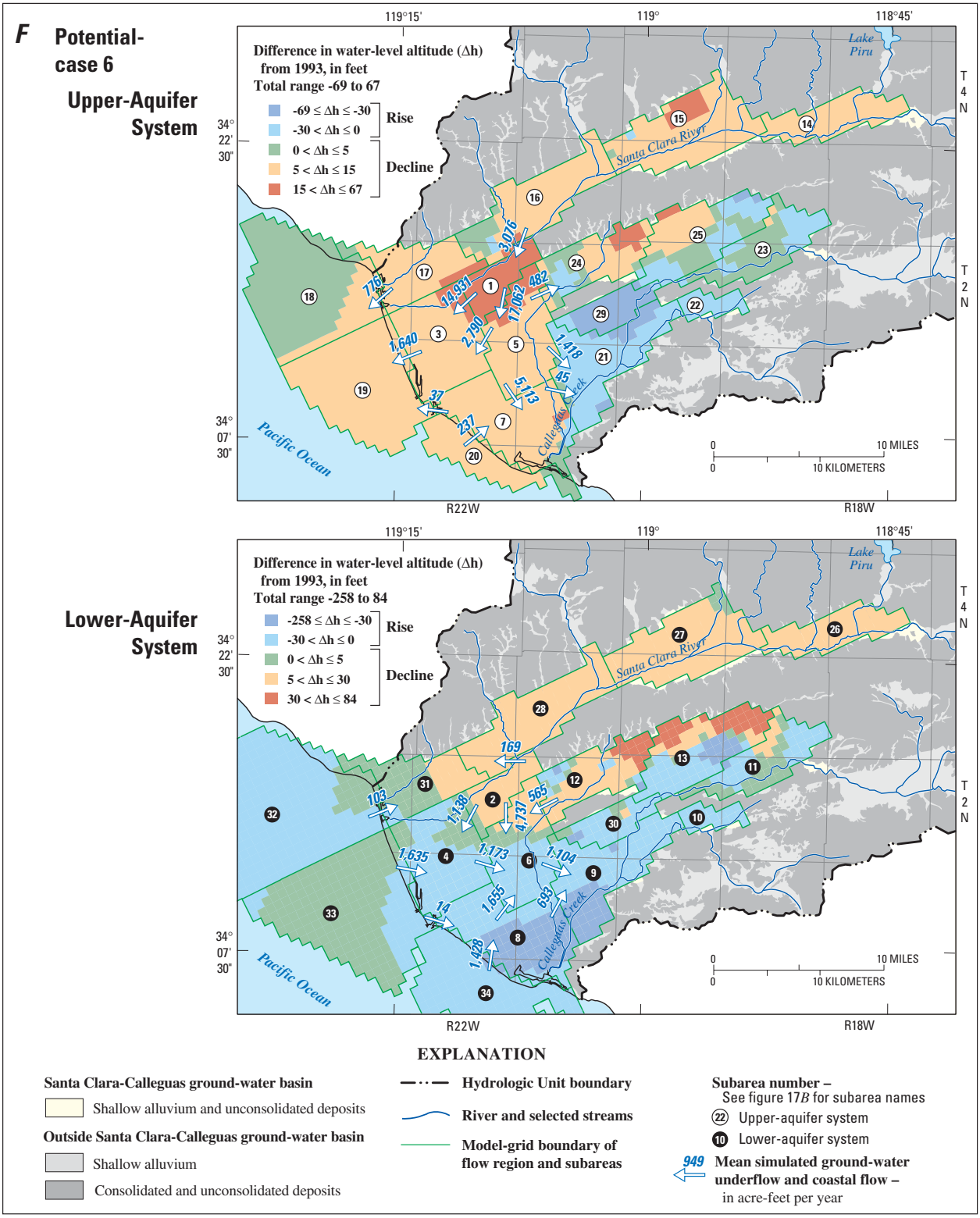

Figure 28—Continued. ***F***, Shifting pumpage from the lower- to upper-aquifer system in the southern Oxnard Plain subarea (potential case 6).

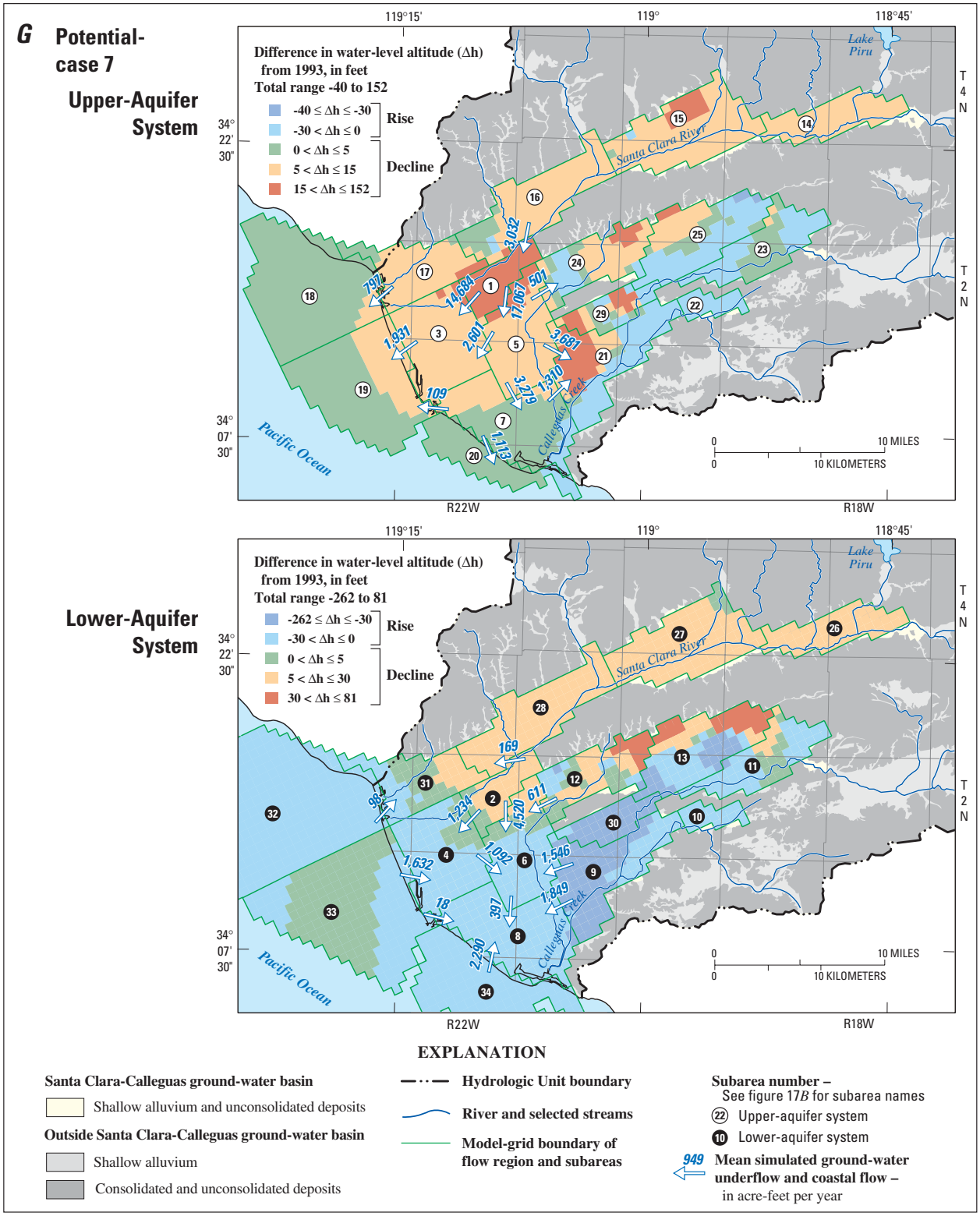

Figure 28—Continued. ***G***, Shifting pumpage from the lower- to upper-aquifer system in the Pleasant Valley subarea (potential case 7).

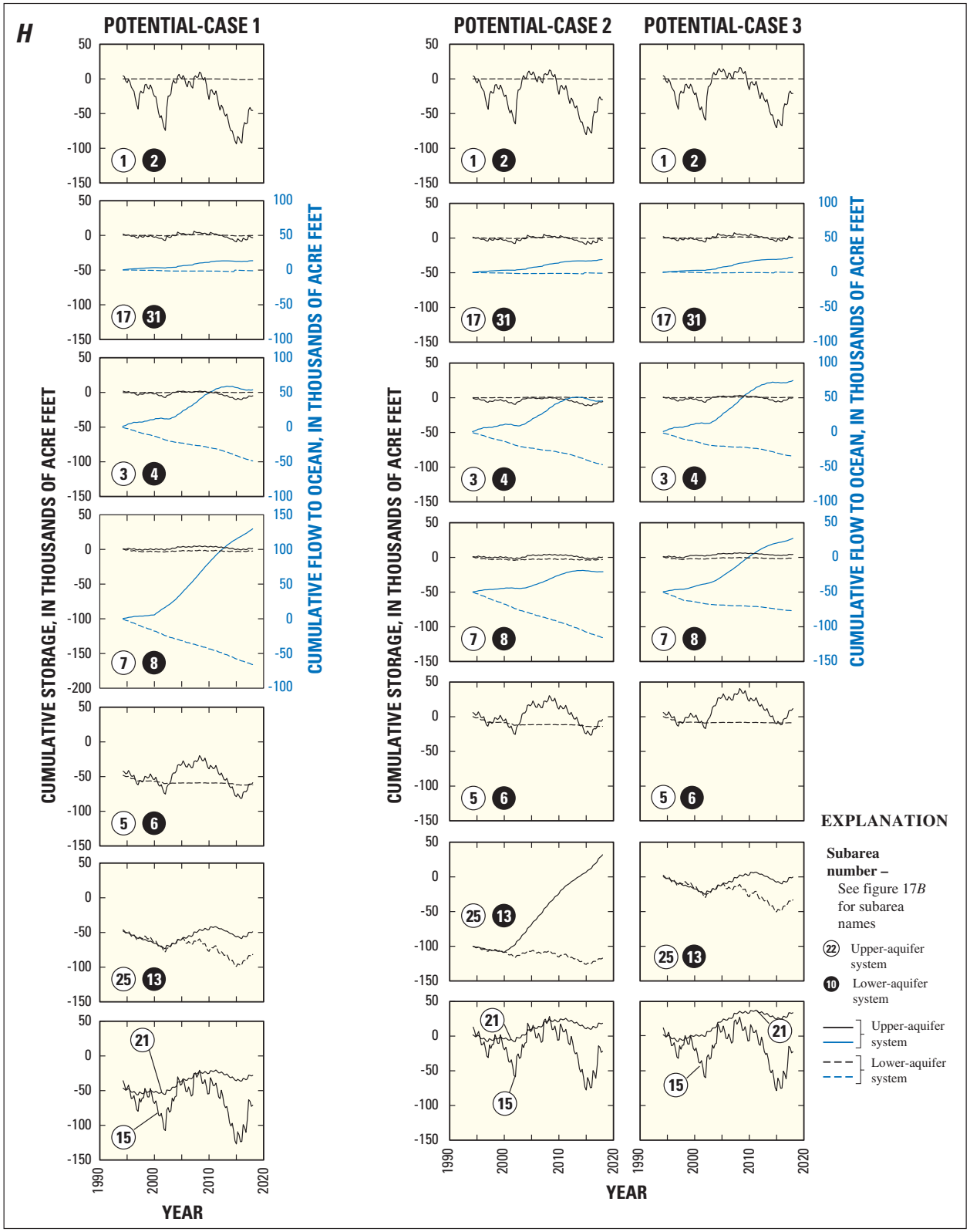

Figure 28—Continued. ***H***, Cumulative changes in ground-water storage and ground-water flow for selected subareas, 1993–2017.

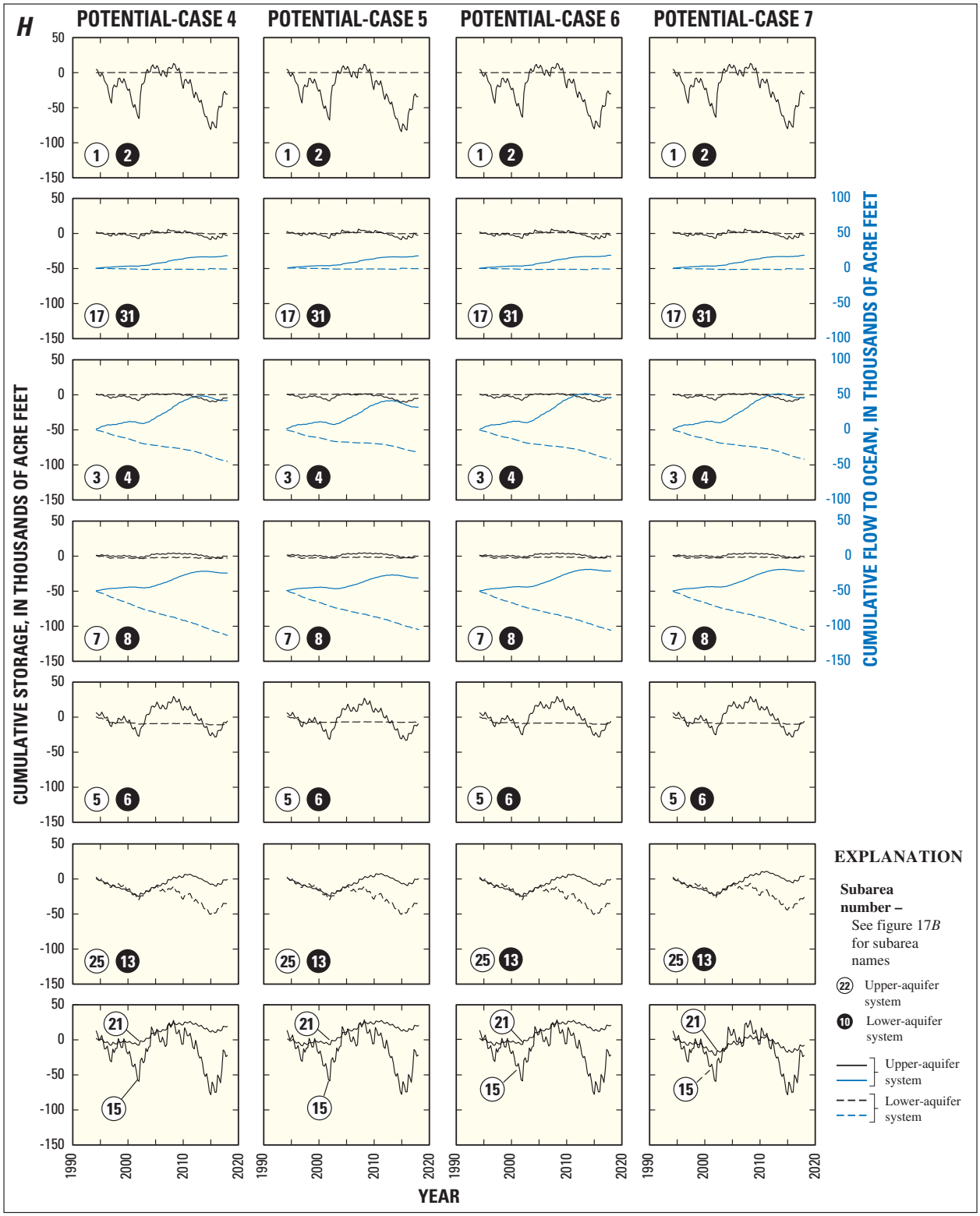

Figure 28—Continued. ***H***, Cumulative changes in ground-water storage and ground-water flow for selected subareas, 1993–2017.

Potential Case 3—Eliminate Agricultural Pumpage in the South Oxnard Plain Subarea

For potential case 3, the pumping of ground water was stopped in the South Oxnard Plain subarea in lieu of additional pipeline deliveries of diverted streamflow or imported water beginning in 1998. This case shows increased recovery in the upper- and lower-aquifer systems throughout the Oxnard Plain and Pleasant Valley subareas relative to base-case 1. This reduction in pumpage increased the coastal seaward flow in the upper-aquifer system and reduced the coastal landward flow (seawater intrusion) in the lower-aquifer system. Stopping pumpage primarily in the lower-aquifer system in the South Oxnard Plain subarea had the largest effect on reducing coastal landward flow (seawater intrusion) of all the potential cases evaluated. Coastal landward flow (seawater intrusion) in the lower-aquifer system was reduced by 48 percent, yet coastal seaward flow in the upper-aquifer system was increased by 85 percent compared with base-case 1 (figs. 27*A* and 28*C*; table 6). The largest net underflow to the South Pleasant Valley subarea was simulated with cessation of pumpage in the South Oxnard Plain subarea (fig. 28*C*, table 6). Similarly, the cessation of pumpage in the South Oxnard Plain subarea resulted in ground-water underflow to the Northeast Oxnard Plain from the South Oxnard Plain subareas—a reversal in underflow relative to the base-case 1 (figs. 27*A* and 28*C*). For cessation of pumpage in the South Oxnard Plain, simulated subsidence was not completely eliminated but was reduced to a few tenths of a foot along the northern boundary with the northeastern part of the Oxnard Plain subareas. This potential case also resulted in an additional 0.1 ft of subsidence over much of the Oxnard Plain Forebay subarea and the adjacent Santa Paula subarea relative to base-case 1. Cessation of pumpage in the South Oxnard Plain also reduced the extent and magnitude of subsidence in the Northeast Oxnard Plain subarea.

Potential Case 4—Shift Pumpage to Upper-Aquifer System in PTP Wells

For potential case 4, pumpage from the Pumping-Trough Pipeline (PTP) wells was shifted from the lower-aquifer system to the upper-aquifer system beginning in 1998. This change produced water-level declines over a larger areal extent in the upper-aquifer system in the Oxnard Plain Forebay subarea (fig. 28*D*) relative to base-case 1 (fig. 27*A*), as well as a small reduction in coastal seaward flow in the upper-aquifer system and a small reduction of coastal landward flow in the lower-aquifer system compared with base-case 1 (fig. 28*D*). The shifting of PTP-well pumpage to the upper-aquifer system also resulted in increased underflow from the lower-aquifer system in the Northeast Oxnard Plain to the South Oxnard Plain and the South Pleasant Valley subareas by 900 acre-ft/yr compared to net underflow in base-case 1 (figs. 27*A* and 28*D*). The shifting of PTP-well pumpage to the upper-aquifer system reduced the extent and magnitude of subsidence in the Northeast Oxnard Plain subarea but had little to no effect elsewhere.

Potential Case 5—Shift Pumpage to Upper-Aquifer System in the Northeast Oxnard Plain

For potential case 5, pumpage throughout the Northeast Oxnard Plain subarea was shifted from the lower-aquifer system to the upper-aquifer system beginning in the year 1998. The change for this simulation is similar to the change in potential case 4. The increase in pumpage in the upper-aquifer system produced increased water-level declines in the Northeast Oxnard Plain subarea, reduced underflow from the Northeast Oxnard Plain subarea to adjacent subareas in the upper-aquifer system, and reduced coastal seaward flow in the upper-aquifer system relative to base-case 1 (figs. 27*A*, 28*E*). The reduced pumpage in the lower-aquifer system resulted in reduced coastal landward flow in the lower-aquifer system (fig. 28*E*). The net coastal seaward flow was decreased by about 1,090 acre-ft/yr in the upper-aquifer system and the coastal landward flow (seawater intrusion) was decreased by about 1,180 acre-ft/yr (figs. 27*A*, 28*E*). The shifting of pumpage to the upper-aquifer system in the Northeast Oxnard Plain subarea also reduced the extent and magnitude of subsidence throughout the Oxnard Plain subareas but did extend some potential subsidence of less than 0.1 ft into the Northwest Oxnard Plain subarea.

Potential Case 6—Shift Pumpage to the Upper-Aquifer System in the South Oxnard Plain Subarea

For potential case 6, pumpage throughout the South Oxnard Plain subarea was shifted from the lower-aquifer system to the upper-aquifer system beginning in the year 1998. The shift in pumpage produced coastal landward flow (seawater intrusion) in the upper-aquifer system and reduced coastal landward flow (seawater intrusion) into the lower-aquifer system in the South Oxnard Plain subarea by about half (fig. 28*F*) relative to base-case 1 (fig. 27*A*). Relative to the base-case 1 projection, shifting pumpage from the lower- to the upper-aquifer system in the South Oxnard Plain subarea resulted in the second largest reduction (33 percent) of total coastal landward flow (seawater intrusion) of all the potential cases evaluated. In addition, shifting pumpage to the upper-aquifer system in the South Oxnard Plain subarea resulted in reduction in coastal seaward flow in the upper-aquifer system, an increase in underflow from the Northeast Oxnard Plain subarea to the South Oxnard Plain subarea, and in a reversal of underflow from the South Oxnard Plain to the South Pleasant Valley subarea in the lower-aquifer system (figs. 27*A* and 28*F*). The net coastal seaward flow was decreased by about 1,750 acre-ft/yr in the upper-aquifer system, and the net coastal landward flow (seawater intrusion) was decreased by about 1,590 acre-ft/yr (figs. 27*A*, 28*F*) in the lower-aquifer system relative to base-case 1. The shifting of pumpage from the lower- to the upper-aquifer system in the South Oxnard Plain subarea yielded the largest combined effect on coastal flow with a reduction of coastal landward flow in the lower-aquifer system and coastal seaward flow from the upper-aquifer system. Similarly, shifting pumpage in the South Oxnard Plain subarea to the upper-aquifer system reduced the magnitude of potential additional subsidence throughout the Northeast and South Oxnard Plain subareas.

Potential Case 7—Shift Pumpage to Upper-Aquifer System, Pleasant Valley

For potential case 7, pumpage throughout the Pleasant Valley subareas was shifted from the lower-aquifer system to the upper-aquifer system beginning in the year 1998. This simulation produced coastal seaward flow in the upper-aquifer system similar to that in base-case 1 and a small decrease of coastal landward flow (seawater intrusion) in the lower-aquifer system compared with that for base-case 1 (fig. 28*G*). Shifting pumpage to the upper-aquifer system in the Pleasant Valley subareas resulted in more flow from the upper-aquifer system in the Northeast Oxnard Plain subarea and a reversal of flow in the lower-aquifer system toward the Oxnard Plain subareas from the South Pleasant Valley subarea (figs. 27*A* and 28*G*). Shifting pumpage to the upper-aquifer system in the Pleasant Valley subareas reduced potential subsidence in the North Pleasant Valley subarea and resulted in reduced subsidence in the Oxnard Plain subareas—a result similar to that caused by shifting pumpage to the upper-aquifer system in the Northeast and South Oxnard Plain subareas.

SUMMARY AND CONCLUSIONS

Ground water from the regional alluvial-aquifer system is the main source of water in the Santa Clara–Calleguas Basin in southern California. A steady increase in the demand for water in the basin since the late 1800s has resulted in streamflow depletion, ground-water overdraft, seawater intrusion, inter-aquifer flow, land subsidence, and ground-water contamination. Construction of reservoirs and discharge of shallow ground water and treated sewage effluent have contributed to regulated flow and modification of river systems in the basin, changing flows in the Santa Clara River and the Calleguas Creek and in some tributaries to predominantly perennial or intermittent flow. The use of ground water and surface water also is affected by wet and dry climatic periods that control the quantity and distribution of streamflow and recharge. These periods, which have persisted since the late 1600s, are estimated to have had periods of about 22, 5.3, and 2.2–2.9 years during the past 100 years. Dry to wet cycle precipitation increases by a factor of 1.8 for winters and by 1.6 for springs.

The Santa Clara–Calleguas Basin in Ventura County, California, is composed of northeast-trending anticlinal mountains and synclinal valleys in the Transverse Ranges physiographic province. The onshore part of the alluvial basin is about 32 mi long and includes about 310 mi^2 bounded by rugged topography. An additional 193 mi^2 of the ground-water basin is an extensive sloping offshore plain truncated by steeply dipping submarine cliffs and dissected by several submarine canyons. The two largest submarine canyons dissect the offshore plain west of Port Hueneme and Point Mugu. The Santa Clara River and the Calleguas Creek and their tributaries drain the basin to the Pacific Ocean.

Growth and increasing water use in the Santa Clara–Calleguas Basin have continued over the last century, and because of the proximity to the Los Angeles metropolitan area, they may continue to transform the basin from an agriculture-based economy to an urban and industrial economy. Agricultural land use increased less than 5 percent between 1969 and 1980, and population in Ventura County increased 28 percent between 1980 and 1992. Agricultural water use increased to a historical high during the 1950s owing in part to the introduction of truck crops and refrigerated railroad transportation. Estimated pumpage ranged from 34,800 acre-ft for the drought years of the 1920s to a maximum pumpage of 301,400 acre-ft/yr during the 1990 drought year.

The Santa Clara–Calleguas Basin consists of multiple aquifers grouped into upper- and lower-aquifer systems. The upper-aquifer system includes the Shallow, Oxnard, and Mugu aquifers. The lower-aquifer system includes the Hueneme, Fox Canyon, and Grimes Canyon aquifers. Layers of the aquifer systems include basal coarse-grained sediments overlying regional unconformities; these coarse-grained layers are the major source of ground-water production and pathways for seawater intrusion. The aquifer systems are surrounded and underlain by consolidated bedrock that forms a relatively impermeable boundary to ground-water flow. Numerous faults act as barriers and boundaries to ground-water flow. The aquifer systems crop out offshore along the edge of the submarine shelf and within the coastal submarine canyons. Submarine canyons have dissected these regional aquifers, providing a hydraulic connection to the ocean through the submarine outcrops of the aquifer systems.

Analysis of hydrological, geophysical, and geochemical data and simulation results indicates that the upper-aquifer system receives most of the natural and artificial recharge, and thus is more dynamic than the lower-aquifer system. Owing to development, many changes have occurred in the regional flow system: streamflow has changed from predominantly floodflows to a combination of regulated flows and floodflows; large quantities of diverted streamflow and treated sewage effluent are used for artificial recharge; streamflow infiltration has increased due to pumpage of ground water; ground water that flowed toward the ocean now flows toward the major pumping centers in the northeastern part of the Oxnard Plain, in Pleasant Valley, and in the western part of the East Las Posas Valley; aquitard compaction has resulted in land subsidence in the southern Oxnard Plain; and vertical flow occurs as leakage between aquifer systems and intraborehole flow within water-supply wells.

A numerical ground-water flow model of the Santa Clara–Calleguas Basin was developed as part of the USGS RASA Program. The flow model was developed to better define the geohydrologic framework of the regional ground-water flow system and to analyze problems affecting water resources of a typical coastal aquifer system. Development of the model included compilation of geographic, geologic, and hydrologic data and estimation of hydraulic properties and flows. The transient-state model was calibrated to historical surface-water and ground-water flows for 1891–1993.

Sources of water to the regional ground-water flow system are natural and artificial recharge, coastal landward flow from the ocean (seawater intrusion), storage in the coarse-grained beds, and water from compaction of fine-grained beds (aquitards). Inflows used in the regional flow model simulation include streamflows routed through the major rivers and tributaries; infiltration of mountain-front runoff and infiltration of precipitation on bedrock outcrops and on valley floors; and artificial ground-water recharge of diverted streamflow, irrigation return flow, and treated sewage effluent.

Most natural recharge occurs through infiltration (losses) of streamflow within the major rivers and tributaries and the numerous arroyos that drain the mountain fronts of the basin. Most streamflow loss occurs during wet-year periods when flows are the greatest, although the percentage of streamflow loss is larger during dry-year periods (37 percent during dry- and 22 percent during wet-year periods). Total simulated natural recharge was about 114,100 acre-ft/yr for 1984–93: 27,800 acre-ft/yr of mountain-front and bedrock recharge, 24,100 acre-ft/yr of valley-floor recharge, and 62,200 acre-ft/yr of net streamflow recharge.

Artificial recharge (spreading of diverted streamflow, irrigation return, and sewage effluent) is a major source of ground-water replenishment to the Santa Clara–Calleguas ground-water basin. Streamflow has been diverted to spreading grounds since 1929, and treated-sewage effluent has been discharged to stream channels since 1930. During 1984–93, the estimated average artificial recharge at spreading grounds was about 54,400 acre-ft/yr, which is about 13 percent less than simulated streamflow recharge (62,200 acre-ft/yr). Estimated recharge from irrigation return flows on the valley floors and treated sewage effluent for 1984–93 averaged about 51,000 acre-ft/yr and 9,000 acre-ft/yr, respectively.

Surface-water outflows from the Santa Clara–Calleguas Basin are streamflow discharged to the Pacific Ocean and to streamflow diversions used for agriculture and artificial ground-water recharge. The streamflows consist of floodflows, regulated surface-water flows, such as releases from Lake Piru and discharge of treated sewage-effluent, and intermittent baseflow from rejected ground water.

Ground-water discharge from the Santa Clara-Calleguas ground-water basin is pumpage, coastal seaward flow to the Pacific Ocean, and evapotranspiration along the flood plains of the major rivers and tributaries. Under predevelopment conditions, the largest discharge from the ground-water system was outflow as coastal seaward flow and evapotranspiration. Pumpage of ground water from thousands of water-supply wells has diminished these outflows and was the largest outflow from the ground-water flow system for the simulation period 1891–93. The distribution of pumpage for 1984–93 indicates that most of the pumpage occurs in the Oxnard Plain subareas (37 percent) and in the upper Santa Clara River Valley subareas (37 percent).

The total simulated pumpage for 1984–93 averaged about 247,000 acre-ft/yr, 146,000 acre-ft/yr from the Fox Canyon Groundwater Management agency (FGMA) subareas and 101,000 acre-ft/yr from the non-FGMA subareas. This large demand for ground water exceeded the natural and artificial supply of surface water and ground water for parts of the two aquifer systems and resulted in an overdraft of the potable water supply. Of the total 1984–93 pumpage, 46 percent was contributed by natural recharge, 22 percent was contributed by artificial recharge from diverted streamflow, 20 percent was contributed by irrigation return flow, and 4 percent was contributed from sewage-effluent infiltration, 6 percent was contributed by storage depletion, and 2 percent was contributed by coastal landward flow (seawater intrusion).

Ground-water pumping has resulted in large water-level declines in the Las Posas Valley and the Pleasant Valley subbasins. A monotonic water-level decline occurred in the Las Posas Valley subbasins from agricultural pumping. In the Las Posas Valley and South Pleasant Valley subbasins, water-level declines of 50 to 100 ft have occurred in the upper-aquifer system, and declines of about 25 to 300 ft or more have occurred in the lower-aquifer system since the early 1900s.

The combination of variable demand from ground-water pumpage and variable supply, which changes in response to climatic cycles, has resulted in large cycles of decline and recovery in ground-water levels in the upper- and lower-aquifer systems. The largest seasonal and decadal changes in ground-water levels occur in the Oxnard Plain Forebay subarea owing to artificial recharge and pumping, and in the South Oxnard Plain and Pleasant Valley subareas owing to agricultural pumping.

The simulated direction of ground-water underflow in the Oxnard Plain is from the artificial-recharge areas in the Oxnard Plain Forebay subarea toward pumping centers in the Northwest and Northeast Oxnard Plain subareas. The mean simulated underflow to the Oxnard Plain subareas from the Santa Paula, West Las Posas Valley, and South Pleasant Valley subareas for 1984–93 was about 5,77; 500; and 5,720 acre-ft/yr, respectively.

Pumpage from both aquifer systems has resulted in large simulated water-level differences between aquifer systems during dry-year periods that range from 20 to 30 ft near the Hueneme submarine canyon, 50 to 90 ft near Mugu submarine canyon in the Oxnard Plain, 10 to 25 ft in the Santa Clara subareas, and 30 to more than 100 ft in the Las Posas Valley subareas. As a result, inter-aquifer flow occurs as leakage. The simulated vertical downward flow from the upper to the lower-aquifer system averaged about 22,700 acre-ft/yr for the Oxnard Plain subareas for 1984–93.

Seawater intrusion was first suspected in 1931 when water levels were below sea level in a large part of the Oxnard Plain. The simulation of regional ground-water flow indicated that coastal landward flow (seawater intrusion) began in 1927 and continued to the end of the period of simulation in 1993. During wet climatic periods or periods of reduced demand for ground-water pumpage, the simulated direction of coastal flow is reversed in the upper-aquifer system from landward to seaward. During the 1984–93 simulation period, the total net coastal seaward flow was 9,500 acre-ft in the upper-aquifer system, which is less than the 16,000 acre-ft/yr coastal seaward flow simulated for predevelopment conditions. During the same simulation period, total coastal landward flow was 64,200 acre-ft in the lower-aquifer system. This simulated coastal landward flow was supported by increased chloride concentrations and increased EM conductivities in many of the coastal monitoring wells.

Water-level declines induced land subsidence that was first measured in 1939. The model indicates that land subsidence began prior to the 1940s, with most of the decline occurring after the drought of the late 1920s and during the agricultural expansion of the 1950s and 1960s. From 1939 through 1993, water-level declines contributed to 2.7 ft of measured land subsidence in the southern part of the Oxnard Plain. For this same period, the model simulated a total 3 ft of land subsidence in the South Oxnard Plain subarea, and as much as 5 ft in the Las Posas Valley subareas. Model results indicate that subsidence occurred primarily in the upper-aquifer system prior to 1959, but in the lower-aquifer system between 1959–93 owing to an increase in pumpage from the lower-aquifer system.

The calibrated ground-water flow model was used to assess future ground-water conditions based on proposed water-supply projects in the existing management plan for the Santa Clara–Calleguas ground water basin and seven alternative water-supply projects. Two different approaches were used to estimate future recharge, streamflow, and climate-related water-demand conditions for input to these model simulations: (1) a 24-year projection (1994–2017) using historical estimates of recharge and measured streamflow, and (2) a 44-year projection (1994–2037) using spectral estimates of future precipitation. The model simulations were used to assess the effects of increased recharge, reduced pumpage, and shifted pumpage (from lower- to upper-aquifer system) on ground-water storage depletion and related coastal landward flow (seawater intrusion) and land subsidence.

The model simulations of the proposed water-supply projects in the existing management plan assume average pumpage from 1984–93 with historical inflows (base-case 1) and with spectral estimates of inflows (base-case 4), a rolling cut back in pumpage (base-case 2), and a step cut back in pumpage (base-case 3). All the simulations of the proposed water-supply projects reduced pumpage in the FGMA areas which resulted in a reduction but not an elimination of storage depletion and related coastal landward flow (seawater intrusion) and subsidence, a reduction in streamflow recharge, and an increase in coastal seaward flow and underflow to adjacent subareas from the Oxnard Plain. However, the immediate reduction in pumpage represented by the step cut-back projection showed the largest reduction in coastal landward flow (seawater intrusion) and land subsidence. A comparison of simulations of future ground-water conditions, based on historical inflows (base case 1) and a spectral estimate of inflows (base case 4), shows increased coastal landward flow (seawater intrusion), storage depletion, and increased land subsidence for base-case 4 due to a drought projected earlier in the spectral estimate of inflows than in the historical inflows. The spectral estimate probably provides a smoother and more realistic transition between historical and future climatic conditions.

Simulations of alternative water-supply projects indicated some differences in hydrologic responses relative to the simulations of the proposed water-supply projects in the existing management plan. Stopping pumpage primarily in the lower-aquifer system in the South Oxnard Plain subarea had the largest effect on reducing coastal landward flow (seawater intrusion) of all the potential cases evaluated. The shifting of pumpage from the lower- to the upper-aquifer system in the South Oxnard Plain subarea yielded the largest combined effect on coastal flow with a reduction of coastal landward flow in the lower-aquifer system and coastal seaward flow from the upper-aquifer system. A seawater-barrier injection projection stopped coastal landward flow (seawater intrusion) into the upper-aquifer system but also resulted in large quantities of coastal seaward flow. The recharge of water in Happy Camp Canyon resulted in water-level rises that were above land surface (not feasible) in the East Las Posas Valley subarea and did not result in significant changes in hydrologic conditions in other parts of the basin.

Water-resource management alternatives may require implementation of feasible demand-side pumpage strategies that do not create adverse effects, such as seawater intrusion and land subsidence, during the driest parts of the dry climate cycles. Management practices should consider the natural climatic cycles that are dominant factors in the supply and demand aspects of the hydrologic budget and hydrologic cycle.

Management of the regional-aquifer system may require the implementation of feasible supply-side recharge projects that do not create adverse effects during the wettest parts of the wet climate cycles; such effects include the potential for liquefaction or contaminant mobilization from water levels that could approach the land surface. Near-surface ground-water levels currently controlled by ground-water pumpage along Arroyo Simi in Simi Valley could occur in areas, such as South Las Posas Valley subarea and the Oxnard Plain Forebay, where additional recharge projects are planned. Contaminant mobilization of organic and inorganic constituents from agricultural and treated sewage effluent can occur when unsaturated sediments become saturated or semiperched systems are hydraulically reconnected to the upper-aquifer system by rising water levels. Evaluation of future management projects may require simulating multiple projects as opposed to individual water-supply projects as was done for this study. Optimization modeling may be used to better evaluate the effects of multiple water-supply projects, allocate the final distribution of resources among the final set of supply and demand components, and delineate the limits of feasibility of any combination of water-supply projects and water-resource management policies.

SELECTED REFERENCES

Adams, F., 1913, Irrigation resources of California and their utilization: Washington, U.S. Government Printing Office, U.S. Office of Experiment Stations series, Bulletin 254, 95 p.

Bennett, G. D., Kontis, A. L., and Larson, S. P., 1982, Representation of multi-aquifer well effects in three-dimensional ground-water flow simulation: Ground Water, v. 20, no. 3, p. 334–341.

Blake, T.F., and Larson, R.A., eds., 1991, Engineering geology along the Simi-Santa Rosa Fault system and adjacent areas, Simi Valley to Camarillo, Ventura County, California: Association of Engineering Geologists, Southern California Section, [Los Angeles, Calif.], 1991, Annual Field Trip Guidebook, 2 v.

Blaney, H. F., and Criddle, W. D., 1950, Determining water requirements in irrigated areas from climatological and irrigated data: [Washington], Soil Conservation Service, 48 p.

———1962, Determining consumptive use and irrigation water requirements: U.S. Department of Agriculture, Agricultural Research Service, Technical Bulletin 1275, 59 p.

Brownlie, W.R., and Taylor, B.D., 1981, Sediment management for southern California mountains, coastal plains, and shoreline—Part C., Coastal sediment delivery by major rivers in southern California: California Institute of Technology, Environmental Quality Laboratory, EQL Report 17-C, 83 p.

California Department of Public Works, 1934, Ventura County investigation: California Department of Public Works, Division of Water Resources Bulletin 46, 244 p.

———1950, Crop survey—Ventura County, surveyed 1949–50 [map]: California Department of Public Works, Division of Water Resources [map available at California Department of Water Resources, Map Library, 1416 9th Street, Sacramento, CA 95814].

California Department of Water Resources, 1958, Sea water intrusion in California: California Department of Water Resources Bulletin 63, 91 p.

———1964, Names and areal code numbers of hydrologic areas in the Southern District: [Sacramento, Calif.], California Department of Water Resources, 57 p.

———1965, Sea-water intrusion: Oxnard Plain of Ventura County: California Department of Water Resources Bulletin 63-1, variously paged.
———1967, Ground water basin protection projects: Oxnard Basin, salinity barrier, Ventura County: [Sacramento, Calif.], California Department of Water Resources, Progress Report, 132 p.
———1970, Memorandum Report for Southern District, Ventura County land use survey: 1969 Ventura County and Upper Santa Clara River Drainage Area Land and Water Use Study: California Department of Water Resources, maps 63-44 Camarillo, 61-45 Fillmore, 62-45 Moorpark, 63-45 Newbury Park, 63-43 Oxnard, 61-46 Piru, 62-44 64-44 Point Mugu, 62-44 Santa Paula, 61-44 Santa Paula Peak, 62-43 Saticoy, 62-46 Simi, 62-42 Ventura.
———1971, Sea-water intrusion: Aquitards in the coastal ground water basin of Oxnard Plain, Ventura County: California Department of Water Resources Bulletin 63-4, 569 p.
———1974a, Mathematical modeling of water quality for water resources management. Volume 1, Development of the ground water quality model: [Sacramento, Calif.], California Department of Water Resources, Southern District, 204 p.
———1974b, Mathematical modeling of water quality for water resources management, development of the ground water quality model. Volume 2, Development of historic data for the verification of the ground water quality model of the Santa Clara–Calleguas area, Ventura County: [Sacramento, Calif.], California Department of Water Resources, Southern District, 114 p.
———1975, Compilation of technical information records for the Ventura County cooperative investigation: [Sacramento, Calif.], California Department of Water Resources, v. 2, 234 p.
———1981a, Ventura County and upper Santa Clara River Drainage Area Land Use Study 1980: District Report: [Sacramento, Calif.], California Department of Water Resources, Southern District, 25 p.
———1981b, Standard land use legend: [Sacramento, Calif.], California Department of Water Resources, 8 p.
———1988, Ventura County and the upper Santa Clara River drainage area land use survey, map 63-43 Oxnard, Calif.: Unpublished map series on file with California Department of Water Resources, Southern District.
California Division of Oil and Gas, 1977, Subsidence study of Oxnard Oil Field and vicinity, Ventura County, California: California Department of Conservation, Division of Oil and Gas Report, 45 p.
California State Water Resources Board, 1956, Ventura County Investigation: [Sacramento, Calif.], California Water Resources Board, Bulletin 12, v. 1, variously paged.
CH2M HILL, 1992, North Las Posas Basin ASR demonstration project: Denver, Colo., variously paged [available from Metropolitan Water District of Southern California, 700 N. Alameda St., Los Angeles, CA 90012].
———1993, Hydrogeology and three-dimensional groundwater flow model of the Las Posas Basin, Ventura County, California: Denver, Colo., variously paged [available from Metropolitan Water District of Southern California, 700 N. Alameda St., Los Angeles, CA 90012].
County of Ventura Public Works Agency, 1975, Compilation of technical information records for the Ventura County cooperative investigation: [Sacramento, Calif.], California Department of Water Resources, 28 p.
———1990, Oxnard Plain of Ventura County, 1989 seawater intrusion study: [Sacramento, Calif.], California Department of Water Resources, 5 p.
Dahlen, M.Z., 1992, Sequence stratigraphy, depositional history and Middle to Late Quaternary sea levels of the Ventura shelf, California: Quaternary Research, v. 38, no. 2, p. 234–245.
Dahlen, M.Z., Osborne, R.H., and Gorsline, D.S., 1990, Late Quaternary history of the Ventura mainland shelf, California: Marine Geology, v. 94, no. 4, p 317–340.
Dal Pozzo, P., 1992, Stream loss and stream loss blockage in Santa Paula Creek: United Water Conservation District, open-file report, 17 p.
Densmore, J.N., 1996, Data from ground-water monitoring wells in the Oxnard Plain, Pleasant Valley, and Las Posas subbasins, Ventura County, California, 1989–95: U.S. Geological Survey Open-File Report 96-120, 179 p.
Densmore, J.N., Middleton, G.K., and Izbicki, J.A., 1992, Surface-water releases for ground-water recharge, Santa Clara River, Ventura County, California, *in* Herrmann, Raymond, ed., Managing Water Resources during Global Change: Proceedings of the American Water Resources Association Annual Meeting, Jackson Hole, Wyoming, p. 407–416.
Dettinger, M.D., Ghil, M., Strong, C.M., Weibel, W., and Yiou, P., 1995, Software expedites singular-spectrum analysis of noisy time series: Eos, Transactions of the American Geophysical Union, v. 76, no. 2, p. 12, 14, 21.
Dibblee, T.W., 1988, Geologic map of the Ventura/Pitas Point Quadrangles, Ventura County, California: Santa Barbara, Calif., Dibblee Geological Foundation, Dibblee Foundation Map series, DF-21, scale 1:24,000.

———1990a, Geologic map of the Fillmore Quadrangle, Ventura County, California: Santa Barbara, Calif., Dibblee Geological Foundation, Dibblee Foundation Map series, DF-27, scale 1:24,000.
———1990b, Geologic map of the Santa Paula Peak Quadrangle, Ventura County, California: Santa Barbara, Calif., Dibblee Geological Foundation, Dibblee Foundation Map series, DF-26, scale 1:24,000.
———1991, Geologic map of the Piru Quadrangle, Ventura County, California: Santa Barbara, Calif., Dibblee Geological Foundation, Dibblee Foundation Map series, DF-34, scale 1:24,000.
———1992a, Geologic map of the Simi Quadrangle, Ventura County, California: Santa Barbara, Calif., Dibblee Geological Foundation, Dibblee Foundation Map series, DF-39, scale 1:24,000.
———1992b, Geologic map of the Moorpark Quadrangle, Ventura County, California: Santa Barbara, Calif., Dibblee Geological Foundation, Dibblee Foundation Map series, DF-40, scale 1:24,000.
———1992c, Geologic map of the Santa Paula quadrangle: Ventura County, California: Santa Barbara, Calif., Dibblee Geological Foundation, Dibblee Foundation Map series, DF-41, scale 1:24,000.
———1992d, Geologic map of the Saticoy quadrangle: Ventura County, California: Santa Barbara, Calif., Dibblee Geological Foundation, Dibblee Foundation Map series, DF-42, scale 1:24,000.
Dibblee, T.W., and Ehrenspeck, H.E., 1990, Geologic Map of the Camarillo and Newbury Park Quadrangles, Ventura County, California: Santa Barbara, Calif., Dibblee Geological Foundation, Dibblee Foundation Map series, DF-28, scale 1:24,000.
Duell, L.F.W., Jr., 1992, Use of regression models to estimate effects of climate change on seasonal streamflow in the American and Carson River basins, California–Nevada, *in* Herrmann, Raymond, ed., Managing water resources during global change: AWRA 28th annual conference and symposium: An international conference, Reno, Nevada, November 1–5, 1992: Bethesda, Md., American Water Resources Association, p. 731–740.
England, Evan, and Sparks, Allen, 1988, GEO-EAS (Geostatistical Environmental Assessment Software) User's Guide: Environmental Monitoring Systems Laboratory Office of Research and Development, U.S. Environmental Protection Agency, Las Vegas, Nevada, EPA600/4-88/033, variously paged.
Farnsworth, R.K., Thompson, E.S., and Peck, E.L., 1982, Evaporation atlas for the contiguous 48 United States: U.S. Dept. of Commerce, National Oceanic and Atmospheric Administration, National Weather Service, NOAA Technical Report NWS 33, 26 p.
Finkle, F.C., 1909, Report on irrigation project for Lower Santa Clara Valley, Ventura County, California to Messrs. James H. Adams & Company and Wm. R. Staats Company: Consulting Engineer Report, 91 p.
Fox Canyon Groundwater Management Agency, 1997, Ordinance 5.5: An ordinance to reduce groundwater extractions: Board of Directors of the Fox Canyon Groundwater Management Agency, 13 p. [ordinance available from the California Water Resources Division, Ventura County Government Center, Administration Building, 800 South Victoria Avenue, Ventura, California 93009-1600].
Freckleton, J.R., Martin, Peter, and Nishikawa, Tracy, 1998, Geohydrology of storage unit III and a combined flow model of the Santa Barbara and Foothill ground-water basins, Santa Barbara County, California: U.S. Geological Survey Water-Resources Investigations Report 97-4121, 80p.
Freeman, V. M., 1932, Report on the study of capacity of underground reservoirs and calculated depletion and replenishment of underground stored water during the period January 1928 to March 1, 1932: [Santa Paula, Calif.], Santa Clara Water Conservation District Report, 27 p.
———1968, People-land-water: Santa Clara Valley and Oxnard Plain, Ventura County, California: Los Angeles, Calif., Lorrin L. Morrison, 227 p.
Galloway, D.L., Hudnut, K.W., Ingebritsen, S.E., Phillips, S.P., Peltzer, G., Rogez, F., and Rosen, P.A., 1998, Detection of aquifer system compaction and land subsidence using interferometric synthetic aperture radar, Antelope Valley, Mojave Desert, California: Water Resources Research, v. 34, no. 10, pp. 2573–2585.
Gardner D., 1995, Summary of operations report—Mound Basin ground water management program construction of monitoring wells: Ventura, Calif., Fugro West Inc., variously paged [available from City of San Buenaventura].
Greene, H.G., Wolf, S.C., and Blom, K.G., 1978, The marine geology of the eastern Santa Barbara Channel, with particular emphasis on the ground water basins offshore from the Oxnard Plain, southern California: U.S. Geological Survey Open-File Report 78-305, 104 p.
Grunsky, C.E., 1925, Report on the water resources of the Santa Clara River Valley: C.E. Grunsky Company, Engineers, 100 p.

Hanson, R.T., 1989, Aquifer-system compaction, Tucson basin and Avra Valley, Arizona: U.S. Geological Survey Water-Resources Investigations Report 88-4172, 69 p.

———1995, Land subsidence in the Oxnard Plain of the Santa Clara–Calleguas basin, Ventura County, California [abs.], *in* Prince, K.R., Galloway, D.L., and Leake, S.A., eds., U.S. Geological Survey Subsidence Interest Group conference, Edwards Air Force Base, Antelope Valley, California, November 18–19, 1992: Abstracts and summary: U.S. Geological Survey Open-FIle Report 94-532, p. 37–39.

———1996, Postaudit of head and transmissivity estimates and ground-water flow models of Avra Valley, Arizona: U.S. Geological Survey Water-Resources Investigations Report 96-4045, 84 p.

Hanson, R.T., and Benedict, J.F., 1994, Simulation of ground-water flow and potential subsidence, upper Santa Cruz Basin, Arizona: U.S. Geological Survey Water-Resources Investigations Report 93-4196, 47 p.

Hanson, R.T., and Dettinger, M.D., 1996, Combining future ground-water and climate scenarios as a management tool for the Santa Clara–Calleguas basin, Southern California [abs.]: Eos, Transactions, American Geophysical Union, v. 77, no. 46, p. F55.

Hanson, R.T., and Nishikawa, Tracy, 1992, Flow-meter data: an important addition to aquifer-test analysis for modeling layered aquifer systems [abs.]: Eos, Transactions, American Geophysical Union, v. 73, no. 43, p. 165.

———1996, Combined use of flowmeter and time-drawdown data to estimate hydraulic conductivities in layered aquifer systems: Ground Water, v. 34, no. 1, p. 84–94.

Harbaugh, A.W., and McDonald M.G., 1996, User's Documentation for MODFLOW-96, and update to the U.S. Geological Survey modular finite-difference ground-water flow model: U.S. Geological Survey Open-File Report 96-485, 56 p.

Holzer, T.L., 1981, Preconsolidation stress of aquifer systems in areas of induced land subsidence: American Geophysical Union, Water Resources Research, v. 17, no. 3, p. 693–04.

Hsieh, P.A., and Freckleton, J.R., 1993, Documentation of a computer program to simulate horizontal-flow barriers using the U.S. Geological Survey's modular three-dimensional finite-difference ground-water flow model: U.S. Geological Survey Open-File Report 92-477, 32 p.

Ireland R.L., Poland, J.F., and Riley, F.S., 1984, Land Subsidence in the San Joaquin Valley, California, as of 1980: U.S. Geological Survey Professional Paper 437-I, 93 p.

Izbicki, J.A., 1991, Chloride sources in a California coastal aquifer, *in* Peters, H.J., ed., Ground water in the Pacific Rim countries: Proceedings of the symposium sponsored by the Irrigation and Drainage Division of the American Society of Civil Engineers, Honolulu, Hawaii, July 23–25, 1991: New York, American Society of Civil Engineers, p. 71–77.

———1992, Sources of chloride in ground water of the Oxnard Plain, California, *in* Prince, K. R., and Johnson, A.I., eds., 1992, Aquifers of the Far West: Papers presented at AWRA Symposium on Water Supply and Water Reuse, 1992 and beyond, June 2–6, 1991, San Diego, California: Bethesda, Md., American Water Resources Association, AWRW Monograph series, no. 16, p. 5–14.

———1996a, Seawater intrusion in a coastal California aquifer: U.S. Geological Survey, Fact Sheet 125-96, 4 p.

———1996b, Source, movement, and age of ground water in a coastal California aquifer: U.S. Geological Survey, Fact Sheet 126-96, 4 p.

Izbicki. J.A., and Martin, Peter, 1997, Use of isotopic data to evaluate recharge and geologic controls on the movement of ground water in Las Posas Valley, Ventura County, California: U.S. Geological Survey, Water-Resources Investigations Report 97-4035, 12 p.

Izbicki. J.A., Martin, Peter, Densmore, J.N., and Clark, D.A., 1995, Water-quality data for the Santa Clara–Calleguas hydrologic unit, Ventura County, California, October 1989 to December, 1992: U.S. Geological Survey, Open-File Report 95-315, 124 p.

Jakes, M.C., 1979, Surface and subsurface geology of the Camarillo and Las Posas Hills Area, Corvalis, Ore., Oregon State University, M.S. thesis, 105 p.

Jiang, N., Neelin, D., and Ghil, M., 1995, Quasi-quadrennial and quasi-biennial variability in the equatorial Pacific: Climate Dynamics, v. 12, p. 101–112.

Johnson, R.L., and Yoon, Y., 1987, Report on Santa Rosa groundwater basin management plan: Boyle Engineering Corp. consulting report for city of Thousand Oaks and Camarosa County Water District, no. VT-T01-107-05, variously paged.

Kennedy, M.P., Greene, H.G., and Clarke, S.H., 1987, Geology of the California continental margin: Explanation of the California continental margin geologic map series: Interpretive methods symbology, stratigraphic units, and bibliography: California Division of Mines and Geology Bulletin 207, 110 p.

Keppenne, C.L., and Ghil, M., 1992, Adaptive spectral analysis and prediction of the Southern Oscillation Index, Journal of Geophysical Research, v. 97, p. 20449-20554.

Koczot, K.M., 1996, Estimating rates and patterns of historical ground-water pumpage for irrigation using a geobased numerical model: San Diego, San Diego State University, Masters Thesis, 111 p.

Law/Crandall Inc., 1993, Water Resource evaluation Santa Paula ground water basin, Ventura County, California: Consultants Report to United Water Conservation District, March 1993, 71 p.

Leake, S.A., and Prudic, D.E., 1991, Documentation of a computer program to simulate aquifer-system compaction using the modular finite-difference ground-water flow model: U.S. Geological Survey Techniques of Water-Resources Investigations, book 6, chap. A2, 68 p.

Mann, John F. Jr. and Associates, 1959, A plan for ground water management –– United Water Conservation District: La Habra, California, [consulting ground-water geologists], 131 p.

Martin, Peter, 1986, Southern California alluvial basins regional aquifer-system study, *in* Sun, R.L. (ed.), Regional Aquifer-System Analysis Program of the U.S. Geological Survey— summary of projects, 1978–84, U.S. Geological Survey Circular 1002, p. 245–247.

———1993, Southern California basins interim report: 12 p.

Martin, Peter, and Berenbrock, Charles, 1986, Ground-water monitoring at Santa Barbara, California: Phase 3--Development of a three dimensional digital ground-water flow model for storage unit I of the Santa Barbara ground-water basin: U.S. Geological Survey Water-Resources Investigations Report 86-4103, 58 p.

McDonald, M.G., 1984, Development of a multi-aquifer well option for a modular ground-water flow model, *in* Proceedings of the National Water Well Conference on Practical Applications of Ground Water Models Aug. 15–17, 1984, variously paged.

McDonald, M.G., and Harbaugh, A. W., 1988, A modular three-dimensional finite-difference ground-water flow model: Techniques of Water-Resources Investigations of the U.S. Geological Survey, book 6, chap A1, 586 p.

McDonald, M.G., Harbaugh, A.W., Orr, B.R., and Ackerman, D. J., 1991, A method of converting no-flow cells to variable-head cells for the U.S. Geological Survey modular finite-difference ground-water flow model: U.S. Geological Survey Open-File Report 91-536, 99 p.

National Atmospheric and Oceanic Administration, 1994, The International Tree Ring Data Base, NOAA's World Data Center-A for Paleoclimatology, Boulder, Colorado, 1994.

Neuman, S.P., and Witherspoon, P.A., 1972, Field determination of the hydraulic properties of leaky multiple aquifer systems: Water Resources Research, v. 8, no. 5, p. 1284–1298.

Nishikawa, Tracy, 1997, Testing alternative conceptual models of seawater intrusion in a coastal aquifer using computer simulation, Southern California, USA: Hydrogeology Journal, v. 5, no. 3, p. 60–74.

Pollock, D.W., 1989, Documentation of computer programs to compute and display pathlines using results from the U.S. Geological Survey modular three-dimensional finite-difference ground-water flow model: U.S. Geological Survey Open-File Report 89-381, 188 p.

Predmore, S.K., 1993, Use of a geographic information system to identify abandoned wells: U.S. Geological Survey Open-File Report 93-147, 1 sheet.

Predmore, S.K., Koczot, K.M., and Paybins, K.S., 1997, Documentation and description of the digital spatial data base for the Southern California Regional Aquifer-System Analysis Program, Santa Clara–Calleguas Basin, Ventura County, California: U.S. Geological Survey Open-File Report 96-629, 100 p.

Press, W.H., Flannery, B.P., Teukolsky, S.A., and Vetterling, W.T., 1989, Numerical recipes— The art of scientific computing (FORTRAN Version): Cambridge University Press, New York, 702 p.

Prudic, D.E., 1989, Documentation of a computer program to simulate stream-aquifer relations using a modular, finite-difference, ground-water flow model: U.S. Geological Survey Open-File Report 88-729, 113 p.

Prudic, D.E., and Herman, M.E., 1996, Ground-water flow and simulated effects of development in Paradise Valley, a basin tributary to the Humboldt River in Humboldt County, Nevada: U.S. Geological Survey Professional Paper 1409-F, 92 p.

Quinn, W.H., and Neal, V.T., 1987, El Niño occurrences over the past four and a half centuries: Journal of Geophysical Research, v. 92, no. C13, p. 14449–14461.

Reichard, E.G., 1995, Ground-water/surface-water management with stochastic surface-water supplies: A simulation-optimization approach: Water Resources Research, v. 31, no. 11, p. 2845–2865.

Santa Barbara County Water Agency, 1977, Adequacy of the ground-water basin of Santa Barbara County: Santa Barbara County Water Agency, chap 4, p. 1–14.

Stamos, C.L., Predmore, S.K., and Zohdy, A.A.R., 1992, Use of D-C resistivity to map saline ground water, *in* Engman, E.T. (ed.), Saving a threatened resource—in search of solutions: Proceedings of the irrigation and drainage sessions at Water Forum ‘92, Baltimore, Md., p. 80–85.

Taylor, B.D., Brown, W.M., and Brownlie, W.R., 1977, Sediment management for southern California mountains, coastal plains, and shoreline—Progress Report No. 3: Environmental Quality Laboratory, California Institute of Technology, Open File Report 77-8, variously paged.

Turner, J.M., 1975, Ventura County water resources management study—Aquifer delineation in the Oxnard–Calleguas area, Ventura County: Technical Information Record, January 1975, Ventura County Department of Public Works Flood Control District, 45 p.

United Water Conservation District, 1983, Appendix for report on proposed Freeman Diversion Improvement Project, Public Law 84-984.

———1986, Hydrologic conditions of water resources within United Water Conservation District: Report for Water Year 1984–85 beginning October 1, 1984 and ending September 30, 1985, 18 p.

———1991, Untitled: Unpublished map delineating groundwater basins in the United Water Conservation District: Ventura County, Calif. [on file with United Water Conservation District].

Vautard, R., Yiou, P., and Ghil, M., 1992, Singular-spectrum analysis: A toolkit for short, noisy chaotic signals: Physica D, v. 58, p. 95–126.

Ventura County Board of Supervisors, 1988, Ventura County general plan, goals, policies, and programs—hazards appendix: Ventura County Board of Supervisors document no. 1D297-1.90 and no. I198, adopted May 24, 1988, 146 p.

Ventura County Public Works Agency, 1973, Santa Paula Creek Percolation Study: Ventura County Department of Public Works, Flood Control District, Hydrology Section, 18 p.

———1990, Quadrennial report of hydrologic data 1985–88: Ventura County Department of Public Works, Flood Control Department, variously paged.

———1993, Quadrennial report of hydrologic data 1989–92: Ventura County Department of Public Works, Flood Control Department, Planning and Regulatory Division, Hydrology Section, variously paged.

Ventura County Resource Management Agency, Environmental Health Department, 1980, 208 Areawide waste treatment management planning study: Technical appendix G, p. 341–356.

Webb, R.H., and Bettancourt, J.L., 1990, Climatic variability and flood frequency of the Santa Cruz River, Pima County, Arizona: U.S. Geological Survey Water-Supply Paper 2379, 40 p.

Weber, F.H., Kiessling, E.W., Sprotte, E.C., Johnson, J.A., Sherburne, R.W., and Cleveland, G.B., 1976, Seismic hazards study of Ventura County, California: California Department of Conservation, California Division of Mines and Geology Open-File Report 76-5, 396 p., pls. 3A and 3B.

Yerkes, R.F., Sarna-Wojcicki, A.M., and Lajoie, K.R., 1987, Geology and Quaternary deformation of the Ventura area, *in* Recent reverse faulting in the Transverse Ranges, California: U.S. Geological Survey Professional Paper 1339, p. 169–178.

Yeats, R.S., 1983, Large-scale Quaternary detachments in the Ventura basin, southern California: Journal of Geophysical Research, v. 88, p. 569–583.

Zohdy, A.A.R., Martin, P., and Bisdorf, R. J., 1993, A study of seawater intrusion using direct-current soundings in the southeastern part of the Oxnard Plain, California: U.S. Geological Survey Open-File Report 93-524, 138 p.

THIS PAGE LEFT BLANK INTENTIONALLY